Early Extractive Iron Metallurgy in N Greece: a unified approach to regional archaeometallurgy.

Euphemia Photos
B.Sc. M.Sc.

Thesis submitted for the degree of Doctor of Philosophy
in the Faculty of Science
University of London

University College
Institute of Archaeology
University of London
August 1987

"Scraping the weathered granite to release the iron sands,
Japan, last century"

(the author is indebted to Mr K Kubota for this watercolour).

ABSTRACT

Aspects of early Greek extractive iron metallurgy are investigated here, for the first time, with particular emphasis on Macedonia, Greece's most metals-rich province. The subject is approached experimentally by considering equally the ores, slag and artefacts of iron in Macedonia, through the analytical examination of archaeological slag and artefacts, the experimental smelting of Macedonian ores and subsequent analytical investigation of the slag and blooms produced.

The mineral resources geology of Macedonia is presented. The historical background to mining and metal working in Macedonia from the Early Iron Age (tenth century BC) to the turn of the present century is documented. The literature on the introduction of iron into Greece, and the East Mediterranean more generally, is critically reviewed, and in the light of results obtained, especially from Thasos, it is argued that the origins of iron making in Macedonia, if not elsewhere in Greece, should be sought locally during the Late Bronze Age.

Despite the absence of excavated furnace remains, it has been possible, through analytical examination of metallurgical waste, to trace the operation of the bloomery in Macedonia continuously for nearly thirty centuries. That a considerable variety of iron ores were exploited was elucidated by the analysis of slag inclusions in a large number of iron artefacts from Vergina and from sites on Thasos and the East Macedonian Mainland, spanning chronologically the Early Iron Age to the Byzantine period. The titanium-rich magnetite sands on Thasos and at Vrontou on the Mainland were shown to have been worked from the Hellenistic/Roman to the turn of this century. A second century BC nickel-rich bloom found at the Hellenistic site at Petres in West Macedonia testified, for the first time, to the smelting of nickel-rich iron laterites in Greece, while the manganese-rich iron deposits in Palaia Kavala district were worked for their precious metals content, probably during Ottoman times and perhaps as early as the Classical period. It is suggested that the Skapte Hyle of the classical texts may be located in the Palaia Kavala district.

A fresh appraisal of the depiction of furnaces on Black and Red Figure Attic vases of the sixth and fifth centuries BC suggests that the bloomery process may have developed at that time to a level not previously suspected. The classical texts, the function of the cauldron on the furnace top and experimental meltings carried out in the process of this work all point to the production of wrought iron/steel through the decarburisation of high carbon iron in a fining hearth. It is argued that the furnaces depicted on the vases are themselves fining hearths, the cauldron sealing the furnace top in order for the air blast to be directed over the molten mass.

Acknowledgements

The author wishes, foremost, to express her sincere gratitude to Prof. R F Tylecote for his constant guidance, criticism and support throughout this research project and others carried out during the last four years. Also to Dr. N J Seeley for stimulating exchange of ideas and optimism in 'difficult' times.

The author is deeply indebted to Dr. Ch. Koukouli-Chrysanthaki of the Kavala Ephoria and Mr. G Gialoglou of IGME, Xanthi for acquainting her with the vast metallurgical remains of East Macedonia and the Macedonian life and character. Their invaluable assistance and undiminished enthusiasm made this work particularly rewarding and enjoyable. Also to Dr. R E Jones for editorial assistance and a little more.

Particular thanks are extended to Mr. I Young of the Geology Department, University College London for the use of the Electron Microprobe, Dr. A Mackay and Ms H Corry of Birkbeck College for access to XRD and SEM instrumentation, Dr. G Mariner of Bedford College for XRF facilities. For initiating me into bloomery iron smelting and providing me with insight into the mind of the smith, I owe a great deal to Mr. R Adams of Oxted, Sussex, as well as to other smiths, Messrs. Th Piperides and S Demertzoglou of Kavala.

The author is grateful for the financial support provided by the Institute of Archaeology, University of London, the Institute for Archaeometallurgical Studies and the University of London

Central Research Fund.

The author wishes to thank warmly the following:
Dr. R Morell of the National Physical Laboratory, Teddington, for facilities for some laboratory reduction experiments.
Mr. B Hodson, British Steel Coorporation, LLanwern, South Wales for the provision of 400 kg of high grade Australian hematite.
Mrs P Adam-Veleni, Dr. J Vokotopoulou, Ms Th Savopoulou of Thessaloniki Museum for archaeological material and stimulating discussions on Hellenistic and prehistoric Macedonia.
Mr. P Dorrell and Mr. S Laidlaw for generous help to body and soul as well as to photography; Mr. I Morton for assistance with computer programming.

Finally, fellow archaeometallurgists in Britain, Greece, Sweden, Thailand, India, United States, Turkey, Germany, Ireland and many other places, many of whose sites I was fortunate to visit and many others to simply meet. I am grateful to them for long rewarding discussions over many pints (or equivalent) on alternative ways of doing the same thing. Also, to C.S. Smith, with whom I exchanged only a "what a lovely day" one bright morning in Washington in 1981 but whose writings have been a continuous source of inspiration since my first introduction to the field.

CONTENTS

Chapter 1	**Introduction**		
	1.1	Scope and Aims	1
	1.2	Thesis Outline and Methodology	5
Chapter2	**Scientific analyses and thehistorical background to metals production in Macedonia: Neolithic to Ottoman**		
	2.1	Macedonia: from the gold and copper of the Neolithic to the iron of the Early Iron Age	12
	2.1.a	Gold	13
	2.1.b	Copper/Bronze	18
	2.1.c	Iron	25
	2.2	Iron in Mainland Greece and the Aegean, Anatolia and the Eastern Mediterranean	29
	2.2.a	Iron in Mainland Greece and the Islands	29
	2.2.b	Iron in Anatolia and the Eastern Mediterranean	34
	2.3	Metals in the Balkans and Central Europe	37
	2.3.a	Gold/Copper/Bronze	38
	2.3.b	Iron	40
	2.4	Summary and Concluding Remarks on Macedonian Metals from Late Neolithic to Early Iron Age	41
	2.5	Metals and Mining in the Archaic /Classical/ Hellenistic /Roman periods	45
	2.5.a.1	Mining: gold, silver and copper	45
	2.5.a.2	Gold,silver and bronze artefacts	48
	2.5.b.1	Mining: iron	49
	2.5.b.2	Iron artefacts	50
	2.6	Byzantine Mining and metals	50
	2.6.a	Byzantine Mining and Metals: gold, silver and copper	50
	2.6.b	Byzantine Mining: iron	51
	2.7	Ottoman Mining and Metals	52
	2.7.a	Ottoman Mining: gold, silver and copper	52
	2.7.b	Ottoman Mining: iron	55

2.8 Summary and Concluding Remarks on Macedonian Mining and Metals from the Archaic to the Ottoman Periods 56

Chapter 3 **Analytical Investigation of Archaeological and Experimental Ore, Slag and Artefacts**

3.1 Introduction 59

3.2 Geology and Minerals Resources of Macedonia and Thasos 68
3.2.a General 68
3.2.b Iron 73
3.2.b.1 Hematite/Limonite: Thasos 73
3.2.b.2 Manganese rich Iron Ores: Palaia Kavala, EM 74
3.2.b.3 Titanium rich-Iron Sands: Thasos and EM Mainland 76
3.2.b.4 Nickel-rich Iron Laterites: Edessa, Kastoria, WM 83
3.2.c Mixed Sulfides: Chalkidiki and Pangaion 86

3.3 Late Bronze Age Early Iron Age Copper/Iron Slag from the Cemeteries of Kastri on Thasos 87
3.3.a Copper Slags 87
3.3.b Iron Slags 92
3.3.c Discussion 93

3.4 Experimental Bloomery Iron Making at Ashdown Forest, Sussex 103
3.4.a The bloomery 103
3.4.b Smelting procedure 106
3.4.b.1 General 106
3.4.b.2 Preheating 109
3.4.b.3 Smelting 110
3.4.b.4 Products of smelting 112
3.4.c Smithing and its products 114

3.5 Slags from Hematite/LimoniteOresand Iron Artefacts from Mainland Macedonia and Thasos 127
3.5.a Archaeological Slags 127
3.5.b Archaeological Artefacts from Macedonia and Thasos 137
3.5.c Discussion 157

3.6 Titanium-rich Iron Slags: East Macedonia and Thasos 159
3.6.a Morphology and Mineralogy 159
3.6.b Provenance 172
3.6.c Discussion 181

3.7 Archaeological and experimental slag andmetal from Manganese rich-Iron ores
3.7.a Archaeological slag 191
3.7.b Archaeological artefacts 199
3.7.c Experimental slag and metal 201

3.7.d Discussion 202

3.8 Smelting of Nickel-rich Iron Laterites in West Macedonia 218
3.8.a Archaeological evidence 218
3.8.b Experimental evidence 220
3.8.b.1 Experimental evidence: bloom and smelting slag 220
3.8.b.2 Experimental evidence: smithed bloom and forge-welded objects 228
3.8.c Discussion 233
3.8.d The question of smelted Ni-rich vs. Meteoritic iron 238
3.8.d.1 Review of the literature 238
3.8.d.2 Canyon Diablo Meteorite 241

Chapter 4 **Metallurgical furnaces in Greece: archaeological evidence, pictorial representations and documentary references**

4.1.a Introduction 249
4.1.b Archaeological evidence 250
4.1.c Pictorial representations 252
4.1.d Documentary references 255
4.1.e Previous investigators' interpretations of the texts and the vase illustrations 257

4.2.a Proposed new interpretation 260
4.2.b Experimental melting of iron in a shaft furnace 266
4.2.c Were the Greeks making cast iron? 271

4.3 Why the Foundry Cup depicts more than bronze casting 274

Chapter 5 **Conclusions** 285

Appendix 2.1 Chronological Tables 295
3.1.1 Pangaion 296
3.1.2 Directory of sites and their abbreviations 298
3.1.3 Inventory of metallurgical waste collected during surveys on Thasos and the Mainland 300
3.2.1 Thasos gneiss and Vrontou granodiorite 303
3.6.1 Analysis of Ti-rich iron slags from Lesvos 304
3.6.2 Analysis of experimental products from the smelting of Ti-rich iron sands 307
3.7.1 Speiss 310
3.7.2 Experimental smelts with Petropigi ore 313
3.7.3 Analysis of non-ferrous slag 315
3.8.1 Ellingham diagram for oxides 317
3.8.2 Experimental smelts with Ni-rich iron

laterites 318
4.1 Traditional Iron Foundry in Kavala 322

Glossary 324

Bibliography 328

List of Tables

Table 2.1 Catalogue of published gold, copper, bronze and iron objects from Macedonia (LN - EIA) 15
2.2 Analyses of copper/bronze artefacts from Sitagroi 19
2.3 Analyses of copper/bronze artefacts from a number of prehistoric sites in Macedonia 22
3.2.1 XRF analyses of iron ores from Thasos 75
3.2.2 Analysis of undressed Thasos Ti-rich iron sands 80
3.2.3 AA analysis of magnetically separated iron sands 80
3.2.4 Microprobe analysis of iron sands from Thasos 82
3.2.5 Analysis of Ni-rich laterites 86
3.3.1 Microprobe analysis of copper and iron slag from Kastri and Palaiokastro 89
3.3.2 Analysis of metallic prills in copper slag from Kastri and Palaiokastro 90
3.3.3 Summary of differences between Kastri and Palaiokastro slags 100
3.5.1 XRF analyses of slag from N. Greece, Knossos and Athens 129
3.5.2 Microprobe analysis of iron slag from Macedonia 130
3.5.3 Iron artefacts from Kavala and Thasos Museums 139
3.5.4 Analyses of slag inclusions in artefacts from Kavala and Thasos Museums 141
3.5.5 Iron artefacts from Thessaloniki Museum 142
3.5.6 Analysis of slag inclusions in iron objects from Vergina 143
3.5.7 Analysis and metallography of objects from Petres 155
3.5.8 Analysis of slag inclusions in objects from Petres 144
3.6.1 XRF analysis of slag from Thasos 162
3.6.2 AA analysis of slag from Katafyto 162
3.6.3 Microprobe analysis of Ti-rich iron slags from Thasos 165
3.6.4 Analysis of Ti-rich iron slags, EM Mainland 168
3.6.4a (extracted from Tables 3.6.3 and 3.6.4) 171
3.6.5 Iron slags fro. various locations in Greece 174

3.6.6 Ti and V contents in artefacts 177
3.7.1 Analysis of silicate phases in Palaia Kavala slag 193
3.7.2 Analysis of metallic phases in speiss 194
3.7.2a (extracted from Table 3.7.2) 196
3.7.3 AA analysis of gold/silver in speiss and slag 197
3.7.4 Analysis of Petropigi slag 198
3.7.5 Analysis of Palaia Kavala ores 200
3.7.6 Analysis of cannon shot from Lekani 201
3.7.7 Anaysis of silicate and metallic phases in experimental slag and bloom 202
3.7.8 Summary of experimental results 203
3.8.1 Analysis of metallic prill in Petres slag and bloom 218
3.8.2 Analysis of silicate phases in Petres slag 219
3.8.3 Nickel distribution in the bloom of various smelts 223
3.8.4 Size and Ni content of Ni-rich prills 224
3.8.5 Analysis of silicate phases in experimental slag 225
3.8.5a (extracted from Table 3.8.5) 224
3.8.6 Analysis of metallic phases in experimental slag and bloom 227
3.8.7 Silicate phases in experimental smithing slag 231
3.8.7a (extracted from Table 3.8.7) 230
3.8.8 Metallic phases in smithed blooms 232
3.8.9 Effect of nickel impurities in iron on diffusion times 234
3.8.10 Analysis of Canyon Diablo Meteorite 242
4.1 Outline of experimental melting procedure 269
4.2 Analysis of products of experimental melting of cast iron 270
4.3 Composition of iron bar from Saugus,USA 272

List of Figures

Fig. 1.1 Map of Northern Greece 10
1.2 Map of Thasos showing the main ferrous and non-ferrous mineral deposits 11
2.1 Map of prehistoric sites in Macedonia with occurrence ofgold, copper/bronze and iron 14
2.2 Gold occurrences and sites of 'ancient' mines in Macedonia 16
2.3 Map of Greece with prehistoric and Classical sites 30
2.4 Map of some sites and regions in Asia Minor 35
2.5 Map of prehistoric and Ottoman sites in the Balkans 39
2.6 Map of Archaic, Classical,

Hellenistic and Roman sites in Macedonia 46
3.1.1 Sites in Macedonia sampled for ore, slag and artefacts 60
3.1.2 Sites on Thasos sampled for slag, ore and artefacts 63
3.2.1 Geological map of Macedonia 70
3.2.2 Geological map of East Macedonia 72
3.2.3 $FeO-TiO_2-Fe_2O_3$ ternary phase diagram 81
3.2.4 Map of lateritic deposits in Greece 85
3.3.1 Ellingham diagram for Cu_2S and CuS 100
3.3.2 Map of Euboea 35
3.4.1 Experimental furnace at Ashdown Forest and furnace reactions 105
3.4.2 Map of bloomery installations at Pippingford, Ashdown Forest 107
3.4.3 Flowchart of smelting furnace and smithing hearth products and waste 113
3.5.1 $CaO.SiO_2$-anorthite-FeO phase diagram 131
3.5.2 Plan of Petres, WM 133
3.6.1a,b,c Drawings of slags 160
3.6.2 Distribution of Ti-rich slag types 161
3.6.3 $FeO-TiO_2$ binary phase diagram 164
3.6.4a,b TiO_2 contents in wustite and matrix 175
3.6.5a,b V_2O_5 contents in wustite and matrix 176 176
3.6.6 TiO_2 vs. MnO contents in slags and artefacts 178
3.6.7 MnO vs. P_2O_5 contents in slags and artefacts 180
3.6.8 Samokovo forge 183
3.7.1 Fe-As binary phase diagram 195
3.7.2 Flowchart of precious metals extraction in Palaia Kavala 206
3.7.3 Schematic illustration of experimental furnaceand hypothetical Palaia Kavala furnace 207
3.8.1 Nickel distribution in experimental blooms and Petro 6 222
3.8.2 Nickel distribution in smithed blooms 229
3.8.3 Plot of diffusivity as a function of temperature 235
3.8.4 Ni-Fe binary phase diagram 244
4.1 Compilation of furnace illustrations on vases 254
4.2 Finery hearth 262
4.3 $Fe-Fe_3C$ phase diagram 262
4.4 Furnace and bellows arrangement during iron melting experiment 267

Plates 1-26

CHAPTER 1

INTRODUCTION

1.1 Scope and aims

Recent years have seen an awakening of interest in archaeo-metallurgical studies on Greek material both in Greece and abroad. The investigation of ancient metals technology, whether artefacts or processes, almost invariably requires the close collaboration of scientists and archaeologists. In Greece, this type of collaboration has largely born fruit in the field of artefact analyses (Filippakis et al 1983; Jones 1980) and in mining and extraction of precious and non-ferrous base metals, like copper and lead. The outcome of this inter-disciplinary effort includes the discovery of ancient mines like the gold mine at Kinira on Thasos (Fig. 1.2), first reported by Herodotus (Wagner et al 1981), the ochre mine at Tzines also on Thasos (Fig. 1.2) (Koukouli-Chrysanthaki and Weisgerber 1982), the silver mines at Laurion in Attica (Fig. 2.3) (Conofagos 1980), the location and characterisation of metal-processing sites on Thasos (Pernicka et al 1980), Siphnos and Kythnos in the Cyclades (Gale and Stos-Gale 1984; Gale et al 1985), Nikisiani in the Pangaion (Papastamataki 1986a; 1986b) and finally the ore-dressing facilities at Laurion (Conofagos 1980; Jones 1982, 1984). The archaeological and analytical data led to the elucidation, on the one hand, of questions relating to mining and smelting practices in antiquity and later periods and, on the other, of the provenance of

lead/silver and copper artefacts on the basis of lead isotope analysis. This last project which spans a large section of the Eastern Mediterranean has helped in the identification of mints, like that on Thasos (Gale et al 1980), and has shed considerable light on the patterns of the metals trade during the Bronze Age (Gale and Stos-Gale 1982).

In the field of iron metallurgy, studies have mainly focused on the examination of artefacts rather than processes. These studies have been inspired primarily by industrial metallurgists whose interest in ancient Greek history prompted them to examine the artefacts themselves in search of evidence that would complement or elucidate the relevant references in the classical texts or, even better, provide new interpretations (Conofagos 1981a, 1981b; Richardson 1934; Varoufakis 1979; Livadefs 1956; Piaskowski 1982). Besides discussing manufacturing techniques (for instance, decarburisation and quenching), most of these researchers were intent on providing a wider view of the state of ancient iron technology. They drew conclusions on aspects of ore and metals processing, despite the relative lack of data on metallurgical waste (slag, furnace remains), data which in any case is mostly of recent date (Davies 1926; Rostocker and Gebhard 1981; Backe-Forsberg and Risberg 1985; Photos et al 1985;). As a result, evidence for ore mining, dressing and extraction has been at best sparse, since most of the analysed metallurgical waste was associated with smithing/forging activities. The writer is keenly aware of the importance of characterisation and elucidation of the extractive processes in early Greek metallurgy. It was partly to

redress the balance in their favour that this thesis was written.

The region under investigation in this work is northern Greece and particularly Macedonia, the richest region of the country in minerals and metalliferous ores (Fig 1.1). Macedonia is the sector of a historically larger geographical unit, politically divided today between Albania, Yugoslavia, Bulgaria and Greece (Hammond 1972; 1979). Its cultural tradition, at least as far as the history of the Greek people is concerned, is irrevocably associated with Philip II, Alexander the Great and their successors, the Macedonian kings of the Hellenistic period. Macedonia's unique position at the crossroads between the Balkans, Asia Minor and the Aegean makes it especially interesting in the study of the development of metallurgical technology. The province is broadly divided into three regions: Western Macedonia (WM) stretching from the Albanian borders to the River Axios, Central Macedonia (CM), the area between the Rivers Axios and Strymon and Eastern Macedonia (EM), the area between the Rivers Strymon and Nestos (Fig 1.1).

In Macedonia, there are archaeological indications of indigeneous metals production spanning a period of nearly sixty five centuries from the Late Neolithic (second half of the fifth millennium BC), during which there is the first evidence for gold and copper working, to the turn of this century. Thus, Macedonia with its rich minerals deposits presents a unique opportunity for a diachronic study of iron ore exploitation and extraction and metals processing from the Early Iron Age (10th c. BC) onwards.

The term 'early' in the title of this thesis has been used in

a broad sense. In as far as the absence of any iron furnace remains in Macedonia can allow one to draw relevant conclusions, 'early' relates to bloomery iron making. This, it appears, was until the Middle Ages the only method the West knew of producing wrought iron (that is, iron containing 0.02% carbon) by the direct reduction of iron ores. The blast furnace with its production of cast iron (2-4% carbon, with silicon, manganese and other impurities) which had to be decarburised to malleable wrought iron, gradually substituted but did not completely replace the bloomery. Although there were a number of modifications in scale, fuel and the method of driving the bellows, bloomery iron-making continued until the end of the last century in many parts of the world. Therefore, given the conservative nature of iron technology in Western Europe, it was not imperative to study the metallurgical remains of only one period in Macedonia (in any case, the data would not have been sufficient), but rather to investigate as much of the material evidence at hand as possible.

In this work, a unified approach to the study of extraction metallurgy in Macedonia is applied. This approach involves the collation of all information relating to the metallurgical remains in the region. This includes the knowledge of the minerals resources of the area and the historical/literary descriptions, when available, as well as the scientific examination of the archaeological finds (metallurgical waste and artefacts). This corpus of data needs to be put into an archaeometallurgical perspective which is provided by carrying out a set of experimental smeltings and smithings in the field. These experimental

simulations do not attempt to be an accurate reproduction of the ancient processes but rather to serve as the testing ground for a number of hypotheses put forward by the archaeological and analytical data. The author is certainly aware that a hypothesis cannot be tested unless the experimental conditions which are set to test it can be adequately controlled and monitored. However, all bloomeries, wherever and whenever they operated, surely relied primarily on experience gained from trial and error. Despite this accumulated experience, the low yields are inherent in this process, a fact which eventually forced smelters to devise alternative paths to wrought iron production. The metallurgical waste in archaeological sites is the cumulative result of many intermediary stages in the process over a number of successful and failed runs. It was in an attempt to elucidate the waste and metal produced at each step that these experimental smelts were undertaken. Although presentation of the procedural details of these experimental smelts is confined in this thesis mostly to appendices to avoid a break in continuity, the experiments have formed the backbone of this work and the basis on which a number of interpretations have been formulated.

1.2 Thesis outline and methodology

In this thesis, a considerable number of topics are discussed, which have arisen from the analytical examination of both archaeological material and experimental results. To cover most of them in detail would far exceed the time limits allocated for this work. On the other hand, to mention them only in passing

would not have given a satisfactory picture of the extreme richness of extractive processes practised in Macedonia throughout its long history. It would not be an exaggeration to say that Macedonia offers a microcosm of most of the archaeometallurgical problems encountered anywhere in the world.

Extractive metallurgy can be investigated through slag and metal analysis. The main analytical tool has been the Electron Microprobe (EPMA) (Cambridge Scientific Instruments Mark V with an EDAX Link 860 x-ray microanalyser) at University College, London, Geology Department. Other analytical techniques, such as X-ray Fluorescence spectrometry (XRF), Atomic Absorption spectrometry (AA) and X-ray Diffraction (XRD), were used and are listed when appropriate. Microprobe analysis provides a unique tool in the examination of mineralogical phases in slag (archaeological or experimental) and metallic or silicate inclusions in metal to determine furnace charge composition, slag mineralogy and temperature and operating conditions. Apart from technology-related issues, this information is essential when attempting to establish the provenance of the ore source, not necessarily in terms of its geographical location but of its typology (eg. phosphorus-rich or manganese-rich iron ores). This line of investigation is possible through the analyses of slag inclusions in iron artefacts.

The thesis is divided into three main parts. The first (Chapter 2) provides a survey of all the existing analytical work on metal objects from Macedonia. It also puts Macedonian metallurgy into a perspective in relation to its neighbours, Asia Minor, the

Balkans and the rest of Greece. This perspective is necessary in examining the question of the diffusion versus independent development of iron technology in Macedonia in the critical period at the end of the Late Bronze Age and the beginning of the Early Iron Age. The question is directly related to the understanding of the development of copper metallurgy in Macedonia in the preceding two millennia, from the Late Neolithic to the Late Bronze Age. Unfortunately, the archaeological and analytical data on copper/bronze objects from Macedonia is minimal compared to that from the rest of Greece for the same period.

The second part (Chapter 3) presents the analytical results from the examination of archaeological slag and artefacts, as well as the results of the experimental smelts. A comparison between the two corpora of data follows. A section is devoted to the description of the experimental field smelts which have taken place at Ashdown Forest, Sussex. The analytical results for slags and artefacts in Chapter 3 are grouped according to the ore type that produced them. Titanium-rich iron slags from Eastern Macedonia (EM) are discussed in the context of the analysis of titanium-rich iron sands that produced them and in conjunction with the experimental smeltings of the same iron sands. Nickel-rich iron slags and 'bloom' from Western Macedonia (WM) are discussed in the context of experimentally smelted nickel-rich iron laterites and smithed nickel-rich iron blooms. Finally, arsenic-rich iron (speiss), in association with manganese-rich slag found in the region of Palaia Kavala in Eastern Macedonia, are discussed again in the context of the experimental smeltings of arsenic-rich iron

ores from the same region. These last smeltings showed very clearly that at least in recent periods the division between ferrous and non-ferrous extraction metallurgy imposed on the analytical investigation of archaeometallurgical remains, breaks down and that ores were used for more than one economically viable metal.

Archaeological artefacts from various museums in Macedonia have been examined for both their slag inclusions (by EPMA) and metal (metallography). An attempt is made to determine the type of ore source for the manufacturing of some of these objects and thus establish the earliest exploitation of a number of iron ore deposits in Macedonia.

All the remains mentioned above will be presented and discussed in the absence of evidence for archaeological iron-making furnaces. Although a number of furnaces involved in non-ferrous extraction processes have recently been reported by some investigators (Papastamaki 1986a; Conofagos 1980), none has been studied in detail. The only documentary evidence of furnaces exist in the illustrations of metallurgical activities depicted on Black and Red Figure vase paintings of the 6th and 5th centuries BC. Our own experimental furnace was built on this model. There is a substantial literature reviewed in the third part of this work (Chapter 4) about the nature of the metallurgical processes depicted on the vases. Furthermore, a new interpretation is put forward based on a reexamination of the classical texts and the results of our smelting and preliminary iron-melting experiments. It is suggested that these furnaces were used in 'steel fining', a

process by which steel for armoury and weapons was produced uniformly by the decarburisation of high carbon iron rather than the carburisation of wrought iron. Ethnographic parallels from China in the last century corroborate the suggested interpretation. Although the Attic vases can scarcely claim a direct Macedonian connection, the furnaces they illustrate seem to be pioneering in their function.

The last Chapter (5) draws together all the conclusions derived from the study of early extractive iron metallurgy in Northern Greece. It proceeds to suggest directions for future research both in aspects of Greek iron metallurgy as well as in archaeometallurgical problems that transgress regional boundaries and seem pertinent to the fundamentals of the field as a whole.

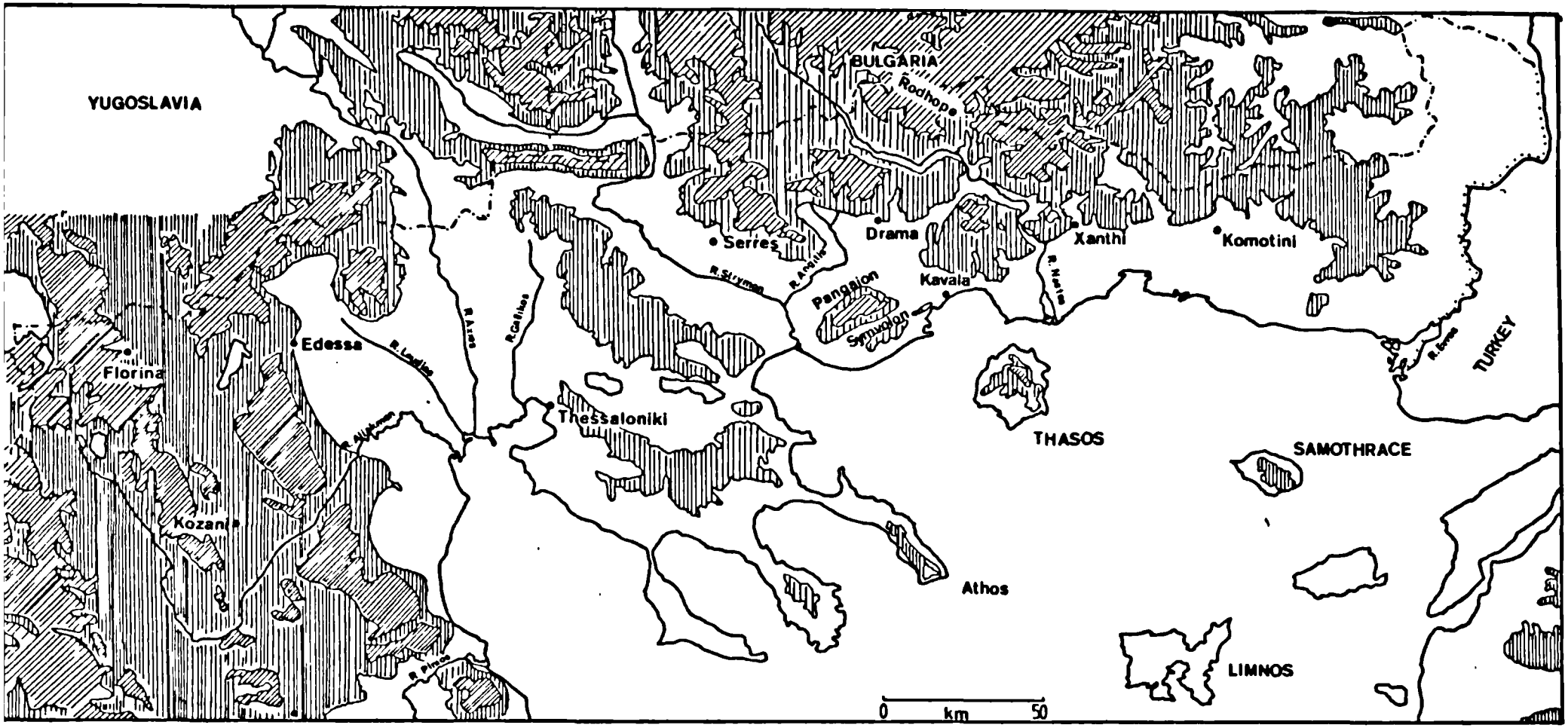

Fig. 1.1 Relief map of Northern Greece (after Naval Intelligence: Greece III, Fig. 22). Contours at 400 |||| and 1000 m ////.

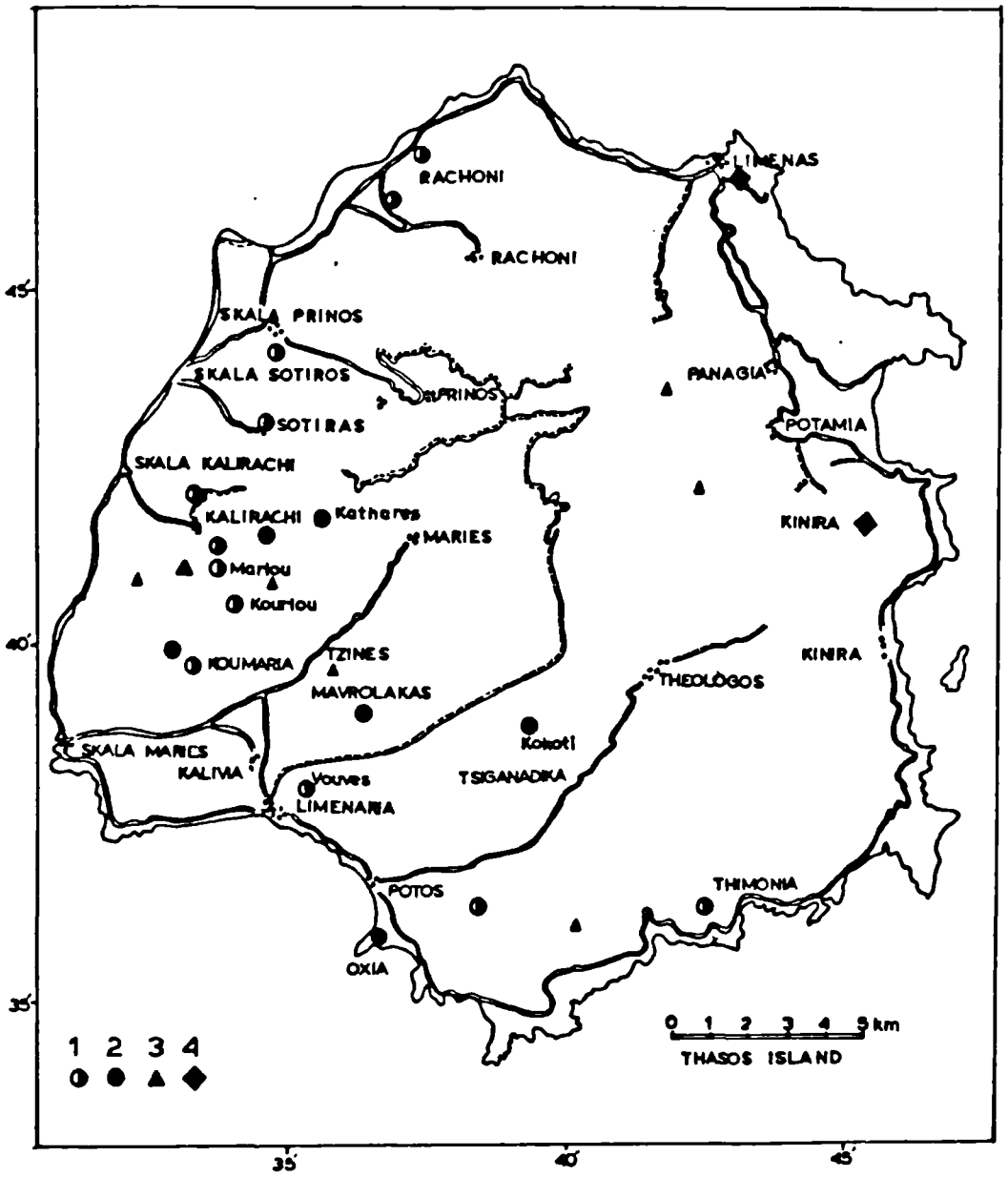

(1) Pb-Zn , (2) Fe-Mn , (3) Cu-Ond , (4) Au-Mines .

Fig. 1.2 Map of Thasos showing the main ferrous and non-ferrous mineral deposits (after Pernicka et al 1980)

CHAPTER TWO

SCIENTIFIC ANALYSES AND THE HISTORICAL BACKGROUND TO METALS PRODUCTION IN MACEDONIA: NEOLITHIC TO OTTOMAN

2.1 Macedonia: From the gold and copper of the Neolithic to the iron of the Early Iron Age

Evidence for metal working in Macedonia begins in the Late Neolithic (LN), (for dates, in calendar years, see appendix 2.1). Settlements like Sitagroi and Dikili Tash in the plain of Drama and Demetra on the River Angitis (Fig. 2.1) were situated well within the metalliferous regions of E. Macedonia and thus within access of the potentially exploitable mineral resources. Although it is very likely that during that early period gold would have been obtained as nuggets from the auriferous beds of the main Macedonian rivers and their tributaries (Davies 1935, 232), it is not easy to assess the early sources of copper. It is currently speculated that copper technology reached Sitagroi, one of the earliest sites with copper artefacts, from the north, namely the Balkans (Renfrew et al 1986, 482).

This section discusses the development in the working of gold, copper/bronze and iron in Macedonia, as can be deduced from the results of analytical studies carried out on metallic artefacts, slag and ores by previous investigators working in the area. The period from the LN to the Early Iron Age (EIA) is described in some detail, since it is during the Late Bronze Age

(LBA) that iron first appears in Macedonia (Davies 1926, 197) in the form of slag. Table 2.1 lists the published gold, copper/bronze and iron objects excavated at various prehistoric sites in Macedonia shown in Fig. 2.1. The objects date to the LN, Early, Middle and Late Bronze Age (EBA, MBA and LBA) and the EIA.

2.1.a Gold

Gold must have been among the first metals to be worked in Macedonia. Its lustre, malleab i lity and accessibility as placer deposits (concentrations of sedimentary origin) in the many river beds in Central and Eastern Macedonia should have attracted the attention of LN inhabitants. Apart from placer deposits, gold in Macedonia occurs in quartz veins (reef gold) and in the Cu-Pb-Zn pyrite mineralization. Fig. 2.2, adapted from Mack (1983), gives a synoptic map of different deposits and the location of ancient mines, caution being applied here to the term 'ancient'. Given the variety of gold sources, it is reasonable to assume that different deposits were exploited at different periods. However, there can be little doubt about the Gallikos river and the Nigrita occurrences, the latter currently being exploited (Mack 1983; Mastoris et al 1979).

The repertory of excavated gold objects in Macedonia is limited (beads, pendants) in comparison with the impressive, contemporary material further north, as for example at the cemetery at Varna (Fig 2.5) in Bulgaria (Ivanov 1978). Evidence for the earliest appearance of gold in Macedonia is dated to the LN levels

Fig. 2.1 Map of prehistoric sites in Macedonia with gold, copper/bronze and iron artefacts.

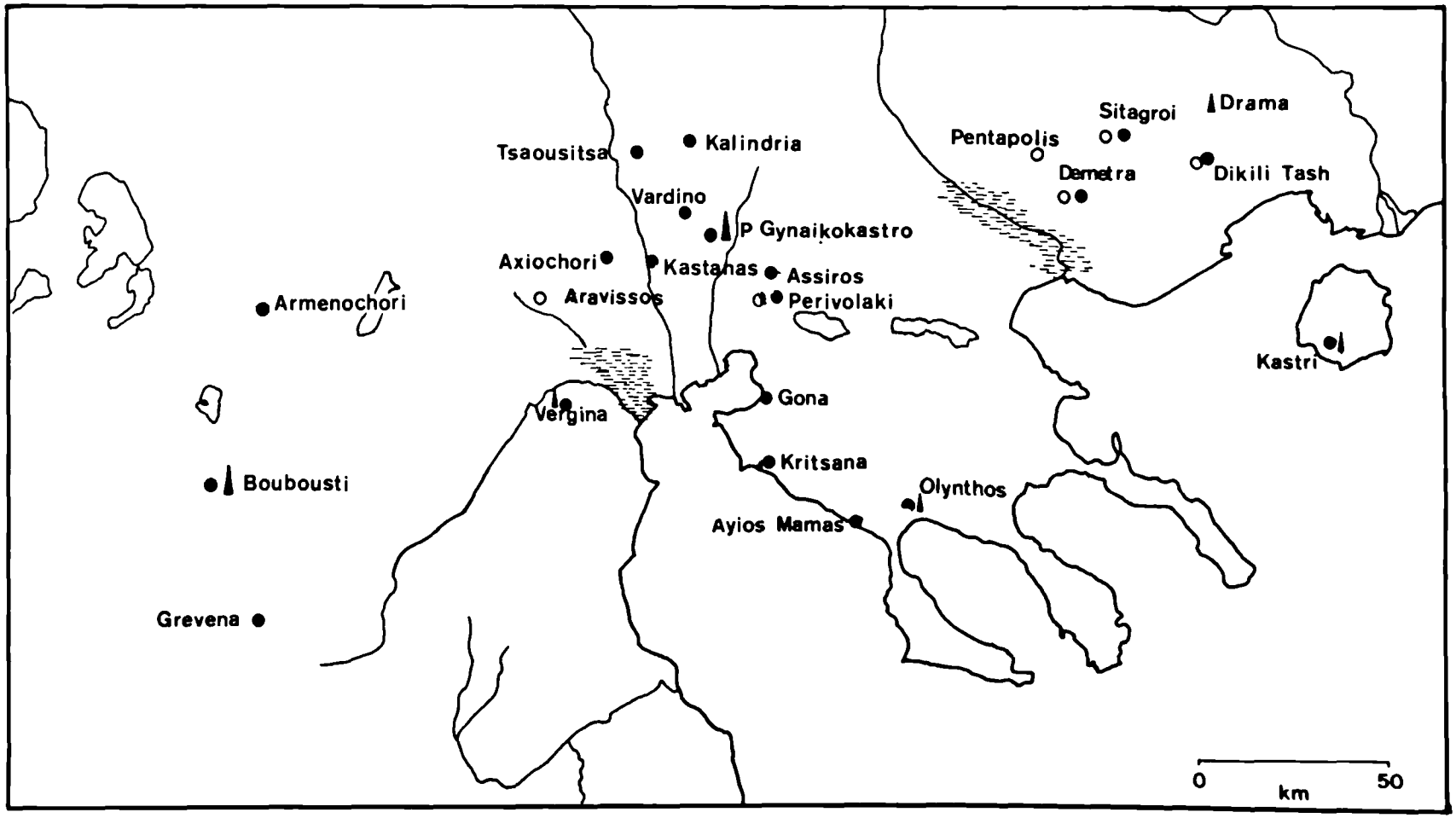
Tsaousitsa
Kalindria
Vardino
P Gynaikokastro
Axiochori
Kastanas
Assiros
Aravissos
Perivolaki
Armenochori
Vergina
Gona
Kritsana
Boubousti
Olynthos
Ayios Mamas
Grevena
Sitagroi
Drama
Pentapolis
Demetra
Dikili Tash
Kastri
0
km
50
Au
Cu
Fe
Bronze

Table 2.1: Catalogue of published gold, copper, bronze and iron objects from Macedonia (LN - EIA)

Site	Metal	Type of object
1. LN - EBA		
Vardino[1]	Cu	pin
Saratse[1] (Perivolaki)	Au	hair pin
"	Cu-As	blade
Kritsana[1]	Cu	pin
Vardaroftsa[1] (Axiohori)	Cu	pin
Sitagroi[3]	Cu, Cu-Sn	beads, pins, awls, hooks,frags.
"	Au	bead
Dikili-Tash[4]	Cu, Cu-Sn	pins,knife
Kastri[8]	Cu, Cu-Sn	pins
Demetra[2]	Cu	beads, foil
"	Au	bead, hook
Aravissos[2]	Au	foils, pendant, bead (or ring
Pentapolis	Au	
2. MBA		
Kalindria[1]	Cu-Sn	blade, disc
"	Au	disc
Gona[1]	Cu-Sn	axe
Vardaroftsa[1]	Cu-Sn	blade
3. LBA		
Vardino[1]	Cu-Sn	fibula, spearhead
Kalindria[1]	Cu-Sn	axe, sickle
Grevena[1]	Cu-Sn	sword
Bouboustí[1]	Cu-Sn	pin
Assiros[5]	Cu-Sn	beads, spiral,coil needle
Kastanas[9]	Cu-Sn	knife,other
Vardaroftsa[1]	Cu-Sn	blade
Kastri[8]	Cu-Sn	weapons,jewellery
4. EIA		
Pateli[1]	Cu-Sn	fibulas (plate, spectacle), horse
Vardaroftsa[1]	Cu-Sn	tweezer frag.
"	Fe	socketed spearhead
Bouboustí[1]	Fe	socketed spearhead
P. Gynaikokastro[6]	Cu-Sn,Fe	weapons,jewellery
Vergina[7]	Cu-Sn	swords. dress pins, fibulas
"	Fe	swords, spearheads, daggers, knives, dress pins, fibulas, arrowheads
Kastri[8]	Fe	knives
Drama[10]	Fe	jewellery,knives,swords

1 Heurtley (1939), Fig. 67 (EBA), Fig. 83 (MBA), Fig. 104 (LBA), Fig. 112 (EIA)
2 Grammenos (1984) 148
3 Table 2.2
4 H. Koukouli-Chrysanthaki, pers. comm.
5 Wardle (1980,260).
6 Th. Savopoulou, pers. comm.
7 Andronikos (1969).
8 Koukouli-Chrysanthaki (1986,appendices VI-VIII)
9 Hanzel (1980)
10 Koukouli-Chrysanthaki (1979,BII)

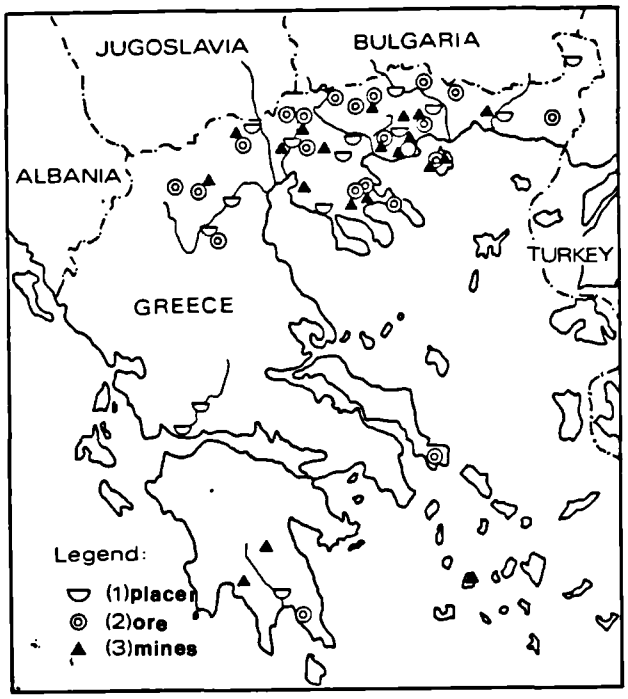

Fig. 2.2 Map of gold occurrences and 'ancient' mines in Greece (after Mack 1983)

(phase III; see appendix 2.1 for dates) at Sitagroi (Renfrew 1979, 360) and Dikili Tash (Theoharis and Romiopoulou 1961), LN levels at Demetra (Grammenos 1984, 149), Aravissos (Grammenos 1984,148) and EBA Saratse (Perivolaki) (Heurtley 1939, fig. 67) (Fig. 2.1 and Table 2.1). The typology of the gold objects ranges from small beads (Sitagroi, Dikili Tash, Demetra), a hook (Demetra), to foils and pendants (Aravissos). The Aravissos material is the richest (Grammenos 1984, fig 56.1-6); the foils are flat, elliptically shaped with one or two holes at the two ends of the ellipse. This typology finds similarities in the Balkans, particularly among the treasures at the cemetery at Varna (Ivanov 1978, fig. 17, 100) as well as to the south at Mochlos in E. Crete (Branigan 1974, pl 20; 2145, dating to Early Minoan II). In Thessaly, two gold pendants have been found, one of them in a LN level at Sesklo (Tsountas 1908, fig 291). Both bear close resemblance to the Aravissos

pendants.

The only two analysed gold objects are those from Demetra (Grammenos 1984, 149) which were examined non-destructively and semiquantitatively by PIXE (proton induced X-ray emission spectroscopy) (E. Mirtsou, pers. comm.). They were cold hammered and consisted of nine parts of gold to one part of silver. Traces of copper and iron were also recorded, but the full compositions were not given. The investigators suggested that auriferous ores in the Pangaion (Fig. 1.1), known from classical antiquity as a source of precious metals, could not be ruled out as the origin of this gold. Since no gold was found in the river sediments around Mount Pangaion, an alternative and more likely source would be the gold placer deposits of the Rivers Loudias and Angitis, in view of the proximity of Demetra to the former and Aravissos to the latter. The Rivers Loudias and Strymon were at the time mostly marshland (Fig. 2.1).

Slag with small quantities of iron oxide and gold from Saratse (Perivolaki) and Vardaroftsa (Axiochori) was analysed and identified as gold slag by Davies (1926, 197). He suggested that it was the product of melting of gold nuggets, but the presence of iron is puzzling since no iron flux is needed to melt gold. It is possible that the 'slag' was weathered pyrite in which gold can often be found (MacDonald 1983, 31). Davies does not give any analyses, and so it is difficult to be certain of the exact identity of this material.

In summary, the Macedonian gold objects dating primarily to

the Late Neolithic have typological parallels in both the north (Balkans) and the south (Central Greece). Since the shapes of these objects are very simple, namely gold foils hammered in elliptical or round forms, and there is no firm evidence that most of the main river beds were not auriferous, it may be safe to assume that Macedonia developed an early, independent gold-working technology from the LN period by shaping and possibly melting gold nuggets.

2.1.b Copper/Bronze

Copper objects appear in a LN context in Mainland Greece in a number of places, a comprehensive list of which is given by McGeehan-Lyritzis (1983) and more recently McGeehan-Lyritzis and Gale (forthcoming). There is a vast corpus of analytical data on arsenical and tin bronzes from the Bronze Age and the Geometric period in Mainland Greece, the Cyclades and Crete, carried out by a number of investigators on material in Greece and in museums abroad. These need not be discussed here, but the reader can refer to a number of publications (in particular, Junghans et al 1960, 1968; Craddock 1976, 1977; Filippakis et al 1983; Gale et al 1985) depending on the area and period of interest.

The earliest analysed copper and bronze objects in Macedonia are from Sitagroi. They are reproduced here with the kind permission of the investigator, Dr E. Slater (Table 2.2). The finds include small pins, hooks, awls, nails, beads and fragmentary pieces. The objects are made of unalloyed copper, at least in the early phases of the settlement, and the presence of impurities

Date Phase	Type	Cu	Sn	Pb	Ag	Sb	S	Si	Fe	Zn	As
II	frag.	90.80	nd	0.40	0.41	nd	nd	nd	0.02	nd	nd
III	frag.	93.20	nd	nd	nd	nd	nd	nd	nd	0.04	nd
	piece	92.39	0.07	nd	nd	nd	nd	nd	nd	nd	nd
	bead	97.50	0.32	0.01	nd	nd	0.06	nd	nd	0.14	nd
	pin	92.00	nd	nd	0.05	nd	nd	3.00	nd	nd	nd
	bead	98.70	nd	0.44	nd	nd	nd	nd	nd	nd	0.28
	piece	94.80	0.82	nd	nd	nd	nd	nd	0.00	0.03	nd
	piece	96.10	0.21	nd	nd	nd	0.01	nd	nd	nd	
	pin	94.40	0.56	nd	0.43	nd	nd	0.08	nd	0.05	0.69
IV	pin	96.05	0.69	nd	nd	0.48	nd	nd	nd	0.09	0.36
	piece	93.20	3.20	2.10	nd	nd	nd	nd	nd	0.40	nd
	bead	62.40	nd	nd	nd	nd	nd	nd	0.21	nd	0.10
	piece	89.55	5.90	4.05	nd	nd	nd	nd	0.06	nd	nd
	piece	96.20	0.12	2.40	nd	nd	nd	nd	nd	0.02	0.40
V	tube	52.00	nd	0.21	nd	nd	nd	nd	0.01	nd	0.31
	pin	97.80	nd	nd	nd	nd	nd	nd	0.02	nd	nd
	hook	97.00	nd	1.39	nd	nd	0.01	nd	nd	nd	1.40
	piece	99.20	nd	0.64	nd	nd	nd	nd	nd	nd	0.05
	frag.	93.20	3.42	0.03	0.13	nd	nd	nd	nd	0.00	nd
	awl	90.30	nd	4.31	0.02	nd	nd	nd	0.65	nd	2.25
	pin	91.20	0.90	nd	nd	nd	0.06	nd	nd	2.34	nd
	awl	92.80	nd	1.78	3.89	nd	nd	nd	0.50	nd	3.89
	piece	94.90	0.01	3.75	nd		nd	nd	nd	nd	nd
	awl	88.40	0.74	6.12	nd	nd	nd	nd	nd	0.16	0.81
	piece	72.30	8.14	0.29	nd	nd	0.42	3.60	nd	0.05	nd
	nail	89.50	0.56		1.45	nd	0.43	0.24	nd	nd	0.72

Table 2.2: Analysis of copper/bronze artefacts from Sitagroi (after E. Slater, pers. comm.)

suggests that the copper was smelted. More specifically, there is no evidence for metal working in Phase I, there is one object from Phase II, eight from Phase III (Table 2.2). It is in Phase IV that bronze artefacts appear for the first time with appreciable tin and lead contents. On the other hand, arsenical coppers with some lead appear later in Phase V or the EBA period. Copper and bronze artefacts were either cast or cold-worked/annealed (E. Slater, pers. comm.). Slag as well as crucible fragments were found in a level dating to Phase II, but it was difficult to conclude whether the slag originated from a smelting or melting operation (McGeehan-Lyritzis and Gale, forthcoming). In carrying out lead isotope analysis, McGeehan-Lyritzis and Gale identified a new source or sources for the copper found at Sitagroi and Late Neolithic sites in Thessaly which could be local or lie to the North. I am indebted to Dr Gale for this information. An in-depth treatment of the Sitagroi metal and slag is due to appear soon in the second volume of the Excavations at Sitagroi.

Most of the objects from LN levels at Dikili Tash were copper with the exception of three tin bronzes (H. Koukouli-Chrysanthaki, pers. comm.). The copper objects were free of impurities, in contrast to the objects from Sitagroi, suggesting the possible use of native copper.

Analyses of objects from LN-EBA Kastri on Thasos, undertaken independently by N.H. Gale and K. Assimenos showed that they were copper (H. Koukouli-Chrysanthaki, pers. comm.) with only few impurities.

In his important survey of prehistoric Macedonia, Heurtley produced a list of bronze analyses carried out by O. Davies and included them as an appendix in the original publication (Heurtley 1939, 254). Table 2.3 gives an adapted version of the data presented in that report as well as an earlier one (Davies 1926). Most of the analyses are semiquantitative, and the objects date from the EBA to the EIA.

The objects from Vardaroftsa (pins and two blades) are interesting because of the unusual combination of their alloying constituents. Two of the objects are tin bronzes (Vard.MBAa and Vard LBA) with high bismuth and nickel contents, while the other two (Vard EBA and Vard MBAb) are even more peculiar combinations of practically every metallic element known! The poor state of preservation of the objects may be partly responsible for the anomalous contents of many elements present. Craddock (1976, 96) attributed the high iron and nickel contents of Vard EBA and MBAb to soil contamination. However, there are clear indications that iron is associated with nickel, at least in the iron ores of W. Macedonia (see section 3.8) and a nickel-rich iron prill was found in slag from Vardaroftsa (see section 3.5). Since iron is often present in copper, nickel would also be expected to be detected in copper associated with iron from these ores.

Two of the objects from Saratse (Sara EBAa and Sara LBA, Table 2.3) were found to be arsenical bronzes with or without tin. The other two objects (Sara EBAb and Sara MBA) might be classed as iron, since it is the only element recorded in appreciable amount, but the date is too early for iron objects. The objects from Gona,

Site/Date	Cu	Sn	Pb	Zn	Bi	Sb	Fe	Ni	As	Ag	Co	Au	S
Vard.EBA	46.27	22.28	13.91	tr	0.89	5.80	3.98	7.09	0.00	0.00	0.00	0.00	0.00
Vard.MBAa	86.26	3.37	0.00	0.00	1.38	0.00	0.82	tr	0.00	0.00	0.00	0.00	0.00
Vard.MBAb	25.94	25.52	0.79	tr	0.00	3.54	11.93	6.49	0.00	0.00	0.00	0.00	0.00
Vard.LBA	78.96	2.14	tr	1.98	3.09	0.40	0.94	1.07	0.00	0.00	0.00	0.00	0.00
Sara.EBAa	92.43	0.09	1.49	0.03	0.00	0.00	0.06	0.00	5.88	0.00	0.02	0.00	0.00
Sara.EBAb	l	s	l	s	tr	tr	m	0.00	l	tr	tr	0.00	0.00
Sara.MBA	s	s	tr	tr	tr	tr	m	tr	tr	0.00	tr	.00	tr
Sara.LBA	74.88	5.07	tr	0.00	0.14	0.11	0.05	tr	2.10	0.00	0.18	0.00	0.00
Gona.MBA	96.00												
Gona.LBA	63.11	2.37	tr	0.00	0.00	1.15	0.07	1.11	0.03	0.00	0.00	0.00	0.00
Krit.EBA	81.79	tr	0.00	0.00	0.06	0.23	0.37	0.00	0.00	0.00	0.00	0.00	0.00
HagMam.LB	m	s	s	tr	.00	.00	.00	.00	tr	.00	tr	.00	tr
Tsaou.IA	74.71	6.79	0.08	0.00	0.00	1.38	0.37	0.00	tr	0.00	0.00	0.00	0.00

m=much
s=some
tr=trace
l=little

Table 2.3: Analyses of copper/bronze artefacts from a number of prehistoric sites in Macedonia (adapted from Davies (1926) and Heurtley (1939, 254)

Kritsana (Krit), Ayios Mamas and Tsaouchitsa (Tsaou) are made either of copper or tin bronze (Table 2.3).

From Servia two copper objects, an amorphous lump of copper (93% Cu, 3% As, 4% Fe) and a needle (95% Cu, 1% As, 4% Fe) have been analysed non-destructively with XRF by R.E. Jones (Ridley and Wardle 1979, 229). The main feature of their compositions is the presence of iron. Iron in copper, a common enough occurrence in Bronze Age artefacts from a number of sites in the East Mediterranean (Cooke and Aschenbrenner 1975), exists as dendrites of iron in a matrix of copper or as a solid solution with copper. The subject is still a matter of ongoing research.

The problem of differentiating between objects produced from native copper and from smelted carbonate ores has been treated by Maddin et al (1980) who concluded that the distinction between worked native copper and that produced from smelted and refined copper that has been worked and annealed is very difficult to make on both chemical and metallographic grounds. Oxhide ingots, for instance, found in Sardinia, known to have been produced from smelted ores, had a purity of 99.7% (Balmuth and Tylecote 1976), suggesting a very efficient refining stage. It is clear from Tables 2.2 and 2.3 that no refining stage intervened between the smelting of the ore and the casting or working of the object.

Native copper may have been available at only a few, if any, of the early settlement sites in Macedonia. The copper ores in the Chalcolithic mines of Aibunar and Rudna Glava in Bulgaria and

Serbia respectively were copper carbonate ores (see section 2.3). Oxide copper ores, albeit of high purity, can be smelted in a small furnace or a crucible at a relatively low temperature and not very reducing conditions (Tylecote 1974). If the first copper ores to be attempted to be smelted in Macedonia were sulfides, (as the sulfur content of some Sitagroi material suggests) their smelting and refining would have required a long period of experimentation compared with carbonates. This may partly explain the belated introduction of copper to Macedonia at least in comparison to the Balkans where both the quantity and variety in typology of the material is impressive.

To summarise, in reexamining Davies's analyses of early bronze objects from Macedonia, the data suggests the smelting of rather complex ores (assuming the analyses represent metal rather than corrosion layers). On the other hand, the more recent analyses of Sitagroi and Kastri material suggest copper or bronze objects with a small number of impurities, originating from smelting of possibly complex ores and in amounts one would expect if no refining stage followed the smelting stage. This implies that the metal was cast in a mould or cold worked directly after being smelted. Finally, the copper objects from Dikili Tash were free of impurities, suggesting, in contrast to other groups of samples, native copper working. It is argued that the belated introduction of copper in Macedonia as opposed to the rest of the Balkans may be due to the more extensive availability of complex sulfide, rather than oxide ores. However, this is only speculation, and researchers currently involved with the problem will no doubt adequately elucidate this

point.

2.1.c Iron

The earliest known attempt to extract iron ores in Macedonia can be dated at least to the 8th millennium BC at Tzines on Thasos (Fig. 1.2). The purpose was to obtain ochres, limonites and hematites (Koukouli-Chrysanthaki and Weisgerber 1982). Bone antler found in situ provided suitable material for dating the mine by the C-14 method.

The sites where iron artefacts have been found in Macedonia are shown in Fig. 2.1 and Table 2.1. Most of them were first surveyed by Heurtley (1939), whose publication of the prehistoric sites in Macedonia still remains one of the most authoritative sources. Naturally, more recent archaeological exploration in the area has added to his list of sites.

Although early iron artefacts have received attention from archaeologists, greater interest has been generated by the evidence from Vardaroftsa (Axiochori) of local iron production, in the form of two pieces of slag, one of LBA and the other of EIA date. Davies (1926) identified them as originating from the production of cast iron and from a bloomery furnace respectively. The chemical analysis provided by Davies (1926, 197) for the LBA sample gives a low total in aluminium and iron oxides (total: 6.5%), high calcium oxide (23%) and silica (69%). The low iron content is indicative of modern blast furnace slag, but it is more likely that the sample was a highly fired ceramic, possibly from

the furnace/hearth wall or lining. Davies originally (1926, 198) postulated, on the basis of this sample, that the LBA smiths of Vardaroftsa produced cast iron, transmitted the knowledge to Asia Minor and the Black Sea coast, where the Hittites were already smelting bloomery iron. The Macedonians learnt and adopted the local method of smelting bloomery since malleable iron is easier to work than cast iron which is brittle. They returned with their newly-found knowledge to Macedonia in the EIA to start producing bloomery iron. In a later publication Davies (Heurtley 1939, 255) reevaluated his original thoughts, which in view of what is known today seem naive, adding "it does not seem that stray examples of cast iron are to be regarded as the source of iron working ".

The present writer's opinion is that more attention should be paid to the EIA level slag which, by virtue of its silicate and iron contents, suggests a fayalitic slag typical of bloomery iron. Our attempt to find in Thessaloniki Museum samples of slag from the same levels at Vardaroftsa as those analysed by Davies proved unsuccessful. Instead, we came across material from later phases which we analysed. The results are presented in section 3.5.

The site most well-known in Macedonia for the abundance of its early iron finds in relation to bronzes is Vergina (Andronikos 1969). The earliest graves at Vergina (Fig. 2.3) have been dated by the excavator to the 11th c. BC, by Kilian to about 1100 BC and by Snodgrass to the 10th c. BC (Snodgrass 1980, 351). Whatever the precise date of the earliest iron finds at Vergina, at least they are not later than the corresponding finds in the South of Greece.

In comparing the artefacts from the cemeteries of Athens and Vergina, Snodgrass (1980, Table 10.3) noted the preponderence of bronze dress pins and fibulae at Vergina (240 out of 241 of all objects in bronze) as well as the total number of iron swords, spearheads, daggers, knives and arrowheads (151 out of 156 objects in iron). The point Snodgrass was making is that the people at Vergina were apparently free to choose the raw material for their objects, shortage of metal being nowhere evident. Nevertheless, Snodgrass has argued that "early Macedonian iron industry, although free of the constraining factors that operated in the south and quite distinct in its overall patterns, shows sufficiently close resemblances in the typology of the swords, knives fibulae and pins to make an independent origin highly unlikely" (Snodgrass 1980, 351).

Since the publication of that article, Prof. Snodgrass has changed his views. In an article submitted for publication, which he kindly allowed the writer to read, Snodgrass (forthcoming) notes that Vergina and Athens seem to lead in iron working over other Early Iron Age centres like Lefkandi in Euboea or Knossos in Crete (Fig. 2.3). His conclusions are based on the evidence for the adoption of iron knives which constitute the majority of functional iron objects in Athens and Vergina as opposed to other types like the javelin in the cemeteries at Knossos and arrowheads at Lefkandi. The knives are thought to be the first form to be shaped into a functional object, and so in Snodgrass' opinion the sites at which they are common developed an iron technology earlier than others.

In Eastern Macedonia at the cemetery of Kastri on Thasos the first occurrence of iron is a knife of the LBA (Koukouli-Chrysanthaki 1986, 1044). The knife has a bronze hilt, whose copper has been shown by lead isotope analysis (by N H Gale), to have a possible Cypriot origin. Despite this early find, and despite the abundance of iron ore deposits on the island, there is as yet little evidence of extensive use of iron during the first phases of EIA on Thasos. This has led the excavator of Kastri to suppose that Thasos lagged behind the Macedonian mainland in adopting the new metal (Koukouli-Chrysanthaki 1986, 1044). Although this may be true, recent evidence of pieces of slag found at the cemetery of Kastri (LBA-EIA) sometimes in the vicinity of iron objects may modify this idea. The concurrence of bronze and iron as well as slag pieces of both types makes this assemblage very important because of its rarity. Discussion of this material is given at some length in section 3.3, but it is of interest to note here that the Kastri metallurgical waste may offer some explanations concerning the transition from the smelting of copper to the smelting of iron ores on Thasos.

Thus, the first evidence for iron slag in Macedonia (Vardaroftsa and Kastri) dates to the 10th c. BC, while iron objects are evident in increasing numbers from the same period onwards particularly in the cemetery at Vergina. Current archaeological theories argue for an independent invention of iron metallurgy in Macedonia, and this hypothesis will be corroborated by our analytical finds on the Kastri copper and iron slag presented in section 3.3.

2.2 Iron in Mainland Greece and the Islands, Anatolia and the Eastern Mediterranean

2.2.a Iron in Mainland Greece and the Islands

For the purpose of this discussion, Mainland Greece encompasses the mainland south of Mt. Olympus from Thessaly to the Peloponnese. Iron is thought to have appeared earlier in southern Greece than in Macedonia, although the question of chronology is still much debated.

The first evidence for iron is a 'cube' from Mavrospelio at Knossos (Fig. 2.3) dating to 1800-1700 BC. The iron 'cube' is described as neither ore nor slag, and it is difficult to deduce its true identity from its photograph, amidst pottery sherds, in the original publication (Forsdyke 1926-27, 279, 296). The author suggests that the piece was kept as a curiosity and does not imply any practical use at that date.

From the LBA (1600-1200 BC) there is ample evidence for iron in Greece in the form of rings, small plaques, pendants from the mainland (Waldbaum 1980, 77), nails, rings, meteorite fragments from Crete (Waldbaum 1980, 78) and a tanged knife and iron fragments from the Cyclades (Waldbaum 1980, 78). The shape and small quantity of iron available suggest that iron was used for decorative purposes. A very detailed account of all iron objects found in Mainland Greece, the Aegean and Crete is given in Waldbaum's excellent, although now outdated, compilation of all the

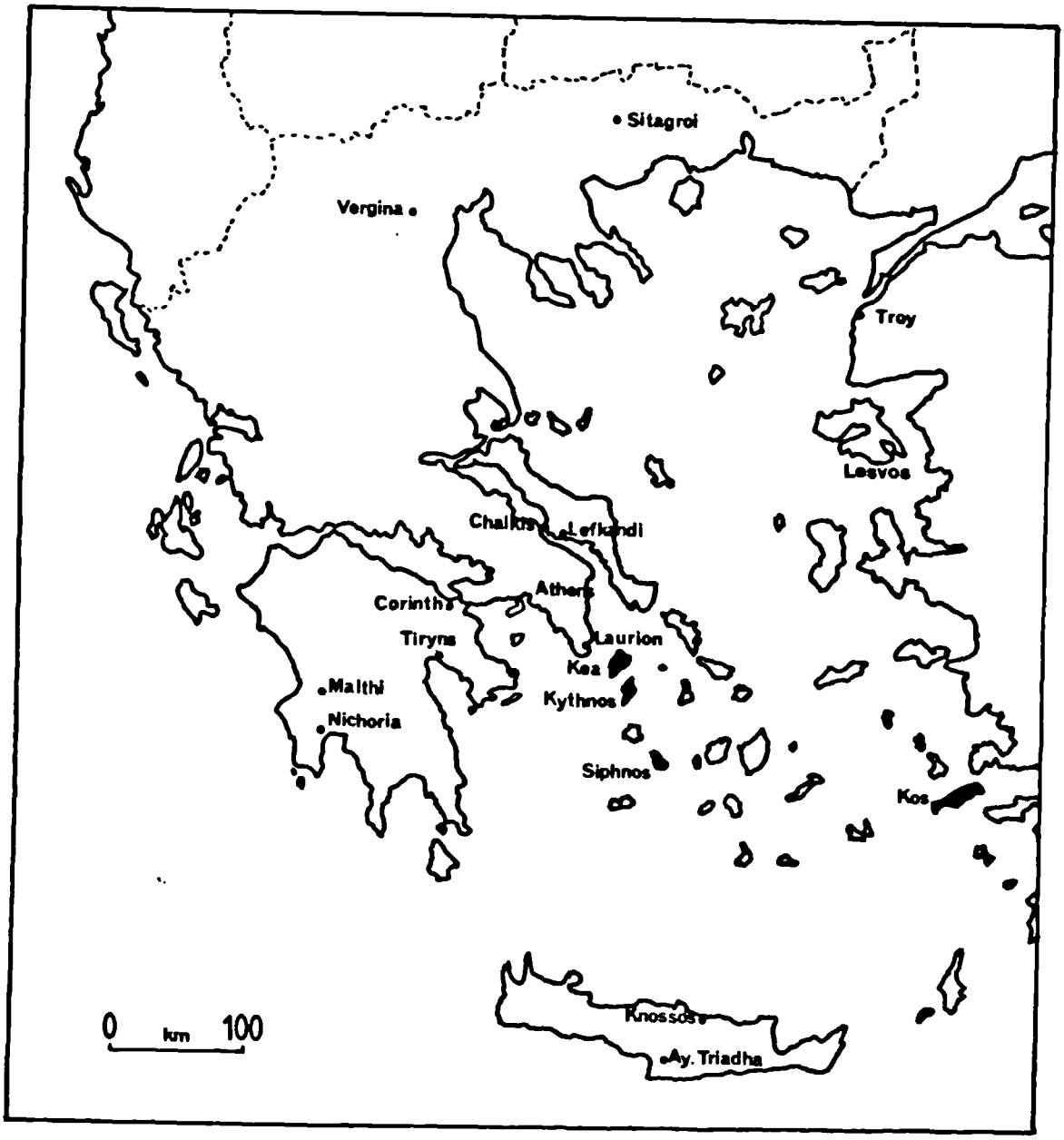

Fig. 2.3 Map of Greece showing prehistoric and Classical sites

material from each period from the LBA to the 10th c. BC (Waldbaum 1978). Vergina is not included in Waldbaum's catalogue.

The sites that have yielded the largest number of functional, as opposed to ornamental, finds in Mainland Greece are Athens (Kubler 1939) and Lefkandi (Popham et al 1980) in Euboea. The Peloponnese, Crete and the Cyclades follow (Snodgrass 1980) (Fig. 2.3). The earliest finds of functional iron come from Athens (an iron dagger with an ivory hilt and pommel (c. 1050 BC) from grave A from the Kerameikos and a similar one from grave B from the same site. An iron dagger from a late SubMycenaean tomb at Tiryns in the Argolid (c. 1050 BC) and also an iron dagger from a chamber tomb in Naxos (Snodgrass 1980, 346-7). None of these objects have been examined metallographically.

As already mentioned, the richest early iron finds are in the cemeteries of Athens (Agora, Kerameikos and other locations in Athens). They include spearheads, swords, knives, dress-pins, fibulae, axes, tools and arrowheads (Snodgrass 1980, Table 10.2). It is clear that during the period 1050-900 BC there is an abundance of iron, while bronze predominates in the period preceding and following it. Bronze is used even for spearheads and arrowheads in the subsequent periods.

Snodgrass advocates a common language, a 'koine', in working iron in the eastern part of Mainland Greece. This is suggested by the peculiar design of an iron pin with a bronze sphere half way along its length to be found in areas as far apart as Mycenae and Thessaly, and carried as an item of trade to the western Aegean to

Kos in the Dodecanese (Snodgrass 1980, 349). Crete also emerges with an extensive iron industry in the 11th c. BC , but it is thought that development there was independent of the Mainland. As was mentioned earlier, Prof. Snodgrass currently believes that Athens and Vergina were probably the first iron-making centers, with Euboea and Crete learning the craft from them.

LBA iron rings from the Peloponnese and Crete have been investigated by Varoufakis (1981; 1982). A number of them had a bi-metallic or tri-metallic bezel consisting of layers of lead and iron or gold, lead and iron. The iron had a high nickel content which prompted the investigator to speculate on the meteoritic source of this iron. Because he was particularly interested in this issue, and despite measured lead contents in the rings sometimes reaching 50%, he calculated the nickel and iron contents in the absence of all other elements (Cu, Pb, Ag). As a result, nickel contents up to 10% were reported to be present in the iron. In his original paper, Varoufakis (1981) presented both his measured and calculated values for nickel, but in subsequent publications he based his arguments on the calculated values only (Varoufakis 1982). This point should be borne in mind when reading his data. In any case, because of the objects' advanced state of corrosion and the possibility for only surface sampling and analysis, Varoufakis could not decide conclusively whether the source of this iron was indeed meteoritic.

The 'iron lumps' of LBA date from Ayia Triadha in Crete (Fig. 2.3) thought to be an iron meteorite (Iakovidis 1970), has been shown by chemical analysis to be corundum (alumina content c. 73%)

(Varoufakis 1982, 317).

Iron 'ore' lumps have been reported in another early context, namely at a LBA level at Malthi in Messenia (Snodgrass 1980, 354) (Fig. 2.3). Iron artefacts like daggers and knives also found in the same context were thought by Snodgrass (1980, 354) to be of more primitive type than at Athens or Tiryns, and so he concluded that some "precocious experimentation with iron was taking place in Messenia as early as the 12th c. BC". It is interesting that the excavator (Valmin 1938), in his discussion of the 'heavy stones', found in an area probably used as a forge because of the presence of ashes, calls them 'sideropetres' (Valmin 1938, 103), a word usually reserved for slag in many parts of Greece. From the description of the material included in a special appendix (Valmin 1938, 412-3), there are strong indications that some of the iron 'ores', as these heavy stones have been identified, could indeed be slag. The blueish-black colour of some of the samples (inv. nos. 1300, 1226, 1104) and the detected presence of silica and manganese found in one of them (inv. no. 1104) strongly points to a slag containing more than a trace amount of manganese rather than "impure quartz, on which manganese is deposited" (Valmin 1938, 413). Such posssible misinterpretations are not included here with the purpose of reflecting badly on the excavator or his/her colleague who carried out the analyses, but rather to draw attention to the need for locating the material (in Kalamata or Olympia museums) and attempting a new examination with the analytical instrumentation available today. This task is not always easy, as our own attempts to reexamine Davies' slag from

Vardaroftsa have shown, since the material, considered rather unimportant in those days, may have been taken as a whole, abroad, for analysis and so may be difficult to locate.

Two spearheads from Mycenae dating to the 7-6th cents. BC were shown by Varoufakis (1973) to be of mild steel (0.13% C) and steel (0.61% C). A third, also analysed, was corroded. The author had suggested that iron (in the form of 'currency bars') was imported from Anatolia, but he has recently reconsidered this view (G. Varoufakis, pers. comm.).

To summarise, the references and analyses (when available) on early iron in the mainland and Crete are discussed here critically. A reexamination of some of that material is urged since it seems that 'ironworking' may not have been as uncommon as we may think during the Bronze Age.

2.2.b Iron in Anatolia and the Eastern Mediterranean

There are fourteen iron objects from the Near East and the Eastern Mediterranean predating 3000 BC. These are smelted of meteoritic iron and were found in Iraq, Iran and Egypt (Waldbaum 1980, 69). The references to meteors and meteorites together with comets, shooting stars and other similar phenomena as they appear in the cuneiform literature have been compiled by Bjorkman (1973). In the same publication iron artefacts dating to the second millennium or earlier with substantial amounts of nickel are also included. The first evidence for iron in Anatolia as well as Egypt and Mesopotamia is in the EBA (3000-2000 BC) with the appearance of

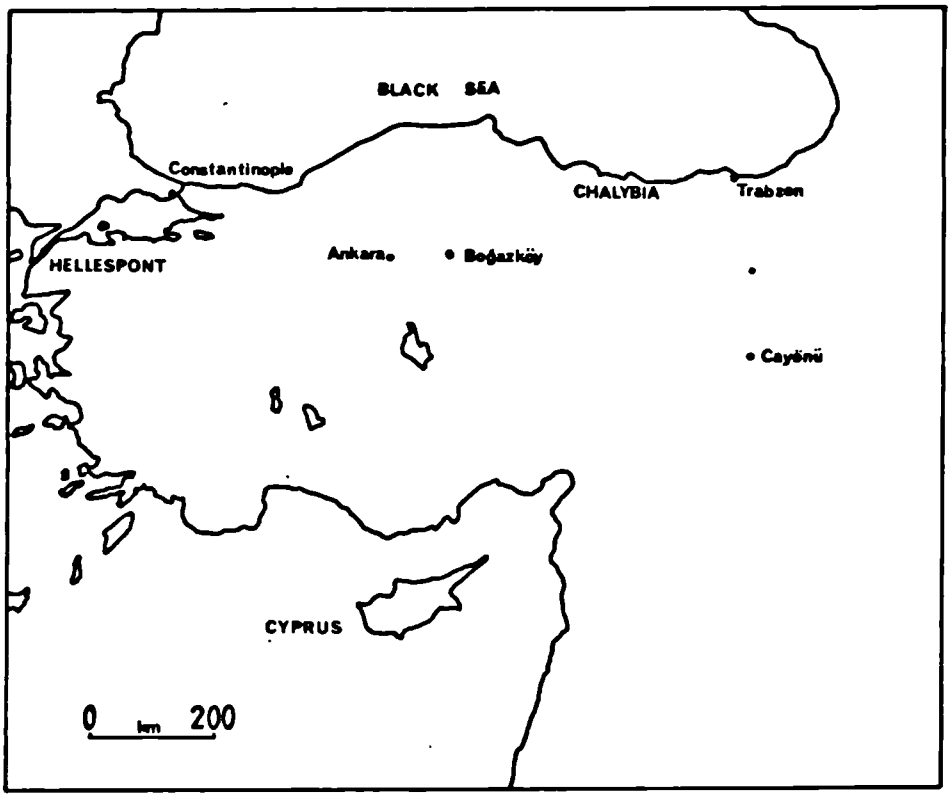

Fig. 2.4 Map of some sites and regions in Asia Minor. Alaca (omitted) is near Boğazköy

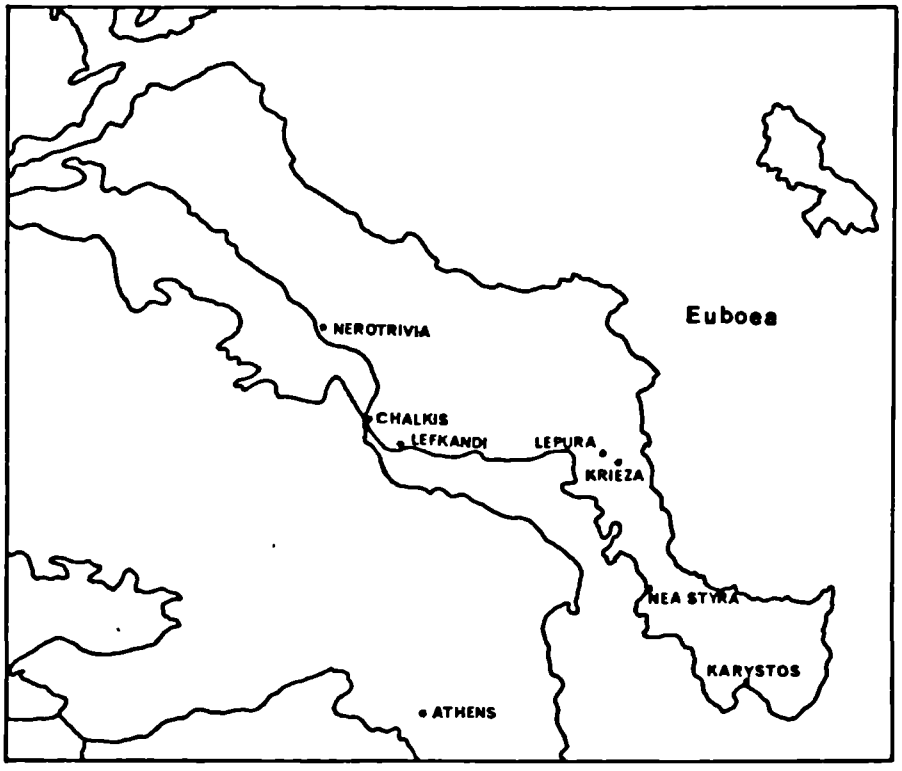

Fig. 3.3.2 Map of Euboea

six objects of meteoritic origin (amulets, pin, plaque, macehead and tools) and six objects of smelted iron ore (a dagger, a dagger blade, a tool and an unidentified fragment) as well as ten unanalysed objects (Waldbaum 1980, 73). As Waldbaum points out, all these examples of early iron are so widely scattered in time and space as to call for caution in drawing conclusions about diffusion of technology (1980, 73). Care should be taken when reading the published literature on meteoritic iron. King Tutankhamun's iron dagger with gold handle has been repeatedly reported as having been made of meteoritic iron, but it is highly unlikely that any analysis was ever carried out on this object (see Waldbaum 1980, 77).

During the MBA, in Hittite centers like Boğazköy and Alaca (Fig. 2.4), some tools and weapons made their first appearance, while arrowheads appeared in Egypt. Thus, for this period there is the marked contrast between Greece on the one hand, the only evidence being that of a 'cube' identified as iron ore, and on the other hand Anatolia where the Hittites had progressed to the shaping of functional iron objects.

It is in the MBA that iron makes its appearance in the Hittite documents as well as Summerian texts as a luxury item to be traded, its value exceeding that of gold (Waldbaum 1980, 76). Waldbaum very eloquently argues on the basis of the celebrated Hittite letter of Hattusilis III to the Assyrian king Shalmaneser I (c. 1250 BC) that, although Hittites may have had written records suggesting knowledge of the smelting of iron ores, the

archaeological record points to the existence of non-meteoritic iron and thus the knowledge of smelting iron ores in other places in the Eastern Mediterranean at the same period. In addition there is no particular abundance of iron objects (tools and weapons) in Hittite lands. Thus, if the Hittites held the 'secret' in iron technology, they saw no great reason in either keeping it or using it to achieve superiority over their neighbours.

Muhly et al (1985, 82) also admit that "we cannot call them (Hittites) innovators, monopolists or disseminators". If, then, iron artefacts appear, albeit in small numbers, in many areas in the Eastern Mediterranean and Anatolia, is there a case to be made for diffusion of knowledge from one center within that region outwards?

Another point of interest is the first appearance of steel. Muhly and coworkers have carried out a series of analyses of early carburised iron from the Eastern Mediterranean. Pigott et al (1982) presented the first evidence for steel in Transjordan: a bracelet with extensive carburization. In two knives from Cyprus dating to the 12th. c. BC, Tholander (1971) detected evidence for carburization and quench hardening testified by the presence of martensite and spheroidised cementite. Despite these valuable examinations, it remains a fact that the number of analyses for early iron in the Eastern Mediterranean is still very small, thereby warranting caution in formulating a final date about the earliest appearance of intentionally produced steel.

2.3 Metals in the Balkans and Central Europe

2.3.a Gold/Copper/Bronze

The autonomous development of copper and gold metallurgy in the Balkans at the end of the Neolithic (Chalcolithic or Eneolithic) has been firmly established on the basis of the evidence for early mining and hoards of gold or copper artefacts found in present-day Bulgaria, Yugoslavia and Rumania with no precedents in the Aegean or Asia Minor (Renfrew 1969).

The Varna treasure in Bulgaria (Fig. 2.5) is the earliest and richest excavated collection of gold artefacts in a Chalcolithic cemetery (4600-4200 BC), predating Troy by nearly 1500 years (Gimbutas 1977a,b). The repertory of shapes is impressive in both gold and copper objects. The gold has been hammered mostly to thin sheets (Ivanov 1978).

Evidence for copper mining in the Eneolithic (early to mid fourth millennium BC) in the Balkans comes from the mine at Rudna Glava (Fig. 2.5) in N.E. Serbia in Yugoslavia (Jovanović and Ottoway 1976; Jovanović 1980) where shafts have been sunk to a depth of 20m and a width of 2m. Another early copper mine dating to the same period is at Aibunar (Fig. 2.5) in Bulgaria. The ore, although malachite/azurite, showed on analysis to contain Pb (1-10%) and Zn (0.1-1%) together with other impurities (Chernych 1978). Copper tools have also been found, but the analysis of an axe-adze and a hammer-axe (Chernych 1978, Table 2) showed very clean copper with only traces (of the order of fourth decimal place) of other elements. This has puzzled the investigators, who concluded that, if the ores contained a host of minor and trace

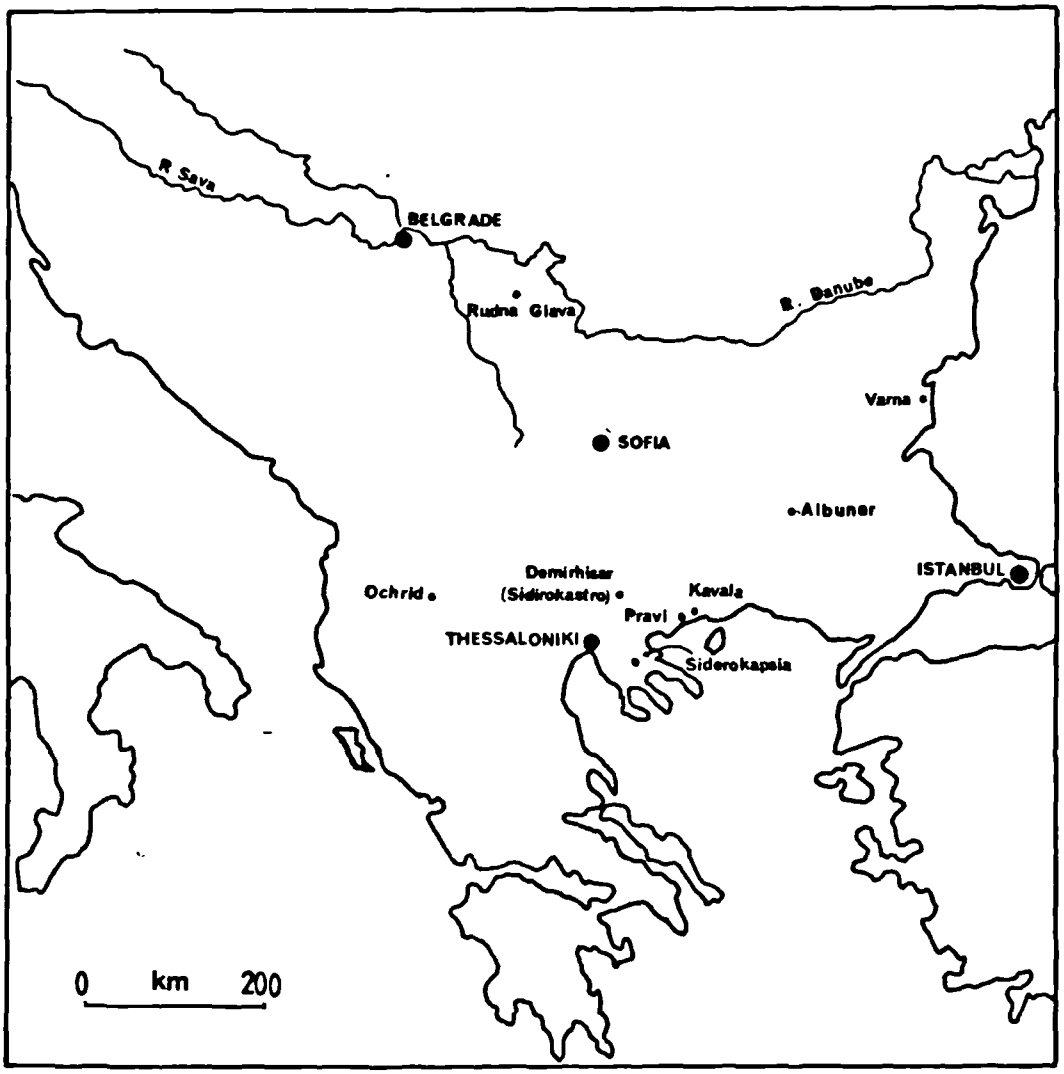

Fig. 2.5 Map of Prehistoric and Ottoman sites in the Balkans

elements, the copper axes were not made of local ores. This observation may or may not be true in view of the purity of metal achieved in the refinement stage. Axe-adzes and hammer-axes, a particular form of tool typology that emerged in the Balkans at the end of the Eneolithic, are the distinctive hallmark of Balkan Chalcolithic metallurgy. They contrast with the more common but less diagnostic early copper objects like awls and needles which have been found in many parts of the world, including the earliest occurrence of copper in the 8th millennium at Cayönü Tepesi in Turkey. (Tylecote 1976,1) Whether the copper of the Balkan axes was indeed smelted or melted native copper is still a matter of debate, but what is not in doubt is that a great deal of thought went into the design of the mould and the shaping of the final object (Charles 1979, 173).

2.3.b Iron

The iron objects in the Balkans or Central Europe by the end of the 2nd millennium are few and far between. In Rumania, at Cernetu in S.E. Transylvania an iron knife and chisel were found with iron bars. This and one or two other occasional finds are all thought to be imports from Anatolia (Hoddinot 1981, 76). The earliest iron objects in central and northern Europe dating to the second millennium are occasional finds in Denmark, Sweden and Slovania (Pleiner 1980, 377).

Some researchers chose to present the material finds in Vergina as evidence for the earliest iron working in Southern

Thrace, on the grounds that the area was the homeland of the Thracian tribe of the Pierries (Hoddinot 1981, 76; Petsas 1964, 255). Were the people buried at the EIA cemetery at Vergina Greeks or Thracians? This is a matter of considerable debate, but it lies outside the scope of this work. Whatever the answer, it is the case that the earliest iron objects at Vergina date to the 10th c. BC and iron does not make a significant appearance in the Balkans until the 8th c. BC (Pleiner 1980, 379). It has been argued that the Balkans had to wait for the advent of Greek colonizers before they were introduced to a fully-fledged Iron Age (Alexander 1962, 130). The dissemination of iron into the Balkans and the routes it followed are based on the evidence that iron artefacts appear in the Balkans and Central Europe later than in Greece and the Eastern Mediterranean. Pleiner (1980, 382) produced a map showing Greece at the epicentre of a diffusion of iron technology originating in the East and moving into the Balkans.

Thus, although the Balkans have a very advanced copper age technology, with a variety of tools and ornamental artefacts far surpassing in style and technique contemporary ones in Macedonia, they are rather slow in substituting their bronze weapons and tools for iron.

2.4 Summary and Concluding Remarks on Macedonian metals from the LN to EIA

Analyses of copper/bronze artefacts from Macedonia (LN-EIA) suggest, on the basis of trace and minor elements present, the use of copper ores as well as the possible use of native copper. It is

clear that after smelting no refining was involved and that the metal was cast or worked as smelted. The evidence for crucible and slag fragments at LN Sitagroi suggests local attempts to smelt or melt metal. McGeehan-Lyritzis and Gale's identification of a new source or sources of copper ores for Sitagroi and sites in Thessaly corroborates the argument for an autonomous development of metallurgy in the area. Of course, the source may prove to be of Balkan origin, but this does not seem likely. It is speculated that availability of complex (sulfide) copper ores may have been a possible reason for the late introduction of copper metallurgy in Macedonia relative to the Balkans.

The earliest iron slag in Macedonia dates to the 10th c. BC and comes from Vardaroftsa and Kastri on Thasos. Iron objects are abundant mostly at the cemetery at Vergina from the same period onwards. The evidence of copper and iron slag in the same context at Kastri together with the metallographic examination of some artefacts from Vergina may shed some light on the introduction of iron metallurgy in the region.

A critical review of the existing literature on the analysis of iron ore, slag and objects is given here particularly with reference to BA iron, in Mainland Greece, the Aegean and Crete. It is pointed out that iron slag may have been evident in a BA context more often than was originally assumed.

In the Balkans, although copper metallurgy had a head start and reached impressive levels in the Chalcolithic relative to the Aegean and Macedonia, it seems to have been slow to substitute

copper/bronze with iron.

It is clear from the discussion in this section and from the work of Waldbaum (1978, 1980) and Muhly et al (1985) that Anatolia and Mainland Greece developed their iron technologies in parallel during the second millennium, Anatolia showing an earlier development but not necessarily a clear dominance in iron-making technology. At the end of that era iron objects appear in large numbers everywhere, heralding the start of the Iron Age for the entire Eastern Mediterranean. This conclusion raises some doubts about the diffusion of iron technology from one region, traditionally thought to be Hittite Anatolia, to one or more centres in the Eastern Mediterranean.

The theory of diffusion of technology is based on relative chronology and typology of artefacts, some sites producing a particular type of artefact earlier than others. As a result, independent invention is claimed at one site, while another site is thought to be 'on the receiving end'. This model tends to overlook two important issues. First, that object typology reflects only the last stage in iron making, that is the shaping of an iron bar/billet, into a functional/ornamental object, and ignores completely all the preceding and equally important stages leading up to the making of the iron bar/billet itself. At Malthi, the probable evidence of metallurgical waste should be used as a good indicator of local, early attempts at iron smelting, irrespective of whether the iron typology at Malthi predates or not that of other centres. Secondly , the assumption that the knowledge of

iron working disseminated from one center tends to overlook the fact that by the EIA many centres were smelting copper ores often in association with iron ores (as flux). Small iron prills or lumps would have been produced from the reduction of the iron ores in the furnace (Wertime 1973). However, the new technology would not have been initiated unless the BA smiths had begun working this new metal with its attendant difficulties: high melting temperature and poor working properties compared to copper.

The introduction of metals technology in a region can only be ascertained with confidence by the presence of slag and other metallurgical waste. Whether the idea behind the production of this waste came from outside or not is really of little consequence. The point of interest is the first evidence for local experimentation with metals and the use of local ores. It could be argued that early bronze smiths of a particular region were importing the raw metal, the only activity required of them being to cast it. The writer believes this assumption to be improbable. In the early stages of copper metallurgy, local experimentation must have followed the sequence: smelting of the ore, making the raw metal and then casting the metal or one of its alloys. It seems highly unlikely that the smith who could cast a bronze object was not also in a position to smelt a copper ore unless the copper he had available was native. It is the opening of extensive trade in metals, the shipment of ingots from a few copper/tin producing areas to the rest of the Mediterranean world, which resulted in specialisation, namely bronze founders not having to be copper smelters as well. Although trade in ingots did not take place until

the LBA in the Eastern Mediterranean, it is possible that the roots of this specialisation had already begun to take place by the EBA, witness the shipment of lead from Laurion to Kea and Lerna during the EBA (McGeehan-Lyritzis and Gale, forthcoming) suggesting that at least some metal trade routes were probably established by that time. Thus, for the periods of experimentation with copper smelting and specialisation induced by trade, one should look well into the LN and no later than the EBA, as one should look for the first steps in the mastering of iron metallurgy well within the Bronze Age.

2.5 Metals and Mining in Archaic/Classical/Hellenistic/Roman Macedonia

2.5.a.1 Mining: Gold/Silver/Copper

Before describing the occurrence and composition of metal objects of the period in question, some introductory remarks on the location of metalliferous ores in Macedonia are necessary. The state-run Greek Institute for Geological and Mining Exploration (IGME) has produced a series of publications relating to the exploitable ore deposits throughout the region (see section 3.2 for a complete reference). With a bias towards ancient metal-working sites, Davies' account (1935) has for long remained an important source of information for anyone working in the area.

Of the three regions of Macedonia (WM, CM, EM), (Fig 2.6), the most important in terms of mineral resources was probably EM, followed by the Chalkidiki peninsula in CM, and the gold placer

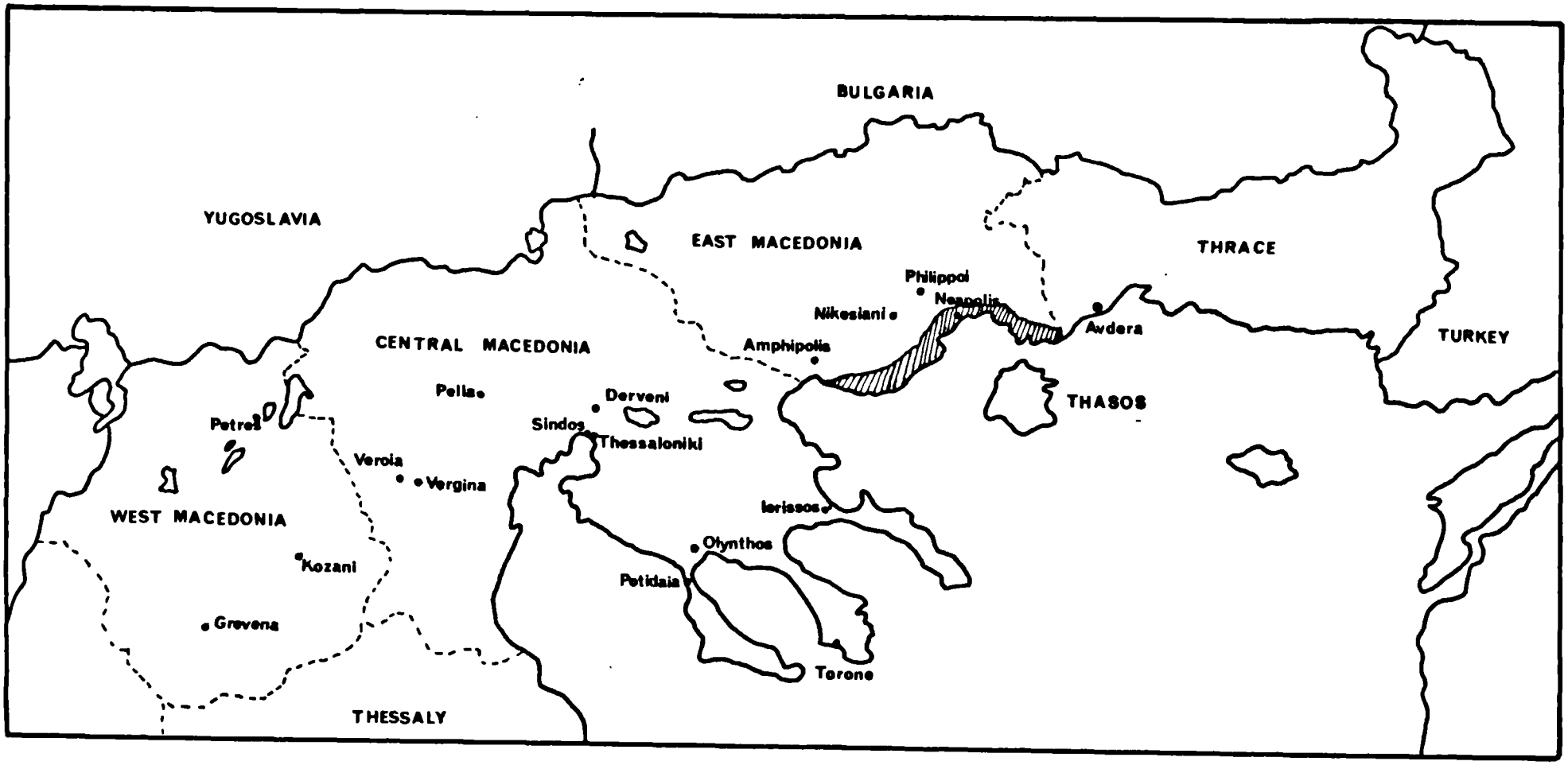

Fig. 2.6 Map of Archaic, Classical, Hellenistic and Roman sites in Macedonia (adapted from Treasures in Ancient Macedonia, Thessaloniki Museum, 17). The shaded area shows the Thasian Peraia.

deposits of the main rivers in the three regions. Strabo (III, 354) mentions gold mines in the Strymon Delta, in the Pangaion and in Crenides near Philippoi (Healy 1979, 46). Until the 4th c. BC when it was conquered by Philip II, EM was Thracian territory with the exception of the coastal region, belonging until the 6th c. BC to Thasos and called the Peraia (shaded area in Fig. 2.6). The bulk of the Thasiot wealth was based on the exploitation of both their own mines and those of the Peraia. The precise location of some of these mines on the Peraia, the Skapte Hyle of ancient sources (Herodotus 6, 46), has not been identified. Two areas are favoured: on or near the Pangaion (Pedrizet 1910; Casson 1926; Lazarides 1976) or in the region of Palaia Kavala (Hereward 1965; Hammond 1979, 72), the area to the north of the modern town of Kavala (Fig. 1.1 and 3.1.1).

The mines on the EM mainland were always the goal behind attempts by the Athenians to conquer and colonise that region as well as breaking up the Thasian hegemony. They did manage to gain control of the area and founded a colony, Amphipolis (Fig. 2.6), only to loose it at the start of the Peloponnesian war. The fact that Thucydides was exiled in Skapte Hyle as a result of his mishandling of the affair testifies to the fact that the Athenians had lost access to the mines on the Thasian Peraia by 422 BC (Koukouli-Chrysanthaki 1979b). Koukouli-Chrysanthaki (1980, 313) recently noted that a) none of the Classical sources locate the Skapte Hyle on or near the Pangaion, and b) the Pangaion would have been well within the Thracian territory. Since it is difficult to accept that the Thasiots had penetrated inland as far as the

Pangaion by the end of 6th-early 5th c. BC when they only managed to found their first colony inland, Crenides, in 360 BC, the second alternative should perhaps be examined more carefully.

Recently two sets of archaeometallurgically-based research projects have been carried out on Thasos. First, there was an attempt to trace the gold mine reported by Herodotus at Kinira (Fig. 1.2), successfully carried out by Wagner et al (1981). Gold grains were found within limonites. The samples were taken from red clay fillings within marble fissures. Second, there was an effort to establish the source of silver for the Thasos mint in the 7th and 6th c. BC (Gale et al 1980). Survey, sampling and analysis of ore from galleries and slag heaps at a number of sites on Thasos associated with the lead/zinc deposits in the western part of the island suggested extensive exploitation probably during the Roman period as well as earlier. TL dating of ceramic fragments from nearby slagheaps revealed smelting during the Roman period. That the Pb isotope compositions of some Archaic (6th c. BC) Thasos coins agreed closely with the isotope ratios of reference material, slag and ores, for the island strengthened the case that silver was extracted from these Pb/Ag ores (Pernicka et al 1980).

2.5.a.2 Gold, silver and bronze artefacts

Fig. 2.6 presents the major sites in Macedonia dating from the Archaic period onwards which have produced an abundance of gold, silver and bronze artefacts often of superb beauty and craftsmanship. Analyses of Hellenistic bronzes have been undertaken by Craddock (1977), but it is not clear how many of

these objects originated in Macedonia. Recently, a complete analysis was made of the bronze crater (ht. 90 cm) from Derveni near Thessaloniki (Fig. 2.6), dating to the end of the 4th c. BC. Varoufakis (1980) showed that the crater's golden colour was due to a high tin content (15%) rather than gold plating. The crater was raised from one single sheet of bronze with embossed figures and cast handles and statuettes welded onto the body. The rim was also made of a separate sheet and welded onto the main body. High tin contents in copper impart hardness to the alloy, and so it is particularly impressive that the bronzesmith was able to raise the bronze sheet to a height of 80 cm without rupturing it (Varoufakis 1980).

Regarding precious metals, Assimenos (1983) produced a set of analyses of the spectacular gold and silver objects from the recently-found important tomb of Philip II, father of Alexander the Great, at Vergina; he elaborated on the techniques of manufacture of some of the objects analysed.

2.5.b.1 Mining : Iron

To our knowledge there exists no documentary evidence relating to iron working in Macedonia in antiquity. Its natural resources in lead and iron are first referenced in geographical manuals of the 4th c. AD (Geographi Graeci Minores II, 523, 51; Totius Orbis Descriptio) as well as another source also of late antiquity, in which Macedonia is presented as a producer of iron, embroideries, bacon and cheese (Expositio Totius Mundi et Gentium,

Ed. J. Rougé 1966).

2.5.b.2 Iron artefacts

Philip II's tomb at Vergina brought to light, apart from gold and silver artefacts, an iron cuirass, its back made of a single sheet of large dimensions (47 cm x 39 cm). Metallographic sections revealed pearlitic structure, suggesting steel rather than iron with very few slag inclusions (Assimenos 1984).

2.6 Byzantine Mining and Metals

2.6.a Byzantine Mining : Gold/Silver/Copper

Very few references exist for mining activities in Macedonia during the Byzantine period. Nevertheless, the Constantinople gold 'sovereign' was the strongest currency for more than six hundred years, even after Byzantium lost most of its eastern provinces to the Arab conquests (Vryonis 1962). This suggests that the empire was self sufficient in precious metals within its own severely diminished borders, and the implication is that Asia Minor, as opposed to Mainland Greece, was primarily the source (Vryonis 1962). However, very little is known about silver mining in Asia Minor in that period, but Turkish archaeometallurgists are presently carrying out surveys in S.E. Turkey where evidence for extensive silver exploitation during Ottoman times, among other periods, is clear (Yenner and Özbal 1986, 317).

In the Theodosian code of the Early Byzantine period (370-386 AD) it is evident that the state had problems in keeping itinerant

Thracian miners looking for gold outside the boundaries of the Diocese of Macedonia (Vryonis 1962). With the Gothic invasion (late 4th c. AD) the mining output had decreased and the situation made worse by the added defection of the Thracian miners expert in following veins of gold, to the Gothic army to avoid taxation (Vryonis 1962, 11). This suggests that, at least during the early Byzantine period, the Macedonian mines were mostly idle. It seems that since early antiquity Thracians had earned the reputation of being capable miners since they often seem to be employed as overseers (epistates) in the silver mines at Laurion (Osborne 1985, 117).

2.6.b. Byzantine Mining: Iron

In the 10th c. AD a Byzantine official, Nicetas Magistros (Westerink 1973), ousted from the court of Constantinople and exiled to the Hellespont between 928 and 946 AD, described in a very poetic way the washing and smelting of beach sands to make iron. In loose translation the text runs as follows: " The river brings iron to the sea like a secret wedding gift by the groom to his bride. But the sea desiring to make her gift public crushes it on the beach in the form of sand in full view to all. This sand is washed, repeatedly and subsequently smelted". Earlier in the passage Nicetas Magistros notes that at the same river mouth the sea sends nodules of iron (Westerink 1973, 63 and 65). This idea of smelting nodules rather than sands is interesting since it is possible that this sand was made into cake balls to be fed into the furnace, as the word 'svolakas' implies in the Byzantine text.
This is probably the first written evidence of smelting of beach

sands in Greek lands after the reference of late antiquity by Pseudo Aristotle (De Mirabilibus Auscultationibus) on the iron sands smelted by the mythical Chalybians on the south coast of the Black Sea in Asia Minor. Given yet a third reference provided by the Spanish ambassador to the court of the Mongol emperor Tamerlane in 1476 AD about smelting iron sands in the same area (Bryer 1982), it is clear that the resources were indeed available and the practice had a long tradition. Smelting of iron beach sands was common practice in Thasos during the late Byzantine-early Ottoman period and on the island of Lesvos, as our results testify (see section 3.6).

The earliest reference to iron workings in EM in historical times is documented in a manuscript from the monastery of Ayia Lavra on Mount Athos dated to 1347 AD. In the document containing privileges given to the monastery by the Serbian monarch Stefan Dušan, iron workings or in Byzantine terminology 'Siderokapsia' were supposed to have taken place in Trelesion, somewhere between Serres and Nevrokopi (Lémerle et al 1979). The document does not specify whether iron was mined or extracted from magnetite sands, but the work of Davies (1935) and Anhegger(1943) rather suggest the latter.

2.7 Ottoman Mining and Metals
2.7.a Ottoman Mining : Gold/Silver/Copper

Belon (1553), a French traveller to Macedonia at the start of the 16th c. AD, gives us the most detailed account, albeit possibly exaggerated in terms of scale of activities, of the operations at

Siderokapsia (Fig. 2.5). Additional information is provided by an official Ottoman report dating to 1589 (Murphey 1980). This report refers to the leading silver mines in Ottoman Rumelia, an area which includes Thrace, the name given to E. and C. Macedonia at the time.

Belon suggests that iron pyrite and marcasite was the type of ore used. No mention is made of galena and/or lead/zinc carbonates as the primary silver ore source. Fuel was wood and charcoal, rather than lignite. Two types of furnaces are described, presumably the smelting and the refining, both being operated by water-driven bellows. The smelting furnace is large and built in the middle of the workshop. It is charged from the top and has two small openings, at the sides, one for molten metal, the other for gases (?). The tuyeres aim towards the furnace floor. The bellows are driven by a water wheel, four rods pushing on the bellows. Seven leats channel water to the wheel. The wheel ends in eight arms, to which eight tuyeres are attached. Four of these are directed towards the smelting furnace, the rest towards the refining. The distinction between smelting furnaces and refining hearths (presumably cupellation hearths for the separation of silver from lead) is the present author's, but Belon himself uses them at one point interchangeably (refining hearths, 'cheminees', smelting furnaces, 'fourneaux'). The hearths are operated with wood. Charcoal is the fuel in the furnaces. Belon specifies that the product coming out of the furnaces is called 'molybdena', while that of the hearths 'molivi'. Belon also adds that 'molybdena' looks more like metallic waste. In section 3.7 the present author

shows, for the first time, that what Belon is probably referring to is speiss. An equally interesting observation in Belon's account is the passage relating to galena and its roasting in a hearth with a combination of wood and charcoal. Belon notes that after the galena is roasted and changes colour it is added to the furnace. The reason for the addition of galena is also explained in section 3.7. The processes described by Belon and the metallurgical waste of similar ones encountered and analysed in Palaia Kavala have been elucidated through smelting experiments carried out by the writer.

The Ottoman report concentrates primarily on the three major mines in EM and CM, namely Siderkapsia, Pravi and Demirhisar (Fig. 2.5). The mines and their outputs (in Troy ounces; 1 Troy ounce = 31.1035 gm) for a particular year are as follows:

Siderokapsia	272,337	(1585 AD)
Pravi	73,560	(1590 AD)
Demirhisar	147,780	(1589 AD)

It is clear from this report that the Ottoman silver mines both in Greece and the Balkans continued their operation well into the early 17th c., in contrast to the situation in Central Europe, where by the mid 16th c. the effect of the importation of cheap silver from S. America resulted in the closure of many of its mines (Murphey 1980, 76).

Belon, who visited Siderokapsia more than a century earlier, reported that there was a mint which had been in operation since the reign of Murad II (1421-1451). This suggests that the mines were being worked, although not necessarily without interruptions, for approximately 200 years.

The Ottoman report (Murphey 1980, 91) gives a short and rather confusing account of the cupellation process which will not be reproduced here. However, a point of interest is the reference to the addition of a precise amount of human excrement (1.2kg), possibly a source of ammonia, to the 'boiling silver' to ensure purity of metal.

2.7.b Ottoman Mining :Iron

Concerning the iron mining of the local hematite and limonite ore sources in Eastern Macedonia, there are references dating from the Early Ottoman period onwards. There was extensive iron production in the region of Eleftheroupolis (Pravi or Pravista in some sources) (Fig. 2.5) even by the end of the 16th c., according to a Turkish firman of the 1583 AD and the accounts of a contemporary traveller, Christoforo Vallier (Anhegger 1943, 206, n.58). This iron production must have intensified by the end of the 17th c. when a foundry was established in Eleftheroupolis in 1698 producing cannon balls and iron for construction material. The goods were shipped to the naval base at Constantinople.

The iron-working activities of Eleftheroupolis are also mentioned in the accounts of a number of travellers who visited the region in the early and late 18th c. (Lucas 1712; Cousinery 1831) as well as in the early 19th c. (Beaujour 1829). Cousinery reported iron slag in the Symvolon mountain range (Fig. 1.1), while Beaujour mentions iron exploitation in the mountains around Eleftheroupolis and the Pangaion. Although, no reference is made to the particular

source of iron ore, Symvolon is known to contain hematitic/limonitic ore deposits as well as iron sands originating from the weathering of the Symvolon granite (Stavropodis and Pourni 1971, 38).

During the Ottoman period the practice of smelting magnetite sands was widespread in the region of southern Bulgaria with important production centers such as Samokovo, Melnik and Perin (Jireček 1886 and 1912; Davies 1935; Anhegger 1943; Georgiev 1971). The practice certainly also extended within the Greek state, to Vathytopos and Katafyto (Fig. 3.1.1). Davies (1935, 228) was not exaggerating when he pointed out that "magnetite sand from the eruptive outcrops of the Rodhope range was as precious to the Balkans as bog ore to Germany" (see Fig. 1.1 for Rodhope range).

2.8 Summary and Concluding Remarks on Macedonian Mining and Metals from the Archaic to the Ottoman Periods

The present knowledge on the mining activities during the Archaic/Classical/Hellenistic periods are summarised, and analytical information on gold/silver and bronze objects is presented.

Documentary evidence on iron mining and artefacts during the same period is at best sparse. Equally sparse is the evidence for the Early Byzantine period suggesting that Constantinople looked mostly east (Asia Minor) rather than west (Mainland Greece) for the procurement of its precious metals. Ottoman precious metals extraction has been better documented in both CM and EM.

Two very interesting references have recently come to light on smelting of iron sands in Asia Minor, rather than Greece, by a 10th c. AD Byzantine official in the Hellespont (Fig 2.4) and a 15th c. AD Spanish ambassador on the shores of the Black Sea. The last one, recalling PseudoAristotle's 3rd c. BC reference of Chalybian iron also in the Black Sea, clearly points to a long tradition of smelting iron sands at least in Asia Minor.

In Macedonia iron workings were first reported in a 14th c. AD document somewhere between Serres and Nevrokopi (Fig 3.1.1) and later on at a number of locations in EM. Since the end of the last century, if not before, the smelting of iron sands, the weathering product of a granitic outcrop, from an inland rather than a coastal location is documented in Bulgaria and present EM.

Two remarks are appropriate here which apply to any archaeo-metallurgical work in any region:

a. Caution should be exercised when consulting modern minerals resources maps with the intention of matching them with metalworking sites or habitation areas as some scholars have attempted recently (McGeehan-Lyritzis 1983). In the absence of an analytical investigation of slag and artefacts which may hope to indicate ore source, the maps are informative only as a guideline and at a general level. This drawback will become obvious in the next chapter when discussing the titanium-rich iron slags of Thasos and the Mainland (section 3.6). Their source of iron ore was the weathered granite of Vrontou and the gneiss of Thasos. This was an important source of iron ore in the late Byzantine and Ottoman

periods but is hardly mentioned in modern ore deposit maps. At the risk of reiterating the obvious, modern minerals resources maps do not necessarily lead to the old workings.

b. A word of caution is also appropriate when interpreting old technical texts, like Belon's for example. Assuming that an author understands the processes he is describing, he is likely to have used names and terminology employed by the miners and smelters he interviewed. This is to be expected since, even today, colloquial terms are used by people in the field which do not necessarily correspond to their mineralogical name. Therefore, it is essential that the modern commentator should have a fair understanding of the relevant processes before attempting any interpretation.

CHAPTER 3

ANALYTICAL INVESTIGATION OF ARCHAEOLOGICAL AND EXPERIMENTAL ORE, SLAG AND ARTEFACTS

3.1 Introduction

When the present work began on Thasos in 1983, very little was known about iron working in the area. More important, it was not always easy to distinguish the remains of iron working (slag, tuyere fragments) from those of lead/silver activities which have already been the subject of archaeometallurgical and geological investigation (Pernicka et al 1980). Nevertheless, veteran well-informed islanders were able to direct us to a multitude of sites, often off the beaten track, where the remains of some type of smelting activity were apparent. It turned out that the majority of these sites on Thasos were related to iron smelting and moreover were remarkably similar to each other, an observation which was later corroborated by the analysis of slags.

The work was extended to the Mainland with the sampling of slag from the Vrontou mountain region (Fig 1.1), slag and artefacts from the Museums in Kavala, Thessaloniki and Thasos, from archaeological sites currently under excavation (Petres, Fig. 2.6) and slag from metal-working sites in the Palaia Kavala district (Fig. 3.1.1). Since no furnaces were located in either of these areas, it became imperative to identify the material and ascribe processes to particular regions on the basis of slag analysis

Fig. 3.1.1 Sites on Macedonia sampled for ore, slag and artefacts.

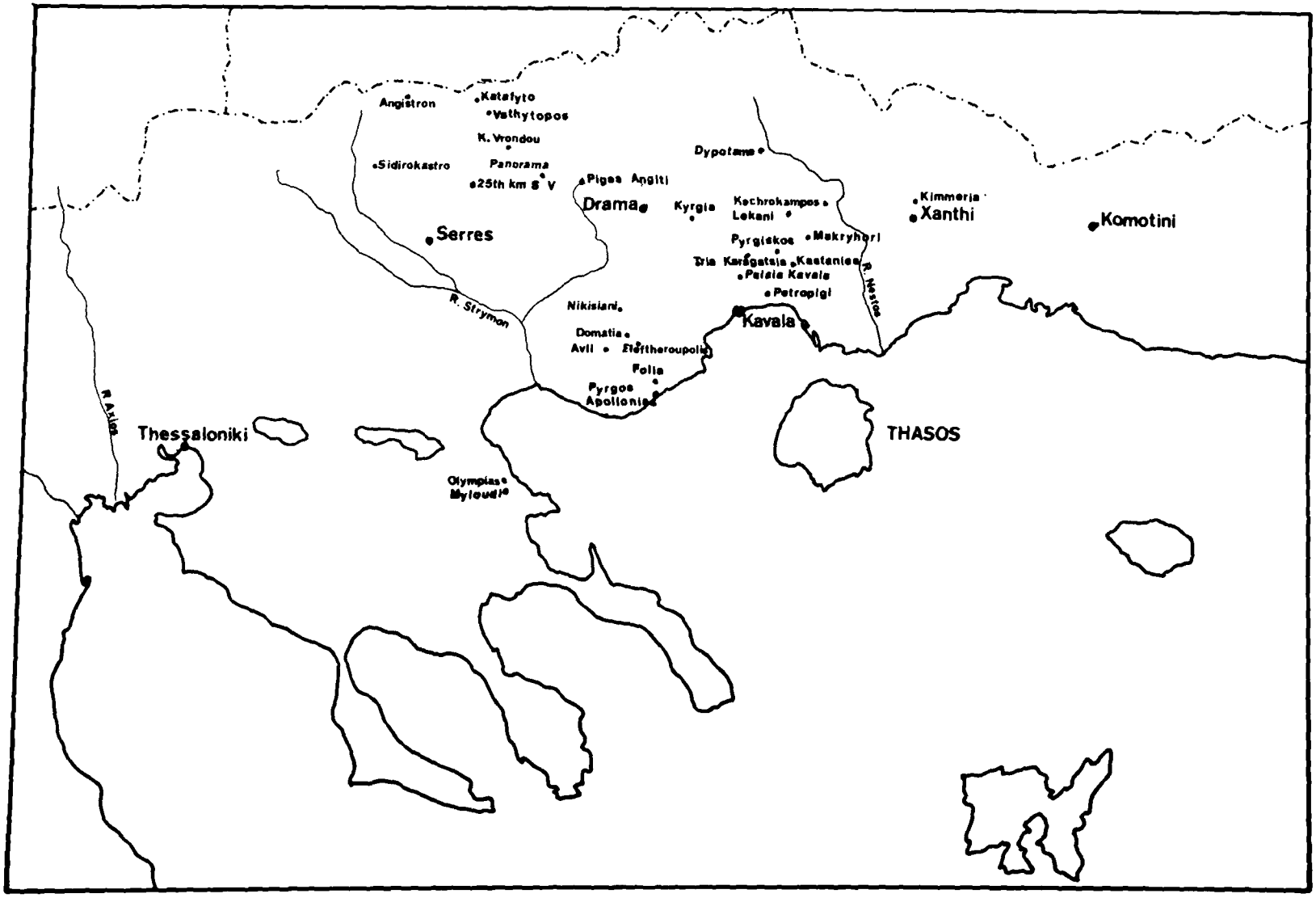
Angistron
Katafyto
Vathytopos
K. Vrondou
Sidirokastro
Panorama
25th km S V
Pigas Angiti
Dypotamo
Drama
Kyrgia
Kechrokampos
Lekani
Kimmeria
Xanthi
Komotini
Serres
Pyrgiskos
Makryhori
Kastanies
Palaia Kavala
Petropigi
R. Nestos
R. Strymon
Nikisiani
Kavala
Domatia
Avli
Eleftheroupolis
Folia
Pyrgos Apollonias
R. Aliakmon
Thessaloniki
THASOS
Olympias
Myloudi

alone.

Ancient metallurgical sites are almost by definition difficult to plan and characterise. Those in Macedonia are no exception to this rule, and the archaeometallurgist's task is rendered all the more difficult by problems associated with the topography, the archaeology and the socio-economic history of that region.

For the archaeometallurgist working with established models of European bloomery iron-making furnace sites, like those in the Weald in England (Tebbutt and Cleere 1973), in Jamptland in Sweden (Magnusson 1986) and in the Holy Cross Mountains in Poland (Bielenin 1974), Macedonia is rather a disappointment. There has, for example, been considerable difficulty in locating a bloomery furnace. A proton magnetometer survey, carried out at Tragi on Thasos in collaboration with R.E. Jones of the British School at Athens, located areas of thermoremanent magnetization, but the furnace remains corresponding to these areas proved very scanty, consisting only of tiny wall fragments. Papastamataki (1986b) has located and excavated a furnace at Nikisiani in the Pangaion, but it is not a bloomery furnace (see section 3.7).

With the exception of the furnace representations on some 6th and 5th c. BC Attic vases (see Chapter 4 for discussion), we know very little about furnace typology at any period in Greek history. We do not know what the bloomery furnace looked like, let alone how it worked. We do not know when the blast furnace was introduced into Macedonia or Greece in general. No blast furnace slags were

found in Macedonia with the only exception at Avli, Pangaion, (see appendix 3.1.1). Blast furnace manganese-rich slags were also found by the author in the southern tip of Euboea (see section 3.6). Slag in Macedonia is either scattered over a few tens of square meters or rises in heaps of considerable tonnage. The sites are located either by the sea or inland near streams or on flat areas on mountain/hill tops. In short, there exists no one typical metal-working area.

To make matters worse, the surrounding mineralisation is equally complex. In one case, Mn-rich iron ores surround a metal-working area where the slag heaps clearly point to non-ferrous smelting. In another, titanium-rich iron slags are found in the vicinity of iron ore deposits which contain no titanium. The reason for the complexity of the sites rests with the pattern of mineral exploitation in Macedonia. It is the result of many centuries of activities carried out on different scales. In addition, the remains which are standing today may or may not be indicative of the original scale of operations. There is also the factor of polymetallism, namely that the ores may have been exploited for more than one metal. Nevertheless, three distinct types of sites have emerged:

1) The iron-working sites on Thasos, including: Mantaloudi, Paidouli, Kalovria, Astris, Theologos, Oxia, Kazani, Tragi and Kato Larnaki (Fig 3.1.2). They are characterised by slag scattered over a few square meters. Some contain a few tens of kg of slag (Oxia, Tragi, K Larnaki), the rest a few hundreds of kg. A few tuyere

Fig. 3.1.2 Sites on Thasos sampled for ore, slag and artefacts.

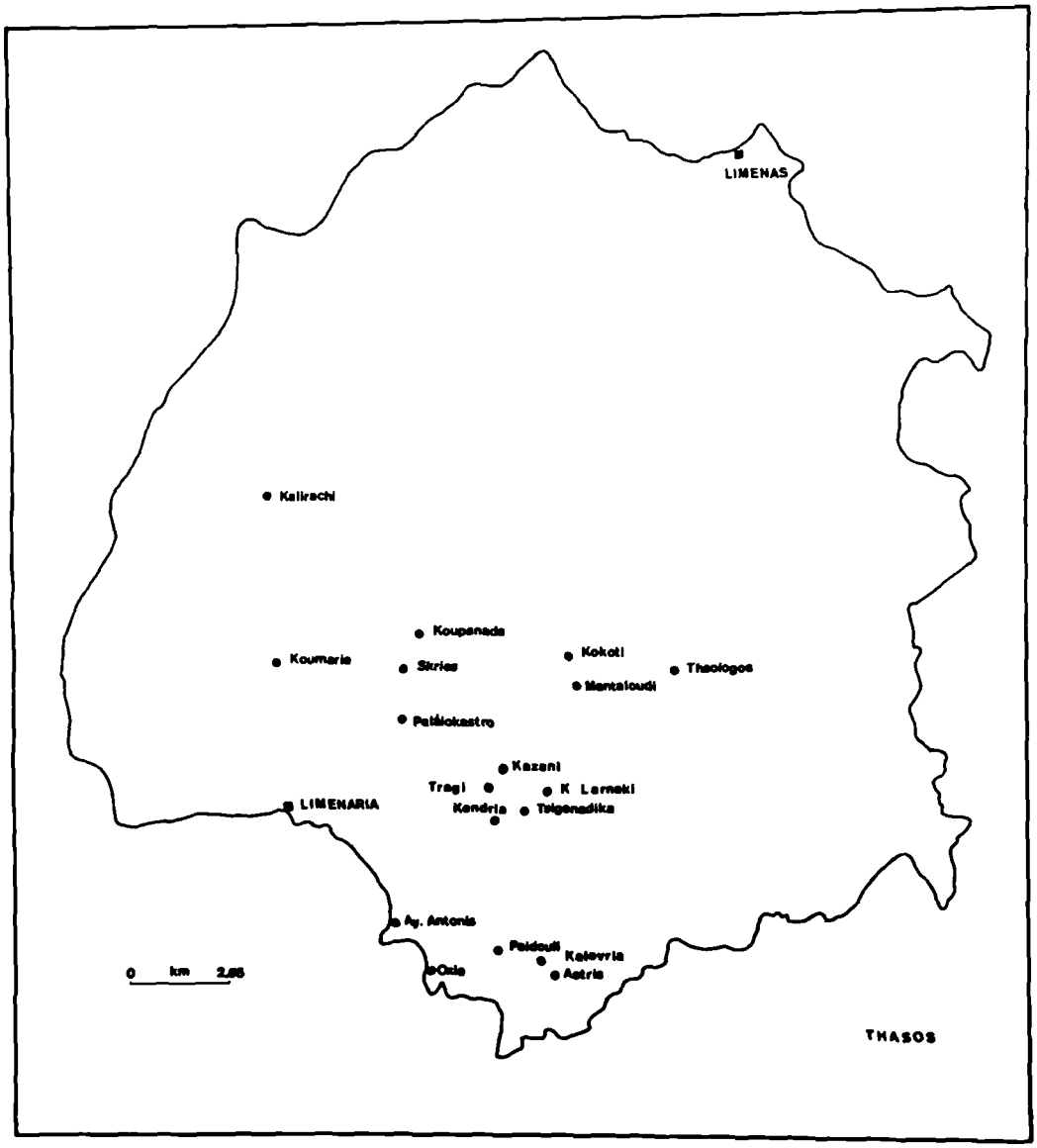
LIMENAS
Kalirachi
Koupenada
Koumaria
Sikries
Kokoti
Theologos
Mantaloudi
Paliokastro
Kazani
Tragi
K Larnaki
LIMENARIA
Kendria
Tsigonadika
Ag. Antonis
Paidouli
Kalovria
Astris
Oxia
0 km 2,05
THASOS

fragments were evident ranging in size from 5cm (Oxia) to 1-2cm (Kazani) inner diameter.

The sites are concentrated in the S. and S.E. parts of the island. They are rather remote and inaccessible with no visible footpaths leading to them and at an altitude of a few hundred meters, mostly on the flat tops or the rather steep slopes of hills. They are situated inland usually 2-3 km from the coast and are not visible from the sea. Natural springs may be present nearby but not in the immediate vicinity of the working area.

Vakalopoulos (1973, 326) points out that fear of piracy in the northern Aegean from the 14th c. forced the inhabitants to abandon the coastal areas and move inland where they were protected by precipitous and inaccessible cliffs. This observation is in accordance with the topography of the iron-working sites we surveyed on Thasos. Thermoluminescence has recently provided valuable independent dating evidence at Oxia and Paidouli. Mrs J Huxtable at the Oxford Research Laboratory for Archaeology kindly carried out dating of one tuyere fragment from each site. The date range (450-700 BP) corresponds to the late Byzantine-early Ottoman period.

2) The iron-working sites of Mainland Macedonia, which include Vathytopos, Katafyto (few hundred tons), the slag heaps at the 25th km of the Serres-Vrontou road (few tons), Piges Aggiti (one-two hundred kg), Sidirochori (one-two tons), Kalapoti, Kimmeria (few tons) and Domatia (Fig 3.1.1).

All these sites are characterised by large slag heaps of the order

of a few tons with one exception, Piges Aggiti. They are located by streams which are often channeled within leats probably built to direct water to water-driven bellows. Some of these sites have been in operation as recently as the turn of the century (Katafyto, G Stavrakis pers. comm.) and remains of large-scale buildings are still visible under thick vegetation at the same site. In a survey at Kimmeria in Xanthi during the mid-1970's the remains of a furnace were clearly evident (Stavropodis 1980).

3) The silver/gold extraction sites at Palaia Kavala which include Makrychori (few hundred tons), Eleftheroupolis (few tons), Tria Karagatsia (few hundred tons), Dipotama (few hundred tons), Pyrgiskos, Kastanies (Fig 3.1.1).

These sites are characterised by large slag heaps, and are all situated in rather inaccessible areas, sometimes on mountain tops, with occasional evidence for leat systems for water supply. Another common characteristic is the presence of speiss, metallic compounds consisting of iron arsenides. They are found within the slag heaps and, although less abundant than the slag, are usually present in the form of plates or lumps of various sizes or prills within the slag.

4) Slag found at archaeological sites. This category includes iron and occasionally copper slag from well stratified deposits. They derive from a variety of ore sources and each type will be discussed individually.

Chapter 3 describes the results of the analytical investigation of the slags and artefacts from the excavated sites

and the undated slags collected during field surveys. Analyses were undertaken to elucidate the extractive processes that gave rise to the slags and to match dated or undated slags and artefacts to particular types of iron ore deposits. Having identified the ore sources, a set of experimental smeltings were carried out with two purposes in mind: to elucidate the nature and composition of the archaeological process-slags and metal, and to appreciate the range of problems associated with smelting these ores in a bloomery furnace.

The chapter begins with an introduction to the geology and mineralization of Macedonia (section 3.2). The archaeological and experimental data are then discussed chronologically and on the basis of iron ore typology. The LBA-EIA copper and iron slags from Kastri are presented first (section 3.3). A brief summary of the bloomery process is included in section 3.4. The discussion is based on the experimental smeltings of a number of Greek iron ores carried out at Ashdown Forest, Sussex, in a shaft furnace resembling those on the illustrations of the 6th and 5th c. BC Attic vases. The various stages in iron making and their associated products and waste are described.

The excavated iron slag and artefacts from the Museums in Thessaloniki, Kavala, Thasos and Pella (excavation at Petres) are then presented in section 3.5. These slags are derived from the smelting of limonitic ores with some phosphorus and/or manganese. The metallographic examination of objects from the cemeteries at Vergina and other locations sheds some light on the technique of

manufacture of some of the earliest functional iron objects in Greece. Section 3.6 expands on the titanium-rich iron slags of Thasos and Mainland EM produced from the smelting of titanium-rich magnetite sands, the product of weathering of the Vrontou granite or the Thasos gneiss. The problems encountered in their experimental smelting are also discussed.

Section 3.7 presents the manganese-rich slags from the region of Palaia Kavala and the arsenic-rich iron (speiss) produced as a byproduct of the smelting of these ores. The process of smelting such ores which usually contain precious metals has been elucidated via the experimental smeltings of iron ore from Petropigi. The suggested method of extraction is corroborated by an eye-witness account by Belon, a French traveller in the Chalkidiki in the 16th c. AD, presented in Chapter 2.

Finally, section 3.8 presents the first evidence for possibly intentional smelting of nickel-rich iron laterites in Greece, at the Hellenistic settlement of Petres in West Macedonia. The experimental nickel-rich iron bloom and slag are discussed in relation to the archaeological evidence from Petres and a sample of meteorite (Canyon Diablo meteorite, Arizona). The purpose of including the meteorite sample is to highlight the points distinguishing terrestrial from meteoritic nickel-rich iron.

The slags discussed in the last three sections contain very diagnostic major and minor elements which partition in the slag or the metal. Thus, it was possible to establish ore-type provenance by carrying out a microprobe examination of metal and slag

inclusions. For the majority of the artefacts analysed, however, which do not contain these diagnostic elements, assessment of their possible ore source would require a sophisticated statistical treatment of their chemical compositions.

An inventory of archaeological sites (and their abbreviations as they appear in various Tables of analyses throughout the text) are given in appendix 3.1.2. An inventory of metallurgical slag, ceramic fragments, ore samples and other material collected during the field surveys in EM are included in appendix 3.1.3. Of these, only the slag and ore were analysed.

3.2 Geology and Mineral Resources of Macedonia and Thasos

3.2.a General

Macedonia is the richest metalliferous region in Greece. As a result, an extensive literature exists on its mineral deposits, the outcome of geological surveys and laboratory investigations carried out on a large scale by the Institute of Geological and Mining Exploration (IGME), as well as private companies with mining interests in specific areas. I have consulted a number of the relevant publications:

* IGME Minerals Map of Greece (Metalogenetikos Chartis tis Hellados, 1973): handbook 1975
* Voreadis (1953) on Thasos
* Maratos and Andronopoulos (1966) on the mineral wealth of Macedonia and Thrace
* Stavropodis and Pourni (1971) on the radiometric survey of

Northern Greece

* Marinos (1982) on the geology and minerals of Greece in general
* Spathi et al (1982) on the manganese iron deposits of Palaia Kavala
* Theophilopoulos (1982) on the iron deposits on Thasos
* Gialoglou and Drymonitis (1983) on the regions currently exploited for minerals resources in EM and Thrace
* Stavropodis (1983) on the radioactive black sands of the Vrontou granite
* Karamatzani and Kaklamani (1983) on the possible exploitation of the Vrontou granite
* Albadakis (1981) and Katsikatsos et al (1981) on the industrially exploited nickel-rich lateritic iron ores of central Greece (Boeotia) and the smaller deposits near Edessa, Garagouni (1971).

The list, by no means exhaustive, naturally focuses on the areas associated with the material analysed in this thesis.

Macedonia is divided into four geotectonic zones of distinct geological age and formation (Fig. 3.2.1). Moving from west to east, the Pelagonian zone consists of metamorphosed and semi-metamorphosed rocks of Paleozoic Age. These were originally sedimentary and igneous types which were converted to schists and marbles. The Vardar Zone encompassing the Axios Valley and the western most of the three prongs of the Chalkidiki (Kassandra) is more complex and consists of ophiolites, volcanics, limestone and flysch. The Kassandra peninsula consists of Tertiary gravels, sands and marls. The Serbo-Macedonian zone, originally part of the Rodhope Massif (the area streching to the Turkish border), is now reclassified to extend only to the Strymon. Both are basically similar, consisting of metamorphic and igneous rocks with granitic

Fig. 3.2.1 The geology of N.E. Greece (after naval Intelligence: Greece III, Fig. 23). A acid lava (trachyte); B granite; C serpentine, diabase, porphyritic gabbro; D gneiss, mica schist and other metamorphic schists; E marble. 1 sandstones, shales and conglomerates (mostly folded Mesozoic); 2 limestones (mostly folded Mesozoic); 3 Tertiary gravels, sands, marls, clays and sinter, all unfolded; 4 alluvium (in places Quartenary).

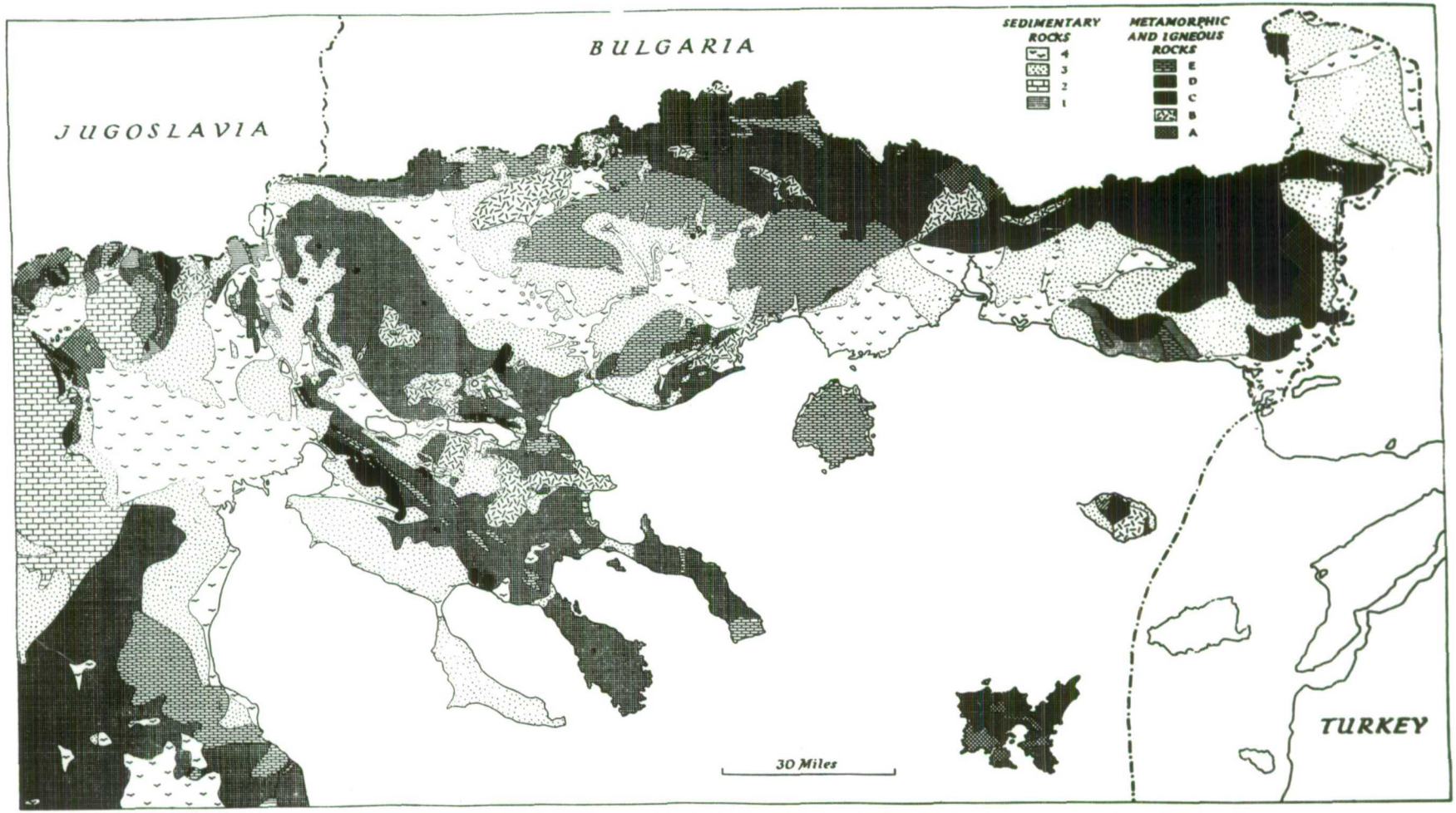
BULGARIA
JUGOSLAVIA
SEDIMENTARY ROCKS
4
3
2
1
METAMORPHIC AND IGNEOUS ROCKS
E
D
C
B
A
30 Miles
TURKEY

masses. The map, Fig. 3.2.2 by Gialoglou and Drymonitis (1983), reproduced here with the kind permission of the authors, gives more emphasis than Fig. 3.2.1 to EM and Thasos.

The mineral deposits of Macedonia with most relevance to this work are the following:

a) the iron deposits of Thasos, the largest in Greece, are predominantly limonite, related to the smithsonite desposits of the island, and contain barite and occasionally copper carbonates (malachite and azurite).

b) the Mn-rich iron deposits of the Mainland opposite Thasos, namely the region of Palaia Kavala, consisting of iron oxides with the additional presence of lead, zinc and arsenic. Gold and silver are also present.

c) mixed sulfides (pyrite, chalcopyrite, galena, arsenopyrite, sphalerite) and their associated oxidised ores. Gold and silver are present.

d) Nickel-rich lateritic iron deposits, although not of the size and potential of those in Lokris and Euboea, occurring in the area around Edessa and Kastoria in WM (Fig 3.2.3).

The partial list is intended to illustrate the difficulties encountered in matching slags to ores and thus elucidating the extraction processes carried out in each area. Slag is the main guide to the ore source, but problems arising from sample inhomogeneity and the fact that slag in the field may be the waste product of more than one process can complicate the interpretation of data.

Fig. 3.2.2 Geological map of E. Macedonia and Thasos (after Gialoglou and Drymonitis 1983).

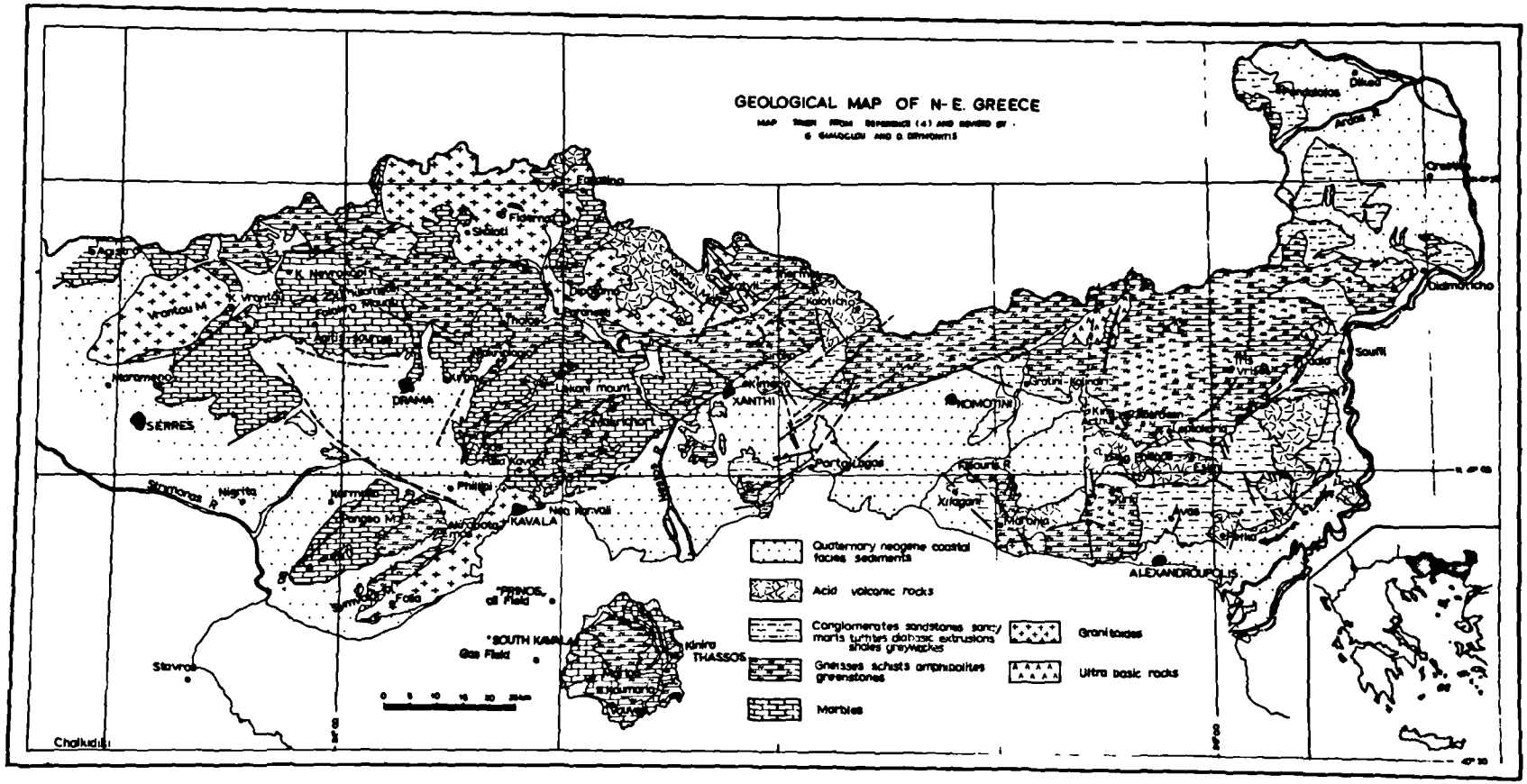
GEOLOGICAL MAP OF N-E. GREECE
SERRES
DRAMA
XANTHI
KAVALA
KOMOTINI
ALEXANDROUPOLIS
THASSOS
Kinira
Stavros
Chalkidiki
Quaternary neogene coastal facies sediments
Acid volcanic rocks
Conglomerates sandstones sand/ marls tuffites diabasic extrusions shales greywackes
Gneisses schists amphibolites greenstones
Marbles
Granitoides
Ultra basic rocks

3.2.b. Iron

3.2.b.1 Limonite/Hematite: Thasos

Geologically, Thasos consists of a series of metamorphic gneiss and marbles lying in succession and in conformity with one another (Voreadis 1953). The iron ore deposits, estimated at eight million tons, are presumed to be of hydrothermal origin and are to be found in the zone of contact between the two types of metamorphic rock. Theophilopoulos (1982) carried out an extensive survey and analysis of the major iron deposits on Thasos. He established four types of iron ore, each one the product of different metallogenic conditions (Theophilopoulos 1982, 31):

Type I - Siliceous: mainly hematite containing manganese compounds, hence its black colour, and thin bands of quartz. It is very hard and not cost effective for exploitation. It is not very common, most of it having undergone transformation to the types below.

Type II - Calcareous: the most common type, and associated with carbonates (including copper) and barite. The major deposits at Mavrolaka, Koupanada, Koumaria-Platania contain this type (Fig. 1.2).

Type III - Colloidal: richer in iron than the other types, low in manganese, silica and carbonates, and derives from Type II. Its colour is black to brown.

Type IV - Soft: limonite with manganese compounds and small concentrations of silicates and carbonates. The colour ranges from

black to red, brown and yellow.

Arsenic-rich iron ores occur at only one location on the island, at Kokoti (c. 1.8% As) (Fig. 1.2). The iron content at Kokoti is higher than elsewhere (54% Fe) (Theophilopoulos 1982, 51).

Table 3.2.1 contains analyses of iron ore collected during the first field survey on Thasos, in the vicinity of surface slag. It was assumed at the time that the slags were the waste product of smelting of those small outcrops. In the event, this did not prove to be the case. None of these ores contained titanium which was present in all the slags examined. In addition, nearly 50% of the 'ore' samples (TSIM, MANTM4, KUPYELLOR, KOK3, Table 3.2.1) collected were too low in iron (high in gangue) to have been charged in an iron-making furnace without some prior enrichment.

3.2.b.2 Manganese-rich iron ores: Palaia Kavala, EM

The iron deposits of the Mainland are of hydrothermal origin and occur in association with manganese (27-43% iron oxide, 18-43% manganese oxide) with the added presence of other elements like Pb, Zn, As, and also Au and Ag. The iron manganese ores derive from the oxidation of sulfides (pyrite, galena, chalcopyrite). The mineralization in this region has been studied extensively by Spathi et al (1982). The discussion included here is extracted from this publication.

The region of Palaia Kavala (Fig. 3.2.2), outlined by the

TABLE 3.2.1 XRF ANALYSIS OF THASOS IRON ORES

	TSIM	MANTM4	MANTM5	OXIM2	TRAGM1	TRAGM2	KUPYELO	KUPBLOR	KOK3	KOK4
SiO_2	9.80	1.93	2.42	5.66	4.90	2.40	13.95	0.50	73.98	2.97
Al_2O_3	4.55	0.08	0.07	0.21	2.85	1.70			1.25	0.05
Fe_2O_3	6.17	5.14	59.70	38.00	32.30	45.90	7.61	53.48	7.81	74.15
MnO_2	1.51	0.04	0.10	2.56	0.05	0.05	0.62	5.03	30.45	0.57
CaO	42.00	68.77	12.04	31.69	30.25	22.85	38.24	16.84	1.08	0.74
MgO		0.83	0.15	0.41	0.40	0.35	0.78	0.49	0.10	0.17
BaO		*23		*1382					0.77	
TiO_2		0.05	0.06	0.01			0.16	0.11	0.09	0.05
K_2O		0.07	0.10	0.03			0.36		0.27	0.04
P_2O_5		0.42	0.14	0.03			0.07	0.01	0.13	0.17
As		*41	*318	*4	0.33	0.50	*33	*10	*31	*183
Cu	0.02	*15	*43	*4			*48	*7	*21	*4
Pb	0.20	0.27	1.07	0.01	0.06	0.11			0.29	0.03
Zn	0.17	*208	*1378	*70	0.28	0.17	*291	*1255	*794	*387
Cr		*2	*22						*22	*28
V		*13		*16					*458	*466
Ag		*7	*5	*5			*1	*5	*1	*5

* denotes ppm

villages of Palaia Kavala, Zygos, Kirgia, Makriplagi and Makrihori, consists of schists with marbles and granitic offshoots. Mineralization occurs as usual at the contact of marbles and mica schists and is developed along two zones, N.E. and N.W. in direction. The former follows the line of occurrences at Mandra Kari, Gorizo Lofos and Giolia, while the N.W. occurrence is evident at the village of Chalkero and the site of Chorissa. It is mentioned in passing here that the occurrence at Gorizo Lofos was visited by the present writer, and slag was picked up in the vicinity about 1km to the south at the site of 'Tria Karagatsia'.

The two directions of mineralization are quite distinct in both chemical and mineralogical terms. In the N.E. the iron manganese ores are associated with Pb, Zn and Ag, while the N.W. is associated with Cu and Au and occasionally Bi. Arsenic is present in both. The iron oxides are goethite, limonite and manganese minerals nsutite (gamma-MnO_2) and cryptomelane (alpha-MnO_2). The alteration of chalcopyrite to goethite suggests that there is an enrichment of copper in lower levels. Very little arsenopyrite was present, and indeed the origin of arsenic in these ores is not well understood (Spathi et al 1982, 87). No ores were collected by the writer during surveys in Palaia Kavala with only one exception, at Petropigi (Fig 3.1.1) on the south-east fringes of the region.

The exploitation of the iron deposits of Palaia Kavala during one or more periods seems to have been extensive, in view of the considerable size of some slag heaps (a few hundred tons).

3.2.b.3 Titanium-rich iron sands: Thasos and EM Mainland

One iron ore source not reported in any of the modern mineral exploration maps is the magnetite (black) sands of Thasos and the Mainland. Still, there is good evidence that these sands were indeed exploited in the region for iron from the 15th c. AD and possibly since the Hellenistic/Roman period (see section 3.6). Although the magnetite deposits on Thasos are very few (Epitropou and Gialoglou, unpublished), magnetite sands are present on the southern shores of the island (Pefkari, Aghios Antonios) (Fig. 3.1.2). They are the result of weathering of gneiss in which titanium is included in amounts up to 1.8% TiO_2. Analysis of Thasos gneiss carried out by G. Gialoglou (Photos et al, in press) is included in appendix 3.2.1. Weathered gneiss is mechanically enriched in magnetite by the effect of seasonal wave action which results in the formation of characteristic layers of black and siliceous sands (Plate 1b) evident in the two locations mentioned above. The thickness of the iron sands layer varies up to 2.5cm. Collection of these sands must have taken place with thin metal sheets or shovels as demonstrated in Plate 1a. The sand would have been dried and subsequently winnowed to remove light quartz particles.

Table 3.2.2 includes analysis of undressed iron sands from Thasos collected from Aghios Antonios near Potos (Fig. 3.1.2) and carried out by XRF. Only the major elements are presented.

Plate 1

(a) Collection of Ti-rich magnetite sands (black patch) at Aghios Antonios, Thasos (plastic bag with black iron sands). Thin metal plates are used as shovels to skim off the black layer.

(b) Multiple layers of black and siliceous sands shown in a shallow section along Aghios Antonios beach, Thasos.

(c) Scraping the Vrontou weathered granite. For comparison with similar Japanese practices last century, see illustration in frontispiece in this thesis.

(d) Magnetite sands accumulating in stream beds at the foot of the granite.

(e) Titanomagnetite grain of Vrontou sand; light phase hematite, dark phase magnetite showing advanced weathering of the grains. 100x

(f) Ulvospinel/ilmenite needles (light grey) exsolving out of magnetite grain (dark grey). 100x

(g) Weathered titanomagnetite grain consisting of hematite (light grey), magnetite (dark grey); inclusions of garnets (black). 100x

(h) Weathered titanomagnetite consisting of hematite (top section), magnetite (bottom section) with garnet inclusion. 100x

Plate 1

a

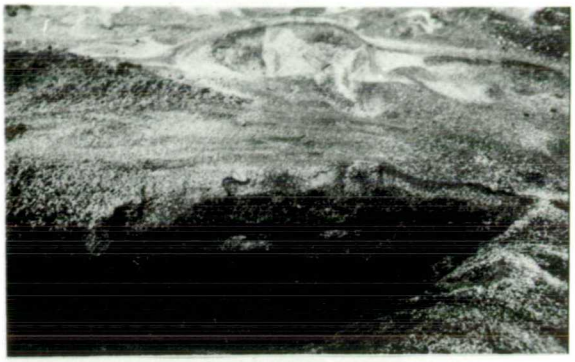

b

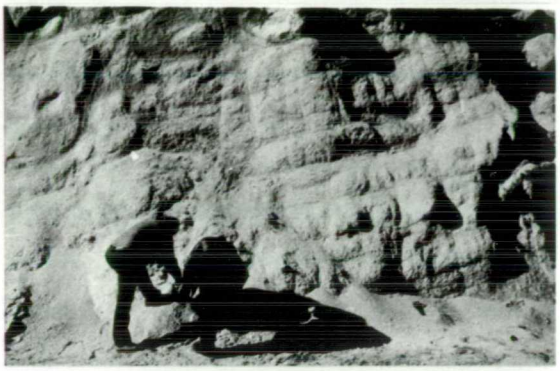

c

d

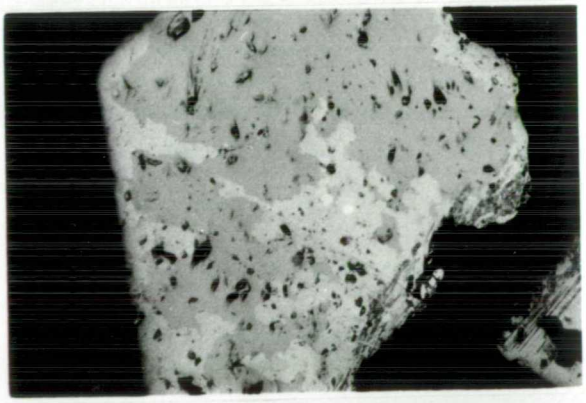

e

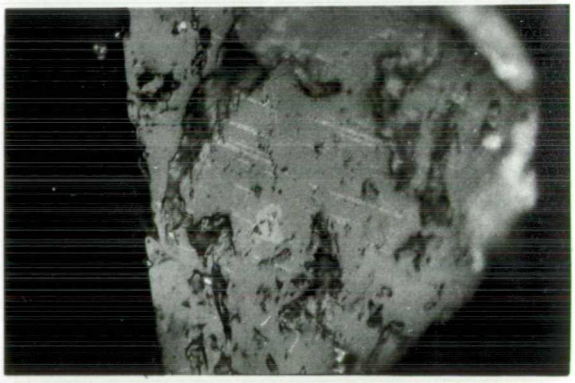

f

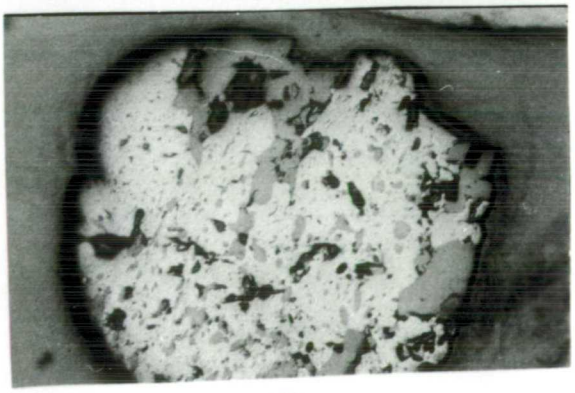

g

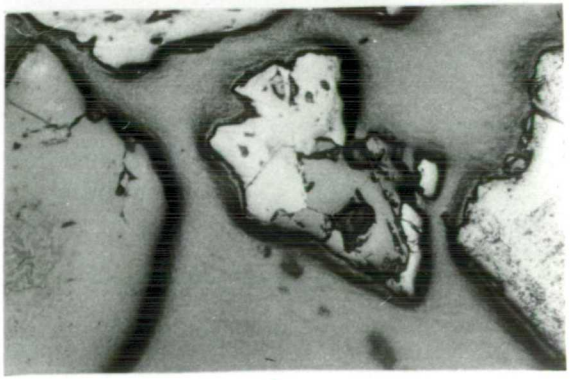

h

Table 3.2.2: Analysis of undressed Thasos iron sands

%age SiO_2	TiO_2	Al_2O_3	Fe_2O_3	MnO_2	CaO	K_2O	MgO
12.04	6.95	6.85	59.55	3.18	3.44	0.16	0.72

Heavy mineral separation of the titanium-rich sands carried out by G. Gialoglou (Photos et al, in press) with trichloro-bromoethane showed that the light fraction consisted of quartz (80%), calcite (10%) and silicates (tourmaline, muscovite and biotite; total 10%). The heavy fraction was subsequently separated into three subfractions using a 15000 Gauss magnet and each was analysed with atomic absorption spectrometry. The first subfraction, constituting about 60% of the total sample, was very magnetic and was picked up at a distance of 5 cm from the magnet. The second was less magnetic (magnet at or near contact) and made up 26% of the total, while the third was completely non-magnetic (14% of the total). The magnetic fractions are magnetites with various amounts of titanium incorporated in the magnetite lattice. The non-magnetic part consists of garnets.

Table 3.2.3: AA analyses of magnetically separated iron sands

	%age								
Fraction	SiO_2	TiO_2	Al_2O_3	Fe_2O_3	MnO_2	CaO	MgO	V_2O_5	Na_2O	LOI
Very magnetic	3.3	4.5	1.7	90.0	0.3	0.5	0.5	0.2	0.1	0.0
Magnetic	6.4	8.9	1.7	81.5	0.3	0.6	0.2	0.0	0.0	1.1
Non-magnetic	27.7	4.1	15.7	36.4	10.4	7.8	1.1	0.0	0.0	1.1

X-ray diffraction of the magnetic portion of the Thasos sands revealed magnetite, hematite, maghemite and quartz. Electron microprobe analysis of mineral grains (Plate 1g-h) are included in

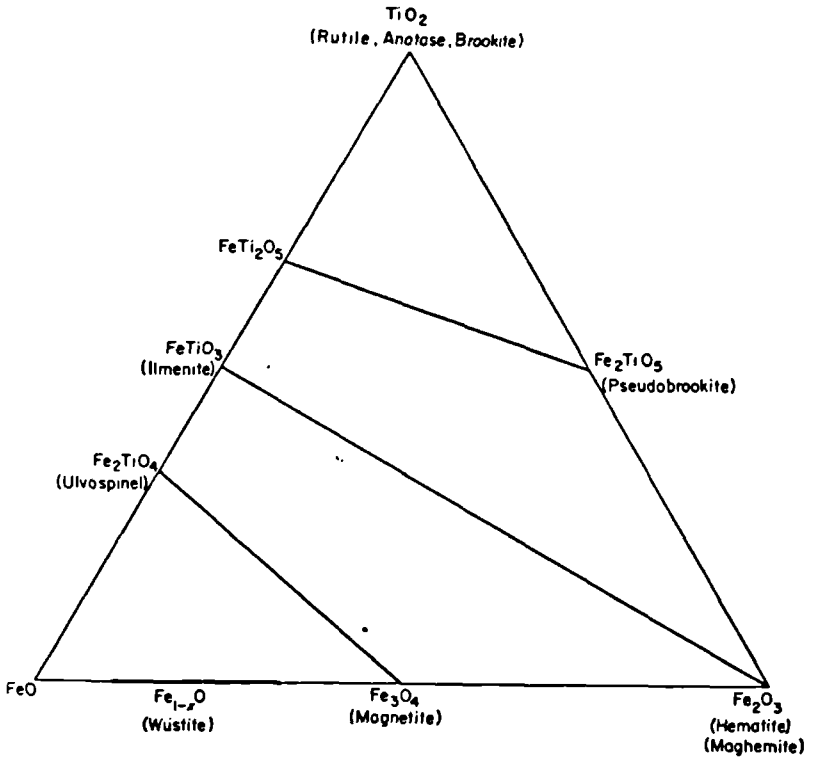

Fig. 3.2.3 $FeO.TiO_2.Fe_2O_3$ ternary phase diagram (after Buddington and Lindsley 1964)

Table 3.2.4. Apart from the gangue material (garnets), (spot analyses 1,2), two types of titanium-rich magnetite grains are included, one with high (spot analysis 4) and one with low titanium (spot analyses 3,5) content. The composition of the grains corresponding to spot analyses 3, 4, 5 can be characterised as solid solutions between FeO-Fe_2O_3 and TiO_2, clearly represented by the diagram in Fig. 3.2.3. Solid solutions of TiO_2 and Fe_3O_4 lie along the line representing the isomorphic series, of which ulvospinel (Fe_2TiO_4) and magnetite are the end members. The distribution of the titanium is spread over the entire grain.

Table 3.2.4: Microprobe analysis of Thasos iron sand

%age	MgO	Al_2O_3	SiO_2	K_2O	CaO	TiO_2	MnO	FeO	Sb_2O_5
Spot 1	4.13	21.09	38.55	0.00	1.77	0.17	22.07	13.66	0.0
Spot 2	0.97	11.45	38.15	0.80	17.87	0.35	2.26	27.46	1.57
Spot 3	0.0	1.54	0.0	0.0	0.0	3.3	0.0	95.15	-
Spot 4	0.0	0.72	1.10	0.0	0.0	21.71	0.0	76.47	-
Spot 5	1.78	3.34	3.34	1.20	1.34	4.26	1.9	81.93	-

FeO represents both Fe^{2+} and Fe^{3+}

On the Mainland, Ti-rich magnetite sands are the products of weathering of the Vrontou granite. Natural enrichment occurs at the foot of the granite in stream beds. In addition to natural dressing, it is probable that ore beneficiation with the use of water channels must also have taken place. Ethnographic parallels of iron sand dressing in Japan give a glimpse of this very efficient but also very labour intensive process (Kubota 1970). The ore is scraped off the weathered granite wall in a manner similar to that illustrated in the watercolour on the front page of this thesis.

Analyses of the Vrontou granodiorite by Karamatzani and Kaklamani (1983) showed that it contains grains of magnetite dispersed in the granitic matrix. They report 2-3% Fe_2O_3 in the granite but with a combination of desliming and magnetic separation a magnetite-rich portion can be obtained with up to 73% Fe_2O_3, thus enhancing considerably the iron content of the 'ore' (Karamatzani and Kaklamani 1983, Table 8). Kubota (1970) and Nishida (1973) report similar results from the beneficiation of iron sands in Japan for the traditional iron-making process, the Tatara.

The iron sands of Vrontou contain both magnetite and ilmenite

and are radioactive due to the presence of uranium containing zircon and thorium compounds (Stavropodis 1983). Stavropodis and Pourni (1971) measured radioactive black sands at the site of Loutra Eleftheron at the foot of the Kavala granite and in the slag heaps of Katafyto, as well as at the 25th km on the Serres-Vrontou road (Fig. 3.1.1). Radioactive slags were also found at Domatia (Fig. 3.1.1) in the foothills of the Pangaion (Stavropodis 1983).

Optical microscopy of the Vrontou sands was quite illuminating (Plate 1e-f). The light phase is hematite, the dark phase magnetite suggesting the partial weathering of the magnetite. This explains the relatively weak magnetism of the Thasos and Vrontou sands.

Plate 1e-f shows light ulvospinel and ilmenite needles exsolving out of the magnetite lattice because of excess titanium. When both minerals have been detected, as in the case of Vrontou sands, it is usually the ulvospinel which exsolves first , followed by ilmenite (Ramdohr 1980, 894). Ulvospinel forms a 'cloth texture' structure seen only under high magnification. Ulvospinel exsolution is a time-dependent phenomenon and has been used to calculate the rate of cooling of iron oxides (Price 1982).

3.2.b.4 Nickel-rich iron laterites: Edessa/ Kastoria, WM

Nickel-rich laterites are essentially hydrated iron oxides containing about 1-1.4% Ni. They cannot be considered nickel ores like the iron nickel mineral pentlandite, a sulphide containing about 35% Ni ($(Fe,Ni)_9S_8$), or garnierites, a nickel magnesium

silicate $(Ni,Mg)_3Si_2O_5(OH)_4$ containing about 45% Ni.

The process of laterization which is also the mechanism of formation of bauxites, the aluminium oxides, involves the leaching of elements like Na, Ca, K, Mg from the parent rock under wet tropical conditions. Such conditions of alternating wet and dry seasons occurred in Greece in the Cretaceous period. During the dry season the leached elements rise to the surface by capillary action and their salts are deposited in situ only to be washed away and redeposited elsewhere in the wet season that follows. The laterites of Greece are formed as crusts on the weathered iron-rich igneous ophiolitic rocks (serpentinites). They have been transported some distance from their source to be deposited as sedimentary rocks in the form of beds and lenses with chromite grains. Under the right pH conditions the solution containing these leached elements can dissolve silica leaving behind aluminium or iron oxides depending on the parent rock. If the original source was a basic igneous rock, laterites were formed, as opposed to bauxites which themselves derive from an acidic granitic rock. Laterites are very common in other parts of the world like S.E. Asia, but they are not always nickel-rich. They have been used as construction material, since, although they can be easily shaped into bricks, once exposed to the air they become cement-like (McNeil 1974).

Fig. 3.2.4 is reproduced from Albadakis (1981) and shows the distribution of the Ni-rich iron deposits in Greece. WM is endowed with lateritic deposits, although not on the scale of those in Lokris. The modern plant at Larymna in Lokris exploits those

Fig. 3.2.4 Distribution of Ni-rich iron laterites in Greece (after Albadakis 1981)

deposits by carrying out reduction in electric furnaces to produce an iron nickel alloy of 70% Fe-30% Ni. Albadakis (1981) also published a number of analyses of lateritic iron ores reproduced in Table 3.2.5 for purposes of illustration. Kastoria is the only location in Macedonia with laterites that are presented here. The Edessa outcrops nearest to Petres, the archaeological site with evidence for smelting of laterites in antiquity, have been reported by Garagounis (1971) to contain 0.8 - 1.55 % Ni. No Cr analysis is given.

Table 3.2.5: Analysis of Ni-rich laterites (after Albadakis 1981)

(%)	Skyros	Kimi	Boeotia	Parnis	Kastoria
Ni	1	1	1	0.7	1
Co			0.1	0.1	0.1
Fe	35	20	33	36	32
SiO_2	25	44	14	40	40
MgO	4	4.5	4	5	1.2
CaO	0.5	1	2	0.6	0.7
Mn		0.3	0.5		
Al_2O_3	11	8	15	11	2.5
Cr_2O_3	3	2.5	3	1	2
S			0.2		
LOI	7		12	5	11

3.2.c Mixed sulfides: Chalkidiki, CM and Pangaion, EM

In C. and E. Macedonia mixed sulfide mineralization is of hydrothermal origin. It consists of galena, pyrite, chalcopyrite and sphalerite. In the western part of Thasos there are argentiferous lead and zinc carbonate deposits, called locally calamine. They occur within marble and are the oxidized zone of the mixed sulfides of the same elements. They are almost always associated with barite (Voreadis 1953).

In the Chalkidiki chalcopyrite and copper oxides occur in the zone of contact of marble and gneiss. The mineralization is associated with the granitic intrusion of the Chalkidiki. At Kimmeria (Xanthi) (Fig. 3.1.1) copper ores, malachite and chrysocolla,are of hydrothermal origin and are also associated with the local granitic intrusion. At Angistron near the Bulgarian border as well as in the Vrontou-Panorama region, mixed sulfide mineralization associated with the Vrontou granite is also present (Fig. 3.2.1) (Gialoglou and Drymonitis 1983). The mixed sulphide mineralization will not be discussed in any further detail. It is mentioned here in connection with Belon, a French traveller to the Chalkidiki in the 16th c. AD. He reports (1553) pyrite being charged in the furnaces there. Microprobe analysis of slags from the same area (Olympias, Myloudi) visited by Belon are presented in appendix 3.7.3.

3.3 Late Bronze Age-Early Iron Age Copper/Iron slag from the cemeteries at Kastri on Thasos

3.3.a Copper slags

Copper slags together with iron slags were found in a LBA-EIA context of the cemeteries at Kastri, namely Larnaki, Tsigganadika and Kendria (Koukouli-Chrysanthaki 1986) (Fig 3.1.2). They come from Tsigganadika graves T14 (D396), T18 (D385, D387), T23A (D383), T23B (384a), T24 (D394a, D395), Larnaki graves L5B11 (D399) and L2ST and Kendria grave K3A/69 (TSIORE). Of these T14 dates to EIA,

T18 to LBA-EIA, T23 and T24 to EIA, Larnaki and Kendria graves to EIA (Table 3.3.1). T23 contains both copper and iron slag.

The copper slags shown in Table 3.3.1 originate from two sites on Thasos, namely Kastri and Palaiokastro. Kastri copper slags (Plate 2b-e) are composed of three phases, of which the silicate matrix is usually the most prominent. The other phases are primarily wustite and fayalite, $2FeO.SiO_2$,an olivine, with some evidence for magnetite distinguished from the wustite dendrites by its plate-like structure. Calcium-rich olivines with less than 5-6% CaO are reported as fayalite, 5-12% CaO as 'fayalite' and more than 12% CaO as kirschsteinite ($FeO.CaO.SiO_2$). Often the glassy matrix can be of kirscshsteinitic composition, and in that case it is reported as matrix. This classification system has been followed throughout the text, in view of the high CaO contents evident in slag from Greece, as opposed to other geographical regions (Photos et al 1985; Photos and Salter 1986).

The Kastri copper slag matrix consists of barium iron silicate ($BaO.FeO.4SiO_2$) with additions of CaO and varied levels of Al_2O_3, BaO substituting for CaO. Electron microprobe spot analyses revealed a concentration of up to 31% barium oxide (Table 3.3.1). The origin of this barium is barite (barium sulphate), a mineral commonly associated with iron deposits on Thasos (Theophilopoulos 1982, 32).

In the majority of the copper slags, copper occurs in both the prills and the matrix (1%-7% CuO). The metallic prills consist primarily of Cu, Fe and S, (D385, Table 3.3.2). The relative ratios

Table 3.3.1: Microprobe analyses of copper and iron slag from Kastri (LBA-EIA) and Palaiokastro (undated), Thasos: silicate phases

Sample No.	Museum No.	Date	Phase	Na_2O	MgO	Al_2O_3	SiO_2	P_2O_5	SO_3	K_2O	CaO	TiO_2	MnO	FeO	BaO	CuO	As_2O_3	Sb_2O_3
Kastri																		
Iron slag																		
L2/ST			wustite	0.00	0.00	0.37	0.54	0.00	0.00	0.00	0.17	0.92	0.26	92.47	0.00	0.00	0.00	
			fayalite	0.00	3.47	0.00	29.81	0.00	0.00	0.00	1.97	0.28	0.96	59.85	0.00	0.00	0.00	
			fayalite	0.00	0.00	0.00	30.44	0.00	0.00	0.00	1.82	0.35	0.86	62.01	0.00	0.00	0.00	
			matrix	0.00	0.00	20.80	33.66	0.72	0.00	3.54	12.61	0.83	0.00	27.25	0.00	0.00	0.00	
D399	L5B11	EIA	matrix	0.00	0.14	3.96	33.16	0.53	0.00	1.33	11.68	0.27	0.54	47.25	0.00	0.00	0.00	
"	"		'faya'	0.00	0.00	1.92	27.21	0.40	0.00	0.00	11.01	0.00	0.32	50.89	0.00	0.00	0.00	
"	"		matrix	0.00	0.00	8.29	36.51	0.94	0.00	2.82	10.18	0.42	0.43	37.36	0.00	0.00	1.05	
D383	T23A	EIA	wustite	0.00	1.06	9.89	0.48	0.00	0.00	0.00	0.29	3.23	0.70	80.35				
			matrix	0.00	0.69	8.95	30.00	0.38	0.00	0.39	13.81	6.07	0.97	27.28				
Cu slag																		
D394a	T24	EIA	matrix	0.00	11.35	0.21	34.69	0.00	0.00	0.00	28.94	0.00	1.36	22.53	0.00	0.00	0.00	
			matrix	0.00	1.05	10.54	48.43	0.56	0.00	2.73	11.51	0.36	0.25	12.49	3.89	4.36	0.93	
			matrix	0.00	1.03	9.61	50.76	0.00	0.00	2.69	10.24	0.46	0.22	12.66	3.56	3.69	0.87	
D384a	T23B	EIA	matrix	0.00	0.00	11.75	36.77	0.00	0.00	2.08	3.27	0.00	0.26	11.64	31.09	2.82	0.00	
			matrix	0.00	4.67	2.45	47.18	0.00	0.00	0.32	20.79	0.00	0.76	19.47	4.40	0.00	0.00	
			matrix	0.00	0.83	1.77	32.45	0.00	0.00	0.81	5.43	0.00	1.28	23.11	29.20	1.71	1.10	
D396	T14	EIA	matrix	0.00	0.00	5.95	36.24	0.28	0.00	2.14	11.78	0.48	0.91	25.37	13.35	1.43	0.00	
			matrix	0.00	6.07	0.00	33.11	0.00	0.00	0.34	22.99	0.00	1.50	31.30	1.86	0.35	0.00	
			matrix	0.00	2.11	10.23	37.86	0.00	0.00	2.55	11.76	0.00	0.78	19.55	15.73	0.39	0.00	
D385	T18,Ap 106	LBA-EIA	matrix	0.00	3.29	2.07	31.99	0.27	0.00	0.34	25.34	0.00	1.25	31.17	2.91	0.00	0.00	
			wustite	0.00	0.61	1.37	0.28	0.00	0.00	0.00	0.36	1.56	0.52	83.78	0.47	0.00	0.00	
D384b	T23B	EIA	matrix	0.00	0.00	9.98	32.09	0.00	0.77	1.44	14.72	0.00	0.85	21.36	16.99	0.73	0.00	
			matrix	0.00	0.00	8.39	29.77	0.00	3.55	2.56	17.60	0.00	0.78	29.25	8.19	0.00	0.00	
TSIORE	K3A/69		matrix	0.86	0.59	3.39	32.67	0.71	0.00	0.64	11.74	0.00	0.00	20.23	29.83	0.00	0.00	
D387	T18,P3	LBA-EIA	matrix	0.63	0.46	3.72	30.56	0.84	0.00	0.85	8.18	0.00	0.00	19.55	33.66	0.00	0.00	
Pal'kastro																		
Cu slag																		
PAL.Th.1		undated	wustite	0.00	0.47	3.10	5.46	0.00	0.00	0.15	2.28	1.55	0.69	83.01	0.00	0.00	0.00	
			wustite	0.00	0.60	2.97	7.71	0.00	0.00	0.38	3.43	1.74	0.93	78.95	0.00	0.00	0.00	
			matrix	0.00	0.44	4.38	34.93	0.00	0.00	2.33	13.51	3.67	1.68	34.12	0.00	0.00	0.00	
PAL.THAS.1		undated	'faya'	0.00	0.48	1.56	45.62	0.44	0.00	0.20	10.76	0.24	0.00	40.04	0.00	1.36	0.00	
			'faya'	0.00	0.40	1.44	43.59	0.40	0.00	0.17	8.80	0.21	0.00	44.18	0.00	1.29	0.00	
			wustite	0.00	0.00	0.58	0.50	0.00	0.00	0.00	0.00	0.41	0.00	93.19	0.00	0.51	0.00	
			wustite	0.00	0.00	0.63	0.87	0.00	0.00	0.00	0.18	0.53	0.00	93.40	0.00	0.33	0.00	
PAL.THAS.2		undated	fayalite	0.00	0.56	1.73	35.43	0.31	0.00	0.13	6.53	0.31	0.19	48.30	0.00	4.33	0.00	
			'faya'	0.00	0.75	1.17	39.87	0.00	0.00	0.18	6.88	0.30	0.00	44.89	0.00	2.87	0.00	
			'faya'	0.00	0.29	1.48	40.44	0.28	0.00	0.31	5.31	0.22	0.00	51.43	0.00	0.72	0.00	
			wustite	0.00	0.00	0.56	0.92	0.00	0.00	0.00	0.13	0.44	0.00	92.19	0.00	0.63	0.00	
THAS.PK		undated	fayalite	0.00	1.09	2.29	44.54	0.00	0.00	0.89	6.33	0.92	0.36	40.95	0.00	0.88	0.00	1.11
			'faya'	0.00	0.51	2.73	48.31	0.00										

Sample No.	Cu	Fe	S	Sb	As	Ag	Pb
D384a	76.77	1.95	29.09	0.00	0.00	0.00	1.15
D384b	68.76	7.11	23.33	0.00	1.21	0.00	0.00
	69.78	5.66	23.22	0.00	0.00	0.00	0.00
	58.13	12.69	27.64	0.00	0.00	0.00	0.00
	51.55	0.93	2.00	25.34	20.18	1.20	0.00
	14.69	0.98	0.50	54.22	11.63	2.02	2.03
	5.99	0.67	1.08	78.28	5.54	3.06	4.05
D385	34.84	29.23	44.89				
	25.35	36.21	32.05				
PAL.THAS.1	96.90	3.20	0.22				
	95.68	4.14	0.37				
THAS.PK	97.14	3.50		2.19			
	97.33	4.20		2.02			

Table 3.3.2: Metallic prills in copper slag from Kastri (EBA-EIA) and Palaiokastro (undated)

of these three elements vary. Some of these prills are Cu_2S with a small amount of Fe (D384a and D384b in Table 3.3.2). It is interesting to note that apart from Cu_2S, a number of these prills contain metallic inclusions primarily of copper, arsenic antimonides or copper antimony arsenides (D384b, Table 3.3.2) with small amounts of iron and sulfur and appreciable quantities of silver and lead. These inclusions can be characterised as speiss, metallic compounds which form insoluble phases in slag (Gilchrist 1980, 232; Rosenqvist 1983, 342). Speiss is a general name encompassing the alloys of heavy metals like iron, cobalt and nickel with arsenic and antimony. In section 3.7 speiss consisting of iron arsenides found amidst slag heaps in the region of Palaia Kavala, EM is discussed in some detail. Precious metals like gold and silver have high affinities for speiss and will partition in that phase in preference to others with the sole exception of lead, which as will be shown again in section 3.7 can be used as a precious metals collector.

The second group of Thasos copper slags presented in Table 3.3.1 comes from Palaiokastro (Fig. 3.1.2). These slags, undated surface finds, are different in composition from those at the cemeteries at Kastri. The absence of barium is notable as is the near absence of sulfur in the copper prills. The prills are primarily copper with some iron and occasionally antimony. The matrix is mainly fayalitic with copper ranging from 1-4% CuO and less than 1% CuO in the magnetite. The majority of iron oxides in these samples is magnetite rather than wustite (Plate 2f,g). No

copper is present in the matrix of sample Pal.Th.1 and, had it not been for the presence of metallic prills containing copper and iron, the slag would have been classified as iron slag. This observation serves as a word of caution when analysing very early material, since the samples available are usually very small in size and number and cannot provide an accurate picture of either furnace conditions or the extractive processes involved.

3.3.b Iron slag

The first evidence for iron exploitation on Thasos is in the form of three pieces of iron slag from two graves at Larnaki and one at Tsigganadika (Table 3.3.1). These cemeteries date to phase IIB2-IIB3 of the EIA (900-700 BC), a period when iron has completely replaced bronze as a working metal (Koukouli-Chrysanthaki 1986, 1043). Iron itself makes its first appearance on Thasos (Kastri) earlier, during phase IIA-IB (1050 BC) in the form of a bimetallic knife with an iron blade and a cast bronze handle (Koukouli-Chrysanthaki 1986, 1044). Analysis of the bronze handle by N.H. Gale showed that the copper was not local but imported possibly from Cyprus, since its lead isotope composition fell within the Cypriot field (Koukouli-Chrysanthaki 1986, 1044).

The iron slag from Larnaki (L2,ST ,Table 3.3.1) contains all three commonly occurring phases, ie wustite, fayalite and a matrix of melillite composition. The latter is a potassium-calcium-iron-aluminum silicate, common in most of the iron slags analysed from Macedonia (see section 3.5 for further discussion). The second sample from Larnaki (D399, Table 3.3.1 and Plate 2a) also contains

the same phases, together with metalic iron prills free of slag inclusions. Arsenic has been detected in its matrix suggesting that the ore source may have been that at Kokoti reported by Theophilopoulos (1982, 51). However, it is difficult to draw conclusions on the basis of one sample only.

The third piece of iron slag is from the cemetery at Tsigganadika (D383, Table 3.3.1). It contains a relatively higher titanium content in the wustite and the matrix compared to the other two, but no other mineralogical phases are evident as to suggest a particular source of iron ore.

3.3.c Discussion

The picture emerging from the analyses of the LBA-EIA copper slags from Kastri and the undated slags from Palaiokastro indicates the use of at least two types of copper oxide ores at the same or different periods. On the one hand, there are the copper ores, malachite and azurite, which occur within the main barite-rich iron deposits of Thasos in places like Mavrolakas and Koumaria-Platania (Fig. 1.2). The slags that derive from their smelting contain sulfur in the metallic prills. On the other hand, there are the copper oxide ores in the vicinity of Palaiokastro, the slags of which contain no barite. The copper prills contain no sulfur, only small amounts of iron and antimony. The role of barite in the Kastri copper slags is of particular importance for two reasons:a) it is the origin of the sulfur in the copper prills, and b) it decreases the viscosity of the slag. Barium sulfate decomposes at

high temperature (the reaction is endothermic) to barium oxide, sulfur dioxide and oxygen:

$$BaSO_4 \longrightarrow BaO + SO_2 + 1/2O_2$$

The reaction can be promoted by localised reducing conditions and the presence of a high SiO_2 content with which barium forms a stable silicate (Rosenqvist 1983, 232). In the present case, a barium silicate glass matrix is formed incorporating iron, alumina and calcium oxides (matrix in Table 3.3.1 and Plates 2b-e). Barium silicate ($BaO.2SiO_2$) forms a eutectic at 1370°C (Levin et al 1964), the lowest of all eutectics formed between BaO and SiO_2. In the Thasos samples the presence of fluxes like FeO or CaO accounting for 15% of the total matrix composition will reduce the melting point of the barium-rich melt. In the process of barite dissociation, SO_2 has reacted with copper resulting in the formation of Cu_2S or matte prills present in the Kastri copper slag. Cu_2S is formed in preference to CuS which dissociates at c. 1120°C (Fig 3.3.1). The reaction of SO_2 with Cu, releasing O_2 in the process, implies that the origin of the copper sulfide prills need not necessarily be a sulfidic ore, as is usually assumed. It is clear from the present discussion that an alternative source of sulfur, such as barium sulfate, should also be investigated.

Viscosity can be estimated by the viscosity index which is the ratio of the sum total of the basic oxides (CaO, MgO, FeO, BaO etc.) over the sum total of the acidic oxides (SiO_2, Al_2O_3) (Bachmann 1980). The lower the viscosity index, the higher the viscosity of the slag, meaning that the viscosity decreases with

increasing amount of basic oxides (Rosenqvist 1983, 312). Thus, it is probable that the copper slags at Kastri were more fluid than those of Palaiokastro given the higher total amount of basic oxides (BaO and CaO). As a result, the Kastri slag would separate better from the metal.

Although the copper slags of Kastri are associated with the main barium-rich iron ore deposits of Thasos, the iron slags from the same site contain no barium. It is difficult to arrive at some definite conclusion as to the absence of iron on the basis of these three slag samples, particularly since it is possible that they are the product of smithing rather than smelting operations.

The presence of iron in copper prills, as observed in the Palaiokastro samples, is a common enough phenomenon in early bronze objects from the E. Mediterranean reported by a number of investigators. Jones (1980) has reported iron contents in bronze objects from the rich EIA cemeteries at Lefkandi in Euboea. The same investigator, in his analysis of pieces of copper/bronze from Servia (discussed in Chapter 2), again reported iron (4% Fe) in the copper. Both sets of analyses were done with XRF energy dispersive analysis, non-destructively. It is possible that their results may have been influenced by surface segregation phenomena. Cooke and Aschenbrenner (1975) suggested that in copper smelting, excess iron oxide which was not taken up by the slag under localised reducing conditions would reduce to metallic iron. As the copper reduces simultaneously, metallic iron (up to 4%) would dissolve into the copper. The presence of metallic prills with this composition in slag from Palaiokastro (Table 3.3.2) corroborates this observation.

Metallic iron produced as a result of copper smelting is found even in more modern practices. Percy (1861, 403) discusses the 'eisensau', or 'bears', ferruginous masses forming at the bottom of the furnace in a non-ferrous smelt. One way of avoiding the formation of this iron is to make certain that sufficient silica is present, so that a fayalite slag forms. Alternatively, the presence of sulfur from imperfect roasting of sulfur-rich ores can prevent the formation of metallic iron since iron will tend to react with sulfur and form matte, sulfur-rich metallic compoounds. Iron can be removed from copper during the refining stage by melting the copper in an oxidising blast and removing the iron as iron oxide in the slag.

It has frequently been reported in the literature that iron oxides were added intentionally as flux during the smelting of copper ores in order to produce a fluid fayalitic slag in combination with the silica in the copper ore. However, it now seems quite clear that iron ores were often found in association with copper ores and so made their way into the furnace accidentally as charge rather than being conscious intentional additions. Pigott (1982, 21) presented an eloquent photograph of a malachite 'pocket' in an iron ore matrix, while Merkel (1983) showed that the charge in the Timna furnaces could contain up to 20% Fe in the copper ore, in addition to the iron-rich nodules (flux) containing up to 48% Fe.

Evidence for copper association with iron ores occurs in the classical texts. The 1st c. AD geographer, Strabo (X,I,9)

refers to a double mine of both iron and copper found above the city of Chalkis in Euboea (Fig. 3.3.3). Although Bakhuizen (1976, 48) purports in his study of the Chalkidean iron industry that Strabo has mistakenly ascribed two locationally separate mines to a single one above the city of Chalkis, he himself (1976, 53) reports the occurrences of both iron and copper elsewhere in the island, near Krieza (Fig. 3.3.2). In any case, what Strabo's reference implies is that such a mine did indeed exist and moreover, by late antiquity, mines would be worked for more than one metal, if the potential was there. Another example of a 'double' mine is Rudna Glava in Yugoslavia, exploited for both copper and iron, albeit at different periods (Tylecote 1982).

The proximity of copper ores to iron ore based on geological observation has led many investigators to suggest that since iron found its way into the furnace, it would reduce to metallic prills, thus suggesting the development of iron metallurgy out of copper metallurgy (Wertime 1973; Charles 1980; Pigott 1982). The Kastri slags provide the first material evidence of what has for some time been speculated, namely the exploitation of copper ore out of iron deposits in the LBA-EIA.

The presence of barium, a unique tracer element in the provenance of the Thasos main iron ore bodies, clearly suggest that the origin of the copper in the LBA-EIA were deposits like that of Mavrolaka, in which copper carbonates are found in small amounts even today (Theophilopoulos 1982, 58). Far from being an intentional addition, hematite/limonite with associated barite (in itself quite heavy and easily distinguishable) entered the furnace

accidentally. It is very likely that metallic prills or small lumps formed as a result of localised, strongly reducing conditions. Early bronzesmiths may have noticed them but were probably not in a position to do much with them, at least initially. The main reason for their lack of success is that they would have tried to work the iron either by melting it as copper or lead or by cold working and annealing it like native copper or gold. But iron with only traces of carbon (wrought iron) melts at temperatures (c. 1550° C) which would be unattainable in the existing hearths and furnaces. In addition, iron would be forged only within a limited range of temperatures according to the impurities incorporated in its matrix. In short, any effort to shape it would result in fracture or no change at all.

Thus to summarise, the analytical data presented here suggest that the early bronzesmiths on Thasos may have been led to the smelting of iron ores through their continuous experimentation with copper ores and the fact that copper ores were extracted from the main iron deposits . This interpretation argues in favour of a likely independent development of iron metallurgy on Thasos and possibly other locations in Macedonia. It would have been more securely verified if the iron slags from the EIA cemeteries at Kastri had also contained barium. But the three samples presented here do not, and they may in fact represent smithing rather than smelting slag. There are six more slag samples from the same context still pending analysis.

Gale (Koukouli-Chrysanthaki 1986) has argued that the majority of

the LBA bronze objects are not made of Thasiot copper. However, the presence of copper slag on the island and the possibility that the correct type of copper ore was not sampled by Gale are two points to bear in mind arising out of the present investigation.

Kastri and Palaiokastro copper slags are clearly process slags, but are they melting or smelting slags? This distinction is not always easy to make. In a effort to establish distinguishing criteria between the two types of process slags, Tylecote (1980, 203) suggested that small amounts of iron oxide associated with high silica, calcium oxide and alumina with relatively high copper (8-40% Cu) contents in the slag are a sound criterion for slags melted in a crucible. Cooke and Nielson (1978) suggested that crucible melting slags usually have a low iron content and a high (SiO_2+Al_2O_3) to (FeO+MnO) ratio compared to smelting slags. In addition, the crucible melting slags have only a small amount of crystalline phases in comparison again with smelting slags.

The presence of barium in the Kastri slags rules out the possibility that they are crucible melting slags since barium would have been removed from the smelting stage. The Palaiokastro slags have high iron contents and copper prills with sufficient impurities for them also to be considered smelting slags. But it is difficult to decide conclusively on such sparse evidence. Thus, the Kastri slags are considered to be the product of smelting and the Palaiokastro slags most probably the same.

Table 3.3.3: Summary of differences between Kastri and Palaiokastro slags

Kastri	Palaiokastro
Date: LBA-EIA	Undated
Ore: copper carbonates	Copper carbonates
Associated with barite-rich iron ore	No barium
Sulfur present in matte prills	Sulfur absent
with speiss inclusions	Copper prills with 4% Fe
Copper in the matrix	No copper in matrix
Smelting slag	Smelting slag?
More reducing furnace conditions (wustite)	Less reducing furnace conditions (magnetite rather than FeO)

Fig. 3.3.1 Ellingham diagram for selected sulfides

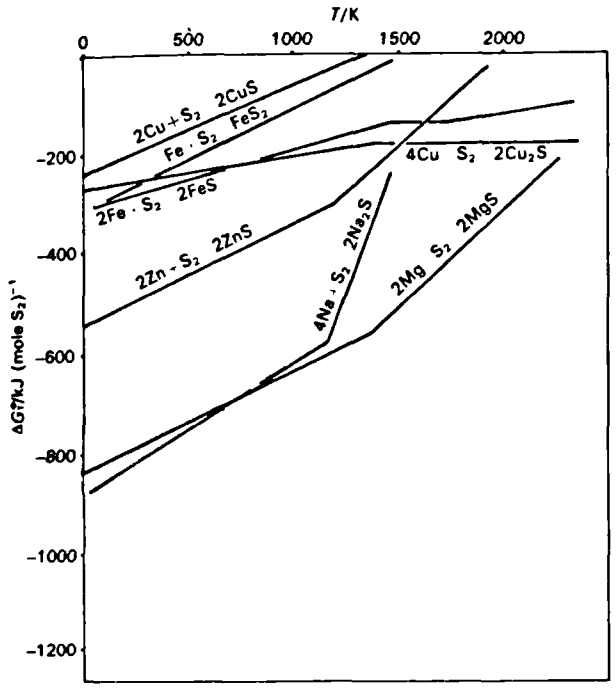

Plate 2

(a) D399. Iron slag, Kastri, Thasos. Dendrites of wustite (light grey), silicate matrix (dark grey), holes (black), amorphous corroded area (grey, middle), metallic iron prill (white). 100x

(b) D384a. Copper slag, Kastri, Thasos. Magnetite (plates), fayalite (lathes), silicate matrix. 200x

(c) D385. Copper slag, Kastri, Thasos. Magnetite (plates), fayalite (lathes), silicate matrix. 200x

(d) TSIORE. Copper slag, Kastri, Thasos. Silicate matrix (glassy), metallic sulfide prills (round), magnetite plates, barium-rich needles. 100x

(e) D394a. Copper slag, Kastri, Thasos. Silicate matrix, barium-rich needles, wustite dendrites (white). 200x

(f) PAL.THAS.1. Palaiokastro, Thasos. Magnetite plates, wustite dendrites (fine), silicate matrix consisting of a fine eutectic of fayalite and mellilite. 100x

(g) PAL.THAS.2. Palaiokastro, Thasos. Magnetite plates, wustite (fine), silicate matrix consisting of a fine eutectic of fayalite and mellilite. 100x

Plate 2

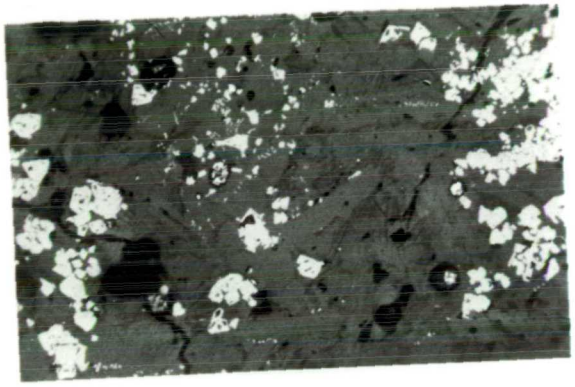

b

c

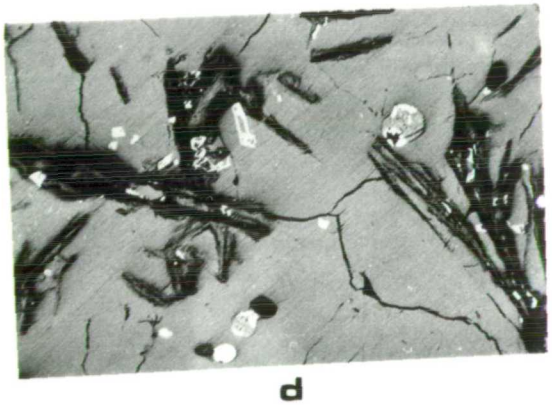

d

e

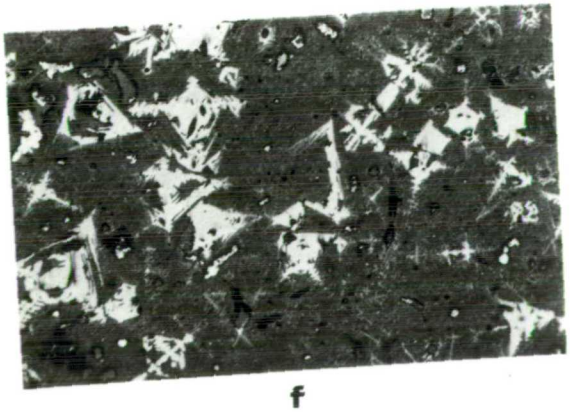

f

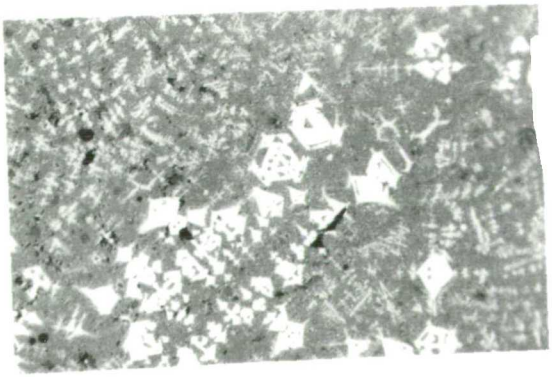

g

3.4 Experimental bloomery iron-making at Ashdown Forest, Sussex

3.4.a The bloomery

The existing literature on the bloomery process is considerable. It consists of eye-witness accounts (Richard 1838; François 1843; Percy 1864; Cline 1937), ethnographic studies in Africa where the process was still extant until relatively recently (Todd and Charles 1978; Avery and Schmidt 1979), laboratory reconstructions aimed at explaining the mechanism of reduction in a bowl and shaft furnace (Wynne and Tylecote 1958; Tylecote et al 1971; Tholander 1986), as well as experimental field smeltings (Cleere 1972; Pleiner 1968) to mention only a select number of references. In addition, a number of doctoral dissertations have been written on various aspects of the process (Fells 1983; Clough 1986; McDonnell 1987). To those should be added the excavated material from bloomery sites in Britain, Europe, Africa and the East, the references for which are numerous. A substantial bibliography can be found in Tylecote (1976) and Tylecote (forthcoming) and Haaland and Shinie (1985).

Given the considerable amount of information existing on the subject, it was decided that the present work would concentrate on the writer's own observations which relate to both the procedure and the products. The detailed examination of the products from each individual smelting/smithing operation would have far exceeded the time limitation imposed on this work and will be dealt elsewhere in due course. The observations relating to procedure are described in more detail. The bloomery iron making involves the reduction of iron oxide to metallic iron (wrought iron) with

only traces of carbon (0.02% C). Wrought iron is malleable, can be forged easily and upon further carburisation can acquire hardness, thus producing a good cutting edge. In practice, however, a varying degree of carburisation of the bloom ranging from wrought iron to cast iron is more often than not the usual product (Tylecote et al 1971); Nosek 1977). To achieve a controlled carburisation, the object had to be in contact with charcoal in the hearth for a considerable period of time to allow diffusion of the carbon in the iron. Some heat-treatment to give the artefact the desired properties followed.

The historical development of the bloomery furnace has for long been considered to follow the sequence: the bowl, the shaft and the stueckofen. The last of these led to the design of the blast furnace (Tholander 1985). Tylecote (forthcoming) has eloquently shown that these three types have been subject to considerable variations in form and operation in various geographical regions, making this classification rather inadequate. The bloomery shaft furnace used in the course of the writer's experimental smelts is shown schematically in Fig.3.4.1. Ore which has not already been roasted in a separate stage will do so in the upper parts of the furnace where conditions are mildly reducing. Carbonates in the ore will decompose and water of hydration will be released at a temperature range of 500-600°C. This results in an increase in ore porosity, enabling furnace gases (CO and CO_2) to penetrate the descending charge. The correct ore particle size is essential in accelerating the process. It should not be too fine, clogging the furnace, nor too coarse requiring long residence time

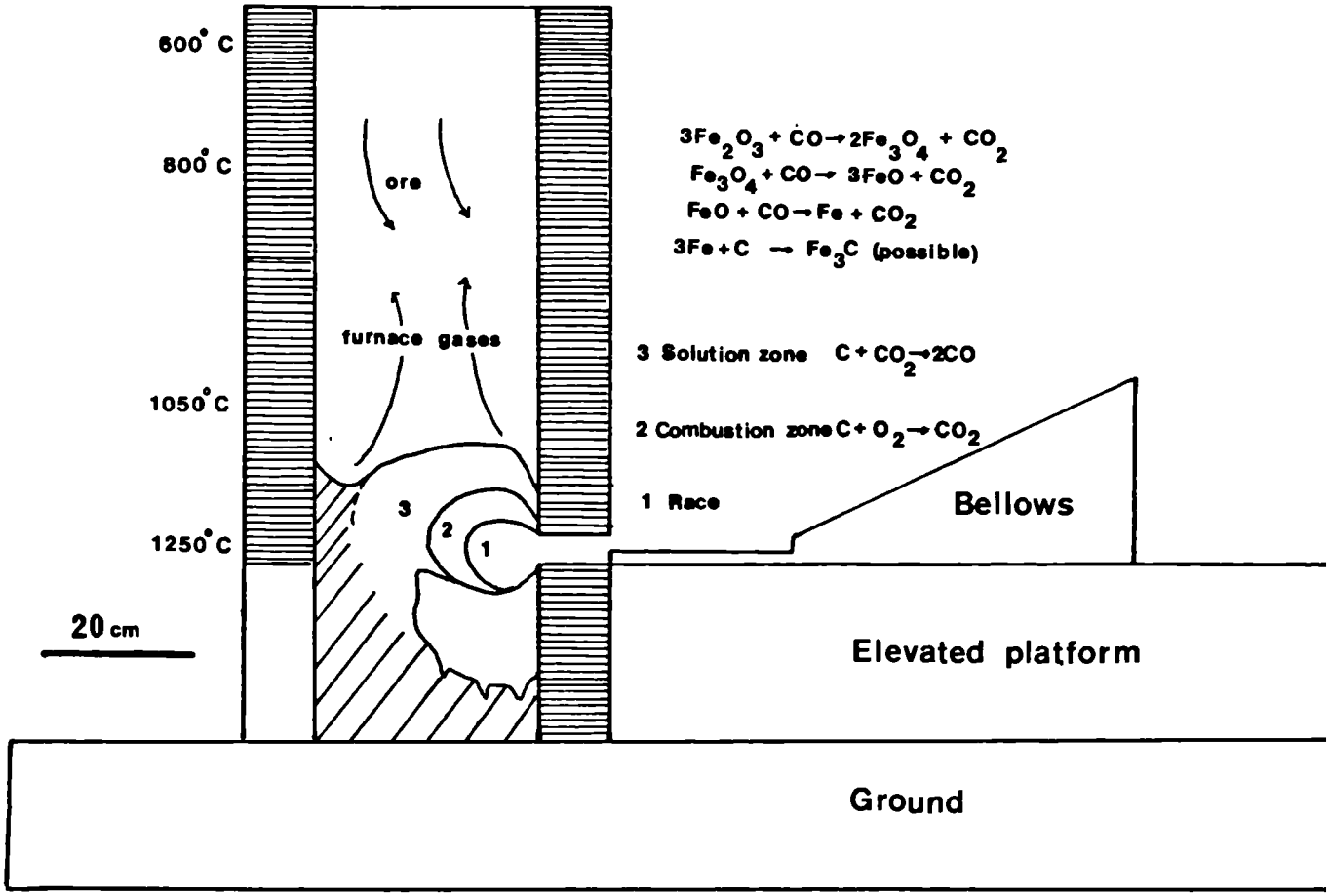

Fig. 3.4.1 Experimental furnace at Ashdown Forest, and furnace reactions

which can only be increased by extending the shaft height. Reduction of hematite (Fe_2O_3), to magnetite (Fe_3O_4) to wustite (FeO) and metallic iron takes place successively, starting at 750-800°C, well above the tuyere zone (Fig. 3.4.1). Carburization of metallic iron to cementite (cast iron) is also possible depending on the fuel/ore ratio. Wustite, either from the reduction of magnetite or the oxidation of metallic iron, once it is near the tuyere zone (the oxidising zone of the furnace), will react with silica in the gangue to form fayalitic slag and dissolving all other oxides present in the charge. Slag can be tapped or left to accumulate at the bottom of the furnace.

3.4.b Smelting Procedure

3.4.b.1 General

The experimental smelts took place at two different locations in Ashdown Forest, Sussex, namely the Pheasantry (TQ445315) (October 1985-March 1986) and at Pippingford (TQ439307) (June 1986-October 1986). Fig 3.4.2 is a schematic representation of the installations at Pippingford, built and maintained by Mr R Adams. The Pheasantry furnace resting on a platform is illustrated in Fig 3.4.1 and Plate 3b. The bellows were of elliptical shape with a valve in the front to prevent air from being sucked back (Plate 3e). There was no monitoring of the air supply which was provided by the bellows and was calculated to be c. 80 l/min. However, some leakage at the seams probably brought this closer to 60 l/min. The bellows were attached to the tuyere with a metal Y tube (Plate 3d), one arm being used as an eyepiece to look into the furnace hot zone

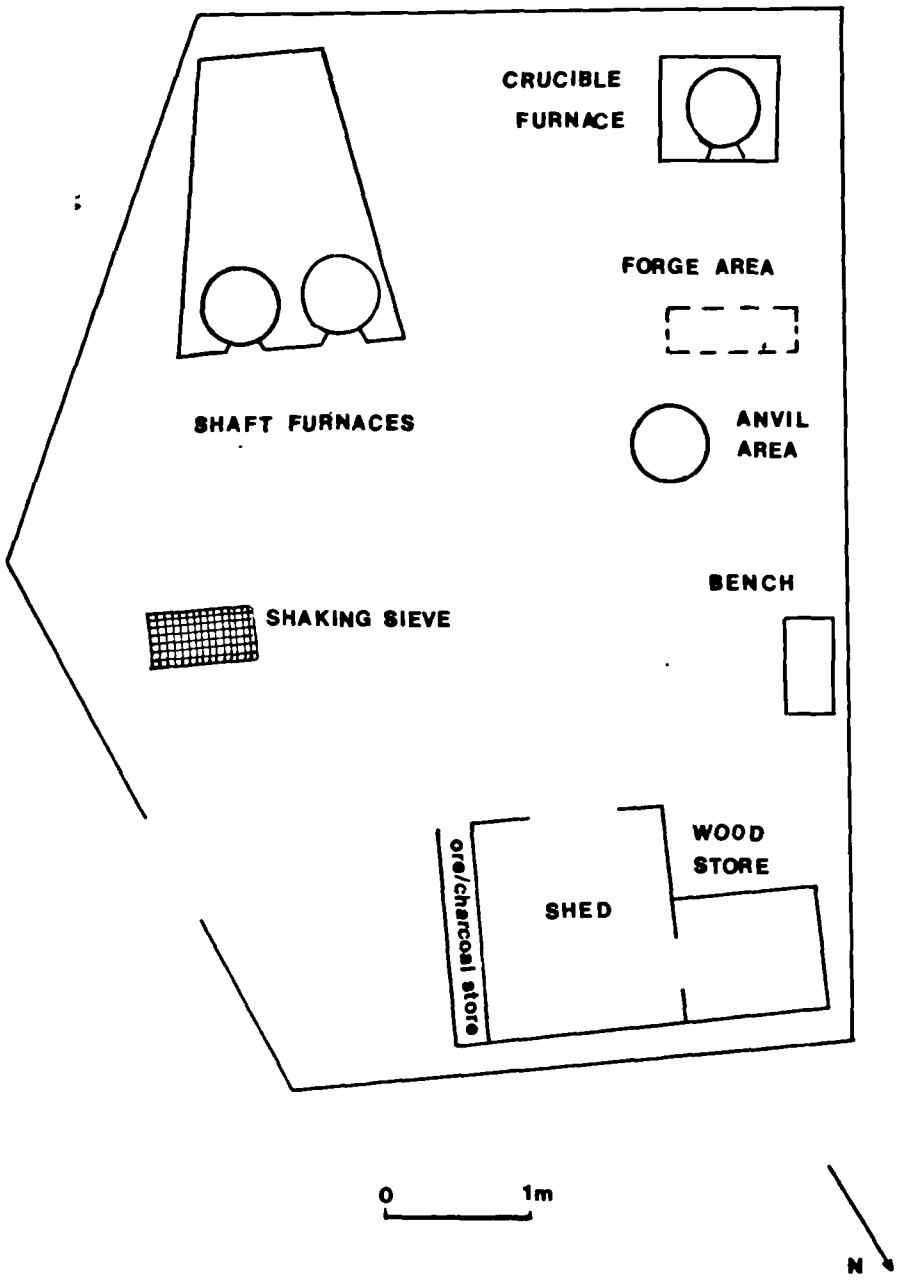

Fig. 3.4.2 Map of Pippingford, Ashdown Forest bloomery iron-making area (adapted from R. Adams, pers. comm.)

while in operation.

The timetable for smelting was set out as follows: one day would be reserved for the preparation of the smelt, a second for the smelt itself and a third (usually after 5 days) for opening the furnace, weighing and sieving the products (slag and bloom) and relining the furnace if needed.

Most smelts were carried out by R Adams and the writer. Occasionally, they would be assisted by a third person who would offer relief with the bellows. The experimental conditions of the smeltings at Ashdown Forest were not strictly controlled, as would have been the case had they been undertaken in the laboratory. It is difficult to smelt in the field, while at the same type keeping a record of the thermocouple readings, air flow rates and furnace gas level unless a corresponding number of assistants were available. As a result, one had to develop a feeling of when things were 'right', which , however, did not necessarily imply that the yield would be satisfactory.

One fact that became soon obvious was that judging the temperature in the hot zone of the furnace by the colour of the flame gave an erroneous idea of a 'high' temperature, which could range anywhere between 950°C and 1200°C. Thus, a thermocouple positioned about 22cm above and to the left of the tuyere was almost always used.

3.4.b.2 Preheating

Preheating of the furnace was perhaps the most important step in the entire smelting cycle since the furnace was outdoors (although always under a plastic roof). The furnace floor, although resting on an elevated platform was still subject to dampness particularly during the winter months when the woods would be under snow. An extensive preheating (minimum two hours) would be essential.

Before preheating, the furnace front arch had to be rebuilt (Plate 3c) since the removal of the previous bloom had partly destroyed it. No modifications could be done to the furnace once preheating started because of excessive smoke (Plate 3c).

Kindling wood and newspapers were spread on the furnace floor and ignited, and chunks of wood (30cm length and 5-10cm diameter) were dropped from the top until they filled the furnace to the rim (about 10kg). The rate of woodburning was very fast (half the charge in less that 10 minutes) when the front arch was left open. This rate was slowed down by sealing most of the front arch and/or partly closing the furnace top. To enhance the draught a chimney (an old milk churn) with an opening at the front (for charging and looking into the furnace) was placed on the furnace. Occasionally an additional chimney (an extra height of 2m from the furnace rim) was fitted on the milk churn. This extra addition was only used when the wood was rather damp and smoked more than usual and the prevailing wind blew in the direction of the operators.

During the preheating with wood stage no bellows were needed, natural draught being sufficient. But when adding the coarse preheating charcoal, it was essential that the flame should not be extinguished, and so the bellows were used rigorously. However, it was found preferable firstly to let the temperature rise slowly, resulting in a uniform heating of the furnace, and secondly to charge the furnace with preheating charcoal all at once rather than in stages because of the cooling effect of each additional batch.

3.4.b.3 Smelting

During the first experimental smelts the first batch of ore was charged directly after the last load of preheating charcoal was added. This was done to increase furnace residence time (FRT), namely the maximum time the ore comes in contact with furnace gases. To calculate the FRT, the bed drop rate is measured. This is the time it takes for the charge to drop a certain distance from the rim of the furnace. However, it was soon realised that the furnace should be allowed to heat up uniformly before ore is charged, since by adding charge to a relatively cool furnace the weight of the furnace bed is increased, preventing combustion gases from rising. Thus, there should be a balance between residence time and an adequately preheated furnace.

Ore and charcoal (1.0-1.5cm diameter) of a pre-specified ratio were loaded into a furnace in a layered form, a layer of ore mixed with some charcoal followed by a layer of charcoal. Charging took place usually at intervals of 15-25 minutes. Once all the

charges were introduced to the furnace, the bellows operator continued to blow at 10-11 blows/minute (Plate 4f), until all but the last one or two charges had reached the tuyere zone. Then the furnace was brought to a shutdown, the bellows were removed and the tuyere hole sealed. The tuyeres remained in situ to be reused unless they were broken. The furnace was sealed usually half an hour after shutdown with an iron lid covered with dry dust both on the top and the front arch. The thermocouple hole was also sealed.

The furnace was opened five days later. The contents emptied from both the top and the arch (Plate 4g) taking care to seive, weigh and put aside charcoal, slag and other furnace contents originating from the area above and below the bloom. The purpose of the exercise was to subsequently study the morphology and mineralogy of the slag as a function of its position in the furnace. Similar methodology was followed for the smithing stage.

The bloom forms directly below the tuyere (Plate 4h), and depending on the yield, protrudes about half way across the furnace. To be removed the bloom had to be forcefully pushed down with an iron rod (Plate 4i) and removed from the front arch (Plate 4j). Some smelts were succesful (Plate 5k) resulting in a large bloom with high yields, other less so (Plate 5l). The bloom was subsequently carried to the anvil where it was cold-hammered to produce a fettled bloom (Plate 5m). Plate 5c1-2 showed two steps omitted in the discussion above, namely the crushing of the ore to about 1cm and the sieving of the charcoal in a moveable sieve suspended on four poles.

3.4.b.4 Products of smelting

In order to better classify and study the furnace contents, the furnace has been divided into three hypothetical zones, namely the bloom, the area above and the area below the bloom (Fig. 3.4.3). This division is based on the assumption that there was sufficient unburnt charcoal within the furnace to hold the material above the bloom in situ. This has been the case for most of our experimental smeltings in view of the high charcoal/ore ratio and the relatively low temperatures the furnace was usually operated at. The remains in the area above the bloom consist primarily of sintered and/or partially reduced ore, the amount depending on the conditions of that particular run and the particle size of the ore.

Below the bloom and on the furnace floor, slag, ashes, ceramic fragments and fines have accumulated. Slag typology can broadly be classified into five groups (drop-like, spongy, vesicular, compact and scale). Experience has shown that many metallic prills never quite form a large mass, either because they are prevented by a viscous slag barrier or because they have been exposed to an oxidizing blast at the tuyere zone and thus have reverted to oxide (FeO). Scale has usually been associated with forging and smithing operations, but it is clear that it has also been obtained as a result of smelting (Plate 6b-f).

Small fired ceramic fragments from the bricks and mortar used for the sealing of the furnace are found amidst the furnace bottom remains. This suggests that not all the partly vitrified/partly unfired ceramic fragments found in a site constitute furnace wall

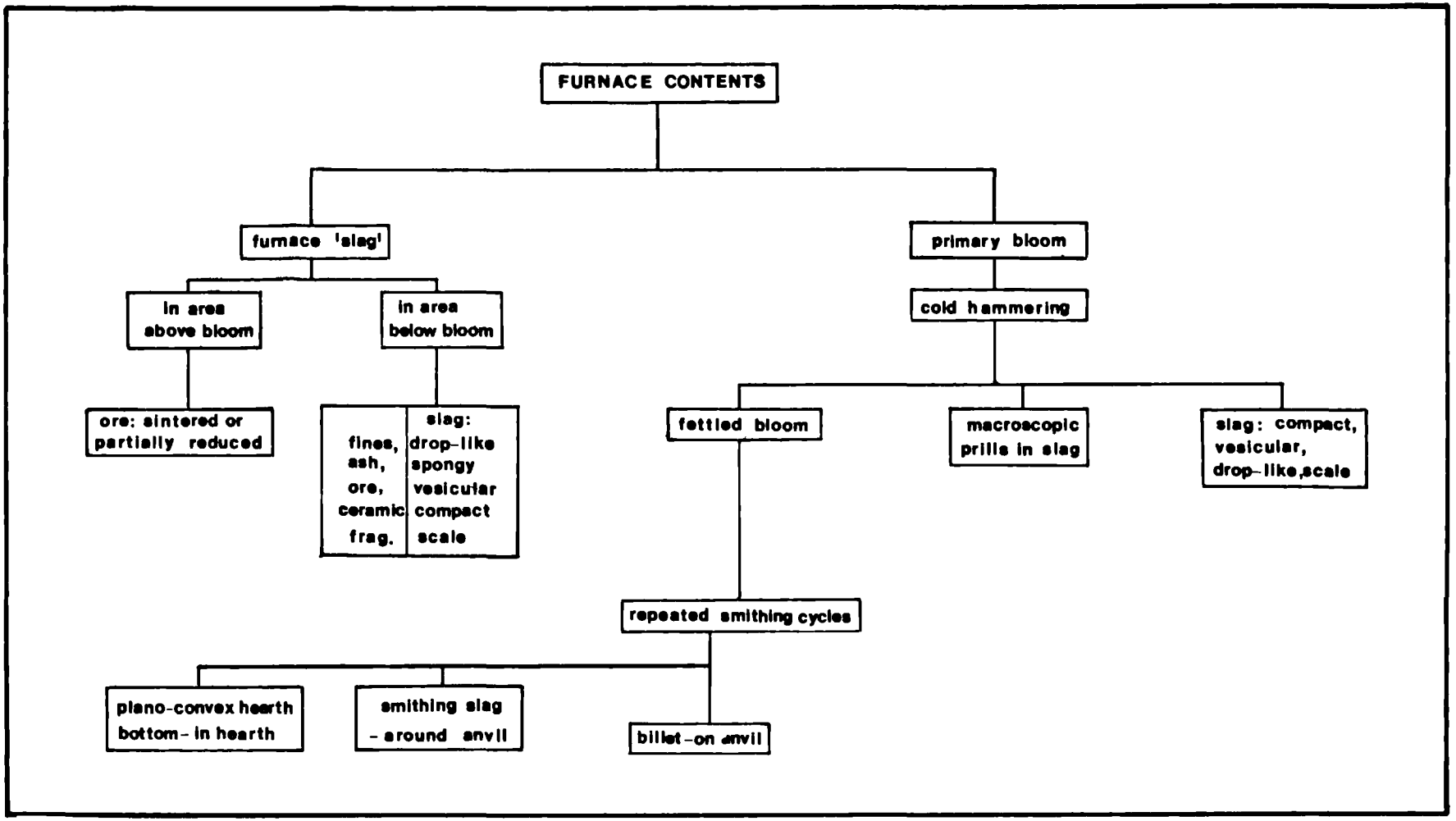

Fig. 3.4.3 Flowchart of smelting furnace and smithing hearth products and waste

and lining fragments. In fact during the course of eighteen smelts, we relined the furnace only twice. Vitrification was extensive around the tuyere zone (the area most in need of relining), but a layer of compact slag formed between the bloom and the wall was not removed with the bloom, and so the wall at this point seldom needed relining.

Once freed from the furnace wall, the primary bloom is then moved on to the anvil and cold hammered (fettled) to remove the outer slag coating and reveal the inner iron mass. It is rare that all metallic iron would coagulate into one mass, thin strips of iron and small lumps are dispersed in the slag (Plate 6bd). These are usually irretrievable and are found in the vicinity of the anvil. They probably constitute a substantial amount of the extensively corroded high-iron 'slag' found in bloomery sites. The slag removed from the primary bloom is similar in typology and composition to the smelting slag collected from the furnace floor.

3.4.c Smithing and its products

A hearth about 50cm wide was built by levelling an area and placing large stones to contain the charcoal. No cavity was made in the hearth floor. Two particle sizes of charcoal were used: bigger chunks (2.5cm diameter) nearer the tuyere, smaller pieces (1-1.5cm) at the opposite end (Plate 6a). The charcoal at the end furthest from the tuyere was sprinkled with water to contain the fire within the center of the hearth.

About 15-20 kg of coarse charcoal was used for the entire process,

which lasted 2-2.5 hours from preheating to the end. This high fuel consumption rate was due to the fact the the hearth area had to be adequately dried before smithing since the area was usually exposed (see Fig.3.4.1). Bellows blowing was kept at 10 blows per minute. Once the hearth was considered ready,the bloom was placed in it and covered in a bed of charcoal. It was occasionally poked to determine the extent of uniform heating. A bloom of dimensions 18x15x10 cubic cm could not be heated from all sides at the same temperature at the same time, the side nearest the tuyere being the hottest. The bloom was kept at a distance of 10-15cm from the tuyere and at intervals turned over to expose new areas to the hot zone. Once uniformly heated, the bloom was transferred with tongs (Plate 6a,b) on to the anvil and there hammered with soft quick blows to remove excess slag. Speed was particularly essential since the rate of cooling of the bloom is very fast.

The cycle was repeated a number of times. The slag had to be squeezed out of the bloom by hammering on the anvil and the metallic core consolidated into a bar. A considerable portion of the smelting slag enveloping the fettled (cold-hammered) bloom ran into the hearth forming the familiar planoconvex-shaped hearth bottoms seen in many archaeometallurgical sites. These hearth bottoms owe their shape not to a cavity in the hearth floor but to the effects of surface tension upon solidification on the level hearth floor. In addition, they form not in the middle of the hearth floor but rather underneath the tuyere, this being the hottest zone. The composition of the smithing hearth bottom should be similar to that of the smelting slag with possibly higher

wustite concentration. However, since large sections of the bloom envelop are also exposed to particularly oxidizing conditions while in the smelting furnace, high wustite sections are also present there in the bloom. The consolidation of the fettled bloom into a billet is only achieved after repeated cycles of heating and hot hammering. The slag scattering in the process around the anvil constitutes the second source, after smelting, of large quantites of slag.

In the course of the experimental smelts, the writer collected all debris from each stage in the smithing process with the aim of establishing slag typology, size distribution and mineralogical composition. One of the problems in the examination of archaeometallurgical debris has always been the difficulty in knowing with any degree of confidence which stage in the iron-making process each sample originated from. Experimental smelts with subsequent analytical investigation of the material are aimed at overcoming at least part of the problem.

Plate 3

(a) Furnace top and Hellenistic mask to invoke the benevolent spirits of iron-making, Pheasantry, Ashdown Forest.

(b) Furnace showing front arch and mouth (top), resting on platform (clay and sand mixture) to enhance insulation.

(c) Preheating of the furnace with wood while slowly sealing the front arch. During preheating only a small hole is left open for draught.

(e) Bellows resting on two wooden beams, held in place by large stones.

(d) Y metallic tube connecting bellows to the tuyere. One arm serves as occular. Joint between Y tube and tuyere is covered with wet clay.

Plate 3

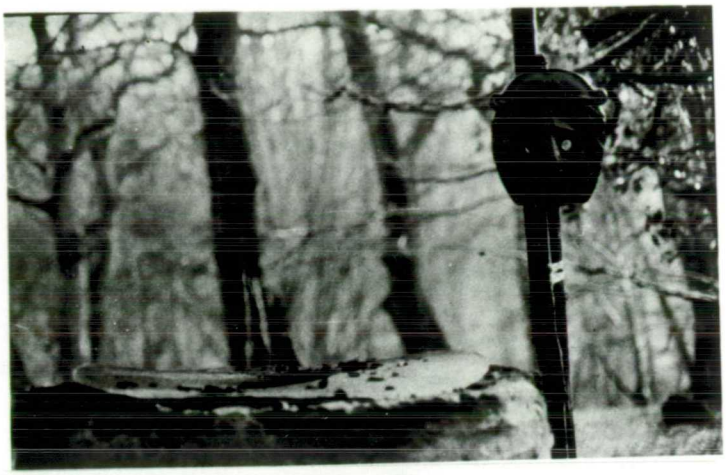

a

b

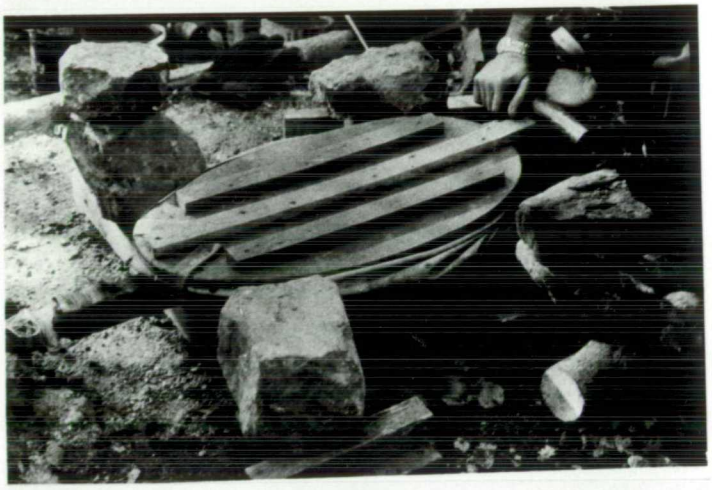

e

d

c

Plate 4

(f) Furnace in operation; bellows operator in position; furnace gases burning with a bluish flame.

(g) Opening of the front arch after five days; partly burnt charcoal, unreduced ore, small ceramic fragments used in the sealing of the arch. The relatively substantial quantity of unburnt charcoal was due to a high fuel/ore ratio charge.

(h) The bloom in situ. Iron rod shows position of tuyere. Themocouple ceramic tube protruding on the right. The furnace has been cleaned. The contents from above and below the bloom have been put aside for further study.

(i) The bloom is freed from the furnace wall by being pushed down with an iron rod. Loosely held slag enveloping the bloom scatters on the furnace floor.

(j) Bloom removed from the front arch.

Plate 4

f

g

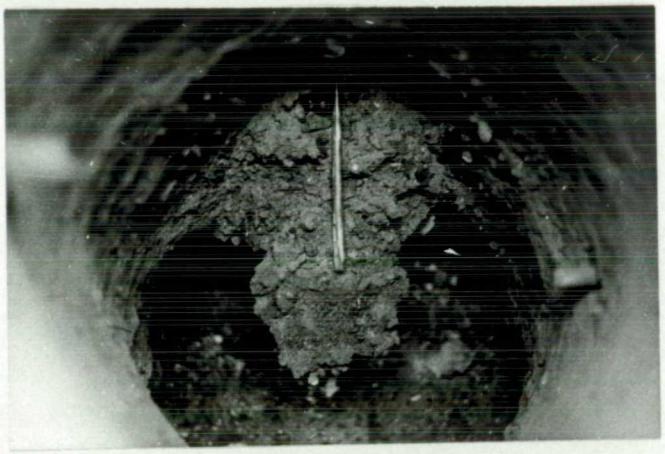

h

i

j

Plate 5

(k) 'Succesful' bloom from X-smelt 5 (nickel-rich iron laterites mixed with high grade australian hematite.

(i) Unsuccesful bloom from X-smelt 4 (laterites on their own).

(m) Cold hammering (fettling) of the bloom after removal from the furnace (five days after the end of smelt).

(c1) Breaking high grade australian hematite to size (about 1-1.5cm) to charge in furnace. Anvil, encassed in a wooden frame serves as the surface.

(c2) Sieving charcoal to remove dust. Commercial charcoal (the only kind used in the experimental smelts) usually contains substantial amount of dust produced in transport and handling, hence it is important to sieve it before use. Sieve is suspended on four poles and it is shaken vigorously with an iron rod.

Plate 5

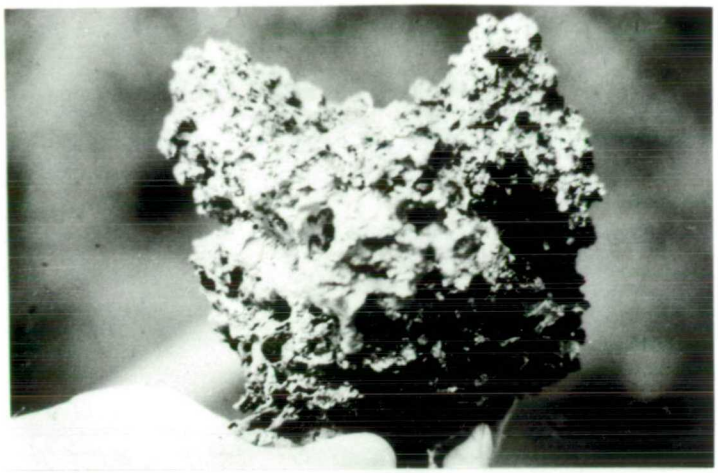

k

m

l

c_1

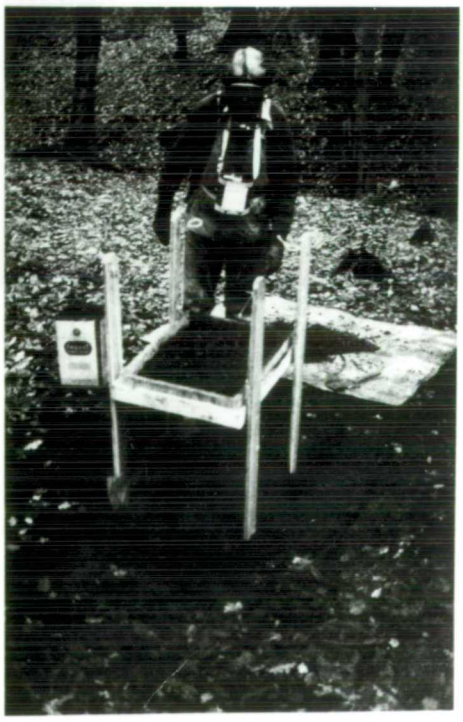

c_2

Plate 6a

(a) Smithing hearth built by surrounding an area with stones and filling with charcoal, coarse near the tuyere, fine at the other end. Bloom is shown in situ, partly exposed. It needs to be turned from time to time to expose new areas to the tuyere.

(b) Hot bloom transfered to the anvil (with tongs) for smithing

(c) Hearth emptied after smithing. Tuyere shown in situ (metal tube) and plano convex smithing hearth bottom formed underneath the tuyere rather than in the middle of the hearth.

(d) The product sequence in iron-making: (clockwise) bloom, billet, artefact. Hammer shown for scale.

Plate 6a

a

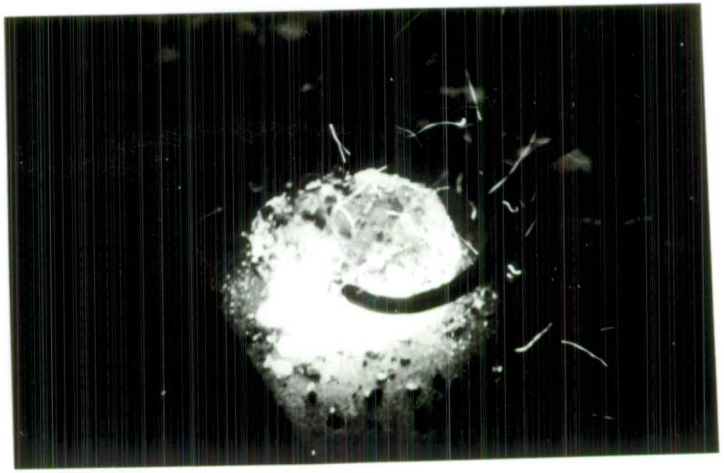

b

c

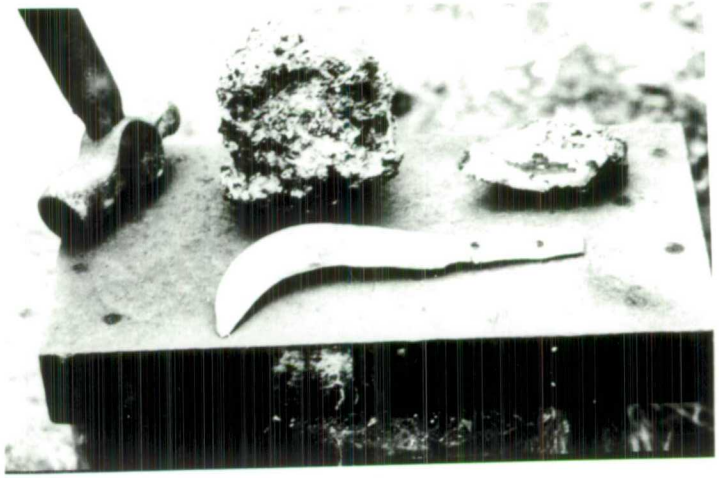

d

Plate 6b

(a) Cross section of a bloom from smelting of high grade australian iron ore. Iron (bright area), slag (dark area). Turned upside down for better view, since normally slag would be at the top and iron collect at the bottom of the bloom.

(b) Cross section of smithed billet from smelting of high grade australian iron ore. Solid iron (both light and dark areas). Area in the middle is not groound and polished as the rest.

(c) same as (a), top view

(d) Smelting slag (dark) with metallic iron prills (light). Iron has not coagulated with the rest of the iron mass. These pieces are irretrievable and constitute a large precentage of the debris around the anvil or in the slag heap.

(e) Typical bloomery slag with charcoal pieces and pores of the kind usually clattering most iron working sites. Initial colour of the slag is dark-grey to black. Upon weathering, slag turns to the familiar dark-brown.

(f) Coat of scale (FeO) enveloping the sintered ore. Scale is one of the most common debris in the smelting cycle and is not associated with smithing or forging only.

(g) Prunning knife made by Mr Th Piperides at Kavala from the other half of the bloom shown in (b) and (c). It was presented to the British Museum, Greek and Roman Department, together with ore, bloom and slag produced from the smelting of Greek iron ores.

Plate 6b

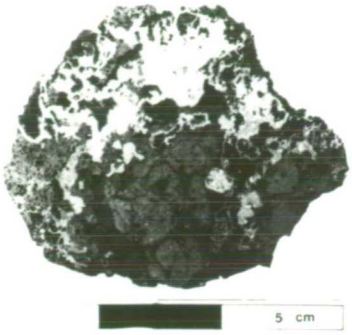

a

b

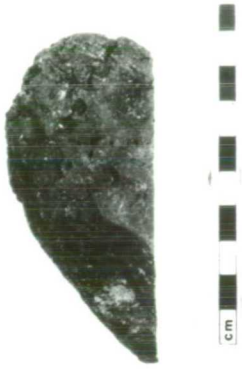

c

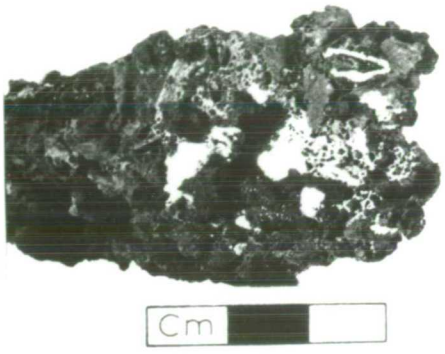

d

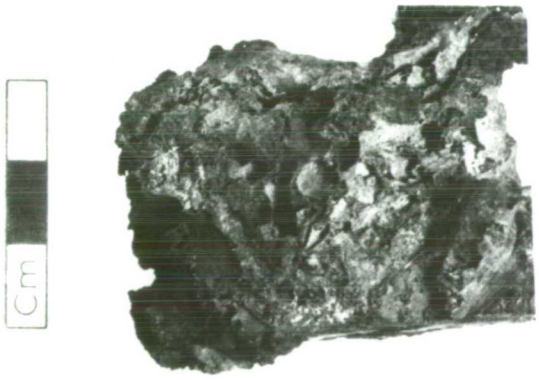

e

f

g

3.5 Slags from hematite/limonite ores and iron artefacts of Mainland Macedonia and Thasos

3.5.a Archaeological slags

This section describes dated and undated slags from a number of archaeological sites. They are grouped together here because, unlike the slags desribed in later sections of this chapter, they contain no specific tracer elements which could assign them to a particular type of ore source. The ore source must be considered to be hematite with some phosphorus and manganese. The material discussed here is bloomery slag and falls into four catergories:

a) early slag (7th-6th c. BC) from Artemission and another site also on Thasos, Limenas

b) early slag from Petres in W. Macedonia (2nd c. BC) (Fig. 2.6) c) 4th c. BC slag from Vardaroftsa (Axiochori) in W. Macedonia (Fig. 2.1).

d) surface slag finds from the Roman Forum at Philippoi (Fig. 2.6), and the vicinity of the 14th c. AD Byzantine tower at Pyrgos Apollonias (Fig. 3.1.1).

The slag from Artemission (ARTE), the sanctuary at Limenas on Thasos, dates to the 7th c. BC (Salviat and Maffre 1980). The original sample measures 8cm x 5cm. The slag was initially thought to have been associated with copper working in view of the existence of copper mines near Limenas (Muller 1979), but its texture, mineralogy and chemical composition clearly point to an iron slag and particularly smithing as opposed to smelting. This observation is corroborated by its context, namely outside the sanctuary.

The distinction between smithing and smelting slags remains a matter of considerable debate (McDonnell 1987) and no attempt will be made to resolve the issue here. Two other samples from Limenas (D354, D356) are also included here.

The bulk chemical composition of the Artemission slag has been carried out with XRF and is included in Table 3.5.1. Comparative material from other sources in Greece are included in the same Table: Hellenistic and Roman slag from theUnexplored Mansion at Knossos (Kn) (Photos et al 1985), six samples from the Athenian Agora (AA) (Mattusch 1977) dating to the 4th c. BC, and one sample from Nea Aghialos, CM (N. AGH). The Agora samples have been kindly provided by Dr E Sakellaraki and that from Nea Aghialos by Mrs E Mirtsou. The high total iron content of these slags (expressed as Fe_2O_3) together with their silica contents, their metallographic structures and the context in which they were all found suggest smithing slags. The three microprobe analyses of ARTE, D354 and D356 in Table 3.5.2 show three phases, namely wustite, fayalite (with considerable calcium) and a silicate matrix. If the CaO content exceeds 12%, the fayalite is considered a calcium-rich olivine, kirschsteinite ($CaO.FeO.SiO_2$). The matrix can be either glassy, of uniform composition, usually an olivine or a eutectic of K, Ca, Al-silicate and kirschsteinite. Plate 7c-e shows the mineralogical composition of ARTE, D354, and D356.

The composition and range of solidification temperatures of

Table 3.5.1

XRF analysis of iron slag from N. Greece, Knossos and the Athenian Agora

Sample	SiO_2	TiO_2	Al_2O_3	Fe_2O_3	MnO	MgO	CaO	K_2O	P_2O_5
ARTE	12.55	0.26	0.30	74.96	0.19	0.65	2.45	0.77	0.30
N.AGH	12.21	0.27	0.34	60.37	0.06	1.53	7.99	2.74	1.41
Kn 54	3.36	0.14	*	75.88	0.03	0.66	6.90	0.08	0.73
Kn 109a	2.16	0.13	*	80.49	0.10	0.49	3.44	0.02	0.27
Kn 109c	9.41	0.17	*	55.64	0.49	2.60	11.12	0.40	1.03
Kn 44	4.48	0.17	*	66.06	0.07	0.97	11.05	0.28	0.84
AA1578	25.66	0.41	3.74	42.05	0.85	1.24	12.22	1.58	0.42
AA1579	9.48	0.27	*	78.55	0.67	0.81	2.62	0.44	0.12
AA1609	6.62	0.20	*	73.49	0.04	0.40	1.91	0.16	0.25
AA1980	77.54	0.55	10.71	14.28	1.52	2.47	3.40	2.11	0.30
AA1581	20.01	0.20	1.90	61.78	0.24	0.92	5.90	1.62	0.20
AA1576	21.42	0.37	2.21	50.36	0.12	1.15	3.44	1.02	0.63

* Al not anal.

Table 3.5.2

Microprobe analysis of iron slags from Macedonia

Sample	phase	Na_2O	MgO	Al_2O_3	SiO_2	P_2O_5	SO_3	K_2O	CaO	TiO_2	Cr_2O_3	V_2O_5	MnO	FeO	NiO	CuO
ARTE	wust.	0.00	0.00	0.94	0.67	0.00	0.00	0.00	0.05	0.24	0.00	0.00	0.03	98.06		
	fayal.	0.00	0.00	0.00	35.96	0.00	0.00	0.00	1.46	0.00	0.00	0.00	0.46	62.13		
	matrix	0.00	0.00	18.86	45.70	0.00	0.00	7.66	11.18	0.00	0.00	0.00	0.05	16.54		
D354	fayal.	0.00	0.99	0.74	29.91	0.00	0.00	0.29	0.96	0.39	0.00	0.00	1.53	65.83		
	matrix	0.00	0.00	17.36	44.02	0.85	0.00	5.61	5.40	0.58	0.00	0.00	0.39	20.03		
	fayal.	0.00	1.70	0.00	29.84	0.00	0.00	0.00	0.49	0.29	0.00	0.00	1.65	67.02		
	matrix	0.00	0.00	20.73	40.86	1.08	0.00	7.51	4.95	0.00	0.00	0.00	0.28	17.61		
	matrix	0.00	0.00	20.30	41.85	1.12	0.00	6.72	5.33	0.69	0.00	0.00	0.19	16.74		
D356	wust.	0.00	0.00	0.66	0.70	0.00	0.00	0.00	0.21	0.58	0.00	0.00	0.87	95.19		
	fayal.	0.00	2.77	0.00	29.72	0.35	0.00	0.00	1.04	0.23	0.00	0.00	2.62	62.37		
	matrix	0.00	0.00	11.13	35.26	1.72	0.00	4.87	4.77	0.30	0.00	0.00	0.00	37.04		
	wust.	0.00	0.00	0.73	0.68	0.00	0.00	0.00	0.17	0.82	0.00	0.00	1.11	94.09		
	fayal.	0.00	5.02	1.23	30.42	0.00	0.00	0.00	2.14	0.31	0.00	0.00	3.03	56.15		
Phil 1	wust.	0.00	0.32	0.95	0.56	0.00	0.00	0.58	0.00	0.76	0.00	0.00	0.27	92.47		
	matrix	0.57	1.14	1.52	33.09	0.86	0.00	0.59	25.22	0.31	0.00	0.00	0.00	41.06		
Phil 2	wust.	0.00	0.81	3.38	1.15	0.00	0.00	0.00	0.00	0.57	0.00	0.00	0.87	86.57		
Pyrg.Ap	wust.	0.00	0.00	0.73	0.65	0.00	0.00	0.00	0.57	0.61	0.00	0.00	2.38	93.52		
	fayal.	0.00	1.76	0.00	30.48	0.00	0.00	0.00	4.75	0.18	0.00	0.00	7.02	54.33		
	wust.	0.00	0.53	0.79	1.17	0.00	0.00	0.00	0.78	0.47	0.00	0.00	2.97	90.31		
Pyrg.Ap	wust.	0.00	0.30	0.73	0.54	0.00	0.00	0.00	0.16	0.67	0.00	0.00	2.48	95.69		
	wust.	0.00	0.00	0.58	0.44	0.00	0.00	0.00	0.00	0.56	0.00	0.00	1.85	96.52		
	wust.	0.00	0.55	0.52	0.36	0.00	0.00	0.00	0.00	0.47	0.00	0.00	2.43	95.48		
	fayal.	0.00	3.28	0.41	30.44	0.37	0.00	0.00	4.70	0.32	0.00	0.00	6.36	55.25		
	fayal.	0.00	3.08	0.00	30.75	0.00	0.00	0.00	4.56	0.30	0.00	0.00	6.39	56.22		
	matrix	0.00	0.00	17.21	35.58	4.09	0.42	5.03	13.17	0.69	0.00	0.00	1.87	20.27		
	matrix	0.00	0.00	15.52	34.85	4.03	0.29	5.53	13.14	0.78	0.00	0.00	1.84	22.34		
M.Th 8	wust.	0.00	0.68	1.06	0.62	0.00	0.00	0.00	0.15	0.75	0.17	0.00	0.00	93.75		
	fayal.	0.45	2.67	0.45	31.14	0.47	0.00	0.33	21.13	0.00	0.00	0.00	0.00	42.31		
	matrix	2.81	0.39	15.93	35.54	3.22	0.21	3.84	14.28	0.23	0.00	0.00	0.00	22.40		
	'prill'	0.00	15.81	0.00	0.00	0.00	0.00	0.00	0.00	0.00	0.00	0.00	0.00	22.89	47.19	
M.Th 7	wust.	0.00	0.56	0.63	0.53	0.00	0.00	0.00	0.43	1.22	0.00	0.00	0.00	93.71		
	matrix	1.66	0.22	16.56	38.97	3.13	0.00	7.79	12.89	0.41	0.00	0.00	0.00	20.35		
	fayal.	0.56	1.80	1.60	32.00	1.31	0.00	0.29	23.49	0.00	0.00	0.00	0.25	38.04		
	fayal.	0.89	0.00	19.46	43.27	0.36	0.00	16.01	0.68	0.00	0.00	0.00	0.00	20.88		
Pet Acr	wust.	0.00	0.00	0.00	0.49	0.00	0.00	0.00	0.26	0.39	0.00	0.00	0.51	87.51		
	wust.	0.00	0.00	0.00	0.42	0.00	0.00	0.00	0.13	0.84	0.00	0.00	1.23	90.89		
Pet 2	wust.	0.00	0.65	0.77	0.35	0.00	0.00	0.00	0.23	0.79	0.00	0.00	0.50	94.86		
	wust.	0.00	0.73	0.92	0.30	0.00	0.00	0.00	0.00	0.58	0.00	0.00	0.55	94.33		
	matrix	0.00	0.00	19.75	28.49	0.00	0.00	4.81	25.21	0.46	0.00	0.00	0.00	17.94		
Pet 3	matrix	0.00	0.61	14.22	39.45	1.53	0.00	1.52	17.34	0.29	0.00	0.00	2.54	23.82		
	wust.	0.00	0.00	0.38	0.54	0.00	0.00	0.00	0.24	0.53	0.00	0.00	1.88	90.74		0.42
Pl Pet1	matrix	0.00	0.56	11.48	38.16	2.98	0.00	7.28	10.33	0.36	0.00	0.00	1.64	26.50		
	wust.	0.00	0.00	1.20	0.74	0.00	0.00	0.00	0.00	0.57	0.00	0.00	1.52	95.57		
Pl Pet2	wust.	0.00	0.64	0.76	1.18	0.00	0.00	0.00	0.36	0.89	0.00	0.00	2.34	89.32		
	matrix	0.00	0.50	11.21	35.51	0.82	0.00	2.16	13.60	0.36	0.00	0.00	3.10	28.88		
Pet 1	wust.	0.00	0.00	0.72	7.35	0.00	0.00	0.00	1.06	0.00	0.00	0.00	0.02	90.84		

		Fe	Ni
Pl Pet2	metal.	91.75	3.54
Pet Acr	metal.	4.49	97.36

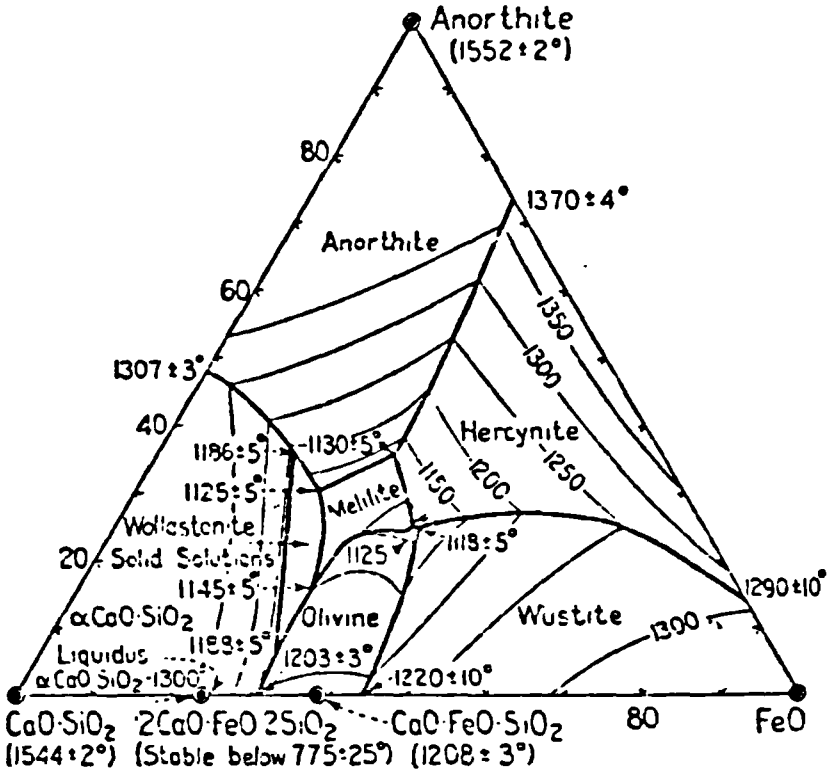

Fig. 3.5.1 FeO–CaO.SiO_2–CaO.Al_2O_3.$2SiO_2$

the slags presented in Table 3.5.2 can be interpreted in terms of the anorthite–CaO.SiO_2–FeO ternary phase diagram (Fig 3.5.1). This is a slight modification of the normally used Anorthite–SiO_2–FeO phase diagram, first put forward by Morton and Wingrove (1969; 1972). The modification is essential because of the high calcium content present in Greek slags which has been determined in samples from other parts of Greece, such as Knossos in Crete (Photos et al 1985). The three main mineralogical phases detected in the slags of Table 3.5.2 are therefore wustite, calcium-rich fayalite or olivine, and potassium-calcium-iron-aluminium silicate or mellilite. The region of solidification of these slags is to be found in the area covering the three minerals in Fig. 3.5.1 at a temperature of c. 1150°C.

Petres is a recently excavated, strongly fortified

Hellenistic settlement on a trapezoidal mound 1.5 km N.W. of the modern village of Petres and 35 km S.E. of Florina (Adam-Veleni 1983). Excavation revealed a number of rooms in what would have been two-storey houses (Fig. 3.5.2). The stratigraphy of the site suggests that the town was built in two phases, the first dating to the end of the 3rd c. BC, the second lasting to the middle of the 1st c. BC when it was destroyed by fire. Petres was more than an agricultural settlement; it was an urban centre whose prosperity was greatly enhanced by its location only 2 km from the Via Egnatia.

Extensive evidence for iron making and working was revealed at the site. A total of 70 kg of slag, generally porous and in a rather poor state of preservation, was recovered from a number of rooms under the destruction layers (Fig. 3.5.2). Black dots indicate rooms in which slag was found. The spread of slag in so many different rooms, some decorated with fine wall paintings, suggested to us that smiths may have occupied the premises after part or all of the settlement, burnt in a fire, had been abandoned and rebuilt closer to the modern village of Petres (Photos et al, in press). Although most of the Petres slag are typical smithing iron slags, two samples contained metallic iron prills with a high nickel content. This was unexpected and of considerble importance since, although analyses and metallographic examination of most of the artefacts from Petres revealed no nickel-rich iron, one shapeless mass of iron, a 'bloom' contained 3% nickel.

The third set of slags in Table 3.5.2 come from Vardaroftsa (MTh 7, 8) (Heurtley 1925-6), dating to the 4th c. BC.

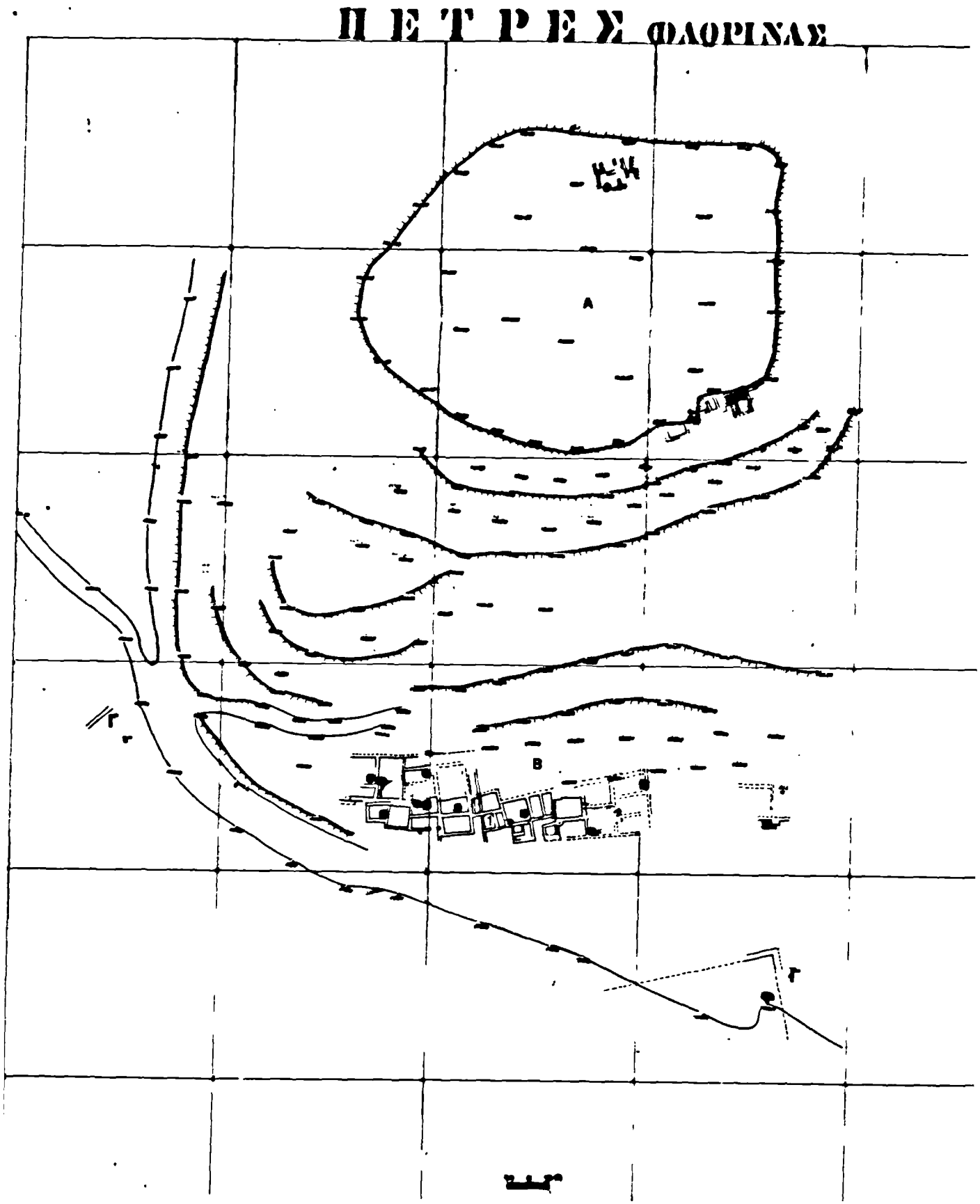

Fig. 3.5.2 Plan of Hellenistic site of Petres,WM (Photos et al, in press). Dots indicate areas within rooms where slag was found. 1 room in which pythos jar with blacksmith's tools and Ni-rich bloom was found.

The polished sections obtained from a lump of slag had the characteristic porous structure, and must have resembled the 'bloomery' slag analysed by Davies (see section 2.1.c). Among the corroded iron prills in the Vardaroftsa slag (M.Th 8) was one with a high nickel content (Table 3.5.2). The rarity of the nickel-rich iron prills in ancient slag exemplified by the single examples from Petres and Vardaroftsa samples is a point of much interest and is discussed in section 3.8.

Among the samples of Table 3.5.2, those with a relatively high Mn content associated with phosphorus come from Pyrgos Apollonias. The site, a Byzantine tower built on the foundations of an earlier tower dating 6th-4th c. BC (Collart 1937), lies at the foothills of the Symvolon mountains where deposits of Mn-containing iron ore have been extracted as recently as the late 1960's, at the mine at Folea (Gialoglou and Drymonitis 1983). The slags found within settlements and particularly working quarters (Petres, Artemission, Vardaroftsa) have been broadly classified as smithing slags on the basis of their compositions, metallography and context. The remainder (Philippoi, Pyrgos Apollonia), predominantly surface finds, are undated. Philippoi slags appear also to be smithing, while the one from Pyrgos Apollonia could be either.

In summary, the slag analyses presented here are obtained from samples produced from ores with no specific tracer element (apart from phosphorus and manganese) which could lead to a particular type of ore deposit. Manganese is not very diagnostic

Plate 7

(a) Petr.2 Wustite dendrite in a fine background of Ca-rich fayalitic lathes and glassy silicate matrix. 100x

(b) Fl.Petr.1 Extensive oxidation of a previously metallic area with slag trapped in the interstices. 100x

(c) Artemission Dendrites of wustite/lathes of Ca-rich olivine in a glassy matrix. 150x

(d) D356 Rectangular-shaped grains of Ca-rich olivine (as well as fine needles); globular wustite at top of section. 200x

(e) D354 Corroded sample: lathes of Ca-rich olivine and dendrites of wustite. 100x

(f) Pyrg. Apol. 1 Globular wustite, Ca-rich fayalite plates ; glassy silicate matrix. 200x

Plate 7

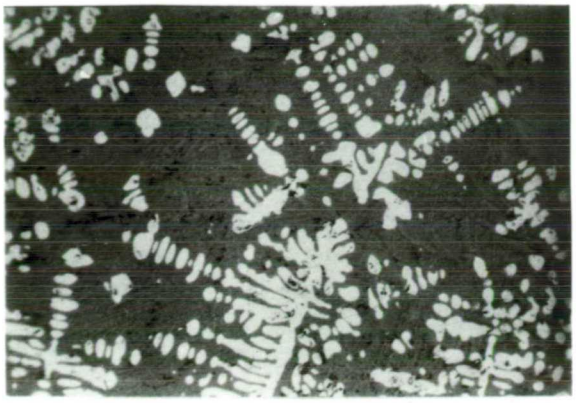

a

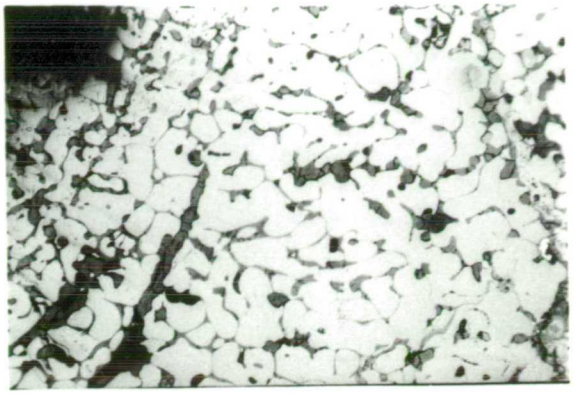

b

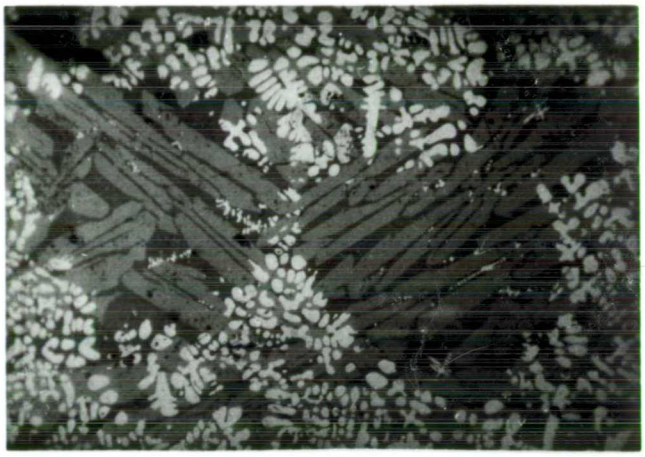

c

d

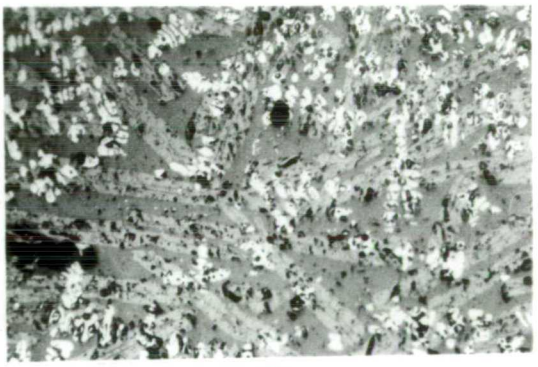

e

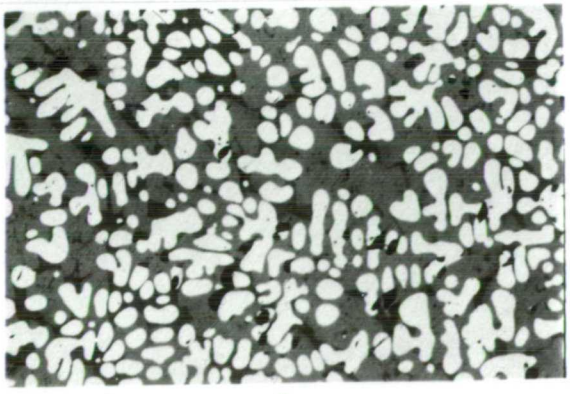

f

because it is a common enough element in iron ores. Phosphorus, on the other hand, even in small amounts in the original ore body, can be characteristic of the ore source since it invariably enters the metal, as well as partitioning in the silicate matrix of the slag inclusions.

The presence of phosphorus in some slag samples suggests that this type of iron ore deposit does exist in Macedonia and should not only be sought in West Crete, as suggested by Varoufakis (1982). Given the limited material and the unstratified context of some of these slags, relatively little archaeological and/or technological information can be deduced from their examination. However, the two nickel-rich iron prill slags from Petres are the first of their kind detected in Greece and the first evidence we have of smelting of lateritic iron ores. The presence of the nickel-rich iron bloom strengthens this observation considerably.

3.5.b Archaeological artefacts from Macedonia and Thasos

A total of fifty iron objects have been sampled from the Museums of Kavala and Thasos, with material from Amphipolis, Drama, Aidonochori on the Mainland, and Limenas on Thasos. Of these only twenty eight (Table 3.5.3) had enough metal to warrant analysis, both metallographic and EPMA slag inclusion analysis (Table 3.5.4). Seventeen artefacts were sampled from the Thessaloniki Museum, of which fifteen were analysed. The objects originated from Vergina, Tsaousitsa and Palaio Gynaikokastro (Tables 3.5.5 and 3.5.6). Finally, six objects from Petres Museum (Table 3.5.8) were analysed by EPMA on both the metal and the slag inclusions in an attempt to

establish the level of alloying elements in the metal (C, P, As, Ni) as well as any trace/minor elements within the slag inclusions which might be indicative of ore typology (Table 3.5.7).

A pioneering study of slag inclusions in British iron artefacts for ore type provenance was carried out by Hedges and Salter (1979). Todd and Charles (1977; 1978) applied the same methodology with a broader aim in mind, namely to elucidate the iron-making processes of the Dimi culture in Ethiopia as a whole, from mining of the ore to the fabrication of the final objects. By linking artefacts to a particular ore source, trade networks could also possibly be illuminated. Todd and Charles argued strongly (1979, 219) for the importance of carrying out studies on all material from a metallurgical site/region (ore, slag, artefacts) before embarking on extensive slag inclusion analysis. This has been the approach followed in the present work as well, since it is essential that all stages in the iron-making process should be studied, not just the final stage of artefact manufacture.

The analysis of slag inclusions (Tables 3.5.4, 3.5.6 and 3.5.8) consisted of either one (silicate of mellilite composition) or two (wustite and silicate) phases and only exceptionally three. Care was taken to avoid sampling inclusions which were part of a welding seam, since the aim was to analyse those inclusions which originated in the smelting cycle. Slag inclusion analysis is a time consuming procedure even with an electron microprobe attached to an energy-dispersive XRF unit, since each area or spot is analysed for

Table 3.5.3: Iron Artefacts from Kavala and Thasos Museums

Sample No.	Typology	Date	Provenance	
Tsi-Kastri	knife	EIA	Kastri	
D330	sword	eighth-seventh c. BC	Drama, Industrial Zone	1
D331	knife	"	"	
D332	tool	"	"	
D334	tool	"	"	
D336	cyl.object	fourth c. BC	Aidonochori (Tragilos)	2
D337	nail	"	"	
D338	tool	Hellenistic/Roman	Limenas, Thasos	3
D340	nail	"	"	4
D345	clamp	Roman	"	5
D346	strigil	"	"	6
D348	knife	"	"	7
D349	nail	"	"	1
D350	nail	"	"	1
D351	"	"	"	1
D352	"	"	"	1
D355	"	"	"	1
D357	"	"	"	7
D360	"	"	"	3
D365	"	"	"	3
D367	"	"	"	7
D369	"	Byzantine	"	8
D370	"	"	"	8
D372	"	"	"	8
D373	"	"	"	8
D374	"	"	"	8

1 Koukouli-Chrysanthaki (1980)
2 Koukouli-Chrysanthaki (1983)
3 Koukouli-Chrysanthaki (1978)
4 Koukouli-Chrysanthaki (1982)
5 Koukouli-Chrysanthaki (1977)
6 Parlama (1973-74)
7 Koukouli-Chrysanthaki (1983)
8 Bakirtzis (1980)

Table 3.5.4

Sample no.	Phase	Na_2O	MgO	Al_2O_3	SiO_2	P_2O_5	SO_3	K_2O	CaO	TiO_2	V_2O_3	Cr_2O_3	MnO	FeO	CuO
Th.Ts.Tf		0.00	0.00	0.00	0.00	0.00	0.00	0.00	0.11	0.00	0.00	0.00	12.59	84.40	2.90
D330	wustite	0.43	0.40	1.18	10.98	0.50	0.00	1.73	0.00	0.56	0.00	0.00	0.00	86.39	
D332	matrix	1.55	0.63	5.99	33.27	3.64	0.26	3.67	4.32	0.33	0.00	0.00	0.41	49.07	
	wustite	0.52	0.77	3.24	16.68	0.95	0.00	0.57	1.79	0.38	0.00	0.00	0.34	77.60	
D334	'wustite	0.93	0.55	2.37	10.47	0.00	0.00	1.23	5.58	0.49	0.00	0.00	0.36	78.07	
	wustite	0.00	0.49	0.92	2.61	0.00	0.00	0.00	1.08	1.52	0.00	0.00	0.33	91.57	
D336	matrix	1.59	2.59	11.27	56.36	0.64	0.00	5.04	8.80	0.24	0.00	0.00	0.67	12.61	
D337	matrix	0.66	1.92	5.12	35.23	1.49	0.28	4.27	2.05	0.39	0.00	0.00	1.52	48.05	
	wustite	0.00	0.00	0.47	0.32	0.00	0.32	0.00	0.00	0.51	0.00	0.00	0.26	99.79	
D338	matrix	1.34	2.45	14.07	51.46	1.39	0.00	4.62	10.11	5.10	0.99	0.00	1.10	5.47	
	matrix	1.21	2.56	21.17	46.74	1.45	0.00	5.52	11.32	5.51	0.00	0.00	0.00	4.35	
	matrix	1.23	2.46	17.15	53.21	1.17	0.00	4.62	10.34	4.54	0.00	0.00	0.39	3.81	
D340	wustite	0.59	1.61	0.22	0.00	0.00	0.00	0.00	0.16	5.03	0.91	1.36	3.37	84.35	
	wustite	0.55	2.96	1.32	0.35	0.00	0.00	0.00	0.00	4.24	0.59	0.60	3.18	86.83	
D345	matrix	0.00	10.86	37.39	6.01	0.00	0.00	0.32	1.54	6.17	7.96	0.96	0.92	29.47	
	matrix	0.00	7.76	19.23	23.64	0.00	0.00	1.10	6.99	7.97	2.62	0.25	0.95	28.51	
	matrix	0.00	4.18	11.69	29.95	0.00	0.00	1.61	7.99	4.59	0.00	0.00	0.74	44.00	
	wustite	0.00	0.00	0.00	0.29	0.00	0.00	0.00	0.00	0.84	0.00	0.00	0.00	98.09	
	wustite	0.00	0.00	0.00	0.12	0.00	0.00	0.00	0.00	0.63	0.00	0.00	0.00	98.92	
D346	wustite	0.00	0.00	0.00	1.78	1.14	0.00	0.00	0.20	0.00	0.00	0.00	0.19	75.97	
D349	fayalite	0.00	0.85	2.51	20.07	2.54	0.00	0.33	1.37	2.77	0.00	0.18	0.27	69.57	
	wustite	0.00	0.00	0.75	0.81	0.00	0.00	0.00	0.00	4.29	0.00	0.00	0.24	93.00	
	wustite	0.00	0.41	0.91	1.78	0.00	0.00	0.00	0.00	4.21	0.00	0.20	0.00	91.84	
	fayalite	0.00	1.04	3.03	24.09	4.40	0.00	0.53	1.53	1.88	0.00	0.00	0.38	63.85	
	fayalite	0.00	1.03	4.72	14.12	2.19	0.00	0.36	0.74	12.27	0.00	0.00	0.27	67.29	
D351	wustite	0.00	0.82	13.56	54.49	0.61	0.00	2.59	4.37	1.00	0.00	0.00	1.45	21.49	
	fayalite	0.00	0.47	8.64	29.59	0.33	0.00	0.84	2.28	0.61	0.00	0.00	1.22	51.05	
	fayalite	0.00	0.72	3.88	28.61	1.78	0.00	1.21	1.57	0.43	0.00	0.00	1.44	60.48	
	fayalite	0.00	0.54	7.48	29.67	1.23	0.00	1.54	1.94	0.38	0.00	0.00	1.43	54.49	
	fayalite	0.00	0.45	8.03	24.07	1.05	0.00	0.11	1.66	0.50	0.00	0.00	2.48	60.33	
D352	wustite	0.00	0.00	1.52	9.45	0.81	0.00	0.25	2.86	0.66	0.00	0.00	0.00	78.34	
	wustite	0.85	0.56	0.76	3.94	0.00	0.00	0.20	1.40	0.00	0.00	0.00	0.26	85.75	
D355	wustite	0.00	1.35	6.46	35.89	1.99	0.00	2.35	18.85	0.57	0.00	0.00	1.38	31.94	
	wustite	0.00	1.15	4.99	25.46	1.21	0.00	2.09	12.71	0.71	0.00	0.00	1.15	51.88	
	wustite	0.00	1.38	6.44	36.26	1.23	0.00	2.38	17.97	0.49	0.00	0.00	1.33	33.51	
	wustite	0.00	0.38	0.30	0.36	0.00	0.00	0.00	0.00	0.51	0.00	0.00	1.84		

Table 3.5.4		Na_2O	MgO	Al_2O_3	SiO_2	P_2O_5	SO_3	K_2O	CaO	TiO_2	V_2O_5	Cr_2O_3	MnO	FeO
D355	wustite	0.00	1.35	6.46	35.89	1.99	0.00	2.35	18.85	0.57	0.00	0.00	1.38	31.94
	wustite	0.00	1.15	4.99	25.46	1.21	0.00	2.09	12.71	0.71	0.00	0.00	1.15	51.88
	wustite	0.00	1.38	6.44	36.26	1.23	0.00	2.38	17.97	0.49	0.00	0.00	1.33	33.51
	wustite	0.00	0.38	0.30	0.36	0.00	0.00	0.00	0.00	0.51	0.00	0.00	1.84	96.04
D360	wustite	0.00	0.87	0.42	0.95	0.00	0.00	0.00	0.44	0.47	0.00	0.00	2.41	95.37
	wustite	0.00	0.95	1.03	5.47	0.35	0.00	0.34	3.49	0.51	0.00	0.00	1.95	87.38
	wustite	0.00	0.22	0.00	0.14	0.00	0.00	0.00	0.40	0.00	0.00	0.00	0.00	101.38
		0.00	0.00	18.18	64.48	0.00	15.75	0.00	0.00	0.00	0.00	0.00	0.00	1.26
D365	fayalite	0.00	1.43	7.08	31.70	0.38	0.00	2.04	9.34	2.27	0.24	0.00	0.51	48.66
	fayalite	0.00	1.33	5.94	26.12	0.62	0.00	1.79	8.69	1.94	0.28	0.00	0.51	47.67
	matrix	0.00	2.00	8.48	40.86	0.91	0.00	3.01	14.17	3.25	0.45	0.00	0.62	23.57
	wustite	0.00	0.84	1.89	6.71	0.43	0.00	0.46	2.11	2.67	1.01	0.26	0.34	83.95
	wustite	0.00	1.53	1.19	0.45	0.00	0.00	0.00	0.00	2.47	2.92	0.59	0.56	89.36
	wustite	0.00	2.24	0.87	0.26	0.00	0.00	0.00	0.00	2.01	3.29	1.18	0.63	89.53
	wustite	0.00	2.36	1.43	0.00	0.00	0.00	0.00	0.00	2.59	4.14	1.49	0.63	87.39
	fayalite	0.00	0.98	5.83	32.27	1.35	0.00	1.94	6.35	0.91	0.00	0.00	0.37	53.01
D366	wustite	0.00	0.39	2.47	14.45	2.39	0.00	0.71	1.38	0.00	0.00	0.00	0.66	78.51
	wustite	0.73	0.34	0.11	19.04	0.56	0.00	0.48	2.08	0.00	0.00	0.00	0.67	58.28
D369	fayalite	0.00	2.08	2.43	22.45	1.63	0.00	1.75	5.96	0.43	0.00	0.00	0.19	60.36
	fayalite	0.00	1.96	3.25	26.89	3.52	0.00	1.52	5.86	0.38	0.00	0.00	0.00	56.45
	matrix	1.20	0.00	18.05	65.68	0.00	0.00	15.49	0.00	0.00	0.00	0.00	0.00	0.38
D372	wustite	0.00	2.38	0.50	0.22	0.00	0.00	0.00	0.00	0.65	0.00	0.00	0.24	95.47
	wustite	0.00	0.00	0.00	0.33	0.00	0.00	0.00	0.00	0.32	0.00	0.00	0.00	92.73
	fayalite	0.00	0.69	3.95	21.33	1.83	0.00	0.73	5.10	0.45	0.00	0.00	0.71	62.08
		1.20	0.94	3.04	16.82	2.13	0.00	0.93	4.47	0.34	0.00	0.00	0.48	59.95
D373	matrix	0.00	0.74	4.24	32.72	6.06	0.00	1.62	9.71	0.27	0.00	0.00	4.57	39.74
	matrix	0.00	0.59	3.52	27.96	5.57	0.00	1.26	7.96	0.27	0.00	0.00	4.07	50.45
	wustite	0.00	0.62	0.35	0.65	0.50	0.00	0.00	0.00	0.50	0.00	0.00	2.73	94.98
	wustite	0.00	0.42	0.43	0.24	0.50	0.00	0.00	0.00	0.51	0.00	0.00	2.15	95.82
D374	wustite	0.00	10.37	0.57	1.29	0.00	0.00	0.37	0.49	0.00	0.00	0.00	0.31	85.78
	wustite	0.00	8.97	0.44	0.36	0.00	0.00	0.00	0.49	0.00	0.00	0.00	0.32	87.40
	fayalite	0.00	2.14	4.10	25.21	6.23	1.75	6.45	0.39	0.00	0.00	0.00	0.37	40.95
	wustite	0.00	0.47	0.66	1.45	0.42	0.00	0.45	0.77	0.00	0.00	0.00	0.32	91.02

Table 3.5.4: Microprobe analyses of slag inclusions in objects from Thasos and Kavala Museums

Table 3.5.5 Iron Artefacts from Thessaloniki Museum
(for Vergina objects, see Andronikos 1969)

Sample No	Typology	Date (cent. BC)	Provenance
MTh 1	fibula	EIA	P Gynaikokas
MTh 2a (AE 418)	sword (near edge)	EIA	"
MTh 2b (AE 418)	sword (handle)	EIA	"
MTh 3	knife	EIA	"
MTh 9	nail	EIA	Tsaousitsa
MTh 10	spearhead	surface find	Vergina
MTh 11 (I ζ)	spearhead	seventh-sixth	"
MTh 12 (AE 5588)	ring	unknown date	"
MTh 13 (I IV)	sword	seventh-sixth	"
MTh 14a (T VII γ)	spearhead (tip)	probably 9th	"
MTh 14b (T VII γ)	spearhead (socket)	"	"
MTh 15 (Z μ)	sword	mid 9th-mid 7th	"
MTh 16 (Nz25, zIIIa)	knife	eleventh-mid 8th	"
MTh 17 (Z3)	knife	first half 9th	"
MTh 18 (KIa)	spearhead (socket)	probably 8th	"
MTh 19 κχα	knife	late 10th-early 9th	"
MTh 20 (T3a)	arrowhead	c. 900 BC	

Table 3.5.8 Iron Objects from Vergina

Sample no.	Phase	Na_2O	MgO	Al_2O_3	SiO_2	P_2O_5	SO_3	K_2O	CaO	TiO_2	MnO	FeO
M.Th 2a	fayalite	0.97	0.00	7.07	35.06	1.00	0.00	3.11	3.48	0.19	1.51	45.15
	fayalite	0.00	2.45	0.00	28.69	0.00	0.00	0.00	0.89	0.00	0.57	66.79
	fayalite	0.00	2.55	0.00	29.11	0.00	0.00	0.00	1.21	0.00	0.49	65.46
	wustite	0.41	0.00	0.00	0.00	0.00	0.00	0.00	0.00	0.00	0.17	97.96
M.Th 2b	fayalite	0.00	3.90	0.00	30.15	0.00	0.00	0.00	0.50	0.00	0.56	64.63
	fayalite	0.00	0.87	2.48	29.95	0.00	0.00	0.99	4.36	0.00	0.36	61.02
	fayalite	0.56	0.72	2.04	29.67	0.00	0.00	0.47	2.49	0.00	0.39	63.91
M.Th 3	wustite	0.00	9.95	0.57	22.78	0.00	0.00	0.31	2.09	0.00	0.24	70.25
	fayalite	0.82	3.71	5.58	40.63	0.28	0.00	1.67	5.52	0.00	0.00	41.56
	fayalite	1.03	1.72	9.53	41.45	0.00	0.00	3.09	7.17	0.25	0.00	35.93
	wustite	0.52	2.11	0.48	0.41	0.00	0.00	0.00	0.00	0.00	0.00	94.92
M.Th 10	matrix	0.63	1.71	6.01	59.92	0.00	0.00	2.59	17.17	0.54	7.64	3.89
	matrix	0.63	1.57	6.38	59.99	0.00	0.15	2.51	16.35	0.69	6.98	4.02
	wustite	0.93	0.61	1.26	1.73	0.83	0.00	0.33	1.66	0.34	0.43	89.05
M.Th 11	fayalite	0.00	0.57	0.00	29.39	0.00	0.00	0.13	1.78	0.00	2.03	64.39
	fayalite	0.45	0.61	0.00	27.79	0.00	0.00	0.00	1.59	0.00	1.97	66.11
	wustite	0.93	0.61	1.26	1.73	0.83	0.00	0.33	1.66	0.34	0.43	89.05
M.Th 1	matrix	1.96	1.91	12.53	60.01	0.00	0.00	8.27	11.01	0.75	0.16	2.80
	matrix	1.67	2.22	12.79	61.33	0.00	0.00	7.63	10.86	0.62	0.00	3.55
	matrix	1.86	1.92	12.63	60.50	0.00	0.00	7.84	10.67	0.58	0.00	4.22
	matrix	2.09	2.26	13.12	61.16	0.00	0.00	7.97	10.60	0.64	0.00	2.84
	matrix	2.01	2.45	13.25	49.10	0.00	0.00	7.73	12.24	0.77	0.00	10.51
	matrix	1.68	1.88	11.92	58.16	0.00	0.00	7.44	10.08	0.67	0.00	6.04
M.Th 19	matrix	2.28	1.88	15.46	59.79	0.00	0.00	5.53	13.44	0.66	0.19	2.01
	matrix	1.97	1.53	14.48	58.67	0.00	0.00	5.25	13.01	0.67	0.53	4.11
	matrix	2.15	1.52	13.73	53.43	0.00	0.00	4.77	11.65	0.67	0.29	14.97
	matrix	1.86	1.46	15.22	61.04	0.00	0.00	5.49	13.30	0.73	0.62	2.03
	matrix	2.08	1.57	15.08	59.76	0.00	0.00	5.36	13.10	0.54	0.48	2.98

Table 3.5.8	MgO	Al_2O_3	SiO_2	P_2O_5	SO_3	K_2O	CaO	TiO_2	V_2O_5	Cr_2O_3	MnO	FeO	
Petro 1	2.09	0.51	4.82	0.00	0.00	0.00	4.31	0.00	0.00	0.00	0.00	63.23	
Petro 4	0.00	1.92	8.22	1.87	0.33	0.19	3.03	0.00	0.00	0.00	0.00	66.79	
	0.00	0.95	0.95	0.00	0.00	0.00	0.13	0.38	0.00	0.00	0.00	85.62	0.27
Petro 5	0.00	7.72	31.60	3.87	0.00	2.01	10.83	0.24	0.00	0.00	1.66	36.21	
Petro 6	0.00	0.00	0.64	0.00	0.00	0.00	0.25	0.37	0.00	0.00	0.00	88.97	2.17
	0.00	0.00	3.31	0.00	0.00	0.00	0.35	0.00	0.00	0.00	0.00	72.36	
Petro 7	1.01	15.44	48.32	0.00	0.00	5.66	17.48	0.00	0.00	0.00	0.00	6.57	
	0.00	0.00	1.08	0.23	0.00	0.00	0.00	0.35	0.00	0.00	0.00	82.78	0.43
Petro 10	0.00	0.00	0.42	0.00	0.00	0.00	0.38	0.37	0.00	0.00	0.00	73.38	

	Fe	Ni	Cu	Mn	Ti	Si	P
Petro1	97.73		0.30		0.35		
	98.49				0.31		
	98.97		0.16		0.35		
Petro 3	97.51				0.38	0.13	
	98.27				0.39	0.35	
Petro 4	98.27				0.29		
Petro 5	98.41				0.36		
	96.52				0.52		0.52

Table 3.5.8: Analyses of metal and slag inclusions in objects from Petres, WM

Plate 8 Kavala and Thasos Museums Objects

D330 (a) Sword. Ferrite and pea rlite. Uniformly carburized object (about 0.1-0.2% C). Some areas have 0.4% C. Not many slag inclusions, and those that are present are equally dispersed within the matrix. No slag stringers. HV 315, 333, 345. 50x.

D351 (b) Nail. Various degrees of carburization. Many slag inclusions elongated along the line of work (upper right-hand side), others not. Ferrite and pearlite; occasionally ferrite of widmanstaetten structure (centre). Average carbon content: 0.3% C. 200x.

D331 (c) Knife. Wittmanstaetten structure of ferrite. Partly spheroidized pearlite at the grain boundaries. Must have been heated for a prolonged period of time at 700 C. Globular slag inclusions. 400x.

D369 (d) Nail. Ferrite with a medium number of inclusions. Considerable amount of phosphorus in slag inclusions. 200x.

D332 (e,f) Tool. Ferrite wih fine cementite films at the grain boundaries. Considerable number of slag inclusions. Neumann bands (f), parallel within the same grain but changing directions from grain to grain. They are caused by sudden stress and are common in metal with some quantity of phosphorus. Indeed, the matrix of some slag inclusions did contain phosphorus. (e) 100x, (f) 200x.

D334 (g,h) Tool. Ferrite grains with fine cementite at the grain boundaries. Large number of slag inclusions; some elongated in the direction of working. No welding seams. Slag inclusions (h) consist of two phases, silicate matrix (dark grey), wustite globules (light grey). (g) 100x, (h) 400x.

Plate 8

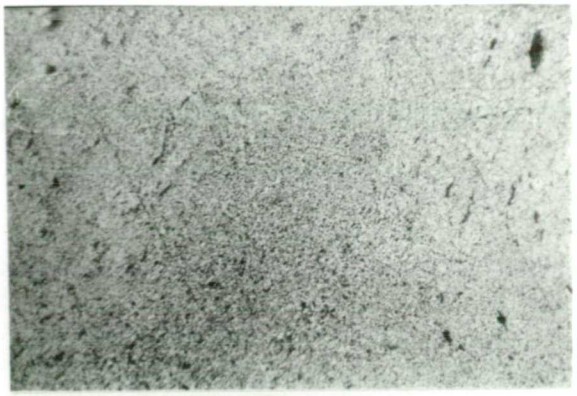

a

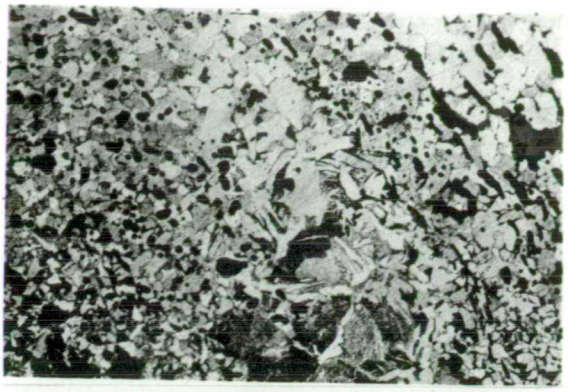

b

c

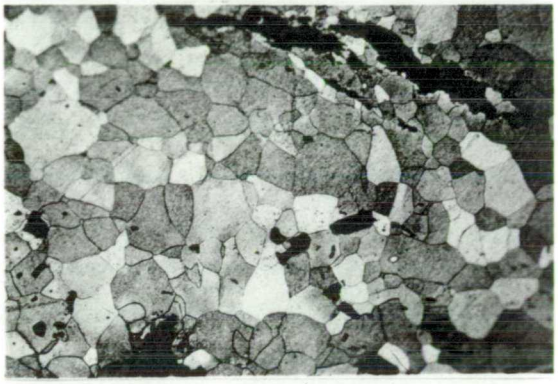

d

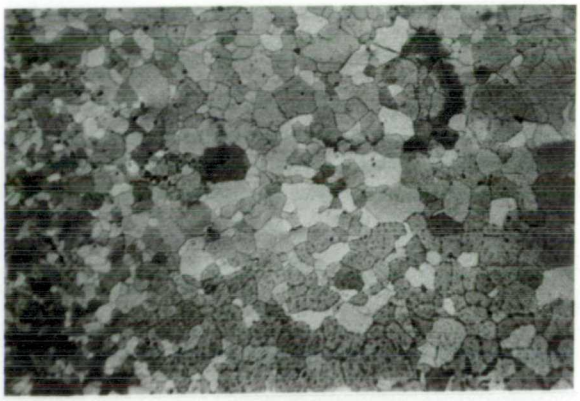

e

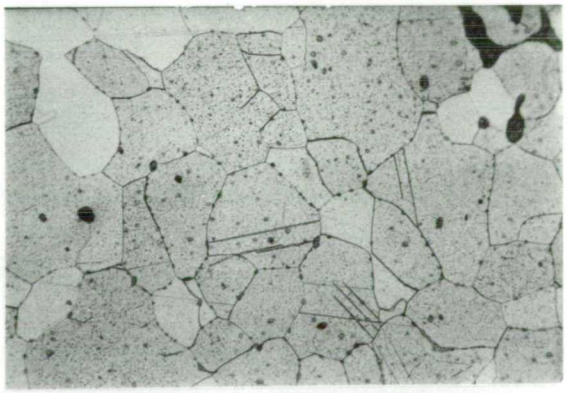

f

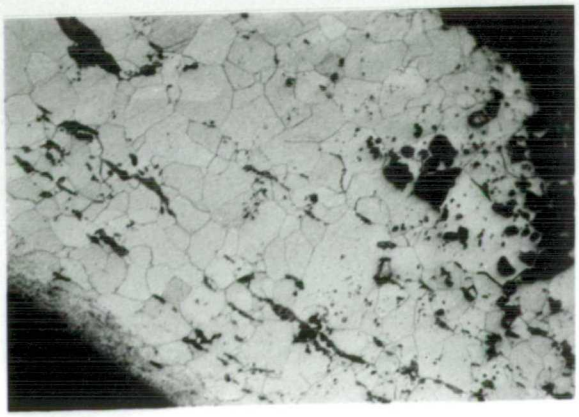

g

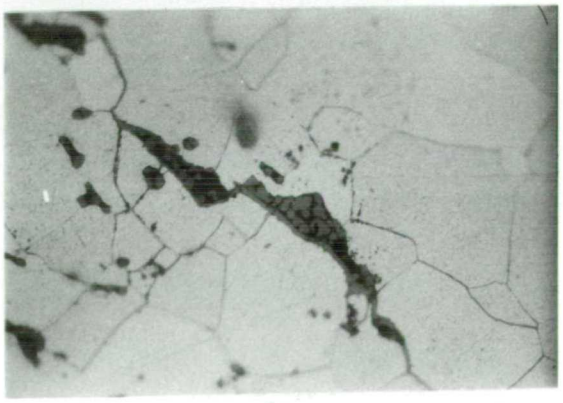

h

Plate 9 Kavala and Thasos Museums Objects (contin.)

D350 (a,b) Nail. Pearlite and ferrite of widmanstaetten structure; C content 0.4-0.5 %. (a) 100 x, (b) 400 x.

D340 (c,d) Nail. Carburization of the edges. Possibly only one sheet of metal. No welding lines or slag stringers. About 0.6-0.7% C at the edges. Ferrite and pearlite (d). No phosphorus. (c) 50x, (d) 200x.

D345 (e) Clamp. Carburization of the egde; ferrite and pearlite. Ferritic matrix, no phosphorus. 100x.

D348 (g,h) Knife. Uniform ferrite with very few slag inclusions. Neumann bands resulting from stress during cold hammering. (g) 100x, (h) 200x.

D348 (f) Knife. Slag inclusion trapped within the matrix of the corroded metal. Rare evidence of a three-phase inclusion with fayalite lathes, wustite dendrites, silicate matrix. Almost certainly a smelting slag inclusion. 200x.

Plate 9

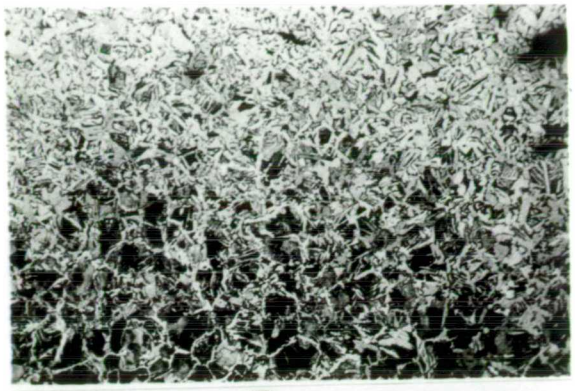

a

b

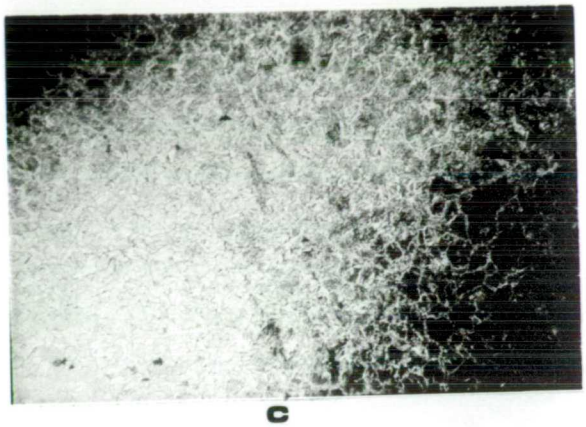

c

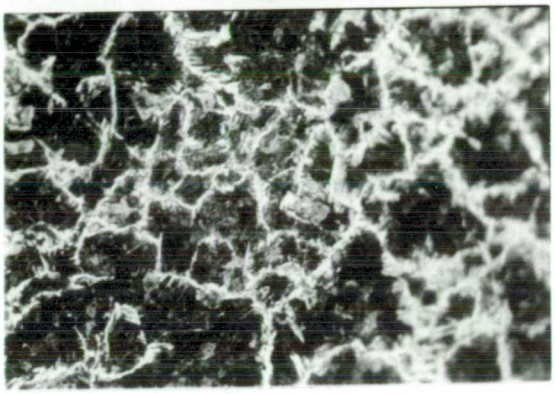

d

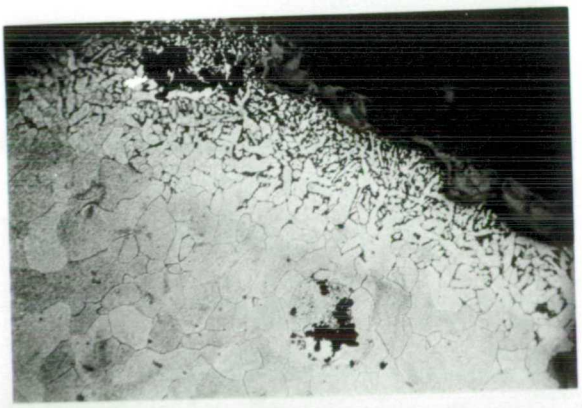

e

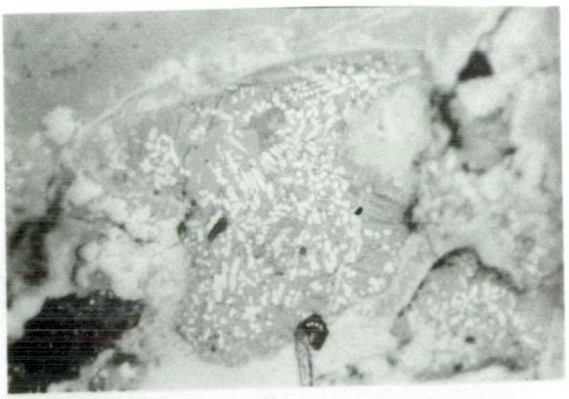

f

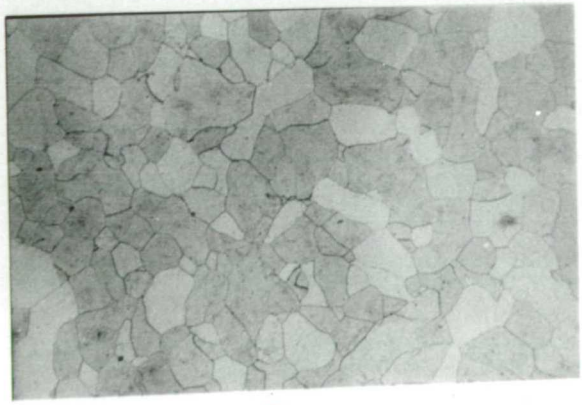

g

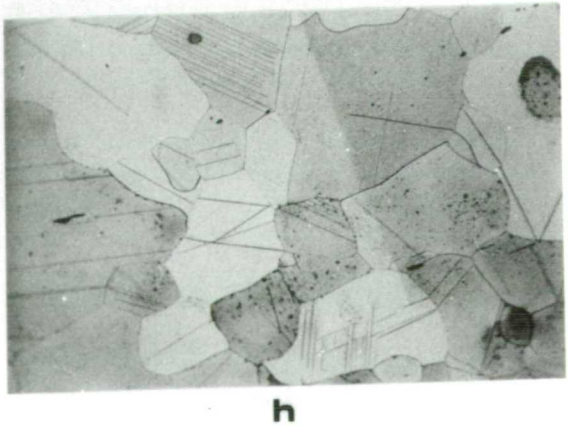

h

Plate 10 Thessaloniki Museum Objects

MTh 1 (a) Fibula. Some areas 0.4% C, most contain about 0.2% C. Pearlite and ferrite in widmanstaetten structure. 100x.

MTh 2(b) (b) Sword (handle). Ferrite with a very large number of slag inclusions. Similar to the composition and metallography of the blade. 200x.

MTh 2a (c,d) Sword (near tip). Ferrite with excessive amount of elongated slag inclusions along the direction of working. Object is probably forge-welded from two or three sheets of wrought iron. Very different from the rest of the sampled objects. Two or three white lines corresponding to welding seams. No carburization of the edges at all. (c) 100x, (d) 200x.

MTh 3 (e,f) Knife. Tip is cold worked, grains partly elongated, pearlite in the grain boundaries, HV 204. Relatively few inclusions. Uniform distribution of F+P thoughout, although edges are decarburized compared to middle section. (e) 200x, (f) 400x.

MTh 9 (g) Nail. Probably martensite with cementite. 400x.

MTh 10 (h) Spearhead. Uneven distribution of carbon. Widmanstaetten structure of ferrite and pearlite (0.1-0.2 %C). Carburization at the edges (0.2 %C), less in the centre. Relatively few inclusions. 100x.

Plate 10

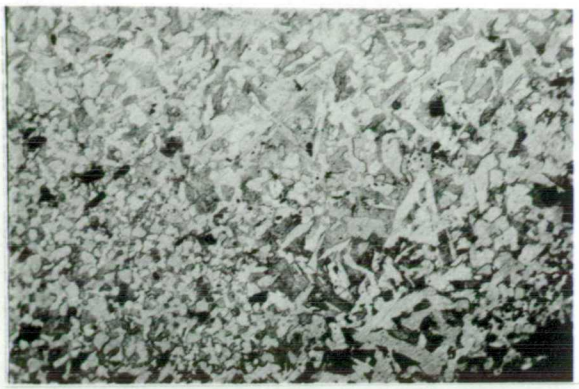

a

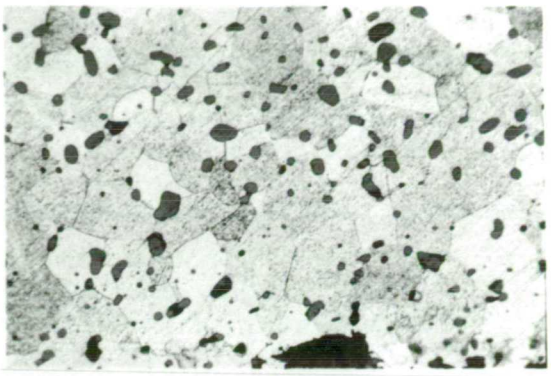

b

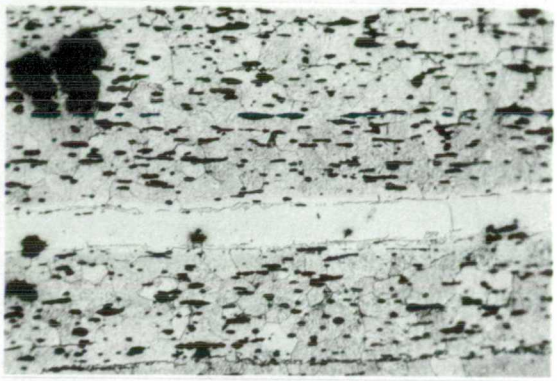

c

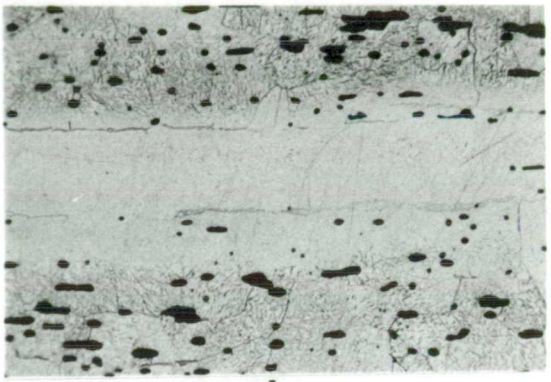

d

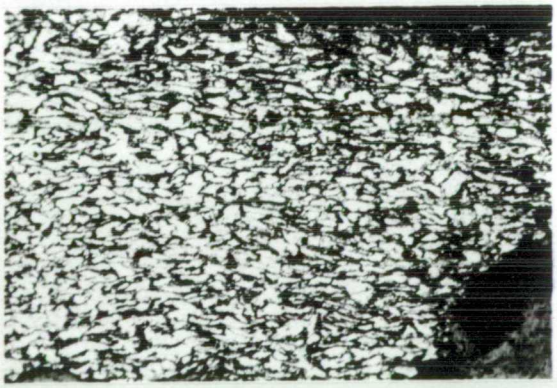

e

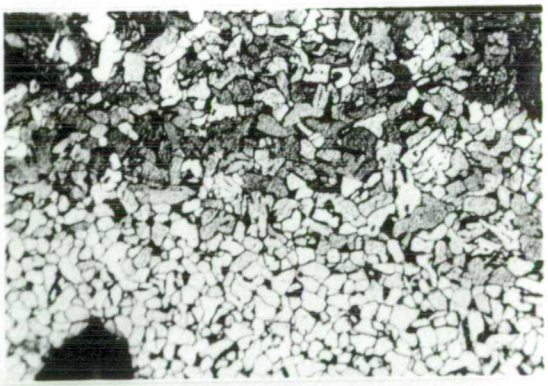

f

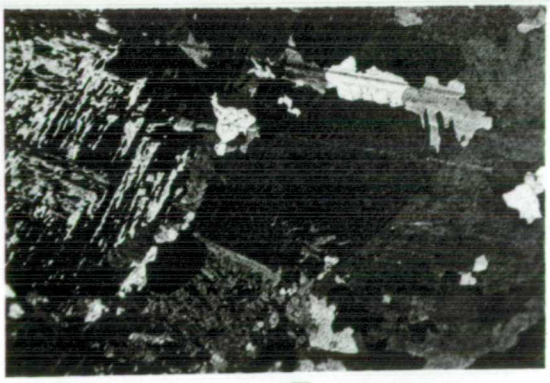

g

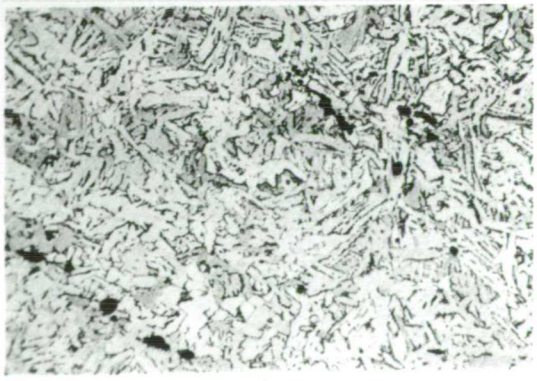

h

Plate 11 Thessaloniki Museum Objects (contin.)

MTh 11 8(a,b,c) Spearhead. Ferrite with probably carbide needles at the tip, HV 108. More carburized in the middle . It seems the pearlite has partially spheroidized (HV 136). Average number of inclusions. Possibly made of three sheets, two low C at the egdes, one high C in the middle. (a) 100x, (b) 200x, (c) 400x.

MTh 13 (e,f) Sword. All ferrite with small round slag inclusions everywhere. Ferrites of various grain size, smaller at the tip and opposite end, and larger in the middle. (e) 100x, (f) 200x.

MTh 12 (d) Ring. Uniform distribution of ferrite surrounded by spheroidized pearlite; 0.2% C; HV 149, 148. Slag stringers elongated along the direction of working. 200x.

MTh 14a (g,h) Spearhead near tip. Ferrite in the middle and F+P at the two egdes (0.4%C). Elongated inclusions because of working in the area of lower C. Various grain sizes. Difficult to establish how many sheets this piece may have been made out of. Inhomogeneous carburization in many areas. It may reflect the inhomogeneity of the bloom. (g) 100x, (h) 100x.

Plate 11

a

b

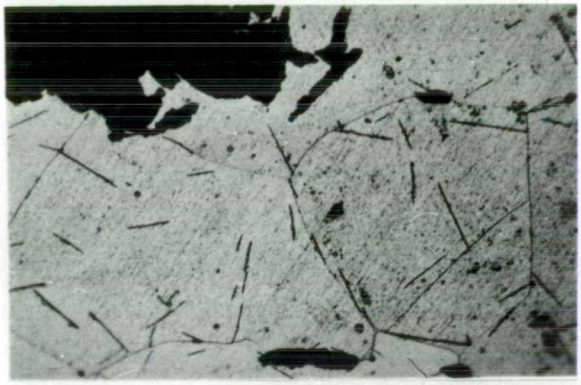

c

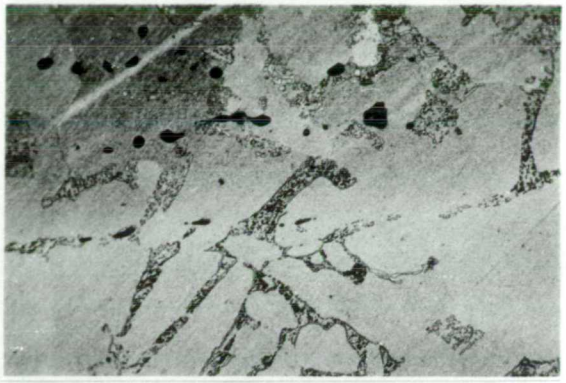

d

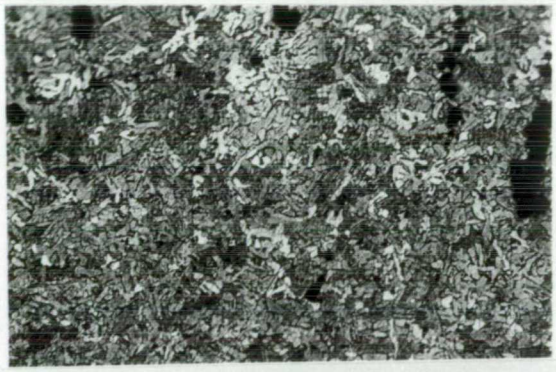

e

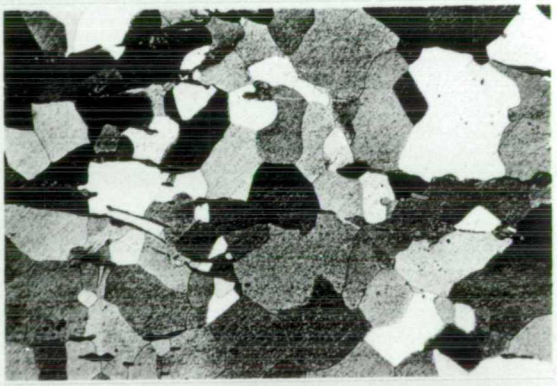

f

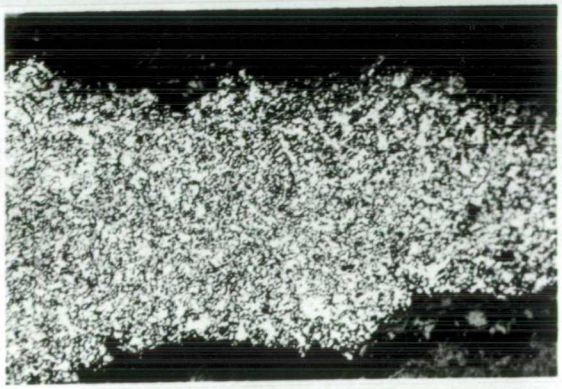

g

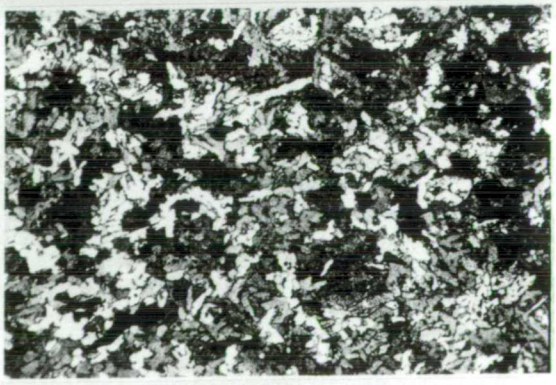

h

Plate 12 Thessaloniki Museum Objects (continued)

MTh 15 (a) Sword. Carbon content in centre of the sample 0.1-0.2 %C. HV 128, but more (0.2-0.3% C) at the tip (HV 148,154 at the tip and HV 128 in the middle). Few inclusions , no welding seams. 200x.

MTh 16 (b) Knife. It is possible this is the result of welding and folding two sheets, one with high carbon, 0.7% C, to one of ferrite (F) and pearlite(P). Welding seam in the middle is characterised by the presence of stringers. The widmanstaetten structure in the middle is nearer the 0.4% C level. Elongated slag inclusions testify direction of working. High carbon area (only P, HV289; P+F, HV215,236). 100x.

MTh 18 (c,d) Spearhead (socket). Originally three separate sheets forged together and then piled. Low C/high C/low C. Upon folding, five layers were evident resulting in a series of low/high/low/high/low carbon areas. The high C areas approach the eutectic (0.8 %C), the low C areas are c. 0.5 %C. Very impressive for an object about 1 cm long and 0.5 cm wide. P, HV 360; P+F, HV 235, 215. (c) 100x, (d) 200x.

MTh 19 (e) Knife. Upper (feathery) bainite. Formed at about 500 C, the result of rapid cooling. Relatively few inclusions. 200x.

D338 (f) Agricultural tool. Ferrite with some pearlite at the grain boundaries. Slag inclusions (black). 100x.

Katafyto nail (g) Ferrite with numerous slag inclusions. 200x.

(h) 'Pearlitic' ghost structure in corrosion area of artefact. 100x.

Plate 12

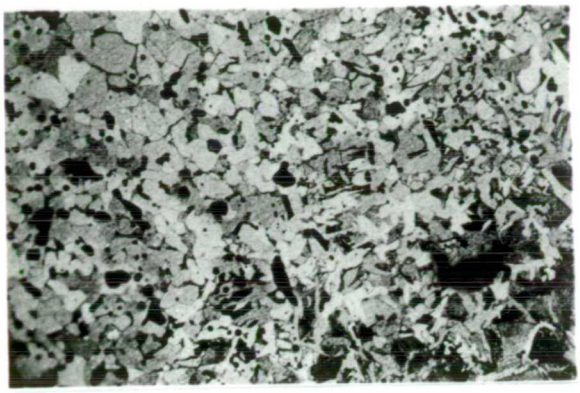

a

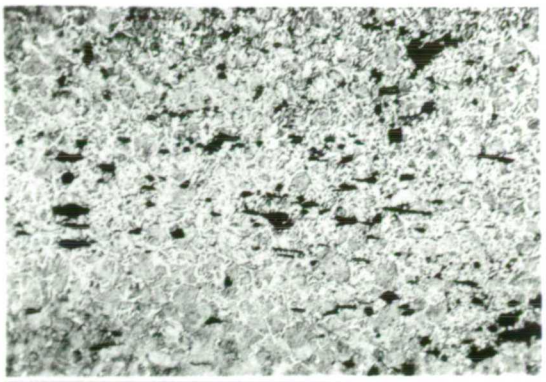

b

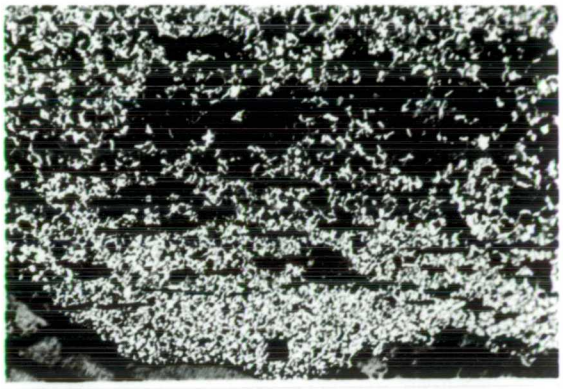

c

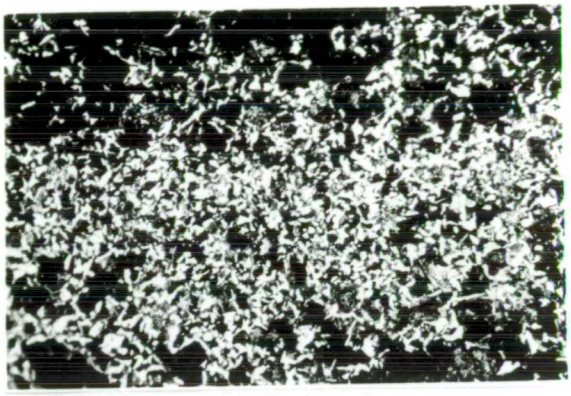

d

e

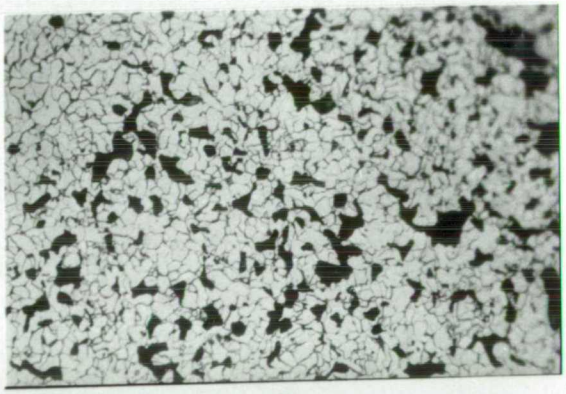

f

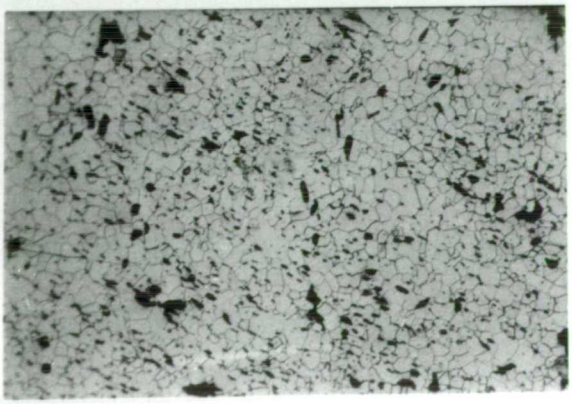

g

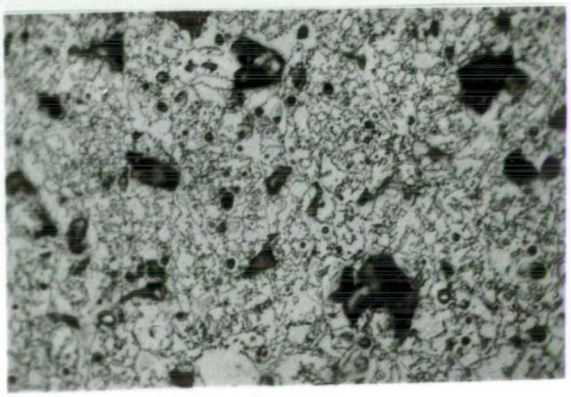

h

Table 35.7

Sample	Typology	Fe %	Cu	Ni	Metallography
Petro.1	handle	98.49	0.34	0.00	Two areas: one is mostly ferriti but with cementite films at the grain boundaries. The other is medium C steel. The two areas ar forge welded. Slag stringers are evident at the interface. **Plate 13a,b,c,d**
Petro. 2	hook	nd	nd	nd	corroded
Petro. 3	strigil	98.26	0.35	0.00	Structure of iron with less than .05% C. It is cooled slowly Large ferrite grains. Black spot are probably carbonitrides, the result of fast cooling and then annealing between 200 and 70 **Plate 13e**
Petro. 4	handle	98.27	0.00	0.00	Iron with about .15%C. Fine ferri grains with pockets of pearlite a the grain boundaries. Cooled moderately fast. HV(200)=196. **Plate 13g**
Petro. 5	nail	98.14	0.14	0.00	Ferrite grains with thin cementit films at the grain boundaries and as stringers. HV(200)=182. **Plate 13h**
Petro. 6	iron lump	95.94	0.00	2.25	Ferrite in matrix of pearlite. Widmanstatten structure. HV(200)=492,348,170
Petro. 7	clamp	98.36	0.00	0.00	Iron with about .15%C. Pearlite a the grain boundaries. HV(200)=185 **Plate 13f**

Plate 13

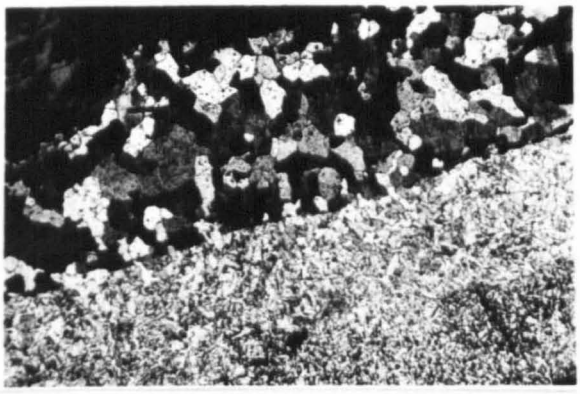

a

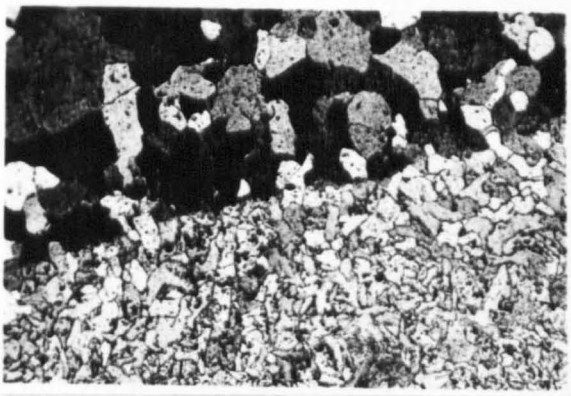

b

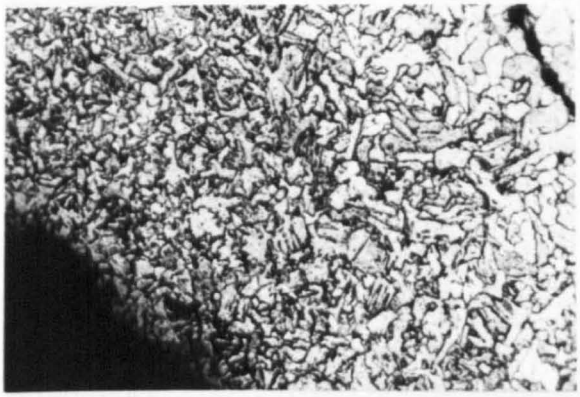

c

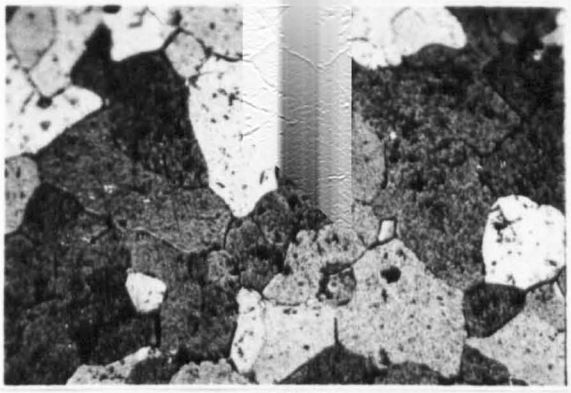

d

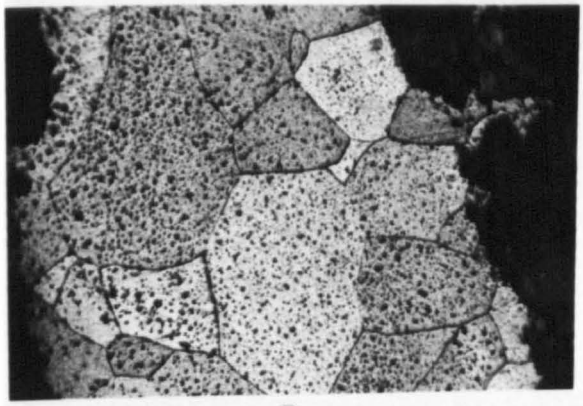

e

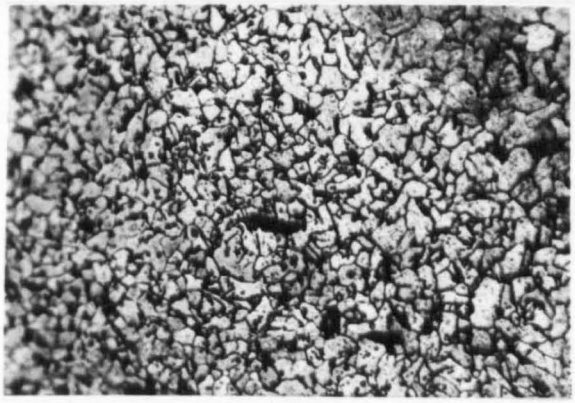

f

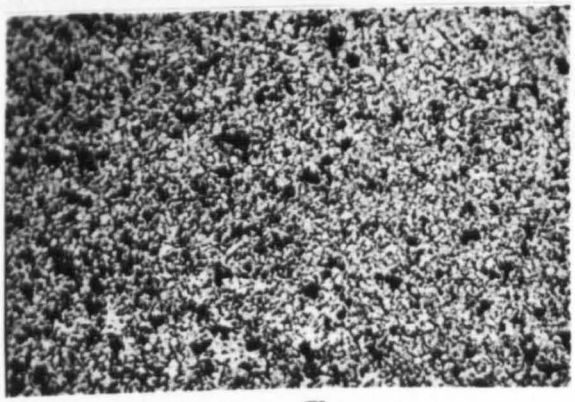

g

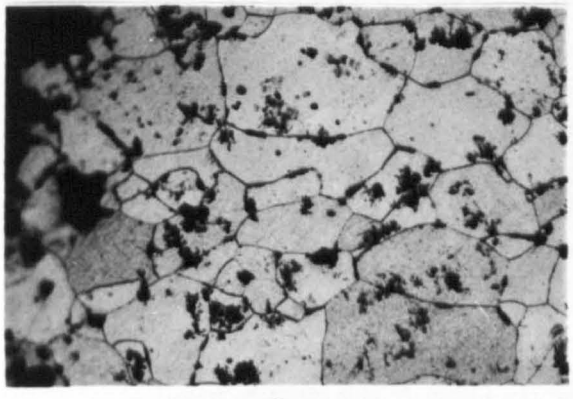

h

a considerable number of minor and trace elements, increasing the data collection time accordingly.

This section only describes the metallographic examination of the three groups of artefacts from the Museums of Kavala, Thasos, Thessaloniki and Pella. The microprobe analyses presented are discussed in the context of provenience in section 3.6. The analyses are by no means exhaustive. A random number of inclusions were analysed and evidence for the presence of Ti, V, Cr, P and Mn was sought. The metallography of each object is discussed in relation to the relevant Plate.

3.5.c Discussion

Most of the swords (three out of four) and all the tools are of ferritic composition. Most of the knives (four out of five) and spearheads (two out of three) are a combination of ferrite and pearlite. Nails and various miscellaneous objects have a varying degree of carburization. There does not seem to be a great deal of control over carburization with the exception of the swords which seem to be ferritic with relatively few slag inclusions (apart from the find from P. Gynaikokastro). It is difficult to establish with certainty the presence of weld lines. Pleiner (1973) pointed out that welding seams even with accompanying slag stringers cannot ascertain that forge-welding between two different metal sheets had taken place. He suggested that iron/steel welding can be clearly distinguished only if the artefact is immediately quenched, since a slow of rate of cooling makes welding seams less discernible. Evidence of martensite or

tempered martensite, suggesting quenching or quenching followed by annealing, was not noticed among the functional objects (tools, knives, etc). Thus, quench hardening does not seem to have been practised. The presence of spheroidized pearlite indicated prolonged heating of iron/steel near the critical temperature. It is interesting that this prolonged heating was observed in decorative objects (fibula, ring, clamp), while the widmanstaetten structure suggestive of fast cooling rate was observed in the functional objects (D330, D331, MTh 10, MTh 14, MTh 15). In addition, the presence of feathery bainite (MTh 19) is also indicative of rapid cooling. The relatively small number of slag inclusions suggests good smithing/forging of the primary bloom.

3.6 Titanium-rich iron slags: Thasos and East Macedonia

3.6.a Morphology and Mineralogy

Iron slags from Thasos and the East Macedonian Mainland are clearly distinguished from iron slags of other localities in Greece. The former are derived from the smelting of titanium-rich magnetite sands which are the product of decompositon of the Thasos gneiss and the Vrontou granite respectively.

Bloomery iron slags are more difficult to describe than blast furnace slags. The latter are usually glassy and compact and relatively easy to identify. Bloomery slag morphology covers a wide range from spongy and porous to glassy and compact. For the present discussion, slag was classified into four groups namely: spongy, semi-spongy to semi-compact, compact and drop-like. Because slags do not photograph well, three drawings of Thasos slags were kindly executed by Mr J Monteadora and are included here to illustrate the prominent features of these types:

(a) compact slag (with ropey structure) (Fig 3.6.1a)

(b) slag with drop-like features (Fig 3.6.1b)

(c) a spongy slag (with a variety of pore sizes) (Fig 3.6.1c)

The drawings are 80% scale.

Of the eighty slag samples collected from sites on Thasos (see appendix 3.1.3), all of them the result of smelting of Ti-rich magnetite sands, 53% were spongy, 28% semi-spongy to semi-compact, 16% compact with or without ropey structure and 3% drop-like. On the Mainland, however, iron slag morphology was different. Of the 99 slag samples collected, 61% were compact (ropey and occasionally glassy), 26% were semi-spongy to semi-compact, 12% spongy and 1%

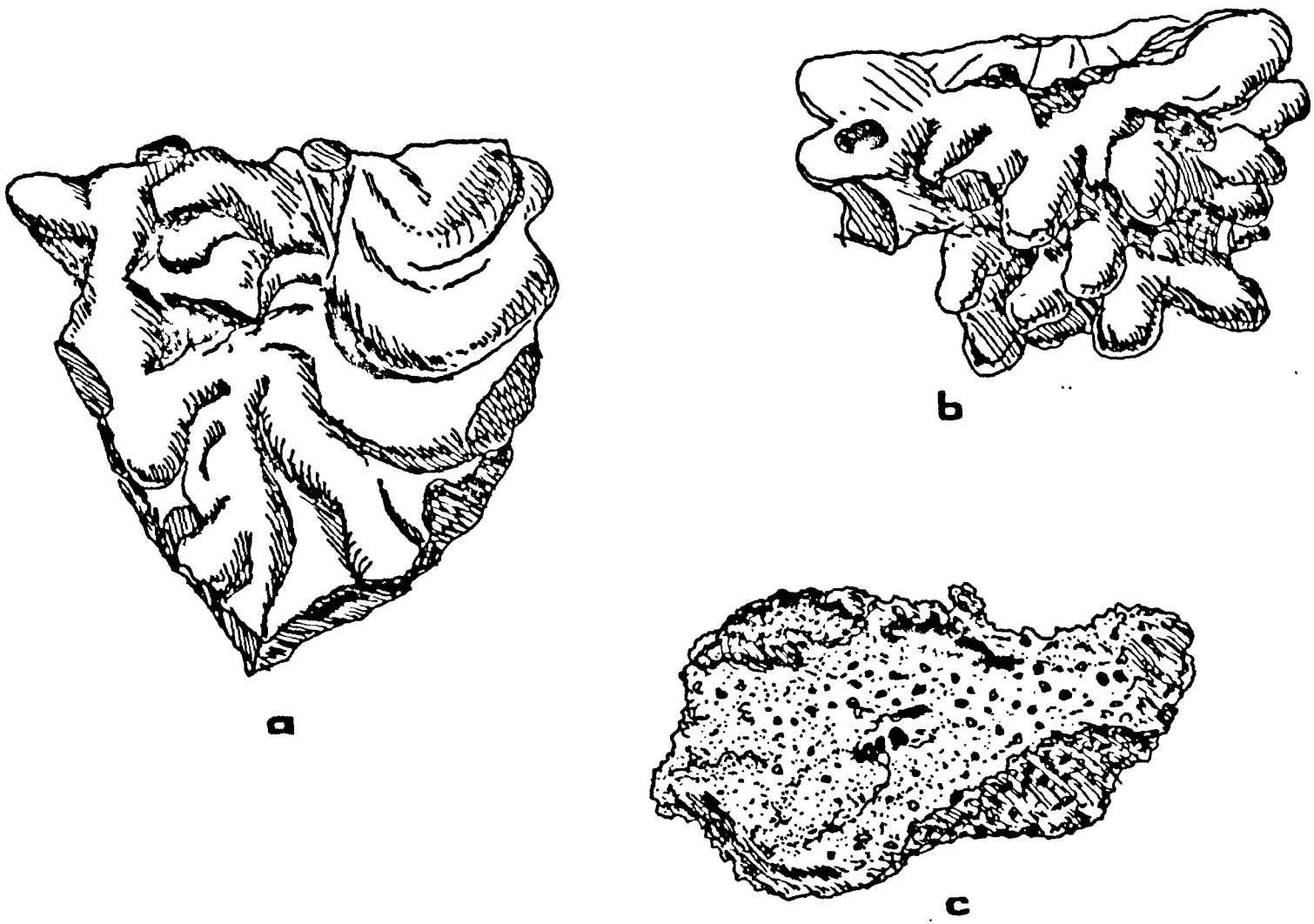

Fig. 3.6.1 Drawing of slag (80% actual size): (a) ropey (tapped) slag, (b) drop-like features in slag, and (c) spongy slag

drop-like. Fig. 3.6.2 is a schematic diagram of the relative percentage of each type of slag from Thasos and the Mainland. Thus, there were more compact slags on the Mainland, possibly the result of an advanced bloomery in a high shaft furnace (Stückofen ?) giving more fluid slags, tapped during the smelting cycle. In Thasos, a smaller type of bloomery with hand-operated bellows and more viscous non-tapped slag may have been in operation. In any case, in both places, the product must have been a spongy bloom hammered mechanically or manually into a bar.

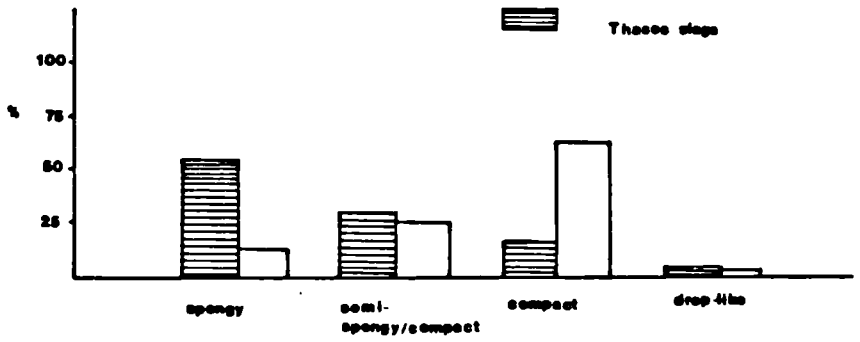

Fig 3.6.2 Distribution of slag types in Thasos and EM Mainland Ti-rich iron slags

Only a small number of slags from Thasos have been analysed by XRF for bulk chemical composition by the present author (Table 3.6.1). Some analyses of slags from Katafyto were carried out by AA at IGME, Xanthi, and are included in Table 3.6.2 for reference. Table 3.6.1 clearly shows the high titanium content in the Thasos slags combined with appreciable iron (shown here as Fe_2O_3) as well

as calcium contents. This amount of titanium sets the Thasos slags apart from those of other geograhical regions in Greece, with the exception of slags from Lesvos (Fig. 2.3) (see appendix 3.6.1). The main difference between the Katafyto slags and those from Thasos is the lower titanium content.

Table 3.6.1: XRF analysis of Thasos slag (Photos et al, in press)

Sample	%age SiO_2	TiO_2	Al_2O_3	Fe_2O_3	MnO_2	CaO	K_2O	P_2O_5	MgO
OXI.2	10.35	12.17	4.66	44.39	1.41	10.57	1.01	0.21	1.10
OXI.1	16.77	6.63	4.41	44.11	0.52	8.67	1.33	0.19	0.75
OXI.4	21.47	11.82	6.50	31.60	0.84	13.34	1.57	0.22	1.21
THE.1	8.79	9.71	1.67	60.10	0.70	8.03	1.14	0.22	0.70
THE.3	6.21	11.41	0.45	65.40	0.83	4.38	0.87	0.16	0.70
THE.4	4.99	8.91	0.75	68.49	0.58	5.50	0.79	0.13	0.46
PAI.1	9.05	13.74	3.13	52.57	0.59	8.33	0.79	0.34	0.90
PAI.2	13.52	9.43	7.61	46.16	0.71	10.90	0.73	0.32	0.73
PAI.3	13.61	9.95	4.62	52.20	0.72	8.18	0.76	0.23	0.75
PAI.4	12.71	12.69	6.58	43.05	0.87	11.32	1.33	0.23	0.98
TSI.3	16.03	10.07	6.04	52.45	0.61	8.95	0.77	0.21	0.74
KAL.1	21.42	13.40	6.62	42.58	0.54	11.85	2.03	0.19	0.96
KAL.2	16.24	4.96	6.30	46.37	0.37	14.36	1.05	0.27	0.95
KAL.4	13.52	15.06	4.51	53.43	0.50	8.89	0.87	0.14	0.66
AST.1	16.48	8.89	6.86	51.65	0.53	11.10	0.72	0.19	0.86
AST.2	15.07	11.51	6.80	47.28	0.49	11.77	1.15	0.15	0.85
AST.3	12.74	11.39	6.12	53.86	0.47	9.74	0.82	0.16	0.80
MAN1.1	12.74	15.09	4.72	56.25	0.60	6.44	1.56	0.10	0.90
MAN2.1	11.82	17.80	4.27	52.20	0.59	10.16	1.95	0.17	0.77

Table 3.6.2: AA analysis of Katafyto, EM slag (Photos et al, in press)

Sample No.	%age SiO_2	TiO_2	Al_2O_3	Fe_2O_3	MnO	CaO	MgO
KAT 1	20.0	3.70	4.95	58.6	0.67	8.00	1.00
KAT 2	14.0	2.15	3.45	67.2	0.55	6.40	1.10
KAT 3	22.0	2.35	5.70	57.9	0.70	8.00	1.00
KAT 4	27.0	2.35	6.10	51.5	0.65	8.40	1.25

	Cu	Zn	V	Cr
KAT 1	0.03	0.18	0.30	0.03
KAT 2	0.03	0.11	0.30	0.03
KAT 3	0.03	0.11	0.20	0.03
KAT 4	0.02	0.09	0.20	0.03

All slag samples from Thasos and the Mainland were examined with the electron microprobe (Tables 3.6.3 and 3.6.4) for two purposes: a) to study slag mineralogy, and b) to match mineralogy and composition of slag inclusions in metal artefacts with that of archaeological slag in an attempt to determine ore provenance. An extract from the Tables 3.6.3 and 4 is given for purposes of easy reference in Table 3.6.4a. The following phases are clearly discerned: ulvospinel (Fe_2TiO_4), wustite (FeO) and a glassy or crystalline matrix. The matrix consists of two phases: a) an olivine of kirschstinitic composition and b) a potassium, aluminium, iron silicate, or mellilite very similar to that found in slags in section 3.5. Fig. 3.6.3 shows the binary phase diagram of FeO-TiO_2 and the solidification range for ulvospinel. The phase diagram most adequately characterising these slags should have been the FeO-anorthite-$CaO.SiO_2$-TiO_2, but the writer was not able to locate such a diagram. Plate 15 show polished sections displaying the characteristic phases in Thasos and EM titanium-rich slags. The average percentage of each phase, calculated by placing a grid over an enlarged photograph of a metallographic section, each phase being recorded at specific intervals, in the slags from Thasos is: 24% ulvospinel, 39% wustite, 35% matrix, 2% metallic prills. This percentage is somewhat different in the slags from the Mainland, which contain overall less ulvospinel with the possible

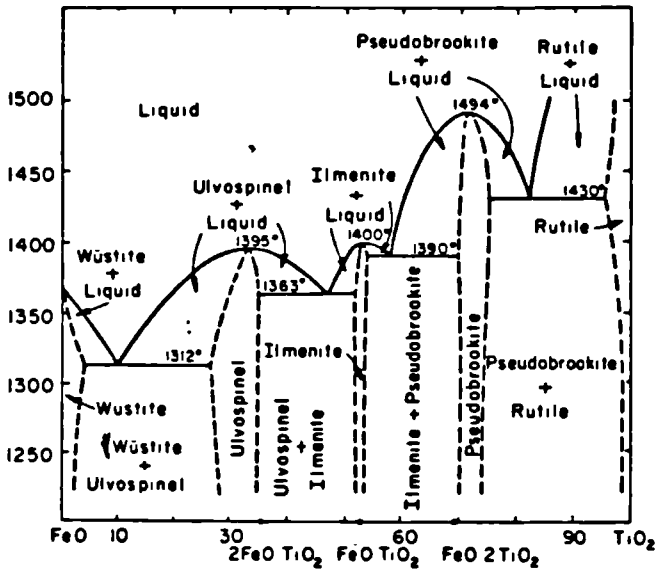

Fig. 3.6.3 $FeO-TiO_2$ binary phase diagram (after Levin et al 1964)

exception of slags from Kimmeria, Xanthi. Ideally, in determining the relative proportions of the phases, one should know which stage in the iron-making stage (smelting or smithing) each sample was derived from, but this is not practically possible when sampling from an archaeometallurgical site. It has however, been possible to do it in the course of our simulation experiments when the slag and metallic remains from each operation were collected and stored for further analysis.

The distribution of titanium in the ulvospinel and the other phases is shown in the line scan and x-ray distribution maps of Plate 14. The titanium line scan (Plate 14g) clearly shows that

Table 3.6.3: Microprobe analysis of Ti-rich iron slags, Thasos

Sample no.	Phase	Na_2O	MgO	Al_2O_3	SiO_2	P_2O_5	K_2O	CaO	TiO_2	V_2O_5	Cr_2O_3	MnO	FeO
KALO 1	ulvo	0.00	0.69	5.42	0.45	0.22	0.20	0.20	25.92	0.63	0.50	0.71	61.45
	ulvo	0.00	0.86	5.60	0.41	0.00	0.00	0.40	25.81	0.00	0.00	0.66	63.92
	matrix	0.00	0.43	7.37	37.29	0.53	3.32	2.08	1.50	0.00	0.00	0.59	28.95
	wustite	0.00	0.61	0.38	0.55	0.00	0.00	0.40	3.02	0.00	0.00	0.60	91.12
TRAG 1	ulvo	0.00	1.17	9.18	0.35	0.00	0.00	0.15	25.15	0.00	0.00	1.41	62.84
	ulvo	0.00	1.02	8.99	0.27	0.00	0.00	0.20	23.05	0.53	0.00	1.10	63.72
	ulvo	0.00	1.00	9.21	0.35	0.00	0.00	0.12	22.57	1.03	0.29	0.96	62.69
	wustite	0.00	0.69	1.02	0.37	0.00	0.00	0.30	5.42	0.00	0.00	0.97	89.82
	wustite	0.00	0.72	0.52	0.53	0.00	0.00	0.61	3.42	0.00	0.00	0.94	92.90
	matrix	0.00	0.43	9.76	34.14	0.81	2.05	18.72	2.72	0.00	0.00	0.71	27.64
	matrix	0.00	0.69	7.96	32.61	0.47	1.48	18.48	1.17	0.00	0.00	1.51	33.58
TRAG 2	ulvo	0.00	0.89	6.39	0.21	0.00	0.00	0.00	28.13	1.16	0.41	1.52	62.50
	ulvo	0.00	1.01	6.43	0.26	0.00	0.00	0.00	28.10	0.60	0.00	1.42	62.58
	wustite	0.00	0.51	0.87	1.88	0.00	0.00	0.91	1.82	0.00	0.00	0.91	93.40
	wustite	0.00	0.45	1.32	1.14	0.00	0.00	0.57	6.39	0.00	0.00	1.02	90.11
	matrix	0.00	0.84	7.30	35.07	0.41	1.50	15.40	1.32	0.00	0.00	1.60	37.21
	matrix	0.00	0.82	6.85	34.60	0.50	1.33	14.68	1.71	0.00	0.00	1.86	37.99
KLAR 1	ulvo	0.00	0.98	8.59	0.55	0.00	0.00	0.51	22.42	0.00	0.27	1.38	65.40
	ulvo	0.00	0.74	8.33	0.40	0.00	0.00	0.46	23.92	0.32	0.00	1.51	63.96
	wustite	0.00	0.72	1.40	0.94	0.00	0.00	0.63	4.63	0.00	0.25	1.46	91.38
	wustite	0.00	0.58	0.30	0.55	0.00	0.00	0.76	1.78	0.00	0.00	1.08	94.25
	matrix	0.00	0.30	8.84	35.39	0.67	2.94	25.44	1.25	0.00	0.00	1.03	21.63
	matrix	0.00	0.50	8.97	35.44	0.84	2.83	25.77	1.33	0.00	0.00	0.90	21.21

Table 3.6.3 (contin.): Microprobe analysis of Ti-rich iron slags, Thasos

		Na_2O	MgO	Al_2O_3	SiO_2	P_2O_5	K_2O	CaO	TiO_2	V_2O_5	Cr_2O_3	MnO	FeO
KAZA 1	ulvo	0.00	0.65	7.73	0.40	0.00	0.00	0.41	23.47	1.10	0.92	0.87	59.73
	ulvo	0.00	1.20	7.77	1.05	0.00	0.00	0.66	23.45	0.00	0.00	0.86	61.30
	matrix	0.00	0.00	10.24	36.62	0.90	4.05	16.83	1.11	0.00	0.00	0.70	28.61
	matrix	0.00	1.17	3.82	24.27	0.00	0.23	21.59	3.04	0.00	0.00	1.19	40.21
	wustite	0.56	0.53	1.61	0.61	0.00	0.00	0.43	5.27	0.00	0.00	0.77	86.92
KAZA 2	ulvo	0.00	0.73	7.59	0.28	0.00	0.00	0.00	26.27	0.63	0.00	1.45	61.20
	ulvo	0.00	0.69	7.18	0.33	0.00	0.00	0.32	25.93	0.00	0.24	1.33	62.22
	matrix	0.00	0.51	0.87	31.63	0.40	0.37	20.97	0.55	0.00	0.20	2.10	43.72
	matrix	0.00	0.00	12.30	37.27	1.28	4.08	16.12	0.77	0.00	0.00	0.81	22.81
KAZA 3	ulvo	0.00	0.85	8.37	0.52	0.00	0.00	0.17	26.75	1.00	0.22	1.42	60.01
	ulvo	0.00	0.94	9.22	0.43	0.00	0.00	0.14	25.53	0.50	0.00	1.53	61.43
	matrix	0.00	1.18	2.78	30.63	0.58	0.49	19.41	1.02	0.00	0.00	2.45	39.83
	matrix	0.00	0.00	16.25	34.61	0.58	2.08	15.09	2.25	0.00	0.00	0.68	26.20
MAN 14	wustite	0.00	0.66	0.70	0.66	0.00	0.00	0.46	5.99	0.00	0.00	1.01	90.20
	matrix	0.00	0.35	6.59	36.05	0.62	2.41	17.75	1.99	0.00	0.00	1.04	32.57
MAN 21	ulvo	0.00	0.80	4.47	0.00	0.00	0.00	0.32	26.85	0.00	0.44	1.15	64.56
	ulvo	0.00	0.75	4.52	0.00	0.00	0.00	0.33	27.45	0.71	0.23	1.21	64.54
	wustite	0.00	0.43	0.47	0.00	0.00	0.00	0.22	1.95	0.00	0.00	0.83	94.98
	matrix	0.00	0.81	0.00	32.61	0.53	0.22	32.48	0.96	0.00	0.00	1.13	32.60
	matrix	0.00	0.41	12.55	34.85	0.66	4.70	21.23	0.80	0.00	0.00	0.77	21.96
	matrix	0.00	0.00	19.46	35.89	0.42	18.63	10.73	0.59	0.00	0.00	0.38	12.16
TSI	ulvo	0.00	1.39	6.05	0.35	0.00	0.00	0.25	29.53	0.62	0.37	1.81	57.68
	matrix	0.00	1.36	8.08	37.79	0.00	0.79	35.84	0.48	0.00	0.00	0.52	12.65
	matrix	0.00	0.00	22.76	37.61	0.00	14.73	8.05	0.47	0.00	0.00	0.58	11.21
TSICE	fayalite	0.00	3.47	0.00	29.81	0.00	0.00	1.97	0.28	0.00	0.00	0.96	59.84
	wustite	0.00	0.00	0.37	0.54	0.00	0.00	0.17	0.92	0.00	0.00	0.26	92.47
	matrix	0.00	0.00	2.80	33.66	0.72	3.54	12.61	0.83	0.00	0.00	0.00	27.25
TSIAR	fayalite	0.00	1.80	0.00	29.55	0.00	0.00	2.71	0.29	0.00	0.00	0.86	63.17
	wustite	0.00	0.42	0.36	0.38	0.00	0.00	0.00	0.54	0.00	0.15	0.33	95.05
	matrix	0.00	1.10	6.10	33.84	0.54	2.78	6.83	0.36	0.00	0.00	0.58	46.30

Table 3.6.3 (contin.): Microprobe analysis of Ti-rich iron slags, Thasos

		Na_2O	MgO	Al_2O_3	SiO_2	P_2O_5	K_2O	CaO	TiO_2	V_2O_5	Cr_2O_3	MnO	FeO
PAI 1	ulvo	0.00	0.92	7.18	0.36	0.00	0.00	0.14	24.88	0.39	0.25	1.06	52.51
	ulvo	0.00	1.32	6.99	0.40	0.00	0.00	0.12	25.25	0.83	0.44	1.21	51.53
	matrix	0.00	0.99	7.88	35.12	0.46	1.02	20.23	1.06	0.00	0.00	0.98	24.77
	matrix	0.00	1.36	10.97	36.90	0.85	0.00	19.93	2.02	0.00	0.00	0.54	16.93
	matrix	0.00	0.00	19.65	44.42	0.00	13.91	1.86	3.25	0.00	0.00	0.10	8.57
PAI 2	ulvo	0.00	0.66	9.43	0.48	0.00	0.11	0.35	24.46	0.00	0.00	0.85	61.95
	matrix	0.00	0.00	16.67	34.54	1.00	2.59	15.59	2.71	0.00	0.00	0.36	24.75
	matrix	0.00	0.77	0.00	31.42	0.57	0.22	21.69	0.48	0.00	0.00	1.21	44.56
PAI 3	ulvo	0.00	0.88	7.46	0.21	0.00	0.00	0.18	27.35	1.00	0.80	0.72	60.79
	ulvo	0.00	0.30	7.25	0.99	0.00	0.00	0.84	25.01	0.00	0.00	0.62	63.37
	matrix	0.00	0.54	2.91	32.07	0.33	0.87	27.64	0.59	0.00	0.00	1.00	42.93
	matrix	0.00	0.76	2.96	31.73	0.40	0.73	15.97	0.73	0.00	0.00	1.14	42.87
PAI 4	ulvo	0.00	0.61	6.55	0.36	0.00	0.00	0.18	25.87	0.00	0.00	0.89	63.51
	matrix	0.00	0.85	2.32	32.20	0.81	0.78	22.81	0.40	0.00	0.00	0.97	39.10
	matrix	0.00	1.44	0.00	30.42	0.72	0.16	21.54	0.48	0.00	0.00	0.82	41.61
OXI 1	ulvo	0.00	1.48	6.30	0.43	0.00	0.00	0.38	26.49	0.00	0.00	2.29	60.25
	ulvo	0.00	1.49	6.38	0.39	0.00	0.00	0.29	26.35	0.00	0.00	2.19	60.27
	wustite	0.00	1.91	1.03	0.00	0.00	0.00	1.08	5.43	0.00	0.00	1.31	86.36
	matrix	0.00	0.00	17.34	32.09	1.00	5.04	20.83	3.74	0.00	0.00	0.97	16.75
	matrix	0.00	1.51	0.00	31.66	0.00	0.14	31.64	0.70	0.00	0.00	2.05	31.84
OXI 4	ulvo	0.00	0.96	7.95	0.47	0.00	0.00	0.00	24.46	0.71	0.64	0.98	60.78
	ulvo	0.00	1.28	7.86	0.20	0.00	0.00	0.20	24.44	0.87	0.00	0.90	62.32
	wustite	0.00	0.32	1.95	1.51	0.00	0.00	0.89	7.88	0.00	0.00	0.72	84.64
	wustite	0.00	0.47	2.12	0.53	0.00	0.00	0.32	10.92	0.00	0.27	1.16	80.89
	matrix	0.00	0.00	7.26	35.86	0.78	1.74	24.70	1.04	0.00	0.00	0.83	24.69
	matrix	0.00	0.00	6.22	36.40	0.69	2.13	24.32	0.95	0.00	0.00	0.77	23.68
THE 1	ulvo	0.00	0.52	5.57	0.49	0.00	0.00	0.54	25.64	0.31	0.00	1.16	62.91
	ulvo	0.00	0.33	5.30	0.39	0.00	0.00	0.20	26.05	0.00	0.00	0.84	65.47
	matrix	0.00	0.75	0.00	31.50	0.27	0.24	29.90	0.74	0.00	0.00	1.09	35.78
	matrix	0.00	0.89	0.00	31.64	0.39	0.00	30.10	0.54	0.00	0.00	1.05	34.30
THE 3	ulvo	0.00	1.02	5.83	0.43	0.00	0.00	0.17	25.92	0.79	0.79	1.15	61.15
	ulvo	0.00	1.08	6.14	0.47	0.00	0.00	0.14	26.12	0.69	0.66	1.03	60.66
THE 4	ulvo	0.00	0.24	5.38	0.31	0.00	0.00	0.41	24.24	0.00	0.00	0.96	60.93
	ulvo	0.00	0.43	5.14	0.27	0.00	0.00	0.61	23.94	0.00	0.00	0.78	62.18
	wustite	0.00	0.21	0.42	0.19	0.00	0.00	0.18	5.76	0.00	0.00	0.92	85.88
	matrix	0.00	0.00	7.66	35.75	0.72	3.48	24.50	1.75	0.00	0.00	0.57	22.69
	matrix	0.00	0.00	7.37	35.34	0.80	3.58	23.38	1.98	0.00	0.00	0.50	23.80

Table 3.6.4: Microprobe analysis of EM Mainland Ti-rich iron slag

Sample	phase	Na_2O	MgO	Al_2O_3	SiO_2	P_2O_5	K_2O	CaO	TiO_2	V_2O_5	Cr_2O_3	MnO	FeO
KATA 1	ulvo	0.00	0.35	5.48	0.50	0.45	0.00	0.00	19.09	8.80	0.46	0.37	65.74
	wustite	0.00	0.35	0.92	0.67	0.00	0.17	0.00	2.00	0.39	0.00	0.00	94.82
	fayalite	0.00	1.70	0.35	30.52	0.00	0.28	2.30	0.60	0.00	0.00	0.89	63.44
	matrix1	0.00	1.60	0.00	31.23	0.39	0.00	17.38	0.46	0.00	0.00	1.18	47.32
	matrix2	0.00	0.00	20.36	50.13	0.00	18.02	1.65	0.35	0.00	0.00	0.17	5.65
	ulvo	0.00	0.48	6.04	0.00	0.37	0.00	0.13	21.81	5.75	0.00	0.65	63.69
KATA 3	ulvo	0.00	0.93	8.08	0.54	0.48	0.00	0.26	17.26	10.88	0.43	0.75	62.83
	wustite	0.61	0.70	0.87	0.77	0.48	0.13	0.30	3.74	0.47	0.00	0.65	92.15
	matrix	0.87	0.91	7.98	36.14	1.88	3.82	11.98	1.22	0.00	0.00	0.81	35.14
KATA 4	ulvo	0.00	0.35	6.38	0.58	0.00	0.21	0.25	24.11	0.00	0.00	0.45	65.39
	matrix	0.00	1.16	3.97	35.70	0.60	2.39	15.65	0.51	0.00	0.00	1.05	45.72
	matrix	0.00	0.00	23.41	56.31	0.76	21.58	0.55	0.00	0.00	0.00	0.00	2.78
	matrix	0.58	1.37	0.00	32.11	0.00	0.00	17.22	0.34	0.00	0.00	1.12	51.74
PIGA 1	wustite	0.00	1.52	2.00	2.52	0.37	0.18	1.61	3.41	1.69	0.00	0.69	85.17
	matrix	0.00	1.20	8.70	34.11	3.39	3.00	25.58	1.67	0.00	0.00	0.39	20.97
	matrix	0.00	1.45	7.40	28.55	2.79	2.59	19.75	2.07	0.56	0.00	0.70	35.08
PIGA 2	wustite	0.00	0.86	0.38	0.75	0.31	0.00	0.31	1.59	1.13	0.20	0.48	92.22
	wustite	0.00	0.88	0.77	1.47	0.30	0.13	0.51	2.53	1.42	0.00	0.45	90.13
	matrix	0.00	0.68	9.38	38.00	3.14	4.69	17.31	1.32	0.00	0.00	0.36	23.54
	matrix	0.00	1.25	7.83	31.96	2.05	3.39	13.35	0.97	0.30	0.00	0.37	36.24
PIGA 3	wustite	0.00	0.99	0.76	0.43	0.00	0.00	0.00	1.87	1.62	0.19	0.45	91.09
	wustite	0.00	0.92	0.76	0.42	0.00	0.00	0.17	1.97	1.80	0.22	0.40	90.95
	matrix	0.00	1.05	8.95	35.74	0.00	3.23	18.79	0.94	0.00	0.00	0.46	26.13
	matrix	0.00	0.98	8.78	34.57	0.00	2.92	18.54	1.01	0.00	0.00	27.75	0.00
SIDI 1	wustite	0.00	0.84	1.24	0.67	0.00	0.12	1.69	5.79	0.50	0.00	0.35	88.93
	wustite	0.00	0.98	1.13	0.58	0.00	0.00	0.18	5.27	0.42	0.00	0.53	82.97
	matrix	0.00	0.59	8.63	38.03	0.00	4.02	15.83	0.32	0.00	0.00	0.30	26.67
SIDI 2	ulvo	0.00	1.21	6.50	0.42	0.00	0.00	0.40	22.36	1.27	0.11	0.43	64.14
	ulvo	0.00	1.35	6.56	1.36	0.00	0.12	0.77	19.21	1.65	0.00	0.41	59.72
	wustite	0.00	0.95	0.40	1.05	0.00	1.90	0.71	1.67	0.00	0.00	0.49	91.81
	wustite	0.00	1.02	0.57	2.06	0.00	0.33	1.18	2.10	0.00	0.15	0.34	88.58
SIDI 4	ulvo	0.00	0.53	5.63	1.28	0.00	0.10	0.80	17.21	0.00	0.22	0.46	70.50
	wustite	0.00	0.64	0.87	0.61	0.00	0.00	0.40	3.69	0.00	0.00	0.43	91.72
	matrix	0.00	0.61	7.70	36.27	1.97	2.84	19.68	1.04	0.00	0.00	0.41	23.87
SIDI 5	wustite	0.00	0.70	0.88	0.69	0.00	0.00	0.37	4.95	0.00	0.15	0.34	89.12
	wustite	0.00	0.59	1.21	0.62	0.00	0.00	0.20	6.01	0.00	0.20	0.26	87.82
	matrix	0.00	0.62	8.15	35.43	1.64	4.33	18.05	1.58	0.00	0.00	0.33	25.36

Table 3.6.4 (contin.): Microprobe analysis of EM Mainland Ti-rich iron slags

		Na_2O	MgO	Al_2O	SiO_2	P_2O_5	K_2O	CaO	TiO_2	V_2O_5	Cr_2O_3	MnO	FeO
KIMX 2	ulvo	0.00	1.51	4.58	0.32	0.00	0.00	0.14	27.48	8.78	0.42	1.08	56.48
	ulvo	0.00	1.52	4.68	0.33	0.00	0.00	0.33	26.41	8.21	0.33	1.00	57.30
	matrix	0.00	1.50	8.28	36.97	1.19	2.95	9.05	1.14	0.00	0.00	1.05	35.39
	matrix	0.00	1.11	7.69	36.09	1.35	2.42	10.40	1.30	0.00	0.00	0.79	37.37
KIMX 3	ulvo	0.00	1.39	4.17	0.37	0.00	0.00	0.18	29.24	5.25	0.00	1.22	59.18
	ulvo	0.00	1.57	4.12	0.34	0.00	0.00	0.23	29.31	4.87	0.00	1.19	5.72
	matrix	0.00	1.26	7.56	37.89	1.63	2.53	11.08	1.64	0.00	0.00	1.24	34.40
	matrix	0.00	1.38	6.31	36.43	1.32	2.26	9.86	1.44	0.00	0.00	1.46	38.42
	ulvo	0.00	1.21	4.45	0.43	0.00	0.00	0.23	29.15	8.65	0.00	1.23	60.51
	matrix	0.00	0.75	9.39	39.23	1.96	2.84	13.01	1.72	0.00	0.00	1.11	29.02
KIMX 4	ulvo	0.00	1.00	4.41	0.47	0.00	0.00	0.00	27.83	0.37	0.16	1.14	62.50
	ulvo	0.00	1.32	4.27	0.24	0.22	0.00	0.00	28.32	2.84	0.17	1.09	60.44
	fayalite	0.00	3.60	0.38	29.73	0.57	0.28	5.31	1.38	0.00	0.00	2.28	55.67
	fayalite	0.00	3.41	0.48	30.99	0.27	0.43	6.45	0.91	2.00	0.00	2.25	55.95
	matrix	0.00	0.00	13.90	39.23	3.07	4.73	14.15	1.70	0.00	0.00	0.59	18.12
	matrix	0.00	13.10	38.84	2.48	14.71	0.00	0.00	1.54	0.00	0.00	0.53	21.83
VATH 1	wustite	0.00	0.68	0.62	0.65	0.31	0.00	0.20	3.23	0.93	0.21	0.48	89.49
	wustite	0.00	0.79	0.46	0.53	0.00	0.00	0.27	3.49	0.99	0.24	0.61	89.32
	wustite	0.00	0.63	0.68	0.53	0.00	0.00	0.25	4.43	1.02	0.00	0.61	89.00
	matrix	0.00	0.86	7.61	37.63	2.88	3.98	15.50	1.03	0.00	0.00	0.56	27.97
VATH 2	wustite	0.00	1.06	0.85	0.50	0.42	0.11	0.00	4.04	2.57	0.34	0.65	86.25
	wustite	0.00	1.11	0.85	0.54	0.28	0.00	0.41	4.94	2.06	0.00	0.80	86.54
	matrix	0.00	0.81	6.63	36.23	3.45	4.51	20.46	0.92	0.00	0.00	0.79	23.80
	matrix	0.00	1.13	6.81	36.50	3.28	4.51	20.70	0.91	0.00	0.00	0.56	23.48
VATH 3	wustite	0.00	0.73	0.73	0.62	0.00	0.00	0.36	3.62	1.47	0.21	0.35	89.74
	wustite	0.00	0.81	0.38	0.52	0.00	0.00	0.26	1.78	0.81	0.20	0.52	91.72
	matrix	0.00	0.95	7.07	30.46	0.00	2.84	15.62	1.70	0.00	0.00	0.36	39.09
VATT 2	wustite	0.00	0.00	1.51	0.52	0.00	0.00	0.49	2.81	0.52	0.00	0.23	89.90
	wustite	0.00	0.51	1.80	0.51	0.00	0.00	0.45	3.06	0.79	0.00	0.35	88.89
	matrix	0.00	0.95	6.70	34.12	0.00	3.73	19.86	0.87	0.00	0.00	0.44	29.76
	matrix	0.00	0.95	7.19	34.53	0.00	3.40	20.34	1.08	0.00	0.00	0.50	28.64
	grain	0.00	0.57	7.35	34.32	0.00	3.83	19.05	1.10	0.00	0.00	0.55	28.26
	grain	0.00	0.87	7.98	33.82	0.00	3.43	17.91	0.00	0.00	0.67	0.62	33.48
VATT 3	wustite	0.00	0.66	0.69	0.55	0.00	0.00	0.33	3.26	0.00	0.27	0.47	92.54
	wustite	0.00	0.66	0.41	0.41	0.00	0.00	0.26	2.53	0.00	0.32	0.53	92.74
	matrix	0.00	0.64	7.43	37.23	2.57	3.01	16.56	1.10	0.00	0.00	0.73	23.86
KIMX 6	wustite	0.00	0.00	1.37	1.11	0.00	0.00	0.45	0.79	0.00	0.00	0.31	94.92
	fayalite	0.00	4.01	0.00	31.47	0.30	0.00	4.65	0.20	0.00	0.00	0.84	59.86
	fayalite	0.00	11.16	0.00	33.23	0.24	0.00	2.42	0.34	0.00	0.00	0.71	53.38
	matrix	0.00	0.48	5.69	32.63	0.00	1.42	15.94	0.29	0.00	0.00	0.74	44.73

		Na_2O	MgO	Al_2O_3	SiO_2	P_2O_5	K_2O	CaO	TiO_2	V_2O_5	Cr_2O_3	MnO	FeO
SEVR 1	ulvo	0.00	0.73	6.49	0.77	0.59	0.00	0.39	19.56	13.00	0.42	0.73	63.69
	ulvo	0.00	1.18	7.04	2.28	0.75	0.27	1.25	19.07	1.01	0.36	0.90	62.21
	wustite	0.00	0.50	0.57	0.63	0.00	0.00	0.26	2.77	0.31	0.00	0.61	91.48
	wustite	0.00	0.91	1.57	0.44	0.23	0.00	0.14	5.13	0.44	0.00	0.00	87.03
	matrix	0.00	1.25	6.09	37.05	4.02	5.37	19.14	0.51	0.00	0.00	0.83	22.92
SEVR 2	ulvo	0.00	0.92	6.71	0.46	0.23	0.00	0.44	19.68	3.74	0.15	0.53	66.30
	ulvo	0.00	1.15	6.69	0.43	0.31	0.15	0.43	20.59	1.02	0.10	0.57	65.27
	wustite	0.00	0.28	1.11	0.57	0.00	0.00	0.32	3.65	0.95	0.17	0.42	87.45
	matrix	0.00	0.97	7.39	34.93	3.21	3.29	24.18	1.41	0.00	0.00	0.54	22.46
	matrix	0.00	0.92	6.57	37.47	3.85	3.97	18.21	0.53	0.00	0.00	0.78	24.83
SEVR 3	wustite	0.00	1.22	0.67	0.37	0.00	0.00	0.39	4.16	0.00	0.00	0.50	90.13
	wustite	0.00	1.23	0.68	0.53	0.00	0.00	0.34	4.25	0.00	0.00	0.69	89.84
	matrix	0.00	1.49	6.76	35.47	2.80	3.26	19.86	1.72	0.00	0.00	0.47	26.85

Table 3.6.4 (contin.): Microprobe analysis of EM Mainland and Thrace (KIMX) - Ti-rich iron slag

Table 3.6.4a: Analyses of Thasos and EM mainland Ti-rich slags extracted from Tables 3.6.3 and 3.6.4

Sample	Phase	%age MgO	Al_2O_3	SiO_2	P_2O_5	K_2O	CaO	TiO_2	V_2O_5	Cr_2O_3	MnO	FeO
KATA3	ulvo	0.93	8.08	0.54	0.48	0.00	0.27	17.26	10.88	0.43	0.75	62.83
SIDI2	ulvo	1.21	6.50	0.42	0.00	0.00	0.40	22.36	1.27	0.11	0.43	64.14
KIMX2	ulvo	1.51	4.58	0.32	0.00	0.00	0.14	27.48	8.78	0.42	1.08	56.48
OXI1	ulvo	1.48	6.30	0.43	0.00	0.00	0.38	26.49	0.00	0.00	2.29	60.25
THE3	ulvo	1.02	5.83	0.43	0.00	0.00	0.17	25.92	0.79	0.79	1.15	61.15
TRAG2	ulvo	0.89	6.39	0.21	0.00	0.00	0.00	28.13	1.16	0.41	1.52	62.50
PIGA2	wust	0.86	0.38	0.75	0.31	0.00	0.31	1.59	1.13	0.20	0.48	92.22
SIDI5	wust	0.59	1.21	0.62	0.00	0.00	0.20	6.01	0.00	0.20	0.26	87.92
VATH2	wust	1.11	0.85	0.54	0.28	0.00	0.41	4.94	2.06	0.00	0.80	86.54
KALO1	wust	0.61	0.38	0.55	0.00	0.00	0.40	3.02	0.00	0.00	0.60	91.12
OXI1	wust	0.47	2.12	0.53	0.00	0.00	0.32	10.92	0.00	0.27	1.16	80.89
THE4	wust	0.21	0.42	0.19	0.00	0.00	0.18	5.76	0.00	0.00	0.92	85.88
KATA1	matr	1.60	0.00	31.23	0.39	0.00	17.38	0.46	0.00	0.00	1.19	47.32
KATA4	matr	0.00	23.41	56.31	0.76	21.58	0.55	0.00	0.00	0.00	0.00	2.78
VATH3	matr	0.65	7.43	37.23	2.57	3.01	16.56	1.10	0.00	0.00	0.73	28.86
SEVR3	matr	1.49	6.76	35.47	2.81	3.28	19.86	1.71	0.00	0.00	0.47	26.82
PAI3	matr	0.54	2.91	32.07	0.33	0.87	27.64	0.59	0.00	0.00	1.00	42.93
OXI1	matr	0.00	17.34	32.09	1.00	5.04	20.83	3.74	0.00	0.00	0.97	16.75
MAN21	matr	0.81	.00	32.61	0.53	0.22	32.48	0.96	0.00	0.00	1.13	32.60
MAN21	matr	0.00	19.46	35.89	0.42	18.63	10.73	0.59	0.00	0.00	0.38	12.16

maximum titanium content concentrates in the ulvospinel and the wustite. The martrix is practically titanium-free. The titanium x-ray distribution maps (Plates 14a-d) show spinel plates grown out of wustite grains. The mechanism of partition of titanium appears to be as follows: if excess titanium is present, ulvospinel will form as titanium exsolves out of the titanium-rich wustite (Plate 14a-d), the remainder partitioning first in the wustite and then in the matrix. If there is not enough titanium to form ulvospinel, the wustite would be enriched in titanium (up to 15% TiO_2). High Ti

was recorded in the slag inclusions of some artefacts and served as a means of provenancing the ore source. However, no ulvospinel plates were detected inthe slag inclusions of the objects probably because of the fast cooling rate experienced during forging. This observation was verified in the course of a laboratory experiment in which iron sands were reduced in a laboratory furnace. 'Ulvospinel' phases were measured after the sample was cooled fast from 1000 C. These phases had the right composition but not the characteristic structure of the ulvospinel plates (Photos et al 1985).

Ulvospinel can accommodate vanadium and chromium as seen in the slags from EM Mainland (Table 3.6.4a). An x-ray distribution map of vanadium in an ulvospinel grain is shown in Plate 14e,f. Vanadium shows the same order of preference as titanium to partitioning, namely first in the ulvospinel, then in the wustite and finally in the matrix.

3.6.b Provenance

The microprobe data discussed in the previous section provided information on slag mineralogy and the partitioning of minor and trace elements in the three major phases ulvospinel, wustite and matrix. In this section an attempt is made to determine the iron ore provenance of the artefacts analysed in section 3.5 and in particular to establish the earliest date for the exploitation of Ti-rich iron sands in Thasos and EM Mainland. To that effect, the TiO_2, and V_2O_5 contents in wustite and matrix were plotted versus the number of samples (slag and objects) in Figs. 3.6.3a, b and

3.6.4a, b. Four sets of data are used:

a) iron slags from various regions in Greece (Table 3.6.5),

b) Ti-rich iron slags from EM (Table 3.6.3)

c) Ti-rich iron slags from Thasos (Table 3.6.4)

d) slag inclusions in artefacts (Tables 3.5.4 and 3.5.6).

Since there is more than one analysis per mineralogical phase, the average TiO_2 composition is used. From Figs. 3.6.3a and b it is clear that Mainland and Thasos slags can be well differentiated from other Greek iron slags on the basis of titanium alone. Slags which consistently show more than 2% TiO_2 in the wustite and the matrix should be considered as having a Ti-rich iron sands provenance. The differentiation is more evident in Fig. 3.6.3a (wustite). Most of the iron objects have less than 1% TiO_2 in wustite or matrix with the exception of six samples (D350, D365, D340, D349, D338, D345) which have more than 2% TiO_2 in both phases.

In an attempt to narrow further the number of objects with a Ti-rich iron sands source, the vanadium content in the wustite and the matrix was plotted for the three slag groups and the artefacts. Figs. 3.6.4a and b show that vanadium can be used as a tracer for a Mainland source since the EM slags are particularly rich in V_2O_5 (in the wustite). Four objects have a high vanadium content, namely D365, D340, D338, D345. Table 3.6.7 summarises the results:

Table 3.6.5

Iron slags from various locations in Greece

Sample	phase	Na_2O	MgO	Al_2O_3	SiO_2	P_2O_5	SO_3	K_2O	CaO	TiO_2	Cr_2O_3	V_2O_5	MnO	FeO	
Pelops.															
Ag. Eli	fayal.	0.00	1.30	4.85	19.76	0.00	0.00	0.89	12.18	0.71	0.00	0.00	1.20	61.49	0.00
	matrix	0.00	1.13	8.41	37.78	0.29	0.00	1.73	24.39	0.41	0.00	0.00	1.07	25.19	0.00
Euboea															
Ag. Dim	matrix	0.86	0.00	7.62	33.49	0.90	0.13	2.23	14.36	0.33	0.00	0.00	0.77	41.45	0.00
	matrix	0.00	0.00	15.87	38.07	1.17	0.35	5.02	14.59	0.61	0.00	0.00	0.22	26.50	0.00
Karysto	wust.	0.00	0.44	0.57	0.31	0.00	0.00	0.00	0.00	0.65	0.00	0.00	0.49	95.23	0.00
	matrix	0.00	0.47	9.31	33.39	0.59	0.00	1.96	7.20	0.35	0.00	0.00	0.89	45.99	0.00
Nea Sty	wust.	0.00	0.00	0.79	0.54	0.00	0.13	0.00	0.17	0.46	0.00	0.00	3.29	93.83	0.00
	fayal.	0.00	2.46	0.00	30.46	0.39	0.00	0.00	3.01	0.25	0.00	0.00	0.00	56.44	0.00
Lepura	wust.	0.00	0.28	0.56	0.36	0.00	0.00	0.00	0.00	0.35	0.00	0.00	5.01	93.77	0.00
Archamp	Bl	0.00	0.00	1.85	13.94	0.00	0.00	0.19	1.38	0.00	0.00	0.00	1.71	80.93	0.00
Sev.Arc	glassy	0.00	0.00	6.16	42.52	0.00	0.14	3.07	19.45	0.00	0.00	0.00	22.00	1.33	0.51
	prill	0.00	0.00	0.99	6.06	6.50	0.00	0.40	2.98	0.00	0.00	0.00	3.16	82.81	0.00
Nero 1	glassy	0.00	0.00	9.37	38.27	0.00	0.00	2.64	17.86	0.00	0.00	0.00	29.01	0.23	0.00
	glassy	0.00	0.00	0.00	32.94	0.00	0.00	0.09	16.59	0.00	0.00	0.00	42.55	0.36	0.00
Nero 2	wust.	0.00	0.00	0.47	0.37	0.00	0.00	0.00	0.00	0.43	0.00	0.00	8.14	86.65	0.00
	matrix	0.00	0.00	1.80	31.08	1.05	0.00	1.46	15.29	0.29	0.00	0.00	12.70	35.71	0.00
Nero 5	matrix	3.94	0.00	18.76	67.68	0.37	0.00	5.68	3.68	0.00	0.00	0.00	0.00	1.03	0.00
	matrix	2.65	0.85	16.65	66.30	1.06	0.00	6.29	1.79	1.05	0.00	0.00	0.00	3.17	0.00
	matrix	4.90	0.00	24.68	59.04	0.23	0.00	1.88	8.24	0.00	0.00	0.00	0.00	0.53	0.00
Ner.	glassy	1.30	0.79	11.03	40.03	0.00	0.88	2.82	1.80	1.11	0.00	0.00	23.29	0.64	0.00
	glassy	0.00	6.48	0.00	33.81	0.33	0.00	0.13	17.95	0.00	0.00	0.00	43.61	0.69	0.00
Attica															
AA.1579	fayal.	0.00	0.00	2.78	31.59	0.00	0.00	0.89	5.67	0.35	0.00	0.00	0.36	56.98	0.00
	matrix	2.14	0.00	21.04	41.77	0.92	0.16	8.46	9.79	0.63	0.00	0.00	0.00	15.75	0.00
AA.1581	wust.	0.00	0.51	0.85	0.25	0.00	0.00	0.00	0.12	0.54	0.00	0.00	0.85	96.02	0.00
	fayal.	0.00	0.95	0.92	30.90	0.70	0.00	0.18	0.17	0.00	0.00	0.00	2.48	57.60	0.00

		Fe	Mn	Ti	Ca	Si	P
Ner	metal.	97.38	1.08	0.23	0.25	0.14	1.06
	metal.	92.47	0.96	0.26	0.34	0.20	4.71
	metal.	92.87	1.00	0.28	0.34	0.20	4.70

Fig. 3.6.4 TiO_2 content in wustite (a) and matrix (b) for: Ti-rich iron slags (EM Mainland, Thasos); non-Ti-rich iron slags from EM and other locations in Greece; artefacts from the Museums of Kavala, Thasos, Thessaloniki and Pella

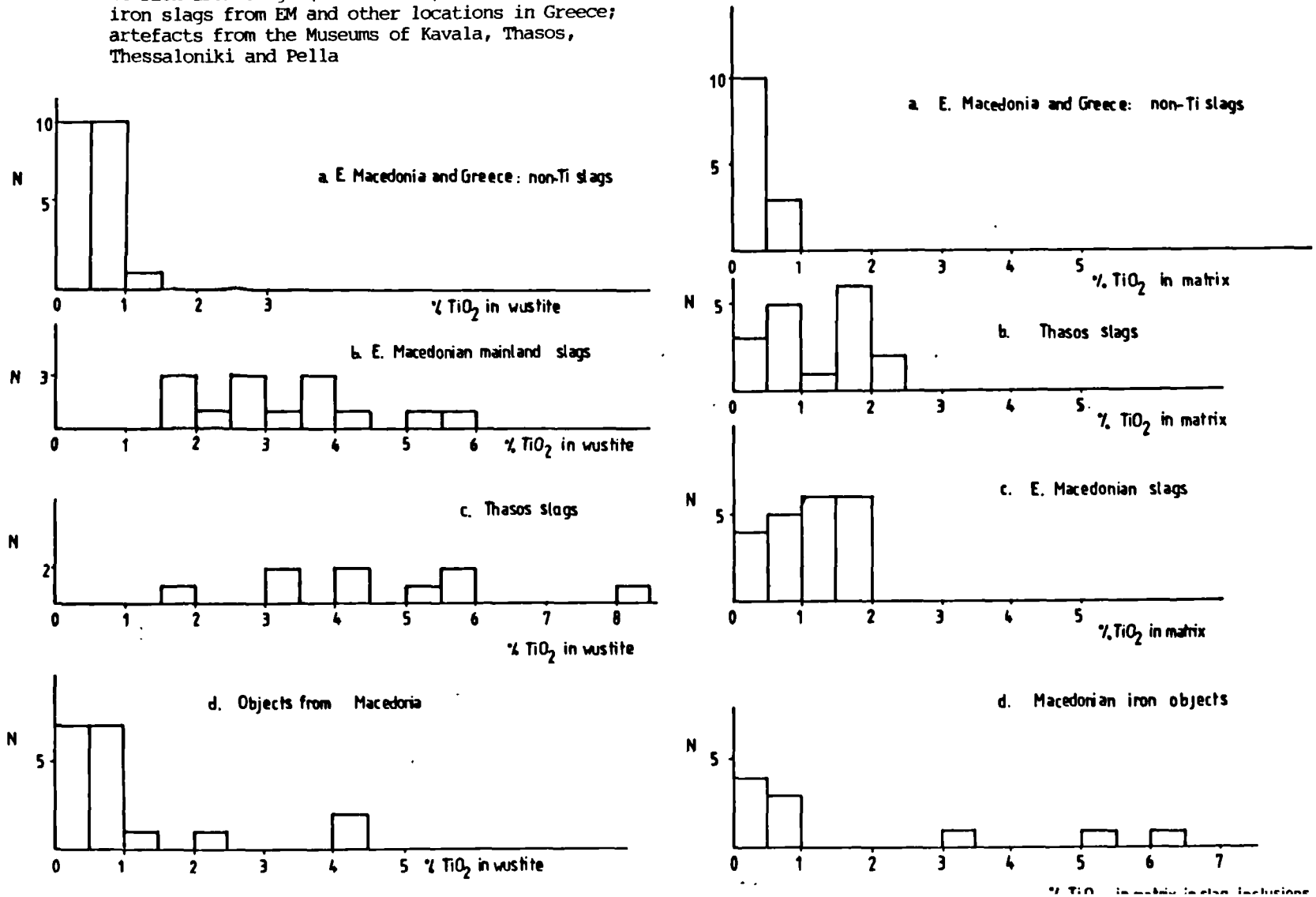

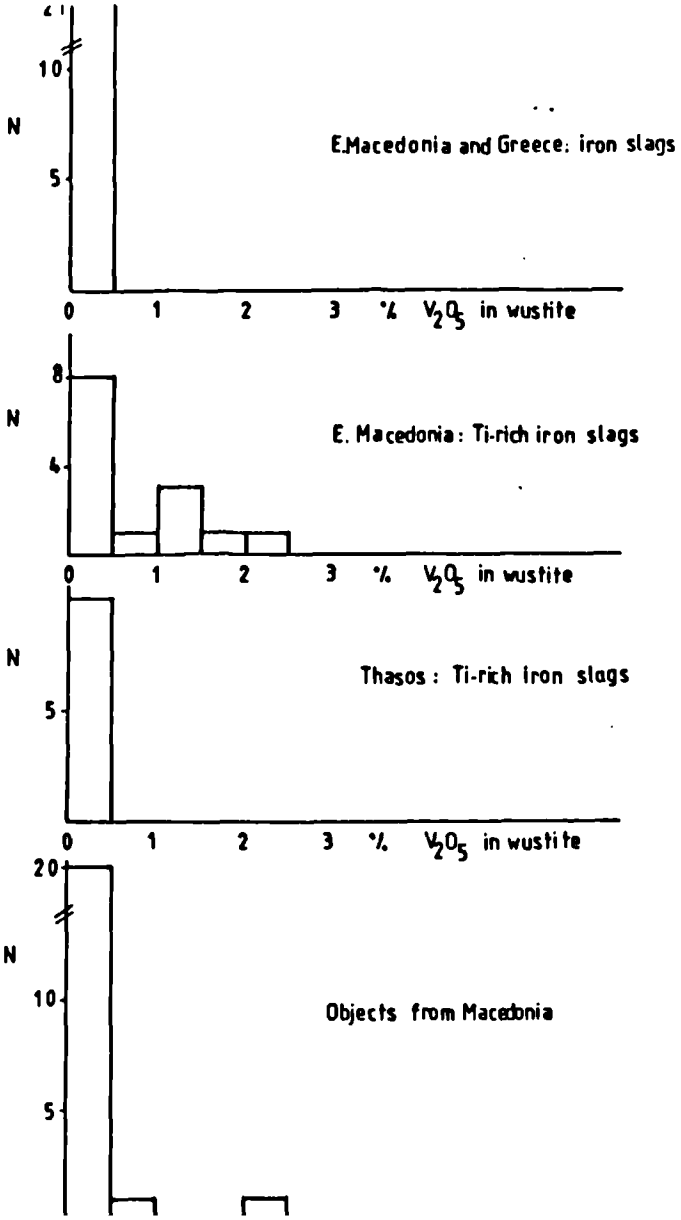

Fig. 3.6.5 V_2O_5 content in wustite (a) and matrix (b) for Ti-rich iron slags (EM Mainland and Thasos), non-Ti-rich iron slags from EMMainland and other locations in Greece, and artefacts from Kavala, Thasos and Thessaloniki Museums

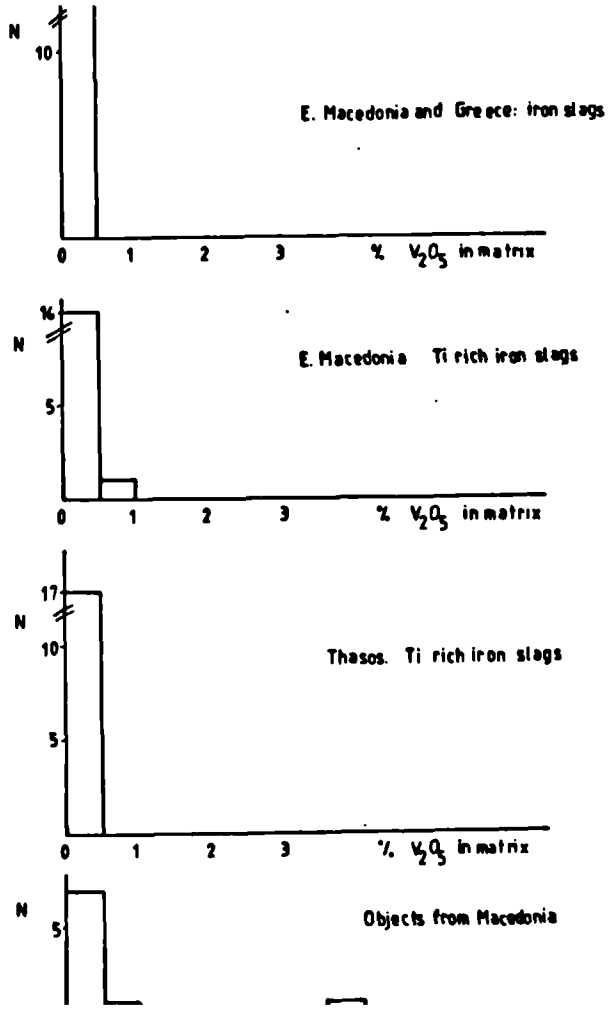

Table 3.6.6: TiO_2 and V_2O_5 contents in artefacts from the Kavala and Thasos Museums

	Wustite	Matrix
TiO_2	D350,365,340,349	D365,338,345
V_2O_5	D365,340	D338,345

From this table it can be deduced that objects D365, D340, D338 and D345 have most certainly been produced from Ti-rich iron sands since their slag inclusions contain all three elements, Ti, V and Cr. It can also be argued that these four objects may have a Mainland origin despite the fact that they have all been found in Limenas, on Thasos. On the other hand, samples D350 and D349, which have only a high Ti-content, argue in favour of a Thasos origin. Since the earliest of these objects date to the Hellenistic/Roman period, it can be concluded that the earliest evidence for the exploitation of iron sands is during that time. The practice continued in the Byzantine period, an observation which has mainly been corroborated by the dating of slag (tuyeres and furnace fragments) from Oxia, Thasos.

The composition of the Macedonian objects has primarily been characterised by the presence of two additional elements namely, manganese and phosphorus appearing in the metal or the slag inclusions thereof. From the binary plots of TiO_2 versus MnO (Fig. 3.6.6a, Thasos slags are not shown) three groups can be distinguished:

Group 1 contains low TiO_2 and low MnO (c. 1%MnO and 1% TiO_2). This group comprises the majority of slags in most parts of Greece.

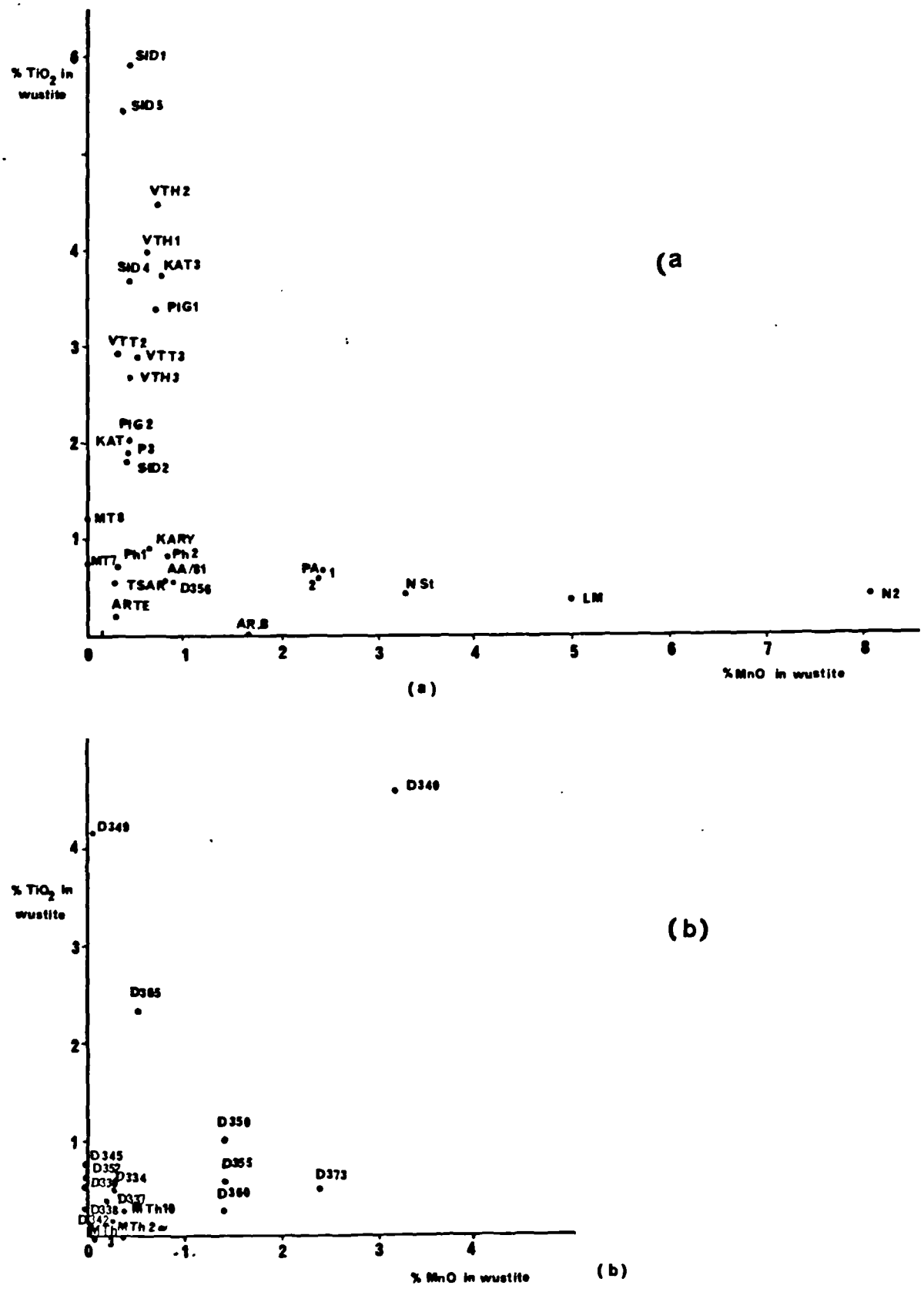

Fig. 3.6.6 TiO_2 vs. MnO contents in slags (a) and artefacts (b)

Group 2 contains slags with a high TiO_2 and low MnO, encompassing most of the EM Mainland and Thasos slags.

Group 3 contains low TiO_2 and high MnO slags, in which the Euboea (Table 3.6.5) and EM slags (Pyrgos Apollonias, Table 3.5.2) are included.

Fig. 3.6.6b shows the same plot for a selection of iron artefacts. Most of the objects fall into Group 1, only two in Group 2 and four in Group 3. The objects in the last group, D350, 355, 360, 373, probably have the Symvolon iron ore body or equivalent as their source, but the evidence is not strong. The slags from Pyrgos Apollonias are also high in Mn and can be associated with these objects. No particular groupings are discernible in plotting the phosphorus (P_2O_5) content versus MnO (Fig. 3.6.7), although admittedly the majority of the sixteen slag samples containing more than 0.5% P_2O_5 are from the Mainland. For this plot, the phosphorus content in the matrix was chosen since this is the phase where most of the phosphorus would segregate in appreciable amounts.

In examining the data for the limited number of artefacts available, the majority fall within the low P, low Mn area of the graph. Three artefacts (D332, D373, Mth10) show some deviation, but that may be due to an insufficient number of analyses. Thus, in summary, it is possible to identify three sources of iron ore in EM and Thasos for the objects analysed: a) hematite ores encountered in a variety of locations with no specific tracer elements, b) the Ti-rich magnetite sands of Thasos or the Mainland c) Mn-rich iron ores similar to those found in the Symvolon mountain. This source

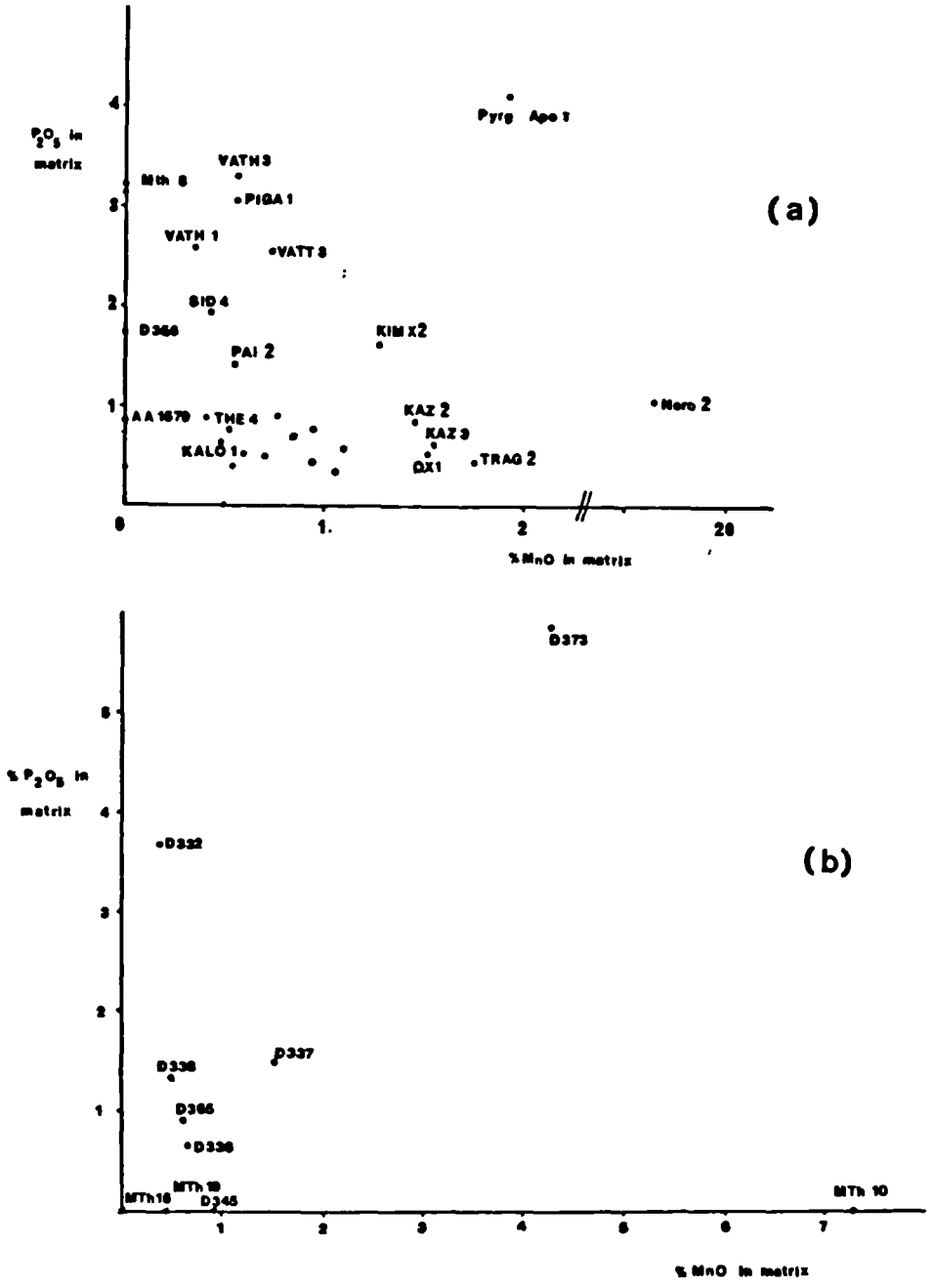

Fig. 3.6.7 P_2O_5 vs. MnO contents in slags (a) and artefacts (b)

may or may not contain phosphorus.

3.6.c Discussion

Evidence is presented here for the first time of the exploitation of Ti-rich magnetite sands on Thasos and the EM Mainland. The iron sands found on the southern shores of Thasos and at the foot of the Vrontou granite on the Mainland are the weathering product of the gneiss and granodiorite respectively. They are naturally enriched by seasonal wave action (Thasos) and washing by streams (Mainland). They are characterised by a high Ti-content found within the magnetite lattice and/or the ilmenite. A considerable amount of the magnetite has weathered completely or partly to hematite. The Mainland iron sands were found to be radioactive due to the presence of uranium and thorium compounds in the Vrontou granite.

The presence of radioactivity can be traced in the slag produced from these iron sands, as in the case of Domatia (Stavropodis 1983). The non-iron constituent of the Thasos sand consists primarily of garnets, while that of the Vrontou granite is primarily epidote, biotite and amphiboles (Karamatzani and Kaklamani 1983, 4).

Both Thasos and the Mainland Ti-rich slags appear to have been produced from the smelting of those Ti-rich sands, since no other Ti-rich iron source is known to exist at either location. Thus, it was the fortunate coincidence of the presence of titanium in the slag which led to the discovery of the ore source. Titanium

appears to be a common constituent of magnetite sands as far afield as Japan (Kubota 1970) and South Africa (van der Merwe 1980) and India (Buchanan 1930). Given the easy access by which iron sands are characterised, they seem to have constituted one of the major sources of iron in many parts of the world.

The Thasos and EM slag mineralogy is characterised by large plates of ulvospinel; with dendrites of wustite and a matrix (glassy or crystalline) of a calcium-rich olivine and mellilite. The phase diagram that most clearly represents the mineralogical phases in these slags with the exception of the ulvospinel is FeO-anorthite-$CaO.SiO_2$. Slag at the EM sites appears more compact and seems to have been tapped. The evidence for leat systems suggest the use of water-driven bellows. Georgiev (1971) illustrates the Samokovo (the word means forge) forges in Bulgaria near the Greek border clearly driven by water wheels (Fig 3.6.8). It is highly likely that the installations at Katafyto and at Vathytopos were similar since old men at both villages recall having helped in the transport of iron sand from locations within present-day Bulgaria (G Stavrakis, pers. comm.).

Ti-rich iron slag on Thasos is found scattered at a number of sites and appears to be the result of small-scale operations. Slag samples from Oxia have been dated to around the 15th c. AD (J Huxtable, pers. comm.). Slag on Thasos often appears in the vicinity of archaeological sites but is not contemporary with the site. This observation should serve as a word of caution against the often readily-made assumption that proximity to an

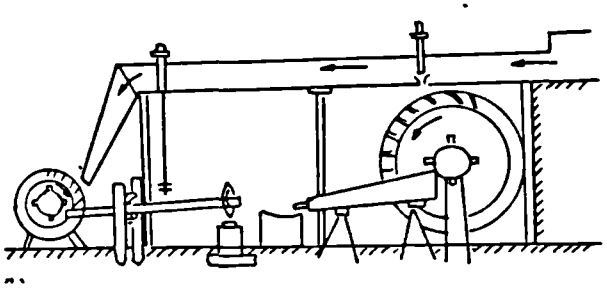

Fig. 3.6.8 Samokovò Forge (after Georgiev 1971) with water (arrows) driving the bellows (right) and the hammer (left)

archaeological site implies contemporaneity. The exploitation of the Ti-rich iron sands raises another important issue, namely that an ore deposit which is hardly considered exploitable today could have served as an important ore source in antiquity or later periods. The smelting of Ti-sands points to a continuous use of bloomery iron at least from the late Byzantine (14th c. AD) to the present century, as can be testified from the slag on Thasos and the Mainland respectively. The study of slag inclusions using Ti, V, and Cr as tracers points to the use of these sands at least since the Hellenistic/Roman period. The practice on Thasos and the Mainland may bear testimony to the continuation of a long tradition of iron sands smelting stretching from the northern coast of Turkey in the Black Sea, to the Northern Aegean. This brings to mind the mythological inventors of iron, the Chalibians, inhabitants of the southern shores of the Black Sea.

Experimental attempts at smelting iron sands pointed to the inherent difficulties in the smelting of such ore in a shaft bloomery furnace. The problems encountered were related to the

containment of the sand in the furnace. There are two ways of achieving this effect: a) by charging large amounts of iron sand (of the order of a few hundred kg per charge as the Chinese did in their blast furnaces) (Wagner 1985), and b) by grinding the ore to a fine size namely 50-70 microns (J Turner, pers. comm.). The sand particle size in the authors' experiments was larger than 100 microns, and the binding material (either organic, glue, or inorganic, clay) either burnt off before the reduction and coagulation of the iron ore was completed or contributed to the formation of large quantities of slag.

In general, these experimental smelts yielded no bloom or cast iron of good quantity, but instead only a great number of small cast iron prills within a glass-rich slag. Further experiments with the smelting of iron sands are suggested in the last chapter. The analyses of the slag and the metallic prills produced in the course of the smelting experiments are presented in appendix 3.6.2 together with the metallography of the products (Plate 16). It can generally be observed that slag microstructure resembles substantially that of the archaeological slag, but the composition of the metallic phases is not consistent with the archaeological evidence.

Plate 14

(a) and (b) THE 4. Photograph and X-ray density map for titanium: angular spinel grains exsolving out of Ti-rich wustite (lighter shade of grey in photograph or black centre in X-ray density map). Original area photographed 0.06 mm^2.

(c) and (d) THE 4. Magnification of (a) with photograph (c) and X-ray density map (d) for Ti. Original area photographed 0.03 mm^2.

(e) and (f) THE 4. Photograh and X-ray density map of vanadium exsolving out of a V-rich wustite: wustite core in the centre. Original area of photograph 0.03 mm^2.

(g) THE 4. Line scan for titanium over angular ulvospinel grain (left side), wustite globule (centre): no Ti detected in the matrix (black background).

Plate 14

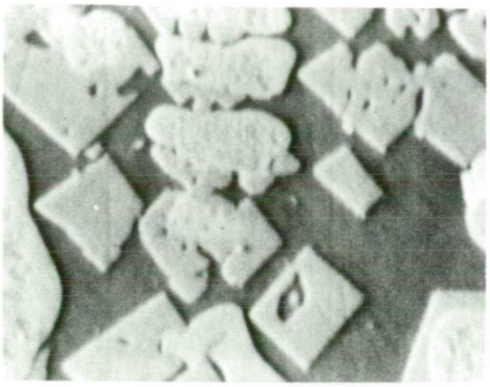

a

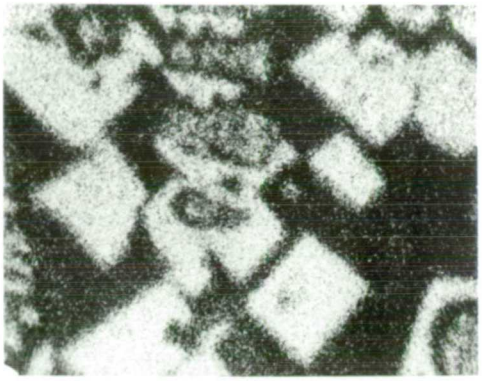

b

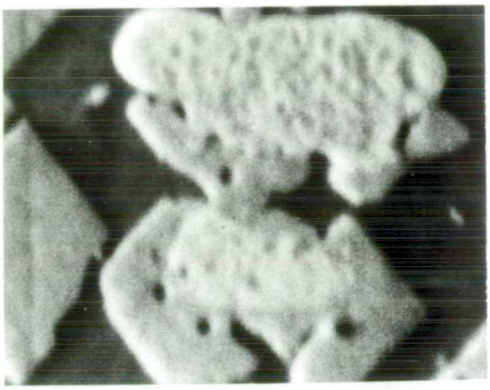

c

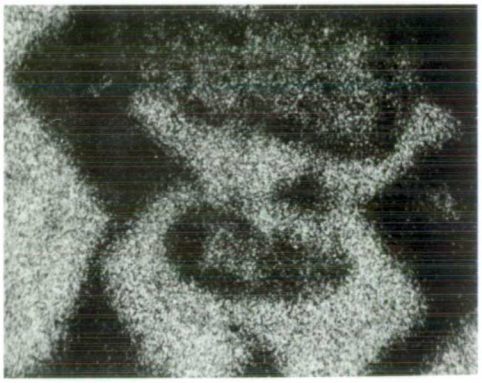

d

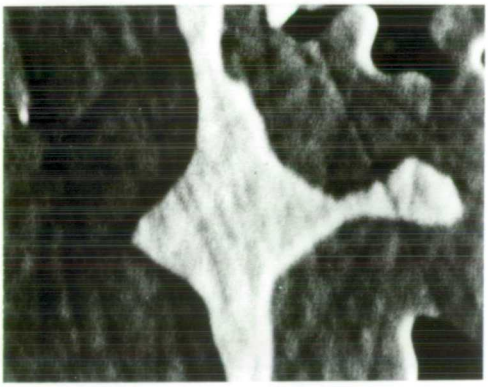

e

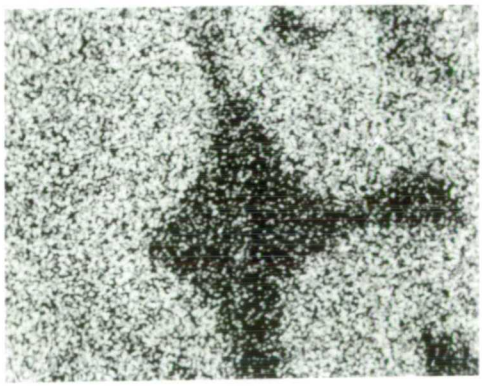

f

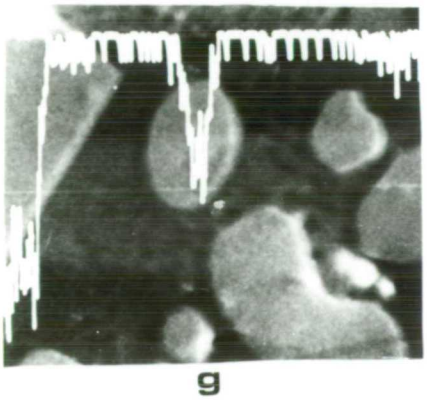

g

Plate 15

(a) KALO 1, Thasos. Ulvospinel plates, dendrites of wustite in a silicate glassy matrix; iron prills (white); black areas are holes. 100x

(b) THE 3, Thasos. Plates of ulvospinel, dendrites of wustite, silicate matrix; metallic prills (white). 100x

(c) THE 4, Thasos. Fine intergrowing of ulvospinel plates with dendrites (or golubles) of wustite. Slow cooling rate allowed complete exsolution of the former from the latter (see also Plate 4); metallic iron (white). 100x

(d) OX 14, Thasos. Well-formed plates of ulvospinel, dendrites of wustite in a silicate matrix; irregularly-shaped metallic prills (white). 400x

(e) PAI 3, Thasos. Plates of ulvosinel in a background of fine dendrites and silicate matrix; a single metallic prill (white, top). 100x

(f) VATHY 3, EM. Fine dendrites of wustite in a silicate matrix. Solidification front in the centre (thick wustite layer). 200x

(g) PIGA, EM. Fine dendrites of wustite in a silicate matrix. 100x

(h) KIMX 3, EM. Ulvospinel plate (enlarged) in a background of Ca-rich olivine (fine lathes) and silicate matrix. 200x

Plate 15

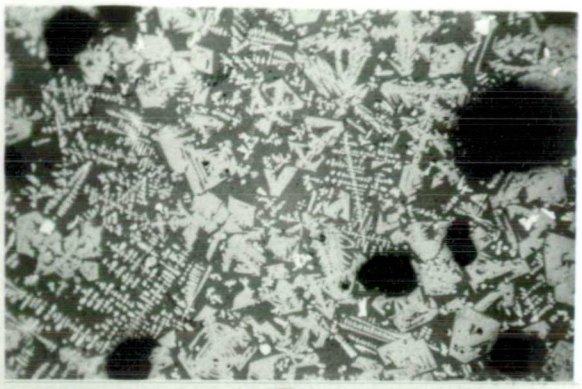

a

b

c

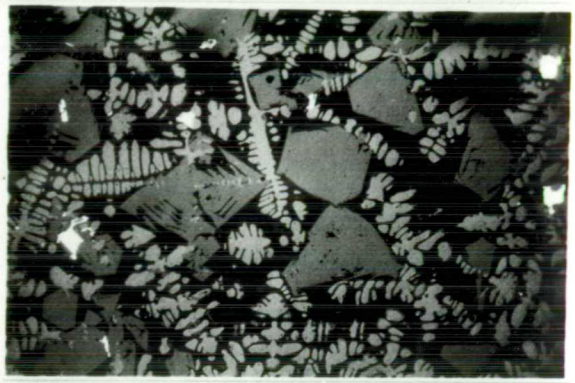

d

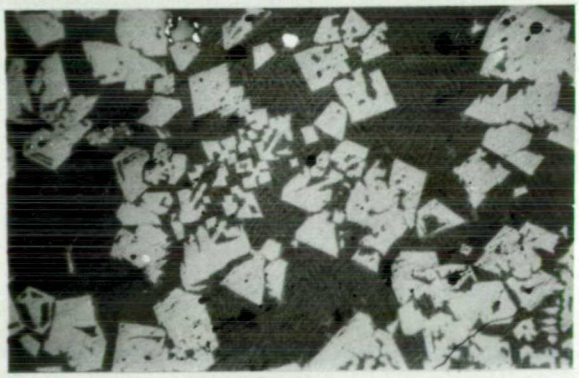

e

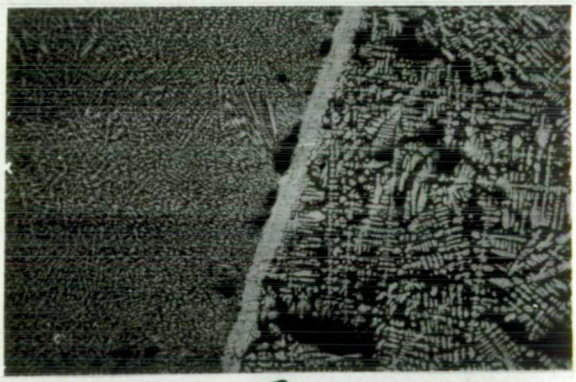

f

g

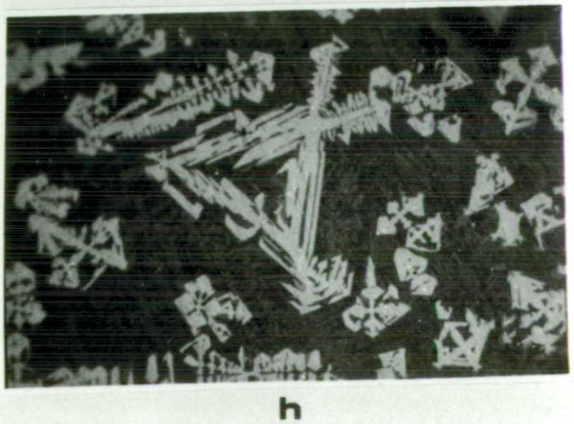

h

Plate 16

(a) X-Sm6IIa. Experimental slag with ulvospinel plate (centre), metallic iron (light), fine wustite dendrites, matrix consisting of a eutectíc of mellilite and kirschteinite. 200x

(b) X-Sm6IIa. Similar to (a). 200x

(c) and (d) X-Sm15. Experimental smelting slag clearly showing ulvospinel plates, calcium-rich olivine lathes and a glassy or crystalline matrix. 200x

(e) and (f) X-Sm2. Cast iron prill with graphite flakes surrounded by pearlite and cementite in the grain boundaries. 200x and 100x respectively, etched.

(g) and (h) X-Sm2. Cast iron prills with regular graphite plates. 100x and 200x respectively, unetched.

Plate 16

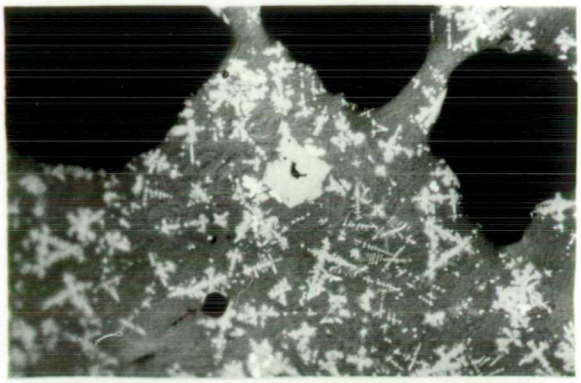

a

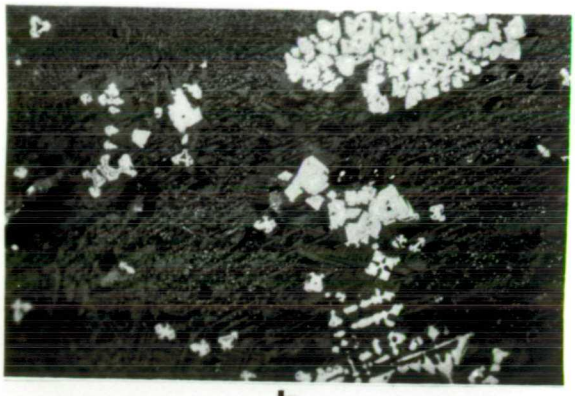

b

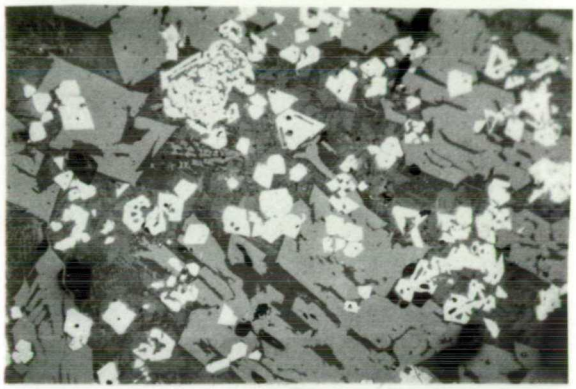

c

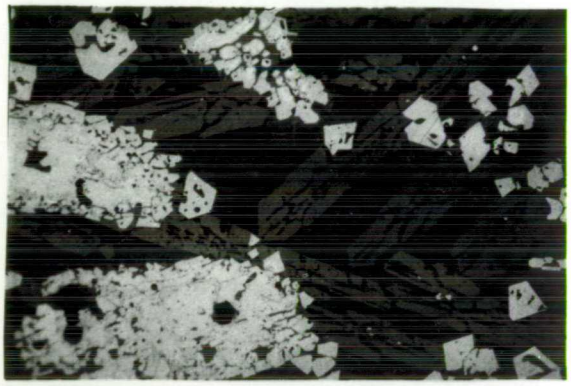

d

e

f

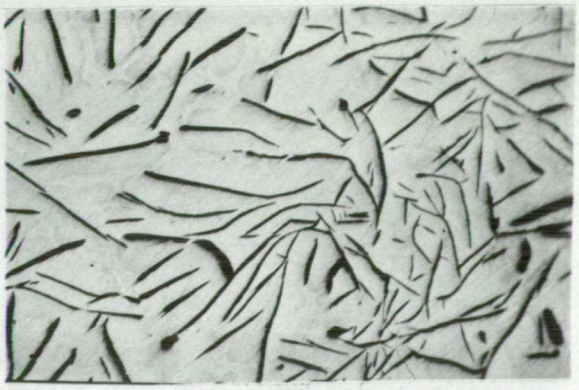

g

h

3.7 Archaeological and Experimental slag and metal from Manganese-rich iron ores (Region of Palaia Kavala)

3.7.a Archaeological Slag

The slags and metal discussed here should, strictly speaking, be treated in the context of non-ferrous metallurgy since it is argued that the metals sought were gold and silver. The work presented here constitutes only the first step in the investigation of the metallurgical activities in Palaia Kavala which is both a village and a district (Fig. 3.1.1). In view of the very extensive scale of metallurgical activities, later steps should include the dating of slags, the mapping and examination of the scale of metallurgical operations in association with local mineralization and possible furnace remains.

In the course of this work seven sites were visited and sampled for slag: Kechrokampos (Kehro), Pyrgiskos (Pyrg), Dypotama (Dyp), Makryhori (Makro), Tria Karagatsia (Kara-3), Kastanies (Kasta) and Petropigi (Fig. 3.1.1), all in the region of Palaia Kavala. Eleftheroupolis (Elefe, EL) is not included in this area, but slag and metal from this site are incorporated in the present discussion. The metallurgical waste of the Palaia Kavala district consists of slag and speiss. Speiss is a magnetic, intermetallic compound of iron, copper arsenides or antimonides, the fractured surface of which is brightly crystalline and resembles cast iron (Plate 20b). For a summary of information on speiss and its earliest evidence in Greece see appendix 3.7.1. The electron microprobe analyses of the slags from Palaia Kavala are presented

in two tables; Table 3.7.1 contains some silicate phases, and Table 3.7.2 the metallic phases, namely speiss (iron arsenides) with matte inclusions (arsenic or antimony iron sulfides).

The main characteristic of the Palaia Kavala slags is the presence of manganese (Table 3.7.1). Slags from Kechrokampos, Makryhori, Tria Karagatsia, Pyrgiskos and Eleftheroupolis consist of three phases: a) a manganese-rich wustite, b) a calcium-rich olivine (kirschsteinite) reported here as 'fayalite', and c) a matrix consisting of either an aluminium-potassium silicate of mellilitic composition or a eutectic of mellilite and kirschsteinite (Plate 17b-d). The olivine constitutes the predominant phase, the matrix making up the interstitial material only. Manganese partitions in all three phases, zinc in the olivine and the matrix, and lead only in the matrix. Lead and zinc are present in too small amounts to form any particular phases. An iron-aluminum oxide phase has been detected in one sample (Kehro-3, Table 3.7.1) and is reported here as spinel. Arsenic occurs in the slag phase of only one sample, from Makryhori, which is not surprising, since arsenic normally partitions in the metallic phase.

Plates 17a-f,h illustrate characteristic areas in slag from various sites in the Palaia Kavala area. Samples Kehro 3, Makry 13, Elefe 5 and Kara 3 display the characteristic three phase mineralogy of wustite, kirschsteinite and the mellilite matrix. Dyp 1 consists of a glassy matrix. Pyrg 3 contains predominantly olivine lathes.

Table 3.7.1

Sample no. – Phase		Na_2O	MgO	Al_2O_3	SiO_2	P_2O_5	SO_3	K_2O	CaO	TiO_2	MnO	FeO	ZnO	Sb_2O_3	PbO
Kara-II	wustite	0.87	0.58	1.12	0.39	0.00	0.00	0.00	0.17	0.43	10.05	85.97	0.66	0.00	
	matrix	0.61	0.85	0.77	10.26	0.49	0.00	0.12	6.35	0.34	11.35	68.65	0.00	0.00	
	matrix	0.00	0.66	1.05	29.65	0.00	0.00	0.65	21.97	0.31	14.35	14.35	0.00	1.94	
Kara-III	wustite	0.63	0.00	1.44	0.57	0.00	0.14	0.00	0.40	0.00	7.26	85.70	0.00	0.00	
	matrix	0.60	0.98	0.96	30.87	1.58	0.00	0.56	22.35	0.17	13.14	28.44	0.00	0.00	
EL-IV	wustite	0.00	0.56	0.52	0.57	0.00	0.00	0.00	0.24	0.51	2.97	94.63	0.00	0.00	
	matrix	0.00	0.70	5.46	34.57	1.14	1.07	2.44	18.53	0.32	4.51	31.25	0.00	0.00	
	matrix	0.00	0.50	6.17	35.52	1.05	1.45	2.85	18.40	0.31	4.22	30.43	0.00	0.00	
EL-I	'fayalite'	0.00	0.51	0.00	31.92	0.69	0.00	0.17	19.53	0.28	4.46	45.48	0.00	0.00	
	matrix	0.49	0.00	19.04	47.41	0.34	0.23	17.28	1.00	0.31	0.34	14.65	0.00	0.00	
	wustite	0.75	0.00	0.39	0.50	0.00	0.00	0.15	0.20	0.68	1.14	93.74	0.00	0.00	
Kehro-3	spinel	0.00	0.81	20.15	0.93	0.00	0.00	0.00	0.43	2.89	1.09	70.80	1.11	0.00	
	matrix	0.00	1.59	17.19	26.01	0.00	0.00	0.11	13.29	2.61	0.96	39.15	0.42	0.00	
Kehro-6	'fayalite'	0.00	1.51	0.79	32.21	1.07	0.00	0.63	26.99	0.30	4.96	32.73	0.00	0.00	
Kehro-4	'fayalite'	0.00	1.33	0.00	29.09	0.49	0.00	0.11	18.03	0.24	6.01	35.17	0.58	0.00	
	matrix	0.00	1.01	10.58	32.39	0.84	0.19	0.49	15.58	0.79	2.14	28.41	0.00	0.00	0.8
	matrix	0.00	1.67	14.04	27.99	0.50	0.00	0.00	14.32	1.88	2.17	30.40	0.00	0.00	0.0

Fig. 3.7.1 Microprobe analysis of silicate phases in Palaia Kavala slag

Table 3.7.2: Microprobe analyses of metallic phases (speiss and matte) in speiss of Palaia Kavala

Sample no.	Phase	Fe	As	Sb	Cu	S	Mn	Ti	Pb	Ag
Kara-3I	speiss	60.92	32.39	1.02	2.08	1.69	0.25	0.00	0.00	
		49.42	43.07	1.83	0.67	2.89	0.32	0.00	0.00	
Kara-3II	speiss	56.18	35.37	1.01	3.17	1.45	0.00	0.00	0.00	
		47.79	43.04	1.89	1.64	1.26	0.00	0.00	0.00	
EL-III	speiss	59.77	36.32	1.27	0.48	0.17	0.00	0.17	0.00	
EL-II	speiss	91.73	6.58	1.11	0.49	0.00	0.00	0.31	0.00	
		59.28	21.75	16.54	1.37	0.85	0.00	0.11	0.00	
		85.13	9.75	5.14	0.46	0.00	0.00	0.23	0.00	
EL-I	speiss	53.72	33.11	3.92	2.01	3.99	0.18	0.14	1.23	
Kehro-1sp	speiss	51.89	33.69	2.92	3.24	0.00	0.00	0.16	0.00	
		79.23	9.38	0.40	0.83	0.00	0.00	0.31	0.00	
Kehro-2sp	speiss	58.23	37.26	1.75	2.71	0.21	0.00	0.23	0.00	
		86.19	11.08	0.31	0.74	0.00	0.00	0.37	0.00	
Kehro-4sp	speiss	55.66	35.05	0.00	0.00	0.83	0.00	0.19	0.41	
Dyp-3sp	speiss	55.27	32.81	8.05	2.16	1.38	0.00	0.25	0.00	
		86.57	10.14	1.09	0.51	0.00	0.00	0.29	0.00	
		77.03	10.37	7.03	0.74	0.18	0.00	0.00	0.00	
		43.63	23.68	18.63	1.82	3.94	0.00	0.21	0.00	
Dyp-5sp	speiss	87.61	10.19	1.34	0.40	0.00	0.00	0.39	0.00	
		55.72	31.33	9.49	1.89	2.07	0.00	0.00	0.00	
		51.41	23.01	14.09	1.81	4.04	0.00	0.18	0.60	
Dyp.H.Me	speiss	85.85	9.89	1.62	0.50	0.13	0.00	0.10	0.00	
		57.14	35.15	4.42	1.83	0.19	0.00	0.22	0.00	
Dyp-4sp	speiss	89.36	9.38	1.15	0.64	0.00	0.00	0.32	0.00	
		40.09	10.99	46.26	2.26	0.00	0.00	0.00	0.00	
		56.54	34.34	6.82	1.86	0.15	0.00	0.28	0.00	
Makro.9sp	speiss	55.32	38.08	5.86	0.97	0.47	0.00	0.30	0.00	
Makro.7sp	speiss	86.39	10.23	1.36	0.27	0.17	0.00	0.28	0.00	
		57.59	35.19	3.78	0.19	0.18	0.00	0.30	0.00	
		61.62	10.49	2.43	0.69	24.96	0.00	0.19	0.00	
	matte	62.43	0.00	0.00	0.58	36.01	0.00	0.22	0.00	
Makro.8sp	speiss	56.13	34.36	6.17	3.17	0.30	0.00	0.22	0.00	
	matte	57.31	3.13	7.65	1.85	26.33	0.00	0.25	0.00	
	speiss	63.29	16.44	7.69	2.63	2.04	0.00	0.29	1.74	
Makro.6sp	speiss	87.14	10.47	0.95	0.39	0.00	0.00	0.29	0.00	
		57.53	35.69	4.51	1.42	0.21	0.00	0.20	0.00	
	Ag-rich	50.11	11.56	5.14	0.79	16.05	0.00	0.16	0.00	0.72
Pyr.Gr.3	speiss	54.67	38.11	1.09	5.78	0.14	0.00	0.13	0.00	

Apart from slag, speiss was found in all of the above sites either in the form of plates (Plate 20b) or as lumps or prills in the slag (Plate 17g). It is produced in the smelting of complex ores, and its presence is usually associated with precious metals extraction. The two distinct arsenic phases encountered, with high and low arsenic contents (Table 3.7.2a, extracted from Table 3.7.2), can be interpreted in terms of the As-Fe binary phase diagram (Fig. 3.7.1).

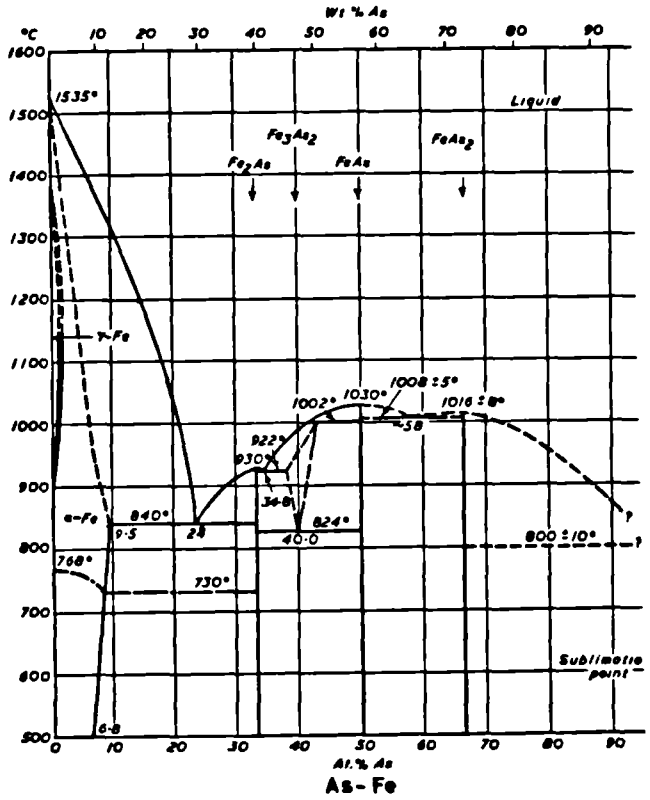

Fig. 3.7.1 The As-Fe binary phase diagram

The predominant phases are shown in Plate 18. These are alpha-iron with 10% As surrounded by a eutectic of alpha-iron and Fe_2As of the composition 35% As-65% Fe. The long lathes (and occasionally the large dendritic globules, Kehro 1sp, Plate 18c,d))

are the low arsenic component which constitutes the main phase. The interstitial material is the eutectic of alpha-iron and iron arsenide (Fe_2As). Given the higher percentage of the alpha-iron phase, the arsenic content in the melt must have been 'hypoeutectic', namely less than 24% As (atomic %) (Fig 3.7.1).

Table 3.7.2a: Analysis of the main As-rich phases in speiss (extracted from Tale 3.7.2)

Sample	%age Fe	As	Sb	Cu	S
Makro.6sp	57.53	35.65	4.45	1.42	0.21
Makro.7sp	57.39	35.19	3.78	0.19	0.17
Dyp.3sp	55.26	32.81	8.05	2.16	1.33
Dyp.4sp	56.54	34.34	6.82	1.84	0.15
EL III	59.79	36.78	1.57	1.13	0.00
Kara 3I	60.92	32.39	1.01	2.08	1.69
Kara 3II	56.18	35.37	1.02	3.17	1.45
Makro.6sp	87.14	10.47	0.95	0.39	0.00
Makro.7sp	86.39	10.23	1.36	0.27	0.00
Dyp.3sp	86.57	10.14	1.09	0.51	0.00
Dyp4.sp	89.36	9.38	1.15	0.64	0.00
EL III	91.73	6.58	1.11	0.49	0.00

Sulfides (matte) and antimony-rich inclusions in speiss

Sample	Fe	As	Sb	Cu	S	Pb	Ni	Zn	Ag
Makro.6sp	49.61	11.72	4.74	0.67	17.11	-	-	11.33	0.72
Makro.7sp	61.22	10.49	2.43	0.68	24.96	-	-	-	-
Dyp.3sp	43.63	23.68	18.63	1.82	3.93	-	-	-	-
Dyp.5sp	51.41	23.01	14.09	1.81	4.04	0.60	0.28	-	-

Sulfide (matte) inclusions are trapped in speiss and are presented also in Table 3.7.2a. They are illustrated in Plate 18e (Makro 7sp, grey inclusions). They are iron arsenic sulfides with small amounts of copper. In one particular case, Makro.6sp, the silver content is high and is associated with zinc with which it has probably formed an intermetallic compound. Speiss can, thus, be

seen to be a precious metals 'trap' in this sample. Antimony which is completely miscible in arsenic is also present. Gold and silver concentrations in speiss are more accurately determined by atomic absorption spectrometry than by electron microprobe analysis. Table 3.7.3 lists the AA analyses kindly provided by Mr N Favas of IGME Xanthi, of speiss and slag for these two elements from sites sampled by the present author.

Table 3.7.3: AA analyses of speiss and slag from sites in the Palaia Kavala region (after N Favas, pers. comm.)

Site	Ag (ppm)	Au (ppm)
Dipotama(sp)	1.2	0.0
Kechrokampos(sp)	62.0	32.0
Makryhori(sl)	119.0	0.4
Kechrokampos(sl)	45.0	12.1

It is evident that gold and silver are found in both the speiss and the slag, probably associated with lead, and that their relative contents vary substantially. The gold content is consistently lower than the silver.

Additional evidence for speiss was found at the site of Petropigi (Fig. 3.1.1; 13 km E. of Kavala and 4 km N.E. of the village of Pontolivado) and in the S.E. fringes of the Palaia Kavala region. Scattered slag (not exceeding a few kg) was found near a disused mine, the shafts of which were still visible together with the waste that was piled next to them. Ore from Petropigi was collected and later charged into the experimental furnace (see appendix 3.7.1), this being the reason why this particular site is treated independently of the other Palaia Kavala

sites. It is possible that the small amount of slag found at the site was not produced from local ore but was brought from somewhere else. The results of analysis of the silicate and metallic phases in a slag sample from Petropigi are presented in Table 3.7.4. The Mn content is very low. The slag matrix is mellilite, and long olivine needles make up the main phase of this slag sample (Plate 19c). Speiss (Plate 19b) is of the same composition and metallographic structure as those at other sites in Palaia Kavala. Lead is present, and a few Fe-Sb-S inclusions as well. These analyses suggest that the source of the Petropigi slag is an ore poor in manganese but rich in lead and possibly silver as well.

Table 3.7.4: Analysis of slag sample from Petropigi

Silicate Phases

%age

Phase	MgO	Al_2O_3	SiO_2	P_2O_5	SO_3	K_2O	CaO	TiO_2	MnO	FeO
'faya'	1.76	1.89	33.35	0.00	0.00	0.42	12.14	0.00	0.52	51.14
matrix	0.56	9.22	40.12	0.59	0.66	1.79	17.93	0.36	0.00	28.67
matrix	0.00	17.45	48.99	0.78	0.52	7.99	8.11	0.38	0.00	12.06

Metallic Phases

Fe	As	Sb	Cu	S	Pb
55.57	34.41	7.07	0.00	0.16	1.60
54.89	33.62	7.04	0.00	0.23	3.60
26.56	16.57	37.69	0.00	0.28	0.00
50.65	6.31	17.79	0.00	14.86	0.00

From the data discussed in this section, it became evident that the source of the slag and speiss in the Palaia Kavala region must be the usually manganese-rich iron ores. These iron ores (mean 26% Fe) are known to exist in the area (Spathi et al 1982), and apart from manganese (mean 10%), they contain arsenic (mean 3%) and

have average lead and silver contents of 0.8% and 56 ppm respectively (Table 3.7.5, after Spathi et al 1982).

The presence of precious metals in both slag and speiss and the absence of any evidence for base metals extraction in the slag heaps suggest that precious metals extraction was the main metallurgical activity in the Palaia Kavala region. It should be noted that not all the Palaia Kavala ores are manganese-rich, Petropigi slag being an example.

3.7.b Archaeological artefacts

There were scarcely any artefacts to be found associated with the slag heaps at Palaia Kavala. The only evidence was a cannon shot and a gun stone of basalt lava found next to each other at Lekani (Plate 20a). They both had a diameter of 7.58cm. The cannon shot weighed about 2 kg; its microprobe analysis, given in Table 3.7.6, consisted of dendrites of alpha-iron with 10% As and matrix consisting of alpha-iron and Fe_2As (Plate 19a). Coring (dendritic structure) is characteristic of casting. Some sulfur-rich inclusions are present.

Iron arsenic alloys are brittle on impact, a property particularly desirable for cannon shot. It is evident that the plaques of speiss found in the field, rather than being thrown away were recycled and made into cannon shot, at least in the Ottoman period. Percy (1864, 76) refers to cannon balls from Sinope in the Black Sea with 16.2% As and from Algiers with 27% As and 1% carbon, but he found no sulphur in the alloy.

Table 3.7.5: XRF analyses of Palaia Kavala ores (after Spathi et al 1982)

'Ακτινοχημική ποσοτική ανάλυση, κύριων στοιχείων δειγμάτων Καβάλας, %

Δείγμα άρ.	Fe	Pb	As	Mn	Zn	Cu	Ba
15002	41 10	0 24	5.66	0 07	0.72	0.049	0 029
15003	28 05	0 74	4 88	0 18	2.00	0.112	0 008
15004	53 50	0 10	0.15	2 15	0.15	0.010	0.046
15005	31 30	6 00	2 83	12 50	0.59	0.150	0.126
15007	16 70	0 65	18.00	0.113	0.015	0.097	0.011
15008	49 80	0 26	1 22	4.60	0.31	0.120	0.036
15009	31 50	0 40	0.43	18 18	1.92	0.040	0.650
15011	–	57.50	9.33	0.32	0.39	0.080	0 032
15014	40 80	0.27	0.50	27.50	5.73	0.039	0.073
15015	27.30	2 30	1.35	20 80	4.95	0.040	0.182
15016	5 20	57 00	8.22	0 43	0.31	0.040	0.032
15017	26 60	3.40	7.37	17 30	1.65	0.090	0.500
15019	18.80	1.50	0.29	32.90	2.20	0.040	0.424
15020	28.70	5 20	0.29	21.80	2.52	0.030	–
15021	18.70	0.75	1.29	31.80	4.10	0.040	0.189
15022 α	21.90	2 00	0.46	27.10	4.00	0.040	0.040
15024	5.60	0.06	0.14	0.02	0.11	4.000	0.017
15024 α	8 00	0.01	–	–	0.44	4.560	0.014
15027	16.60	0.001	0.10	0.03	0 0025	0.011	0.023
15029	31 30	0 40	0.62	16.50	0.79	0.040	0.337
15030	54.20	0.018	10.80	0.02	0.11	0.015	0.021
15031	52.00	0.10	7.25	0.02	0.30	0.023	0.014
15032	17 50	0.254	0.78	10.17	1.48	0.026	0.022
15035	0 90	0 007	0 02	2.90	0 066	0.011	0.015
15039	25.20	2.60	2 83	25.20	1 08	0.160	0.023
15044	40.00	0.10	0.35	0.31	0.10	1.610	0.040
15045	45.00	–	0 35	0.016	0.002	0.240	0.012
15047	0.45	–	0 66	1.737	0.175	0.710	0.021
15048	0.30	0 005	0 006	1.35	0.004	0.006	0 030
15051	27.60	6.20	0.53	16.18	3.90	0.080	0.273
15052	11.30	1.15	0.13	19.30	1.65	0.030	0.156
15053	7.70	1.00	0.51	15.20	0 91	0.040	0.030
15054	46.00	0.35	0.35	–	0.15	0.010	0.044
15055	1.60	0 007	0.038	6.26	0 305	0.008	0.025
15811	46.00	0 020	5.49	7.40	0 043	0.045	0.019
15814	10 64	0 014	0 325	2 55	0.054	0.101	0.140
15815	50 00	0 018	3 090	0 02	0.0015	0.117	0 013
15817	46 00	0 798	5.49	0 044	0 093	0.115	0 085
15819	38 20	0 10	0 25	0 39	0.13	1.210	0.040
15822	30.20	0 40	3.03	15.40	2.15	0.150	0 040
15823	31.00	0 57	16.21	1.07	0 27	0.100	–

'Ακτινοχημική ποσοτική ανάλυση ίχνοστοιχείων δειγμάτων Καβάλας, σέ p.p.m

Δείγμα άρ.	Sb	Cd	Sr	Sn	Bi	Ag	Au
15002	1115	250	60	–	–	15	x
15003	1438	140	80	–	–	25	x
15004	65	–	35	–	–	2	–
15005	268	–	40	–	–	83	1
15007	475	–	50	–	–	10	x
15008	240	–	150	–	–	11	–
15009	210	210	235	–	–	70	0 3
15011	1490	–	–	40	–	420	0 5
15014	660	200	30	–	–	90	x
15015	1060	280	150	–	–	98	0.1
15016	740	–	–	35	–	275	0.2
15017	2490	237	140	5	–	62	1.75
15019	240	250	130	–	–	88	0 1
15020	x°	x	x	x	x	27	0.16
15021	620	700	115	15	–	216	0.18
15022 α	780	90	5	–	–	110	0.18
15024	–^	60	–	–	50	70	1 32
15024 α	–	–	–	15	66	60	x
15027	–	75	5	–	–	3	x
15029	400	200	110	–	–	18	0 08
15030	245	140	10	–	–	10	x
15031	580	35	5	–	–	7	x
15032	4160	420	140	–	–	10	x
15035	–	95	40	–	–	–	x
15039	1100	55	7	–	–	17	x
15044	330	–	–	–	1560	–	22
15045	–	40	–	–	1220	8	x
15047	145	250	5	–	–	–	x
15048	–	135	50	–	–	135	x
15051	250	700	145	115	–	98	0.08
15052	300	250	425	10	–	59	–
15053	4200	30	500	–	–	17	–
15054	37	–	5	–	–	3	4.3
15055	–	140	75	–	–	–	x
15811	655	–	40	–	–	35	x
15814	120	–	30	–	–	75	x
15815	110	45	5	–	–	7	x
15817	610	215	65	–	–	37	x
15819	20	5	–	5840	–	15	4.05
15822	700	200	10	–	–	25	1.47
15823	x	x	x	x	x	18	2.35

Table 3.7.6: Analysis of Lekani cannon shot

	%age Fe	As	Sb	Cu	S
Dendrites	88.03	10.07	0.55	0.31	0.12
Interstitial	58.35	37.25	1.33	1.69	0.31
Matte inclus.	70.77	15.67	2.25	0.83	4.63

3.7.c Experimental slag and metal

The experimental smelting of ore from Petropigi was undertaken in order to establish whether the Palaia Kavala ores can be smelted in a low shaft furnace and whether they were the ones which gave rise to the slag heaps and speiss in the area.

Slag analysis from X-smelt8 involving iron ore from Petropigi showed slag (Plate 20d) with very common mineralogical phases like a calcium-rich olivine and a silicate matrix (Table 3.7.7 and Plate 19d,e) with traces of manganese and some sulphur. The phosphorus content of the slag was 0.5-1% P_2O_5, an equivalent amount to that observed in the rest of the Palaia Kavala slags. No lead was present. Thus, the Petropigi and experimental slags contain the same mineralogical phases. The metallic phases, on the other hand, are quite distinct. The experimental bloom (Plate 20c), a solid piece of iron weighing 2kg envelopped in relatively little slag (Plate 20d) consisted of alpha-iron with arsenic and traces of copper (Table 3.7.7, Plate 19f), arsenic accommodating both antimony and copper in a solid solution. Conditions were strongly reducing in the experimental furnace, given the high fuel/ore ratio (3/1) (appendix 3.7.1) and the fact that very little arsenic was actually lost as As_2O_3. At that temperature range and with a CO/CO_2 >= 1 there was a reduction and a solid state diffusion of arsenic in the

le	phase	Na_2O	MgO	Al_2O_3	SiO_2	P_2O_5	SO_3	K_2O	CaO	TiO_2	Cr_2O_3	MnO	FeO
:om	faya	0.00	0.00	1.53	32.13	0.00	0.00	0.00	5.84	0.00	0.00	0.49	59.11
	matrix	0.00	0.00	11.51	49.44	0.51	0.00	2.14	20.35	0.39	0.00	0.00	13.58
	matrix	0.00	0.00	11.93	43.93	1.15	0.61	1.93	18.53	1.39	0.00	0.00	20.08
	matrix	0.00	0.00	3.14	47.07	0.31	0.14	1.47	20.41	0.59	0.00	0.21	20.17
3dr	faya	0.00	2.13	0.51	31.20	0.00	0.00	0.12	11.59	0.00	0.00	0.36	52.92
	faya	0.00	1.87	0.42	31.07	0.00	0.00	0.00	14.23	0.00	0.00	0.50	50.38
	matrix	0.00	0.00	13.64	40.65	0.73	0.23	3.65	13.09	0.00	0.00	0.23	25.88
	matrix	0.00	0.00	14.48	39.62	0.73	0.13	3.47	14.33	0.33	0.00	0.13	21.21

	Fe	As	Sb	Cu
:om	92.69	4.69	0.00	0.41
	93.16	3.05	0.00	0.34
	94.03	3.03	0.41	0.24
x=0	89.63	5.48	0.99	0.40
x=1220mic	91.01	4.87	0.56	0.39
x=2390mic	92.83	4.54	0.43	0.38
x=3340mic	89.16	7.34	1.21	0.39
x=4310mic	88.53	6.91	1.14	0.56
x=5000mic	90.97	5.46	0.60	0.33

Table 3.7.7: Silicate and metallic phases in experimental bloom and slag (X-smelt 8)

iron.

3.7.d Discussion

Table 3.7.8 gives a summary of the differences between experimental and archaeological slag and metal.

Table 3.7.8

	Experimental	Petropigi	P Kavala region
slag	wustite Ca-rich olivine mellilite matrix	wustite Ca-rich olivine mellilite matrix	wustite (with Mn) Ca-rich olivine (with Zn,Pb) mellilite matrix (with Pb)
metal	As-rich bloom (with Sb,Cu)	Speiss (with Sb,Cu,S,Pb)	Speiss (with Sb,Cu,S, Pb,Ag,Mn,Ti)

The salient points arising from this Table are:

a) the slag mineralogy in both experimental and archaeological samples differs only in the type of minor elements included in the three phases which are common to all three groups. This suggests that the free-running temperature of the slag was the same as that in our experimental furnace, namely not exceeding 1250 C,

b) Petropigi slag and speiss match the analogous samples from other sites in the region of Palaia Kavala suggesting a uniformity of processes practised throughout the Palaia Kavala district,

c) The main metallic product of the experimental smelt was an arsenic-rich bloom. The speiss found at Petropigi, as well as at other sites at Palaia Kavala, was not the only metallic product since it was considered waste, like slag, despite the presence of

some precious metals. This suggests that the metal extracted from the Palaia Kavala furnaces was either lead or copper.

From Fig 3.7.1 it is evident that iron can dissolve up to 9.5% As at 840°C, the amount decreasing at lower temperatures. From probe analysis it can be indeed verified that the arsenic content in the experimental bloom did not exceed 9.5%. X-smelt8 bloom was never molten and thus, upon reduction, a solution of arsenic and iron formed by solid state diffusion. On the other hand, Palaia Kavala speiss was molten and upon solidification two distinct phases were formed. It was precisely this difference in the metallography of the metallic phases of the archaeological speiss and the experimental bloom which shed light, for the first time, on the ore source of the extensive Palaia Kavala slag heaps and the mechanism of its reduction. The production of an arsenic-rich bloom (Plate 20c) suggested that the manganese-rich ores of Palaia Kavala must have been the ore source of the speiss, but they could have never been used in a bloomery. The bloom would be brittle. Instead the ore, with its substantial iron content (Table 3.7.5), and precious metals content would have been charged in a blast furnace. The product of this blast furnace was not cast iron, since archaeological evidence suggests that most of the iron was either combined with arsenic in speiss or in the slag. The precious metals content of these iron ores, particularly silver, clearly point to exploitation of these ores for precious metals.

Where could these metals collect in order to be extracted

from the ore? Since 'early' smelters probably had no way of knowing that precious metals did collect in the speiss, lead was used as a collector. Lead had to be added to the furnace, as galena, and co-smelted with the iron ore because the lead content of Palaia Kavala ores on their own is rather low (0.8% Pb). This view is corroborated by finding lead in the Petropigi slag but not in the experimetal slag produced from Petropigi ore. The product of the hypothetical Palaia Kavala blast furnace was metallic lead (with Ag/Au), which was subsequently tapped out of the furnace. The flowchart of Fig. 3.7.2 illustrates this procedure. The temperature in the Palaia Kavala furnaces must not have exceeded 1250 C (as concluded by slag mineralogy), but the furnace conditions must have been considerably more oxidizing (CO/CO_2 <= 1), at least compared to the bloomery. Fig. 3.7.3 illustrates the differences between the products of the bloomery smelt of the Petropigi ore (a) and those produced in a hypothetical Palaia Kavala blast furnace (b) at the end of the smelt and before tapping.

Once lead was tapped, the slag discarded and the speiss reprocessed, cupellation of the metal would follow, giving litharge and metallic silver/gold (Fig 3.7.2). However, the absence of litharge in the slag heaps, despite its bright yellow or red colour, may suggest that lead was recycled by being recharged in the blast furnace.

It is not known whether there was sufficient gold in the Palaia Kavala ores to warrant extraction by separation from silver. At least in the Chalkidiki Belon (1553) makes quite clear that both

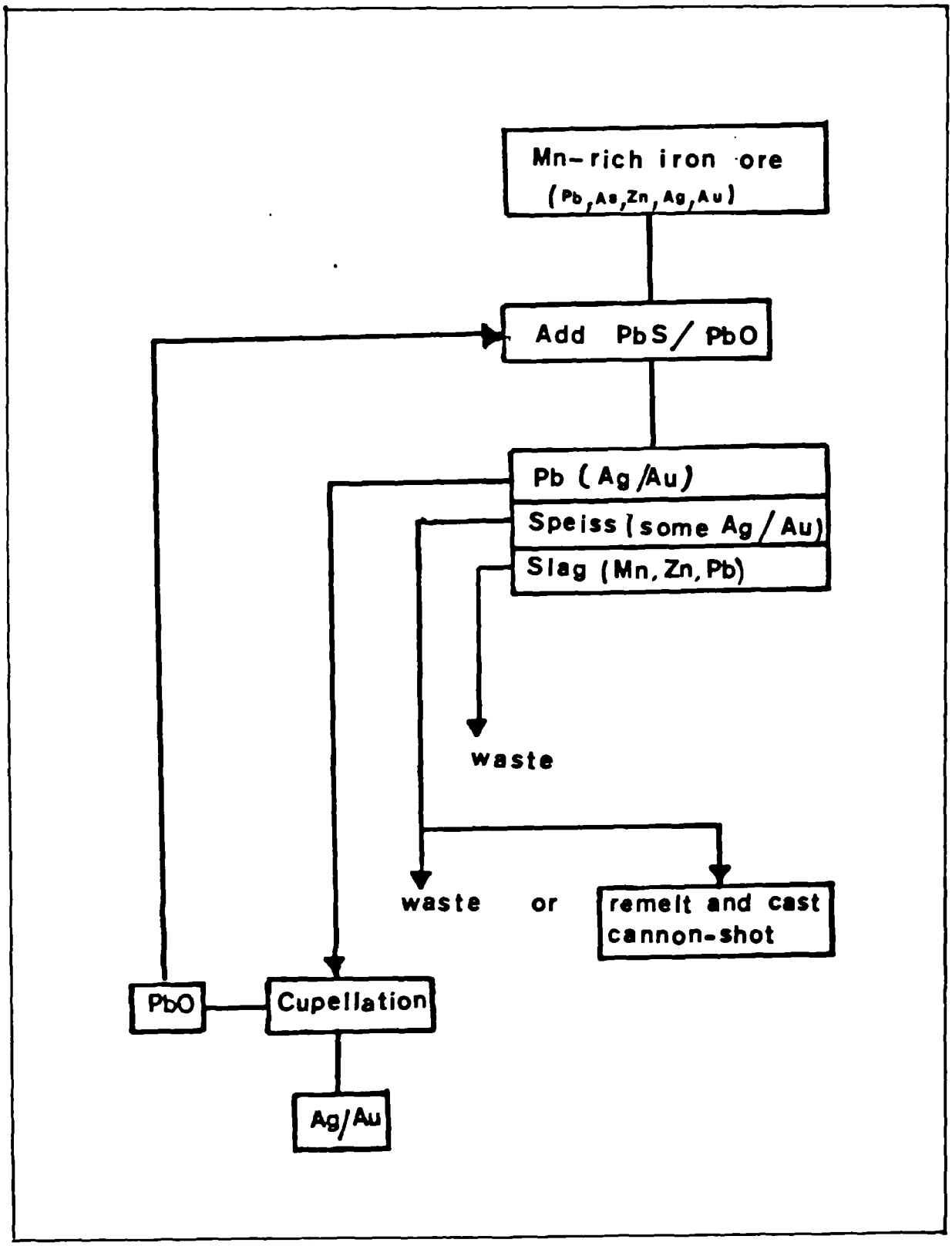

Fig. 3.7.2 Flowchart of precious metals extraction at Palaia Kavala region, EM

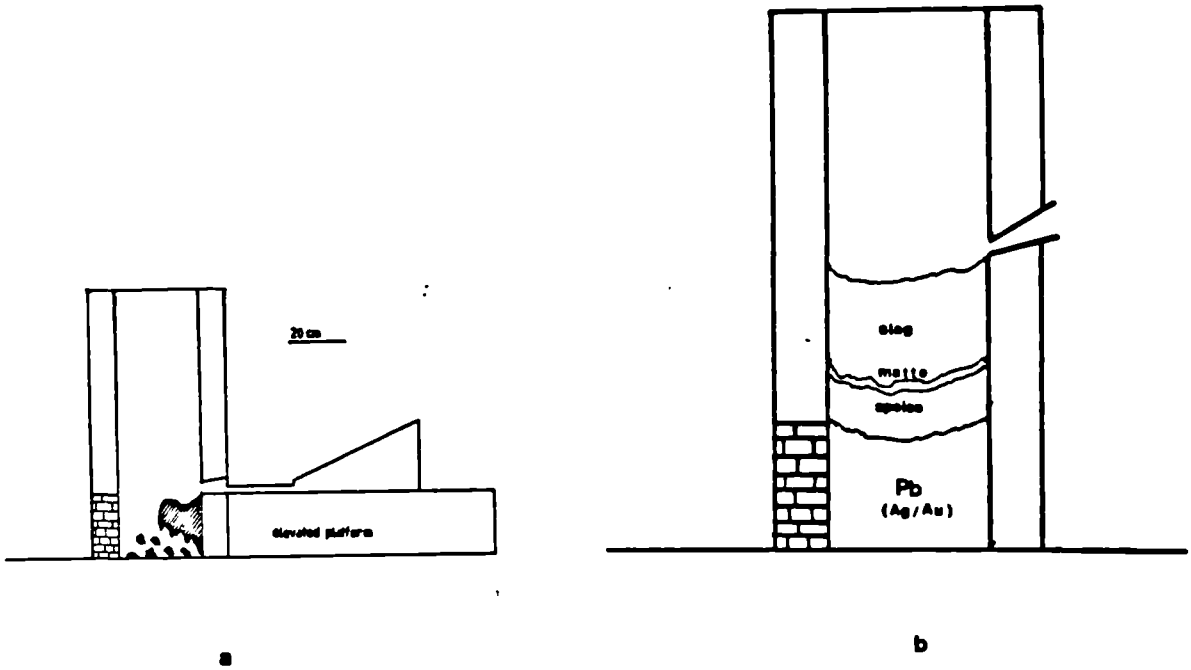

Fig. 3.7.3 Smelting of Palaia Kavala Mn-rich iron ore: schematic illustration of (a) the experimental furnace with bloom , and (b) a hypothetical furnace with lead, speiss, matte and slag before tapping.

metals were extracted. Since the gold content of some Palaia Kavala ores is rather low (Table 3.7.5), it is possible that they were used primarily for silver extraction.

In reference to precious metals extraction in the Chalkidiki, Belon (1553) noted that sulfuric acid was used to separate gold from silver. If the Ag/Au product was digested into hot sulfuric acid, silver would go into solution as Ag_2SO_4, and gold would form a residue and be removed (Ammen 1984, 198). To precipitate the silver, hydrochloric acid should be added. There

are various ways of reducing silver chloride to metallic silver (Ammen 1984, 191), the most likely having been heating with fluxes like sodium carbonate, soda ash and charcoal in the crucible. The separation of Ag/Au with sulfuric acid is unlikely to have been used in antiquity, cementation being the more likely path (Conofagos 1980, 84), involving the heating together at c. 800°C of a gold alloy to be purified with a salt in a sealed crucible. Notton (1974), who carried out an experimental simulation of the cementation process practiced by the ancient Egyptians and described by Diodorus Siculus (1st c. BC) from an adaptation by Agatharcides (2nd c. BC), found that combining all the ingredients mentioned by Diodorus did not necessarily produce a gold of high purity. However, this may have been due to the nature of the crucible which was not sufficiently porous to absorb the lead slag (Notton 1974).

This discussion about gold and silver refining is stricIty conjectural and certainly demonstrates the need for archaeometallurgical work in the area of Palaia Kavala. Papastamataki (1986b) recently excavated a furnace at Nikisiani in the Pangaion which appears to be of Ottoman date (Plate 20e). The excavation revealed a double furnace of two hearths reminiscent of Burchard's furnace in the 16th c. (Tylecote 1976, 99) for lead smelting (Plate 20f). The illustration shows a pair of blast furnaces about 2m high operated by a set of four bellows. Belon (1553) mentions that a "water wheel operated eight arms , four of which press on the bellows of the smelting furnace and the other four are intended for the bellows of the furnace which separate

lead and silver". Belon's account strongly implies that a furnace like Buchard's was indeed in operation in the Chalkidiki in the 16th c., if not in Palaia Kavala as well.

If the manganese iron ores of Palaia Kavala were exploited in antiquity for their silver content then it is possible that the area could possibly be identified as the Skapte Hyle (Koukouli-Chrysanthaki 1980). It is tempting to speculate that, while Skapte Hyle may have been the source of silver in classical antiquity, Pangaion was the source of gold.

To summarise, the experimental smelts were particularly helpful in elucidating the extraction processes in Palaia Kavala. It is suggested that at least during the Ottoman period manganese-iron ores and lead (litharge or lead sulphide) were charged together in a blast furnace, the purpose being the extraction of precious metals. The manganese iron ores were the source, the lead was the collector. The case for equating Palaia Kavala with the Skapte Hyle is cautiously advanced, while recognising the need for more archaeometallurgical work in the area.

Plate 17

(a) DYP 1. Glassy silicate slag of kirschteinitic composition from Dipotama: very different from slags from other sites. 50x

(b) Dypme (200x), (c) Kehro 1sp (50x), (d) Kehro 1sp (100x). Calcium-rich olivine with fine wustite dendrites, speiss prills (d) and a glassy matrix.

(e) Makro 7sp (50x). Slag associated with lump of speiss (not shown here); dendrites of wustite.

(f) Makro 7sp (200x). Slag associated with lump of speiss: fine inter-growth of dendrites (light grey), calcium-rich olivine (medium grey), glassy matrix (dark grey) and black pores.

(g) Kehro 2sp (100x). Speiss prill in slag; speiss composition similar to those in Plate 18.

(h) Pyrg 3 (400x). Calcium-rich fayalite (angular grains) with fine crystals of the same dispersed in the silicate matrix; very fine wustite (bright 'sparkling') constituent; black holes.

Plate 17

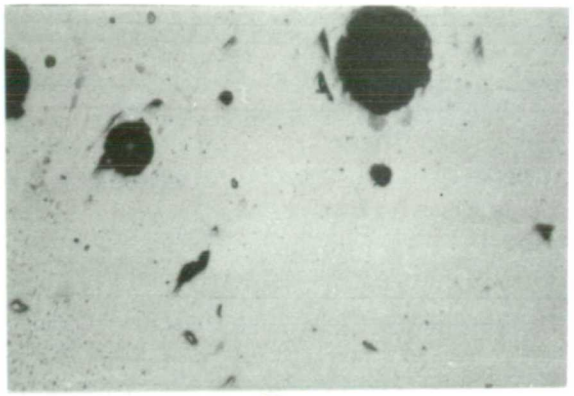

a

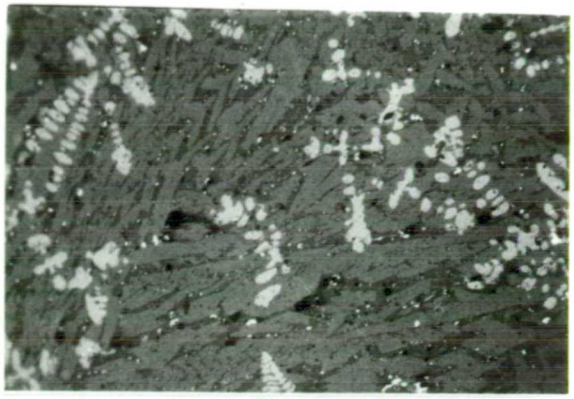

b

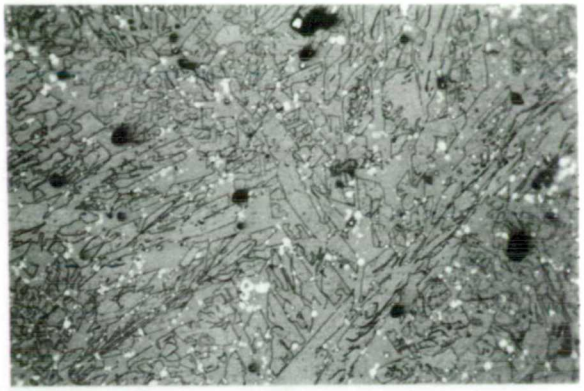

c

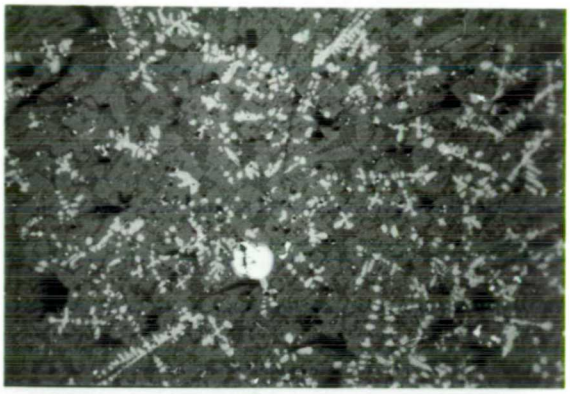

d

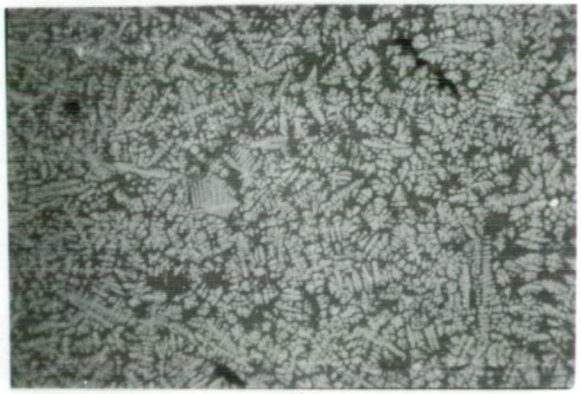

e

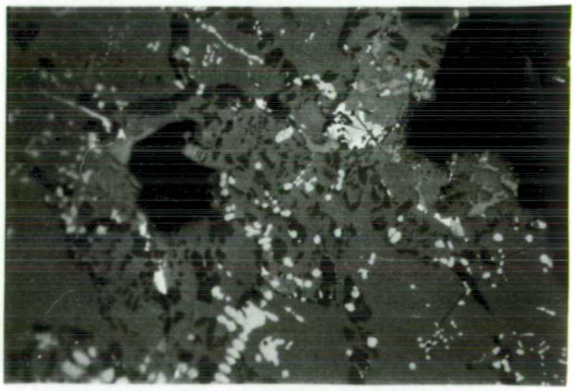

f

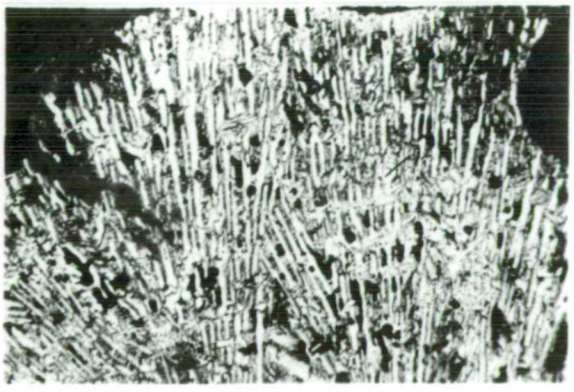

g

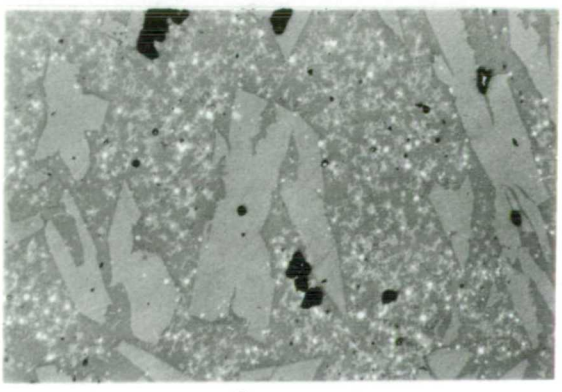

h

Plate 18

(a) Dyp 1 (100X), (b) Kehro 3 (100X), (c) Pyrg 3 (100X), (d) Elefe 5 (200X), (e) Makry 13 (100X), (f) Elefe 2 (200X), (g) Kast 1 (200X) prill in slag, (h) Kast 4 (200X):

The long white-grey lathes are the low arsenic constituent (c. 10% As), the interstitial material is a eutectic of low arsenic and high arsenic (c. 35% As) constituents. The globules occasionally forming a dendritic structure are low in arsenic like the white lathes. Matte inclusions are seen in (f) (light grey inclusions exactly at the center of the photograph. Large black areas in (e), (f), (g) are pores and/or corrosion.

Plate 18

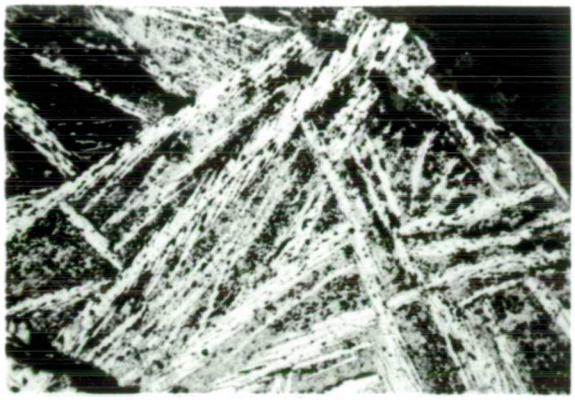

a

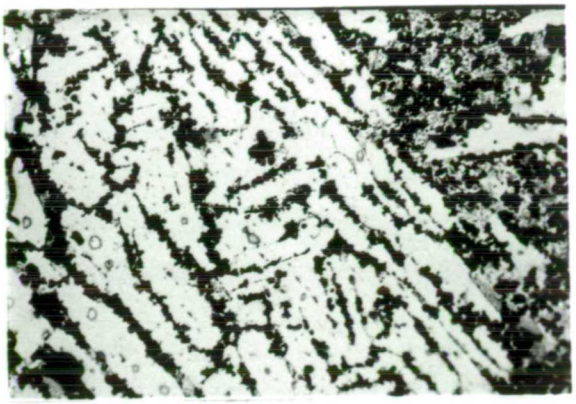

b

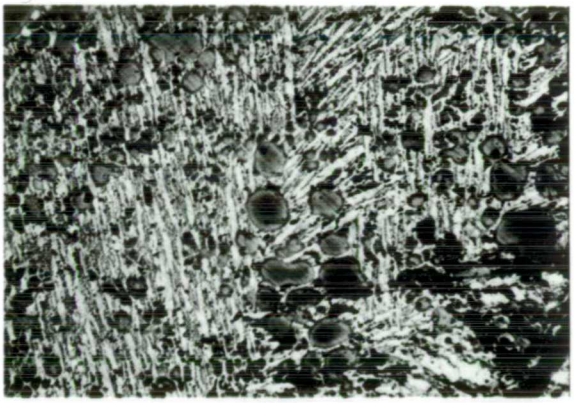

c

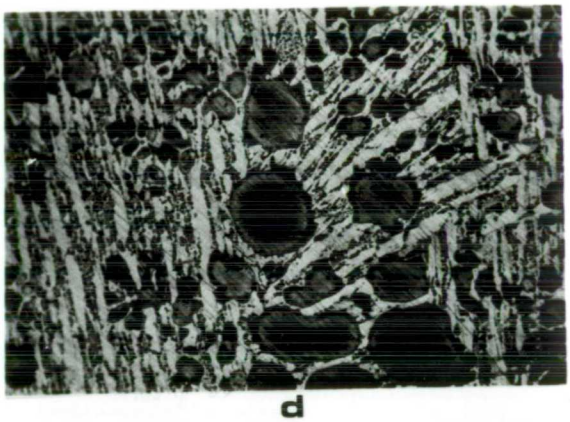

d

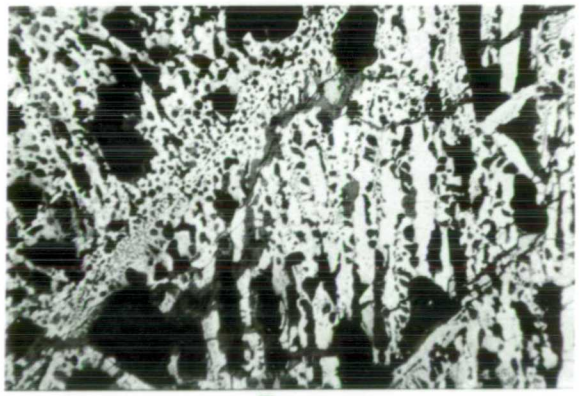

e

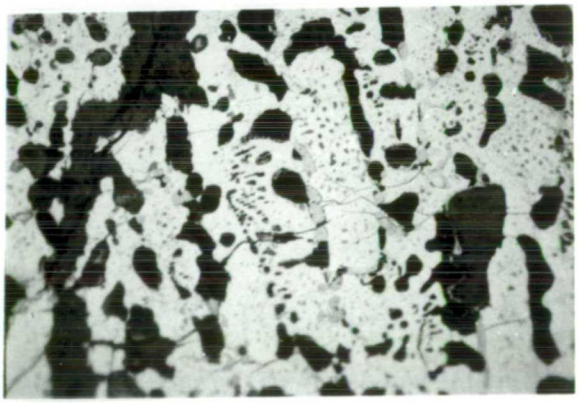

f

g

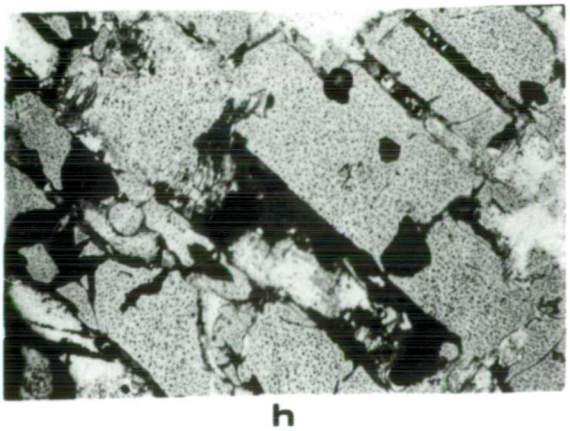

h

Plate 19

(a) Cannon shot from Lekani (Palaia Kavala district) (100x). Low-As dendrites showing coring (the object has been cast) in a matrix consisting of a eutectic of low- and high-As content in the iron.

(b) Petropigi speiss (400x). Similar to samples in Plate 18.

(c) Petropigi slag (200x). Lower section is part of a speiss prill. Calcium-rich olivine needles in a silicate matrix. Note similarity with experimental slag (d).

(d) X-Sm8 slag (200x). Calcium-rich olivine needles in a silicate matrix.

(e) X-Sm8 slag (200x). Other area in a slag with partially reduced iron oxides and some calcium-rich olivine lathes.

(f) X-Sm8 bloom (200x). Experimental As-rich bloom from the smelting of Petropigi ore.

Plate 19

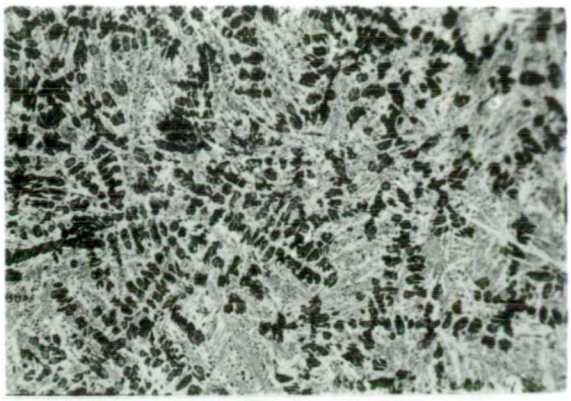

a

b

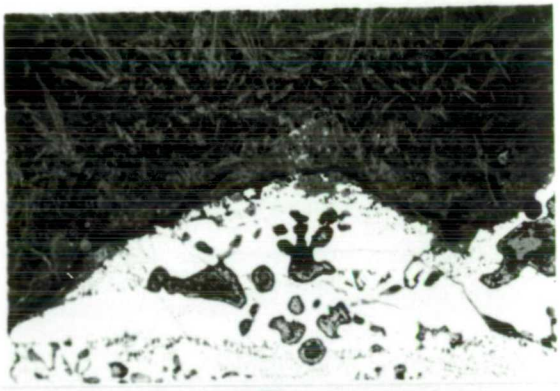

c

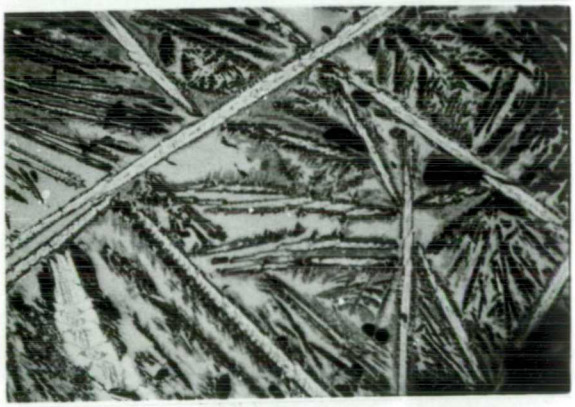

d

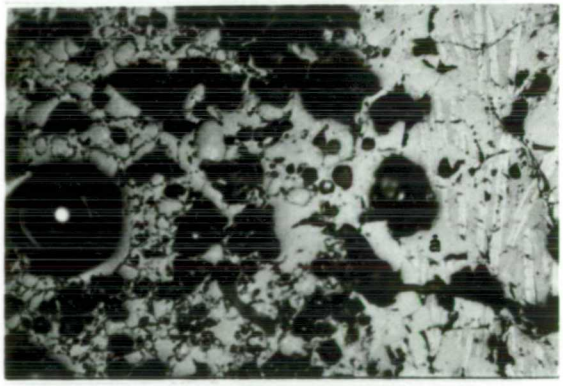

e

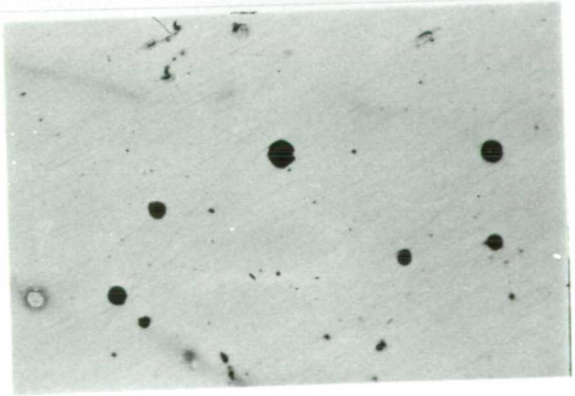

f

Plate 20

(a) Arsenic-rich cannon shot (left), basalt gunstone (right). Diameter: 7.58cm for both.

(b) Plaques of speiss found at Dipotama.

(c) Solid arsenic-rich bloom produced from the smelting of Petropigi ore (X-sm8).

(d) Slag found on the furnace floor at the end of smelting of Petropigi ore. Average size 5-7cm long.

(e) Double hearth furnace at Nikisiani excavated by the Archaeological Service (Division of East Macedonia) (Papastamataki 1986b).

(f) Buchard's double blast furnace for Pb smelting (after Tylecote 1976).

Plate 20

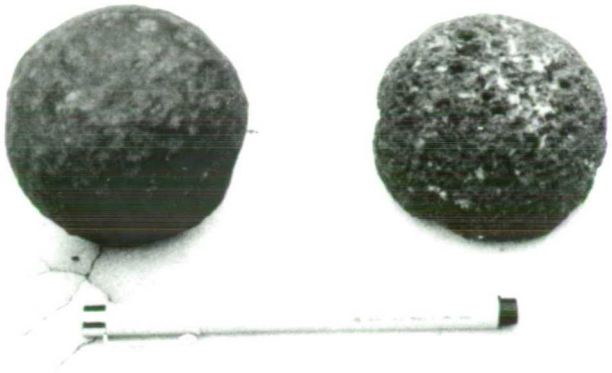

a

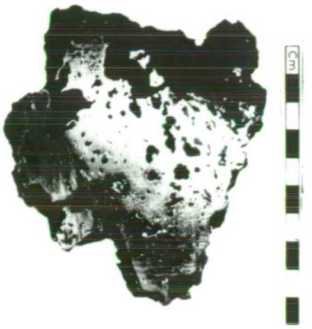

c

b

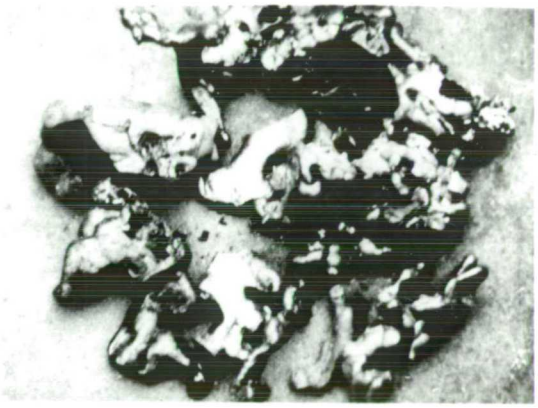

d

e

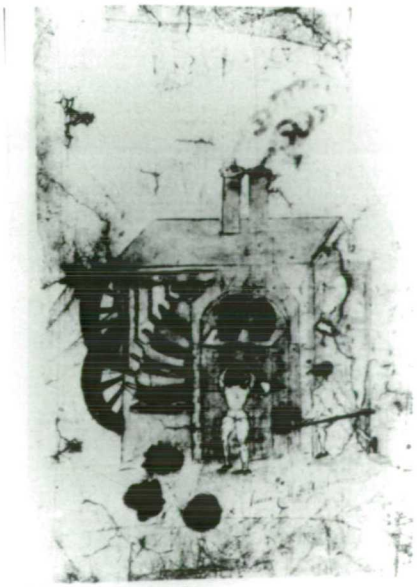

f

3.8. Smelting of Nickel-rich iron laterites in West Macedonia

3.8.a The archaeological evidence

The first evidence for nickel-rich iron in early Greek artefacts of Mycenaean date, presented by Varoufakis (1981; 1982), was discussed in detail in Chapter 2. Nickel contents up to 10% were detected, but the investigator was not able to conclude whether the origin of this iron was meteoritic or terrestrial, since only surface analysis was carried out on the objects. Thus, until now there was no evidence for the smelting of nickel rich-iron ores in antiquity in Greece, despite the presence of known deposits in a number of locations (see Fig. 3.2.4).

It was the iron prills in the slags recovered from the Hellenistic settlement at Petres in W. Macedonia which first suggested that nickel-rich lateritic iron ores may have been smelted in antiquity in Greek lands. Evidence was based on a lump of nickel-rich iron (5cm diameter) found amidst a hoard of blacksmith's tools at Petres (Adam-Veleni 1983) and nickel-rich iron prills in some slag. The analyses of two metallic prills in the Petres slags are given in Table 3.8.1. One prill is nickel-rich iron and the other almost metallic nickel. The majority of the iron prills in these and other slag samples contained no nickel at all.

Table 3.8.1: Analyses of metallic prills in Petres slags and bloom

Sample	%age Fe	Ni
Slag		
Fl-Petr	91.75	3.45
Pet.Acr	4.49	97.36

Analysis of Petres bloom (Petro 6)

Distance between sampling points (in microns)	Fe	Ni
0	92.36	3.47
100	92.35	3.71
220	93.54	3.52
380	92.27	3.27
580	92.85	3.18
980	93.77	3.06
1380	93.79	2.89
2380	93.16	3.16
8380	92.35	3.02

The typical composition of the mineralogical phases in the Petres slag is given in Table 3.8.2. For a complete list of analyses of Petres slags, see Table 3.5.1. Only two phases were evident, an alumina-rich silicate matrix and wustite, both of them typical of most iron slags (Plate 7a,b). Thus, the only evidence suggesting a lateritic ore source is based on a few nickel-rich metallic prills.

Table 3.8.2: Analyses of two slags from Petres

	Matrix		Wustite	
	FlPet1	FlPet2	FlPet1	FlPet2
MgO	0.56	0.51	0.00	0.64
Al_2O_3	11.48	11.21	1.19	0.76
SiO_2	38.14	35.51	0.74	1.18
P_2O_5	2.98	0.82	0.00	0.00
K_2O	7.28	2.16	0.00	0.00
CaO	10.33	13.61	0.00	0.00
TiO_2	0.36	0.35	0.57	0.89
MnO	1.64	3.09	1.52	2.34
FeO	26.58	28.88	85.57	89.32

Table 3.8.1 also presents the microprobe analyses of a line scan across 8.5mm of a sample sectioned from the Petres 'bloom'. The

line scan suggests that the average nickel content is about 3.2%, and random analyses on the same sample showed a nickel content ranging between 2.2 and 3.9%.

The metallography of the Petres 'bloom', shown in Plate 21 a,b, is heterogeneous and consists of . martensite in the middle of the sample (21a) with ferrite and pearlite of a widmanstatten structure at the edges (21b). The presence of nickel makes it difficult to estimate the carbon content visually. In the presence of an average content of 3.1% Ni it has been estimated to be about 0.15-0.2% C. The hardness of the martensite area is 492Hv, the pearlite is 290Hv and the ferrite 170Hv.

3.8.b.1 The experimental evidence: blooms and smelting slag

In the light of the results of the archaeological evidence, a set of experimental smelts was undertaken to compare nickel-rich iron and associated slag produced under known conditions with the Petres slag and bloom. It was expected that experimental reduction of nickel-rich iron laterites should highlight the difference in nickel distribution in the bloom, the smithed billet and the forged objects. Once the pattern of nickel distribution in terrestrial iron was elucidated, comparisons could subsequently be drawn with that in meteoritic iron. A number of mixed ores were charged in the shaft furnace (appendix 3.8.1). More specifically, two smelts were undertaken using only laterites (Xsmelt4 and Xsmelt10), two using a combination of laterites and hematite (Xsmelt5 and Xsmelt7), one using an artificial ore (hematite with reagent grade NiO, Xsmelt3) attempting to simulate an iron-rich laterite, and

finally one with laterite bound in clay (Xsmelt11). Binding laterites with clay became necessary because towards the end of the experimental smelts only finely pulverised ore was available. However, the alumina content of the charge was increased considerably, resulting in a large amount of slag.

The presentation and discussion of the experimental evidence concentrate on both the blooms and the slag. The blooms were examined for their nickel content and distribution as well as their metallography, and the slag for its composition and phase analysis. Finally, a piece of a smithed bloom was forge-welded on to a piece of modern steel (1% Mn) and the nickel distribution in the metal and the mineralogy of the slag inclusions were studied. All analyses were carried out with the EPMA.

Figure 3.8.1 illustrates graphically the Ni distribution in the experimental blooms of smelts 3, 4, 5 and 7 and compares them with that in the Petres bloom. The relevant data (distance from a hypothetical origin versus concentration) are given in Table 3.8.3. In the blooms of Xsmelt4 (Table 3.8.3) and Xsmelt10, both the products of smelting laterites on their own, the distribution along 2.5mm ranged between 3 to 6.5% and 36-38% Ni respectively. Random analyses on the same samples confirmed these results. The distribution of Ni in the blooms produced in Xsmelts 3, 5, 7 (Table 3.8.3), the products of mixing laterites with hematite, and in Xsmelt 11 (laterites and slag) proved to be rather non-uniform. To illustrate this point across a length of 8mm, the nickel content varied between 20% and 67% Ni (X-smelt5, Table 3.8.3). In the bloom

of X-smelt 7 (Table 3.8.3) in the first 1.0cm there was no nickel in the iron, but the nickel content gradually increased to 56% in the remaining analysed section (6mm). In another sample (X-sm11c), in an area of 900 x 800 square microns the composition ranged from 10% Ni to 69% Ni, while in the bloom of X-smelt3 (Table 3.8.3), the nickel concentration fluctuated between 5 and 20%. For additional information on the nickel content in iron in the experimental blooms and metallic slag prills see Table 3.8.6.

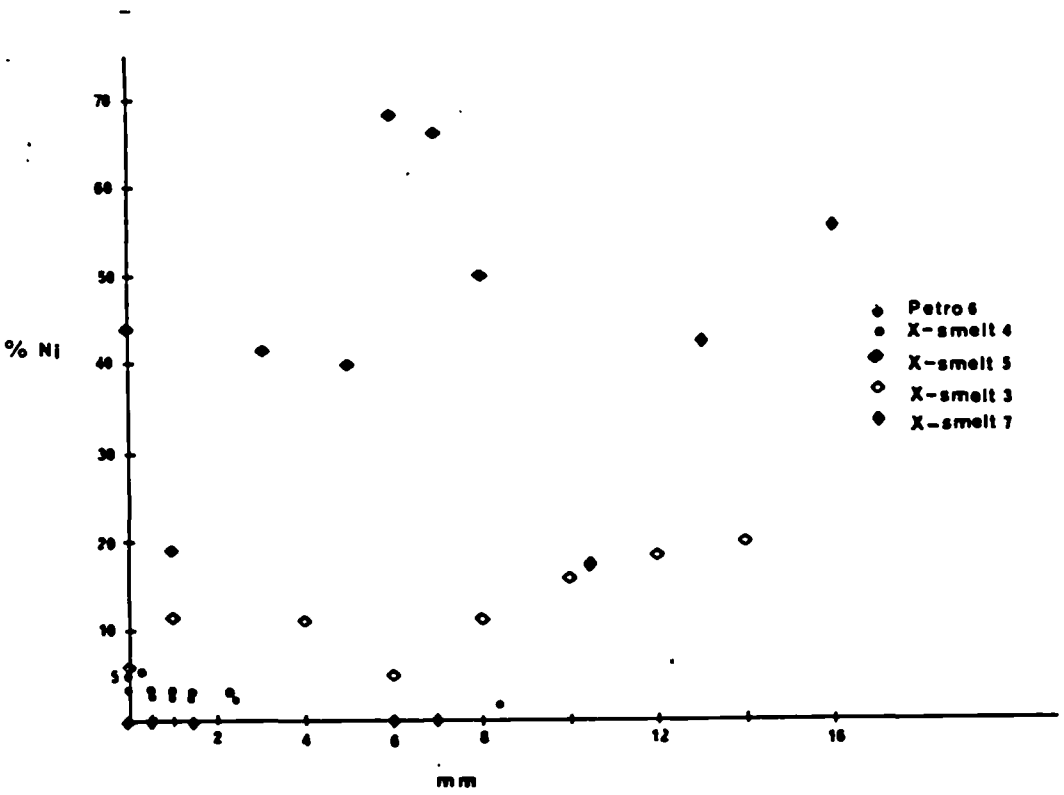

Fig. 3.8.1 Nickel distribution in the blooms of various experimental smelts and in the archaeological bloom (Petro 6). Distance measured in mm

Table 3.8.3: Nickel distribution in the bloom of various smelts

X-smelt 7		X-smelt 3		X-smelt 5		X-smelt 4	
microns	%Ni	microns	%Ni	microns	%Ni	microns	%Ni
0	no Ni	0	6.2	0	44.3	0	6.6
500	"	1000	13.1	60	52.8	40	3.9
1400	"	2000	12.4	1050	19.9	140	4.8
1800	"	4000	12.6	3190	42.1	300	6.5
6000	"	6000	5.5	5090	39.7	500	3.2
7000	"	8000	13.7	5990	67.3	600	3.7
10500	17.5	10000	16.5	7000	66.7	740	3.6
13000	44.3	12000	18.4	8000	53.4	1030	3.3
15900	55.9	14000	20.3			1520	3.3
						2310	3.3

From Figure 3.8.1 it is clear that the blooms produced from artificial ore or laterites mixed with hematites had a varying nickel content which reflects the wide distribution of nickel in the original charge. On the other hand, blooms produced from laterites on their own tended to have a much more uniform nickel content over the same range of analysed distances, although the absolute amount may vary substantially (3-6% Ni or 36-38% Ni).

The metallography of the bloom from X-smelt 3 (Plate 21c) shows pearlite and ferrite. The pearlite occupies the area of the previous austenite grains, the ferrite is in the grain boundaries. Some martensite is also present in the middle of the sample. The metallography of X-smelt5 bloom consists of martensite in the middle, pearlite with ferrite in the boundaries (Plate 21e).

The distribution of nickel in the metallic prills of various sizes found in the experimental slag also varied considerably. Table 3.8.4 illustrates this variation, suggesting that composition does not depend on prill size.

Table 3.8.4: Size and nickel content of nickel-rich prills

Width	sample	Ni%	Fe%
20microns	Xsm10d	31	59
70	Xsm10a	54	45
100	Xsm7e	1.5	93
300	Xsm10a	7	89
330	Xsm10a	15	83

The metallography of the prills varies substantially. Upon etching, Xsm10d revealed the following: the metallic prills have been molten, they are all round, and their carbon content is c. 0.8%. Their composition is more uniform given that they cooled from the molten state (Plate 21f).

The data from the analyses of the silicate phases of the experimental slag are presented in Table 3.8.5a extracted from Table 3.8.5 for easy reference. There are four different phases, illustrated here for one particular sample.

Table 3.8.5a: Silicate phases in slag (extracted from Table 3.8.5)

%age	Chromite	Wust.	Kirsch.	Matrix
Na_2O	0.00	0.00	0.00	2.25
MgO	8.99	0.00	2.58	0.00
Al_2O_3	29.67	0.72	0.00	16.97
SiO_2	0.31	0.46	32.43	40.86
P_2O_5	0.00	0.00	0.38	1.04
K_2O	0.00	0.00	0.00	8.73
CaO	0.14	0.50	28.75	10.69
TiO_2	0.24	0.84	0.00	0.37
Cr_2O_3	0.13	0.21	0.00	0.00
MnO	0.00	0.44	0.59	0.25
FeO	23.67	93.75	35.28	18.76

The phase of particular interest here is chromite (large angular grains in Plate 21h,g,f). This phase contains iron aluminium and chromium. Chromite was evident in slag of all smelts

Sample No.	Na_2O	MgO	Al_2O_3	SiO_2	P_2O_5	SO_3	K_2O	CaO	TiO_2	Cr_2O_3	MnO	FeO	NiO
XSm 7e	0.00	2.66	0.00	30.86	0.00	0.00	0.00	7.05	0.00	0.00	0.68	57.49	
	0.00	0.00	0.62	0.21	0.00	0.00	0.00	0.13	0.00	0.81	0.00	92.12	
XSm 10a	0.00	4.12	11.57	0.43	0.00	0.00	0.00	0.27	0.17	54.07	0.00	28.08	0.74
	0.00	3.83	12.24	0.24	0.00	0.00	0.00	0.23	0.00	55.62	0.00	26.71	0.37
	0.00	1.47	10.54	36.81	0.00	0.00	2.91	19.58	0.58	0.00	0.57	26.15	
XSm 10d	0.00	6.19	20.05	0.00	0.00	0.00	0.00	0.13	0.00	46.93	0.00	25.70	
	0.00	8.99	29.67	0.31	0.00	0.00	0.00	0.14	0.24	37.13	0.00	23.60	
	0.46	4.58	27.44	0.64	0.00	0.00	0.00	0.26	0.35	29.32	0.44	33.30	0.28
	0.00	1.46	19.31	0.34	0.00	0.00	0.00	0.00	0.00	45.11	0.00	34.67	
	0.00	4.94	13.77	0.00	0.00	0.00	0.00	0.26	0.00	52.41	0.00	24.03	
	0.00	3.65	4.67	0.00	0.00	0.00	0.00	0.34	0.00	58.51	0.62	30.76	
	0.00	0.00	0.72	0.46	0.00	0.00	0.00	0.50	0.85	0.21	0.44	93.75	
	0.00	2.58	0.00	32.43	0.38	0.00	0.00	28.75	0.00	0.00	0.59	35.28	
	0.00	4.09	0.00	32.56	0.24	0.00	0.00	29.36	0.00	0.00	0.57	32.45	
	0.00	4.40	0.56	33.07	0.00	0.00	0.15	29.33	0.00	0.00	0.51	32.39	
	2.25	0.00	16.97	40.86	1.04	0.00	8.73	10.69	0.37	0.00	0.25	18.25	
XSm 11	0.00	6.41	9.03	0.28	0.00	0.00	0.00	0.13	0.11	60.45	1.09	22.48	0.28
	0.00	5.81	6.33	0.23	0.00	0.00	0.00	0.00	0.15	65.37	2.69	17.39	
	0.00	0.00	0.37	0.68	0.00	0.00	0.00	0.34	0.43	0.37	0.00	93.93	
	0.00	0.94	2.61	28.21	0.00	0.13	0.00	15.98	0.46	0.00	0.34	50.85	
	0.00	0.28	14.67	59.15	0.00	0.00	4.66	3.49	0.79	0.00	0.17	14.38	
	0.00	0.81	4.74	58.89	0.00	0.00	5.04	6.87	0.48	0.00	0.00	20.18	
	0.00	0.52	21.61	58.28	0.00	0.00	13.05	0.00	0.68	0.00	0.00	6.78	
	0.00	0.00	9.58	64.21	0.28	0.00	6.77	3.31	0.65	0.00	0.00	13.65	
XSm 11a	0.59	8.30	12.72	0.37	0.00	0.00	0.10	0.30	0.00	58.21	0.74	19.81	
	0.00	1.02	18.62	0.00	0.00	0.00	0.00	0.19	0.39	32.21	0.00	45.00	
	0.00	0.84	0.31	0.35	0.00	0.00	0.00	0.25	0.18	0.86	0.24	95.27	
	0.00	0.73	0.27	0.39	0.00	0.00	0.00	0.00	0.22	1.05	0.00	94.29	
	0.75	0.81	14.92	34.19	1.19	0.00	6.02	10.51	0.00	0.00	0.00	27.73	
	0.00	1.16	0.00	0.15	0.00	0.00	0.61	3.72	0.00	0.00	0.14	0.00	
	0.00	0.00	0.00	0.00	0.00	0.00	1.10	0.28	0.00	0.00	0.00	0.93	
	0.26	0.00	0.00	0.33	0.00	1.17	0.00	0.00	0.00	0.00	0.00	0.37	
	0.29	0.00	0.00	0.58	0.14	0.00	0.93	2.56	0.00	0.00	0.00	1.46	
XSM 11b	0.00	6.40	14.85	0.21	0.00	0.00	0.00	0.00	0.00	53.27	0.39	24.35	
	0.53	8.76	15.16	0.00	0.00	0.00	0.00	0.00	0.00	55.69	0.42	19.75	
	0.00	0.33	0.49	0.63	0.00	0.00	0.00	0.23	0.56	0.67	0.00	91.70	
	0.53	0.67	26.07	14.45	0.27	0.00	0.69	6.93	0.99	1.47	0.23	49.78	
	0.64	0.44	24.77	26.09	0.33	0.00	3.96	8.24	0.50	0.00	0.21	34.86	
	0.00	1.89	0.73	31.31	0.00	0.00	0.19	15.72	0.00	0.17	0.28	49.25	
	1.29	0.00	19.78	43.06	1.56	0.00	10.48	8.71	0.57	0.00	0.00	13.66	
XSm 11c	0.00	4.71	12.09	0.73	0.00	0.00	0.00	0.00	0.00	55.11	0.00	25.97	
	0.00	1.93	11.09	10.04	0.00	0.00	0.61	5.26	0.69	19.38	0.29	49.52	
	0.00	0.47	12.69	28.26	0.09	0.14	2.93	10.07	1.29	3.13	0.00	38.64	
	0.00	2.65	6.97	36.06	0.54	0.00	2.62	19.57	0.29	0.30	0.28	30.37	

Table 3.8.5: Microprobe analyses of silicate phases in experimental slag

Sample No	Na_2O	MgO	Al_2O_3	SiO_2	P_2O_5	SO_3	K_2O	CaO	TiO_2	Cr_2O_3	MnO	FeO	NiO	CuO	As_2O_3
XSm 3a	0.00	2.33	8.96	52.05	0.93	0.63	1.85	4.19	1.02	0.00	3.59	21.56		0.27	
	0.00	2.52	10.45	61.28	0.96	0.72	2.01	5.64	1.13	0.00	4.06	10.84			
XSm 3c	0.00	1.26	3.13	33.42	0.39	0.00	0.37	16.87	0.37	0.00	0.20	38.47			
	0.00	0.00	7.89	29.60	0.46	0.00	2.06	13.52	3.12	0.00	0.22	17.11			
	0.00	0.74	0.33	3.70	0.00	0.00	0.00	18.00	0.10	0.00	0.17	42.85			
XSm 3d	0.00	3.86	0.00	33.95	1.16	0.00	0.55	53.76	0.27	0.00	0.12	4.50			
X3Sm b	0.00	0.94	4.78	35.99	0.89	0.00	4.93	22.34	0.70	0.00	0.62	25.32			
	0.00	30.17	38.29	0.00	0.00	0.00	28.28	0.26	0.00	0.00	0.00	1.74			
XSm 4	0.00	1.61	1.28	1.59	0.00	0.00	0.00	0.17	0.35	2.14	0.73	91.76			
	0.00	1.62	0.17	0.39	0.00	0.00	0.00	0.00	0.29	3.77	0.71	94.37			
	0.00	6.61	12.65	5.93	0.00	0.00	0.00	0.59	0.00	52.02	0.97	17.97			
	0.00	3.43	17.64	0.90	0.00	0.00	0.16	1.21	0.94	0.00	0.71	64.42	0.28		
	0.00	4.64	12.58	0.34	0.00	0.00	0.00	0.33	0.75	6.32	0.69	70.05	0.79		
	0.00	4.73	6.00	0.26	0.00	0.00	0.12	0.59	0.43	5.52	0.60	77.44	0.70		
	0.00	2.34	0.62	31.43	0.45	0.00	0.00	29.17	0.00	0.00	0.89	14.22			
	0.00	2.20	0.00	31.72	0.00	0.00	0.00	26.60	0.00	0.00	0.61	11.90			
	0.00	2.61	11.77	35.33	0.00	0.00	0.71	37.32	0.00	0.39	0.24	12.08			
	0.00	0.00	15.04	37.51	3.13	0.00	5.45	18.26	0.59	0.20	0.29	16.16			
XSm 4c	0.00	6.94	29.92	0.37	0.00	0.00	0.00	0.36	0.20	11.35	0.15	28.44			
	0.00	2.50	20.44	7.35	0.65	0.00	0.00	5.28	1.25	1.62	0.55	54.58	1.75		
	0.00	3.68	6.53	25.93	0.25	0.00	0.00	23.24	0.27	0.00	0.87	18.64	0.28		
	0.00	0.88	7.74	34.07	1.02	0.00	0.00	19.86	0.00	0.00	0.68	31.72			
	0.00	1.28	4.52	13.05	0.00	0.00	0.00	11.00	0.49	0.00	0.42	70.70			
	0.00	2.67	12.21	33.70	0.00	0.00	0.00	36.80	0.00	0.00	0.21	14.30			
XSm 4e	0.00	5.24	20.81	1.98	0.00	0.00	0.00	0.17	0.00	42.81	0.60	20.50	0.23	0.62	
	0.00	4.57	18.49	10.00	0.00	0.00	0.00	6.80	0.38	20.03	0.55	37.64			
	0.00	1.77	9.58	33.54	0.81	0.00	0.00	23.67	0.64	0.00	0.55	27.72			
	0.00	1.69	9.69	29.95	0.87	0.00	0.00	21.05	0.86	0.00	0.55	34.69			
XSm 5	0.00	0.57	14.06	33.76	0.89	0.75	7.65	19.12	0.28	0.19	0.30	23.27			
XSm 5Ib1	0.00	0.00	0.00	0.27	0.00	0.00	0.00	0.00	0.00	0.00	0.00	95.19	0.86	0.29	
	0.00	1.70	1.86	4.33	0.00	0.00	0.73	2.60	0.47	0.00	0.83	85.15	0.33		
	0.00	0.59	11.50	12.32	0.00	0.00	7.91	1.05	0.66	0.19	0.46	64.40			
	0.00	0.73	17.43	33.09	0.66	0.00	9.25	24.24	0.28	0.00	0.17	11.64			
XSm 5IC2	0.00	0.83	0.95	0.43	0.00	0.00	0.00	0.11	0.62	2.50	0.48	87.70			
	0.00	0.00	5.30	21.22	0.00	0.00	0.00	1.28	0.00	0.00	0.00	79.81			
XSm 111a1	0.00	0.00	0.00	0.51	0.00	0.00	0.00	0.00	0.00	0.22	0.00	96.85	1.64		
	0.00	1.21	0.35	32.32	0.49	0.00	0.27	26.97	0.00	0.00	0.29	37.44			
	0.00	0.00	12.15	37.21	4.54	0.00	10.59	14.51	0.17	0.00	0.00	14.21			
XSm 111C1	0.00	6.68	6.65	0.53	0.00	0.00	0.00	0.45	0.15	65.68	0.65	18.48			
	0.00	5.85	11.75	0.24	0.00	0.00	0.00	0.19	0.00	56.37	0.54	22.29			
	0.00	0.58	7.55	26.76	0.39	0.00	0.00	12.46	0.67	0.00	0.35	48.67	0.36		
	0.00	1.64	4.35	31.43	0.00	0.00	2.25	13.22	0.30	0.17	0.34	46.11	0.34		
	0.00	1.16	6.47	22.00	0.00	0.00	0.00	10.10	0.63	2.13	0.39	55.44	0.37		
	0.00	1.40	6.59	22.05	0.00	0.00	0.00	13.81	0.92	0.67	0.42	52.59	0.26		
	0.00	0.68	1.51	40.40	0.00	0.00	7.75	11.28	0.13	0.00	0.30	28.06			
	0.00	0.00	14.80	39.63	0.00	0.00	9.15	8.90	0.51	0.30	0.00	29.46			
XSm 7a	0.00	0.36	6.69	0.73	0.00	0.00	0.00	0.17	2.15	1.42	0.00	84.75			
	0.00	0.51	3.38	33.16	0.53	0.00	1.19	16.91	0.00	0.00	0.37	45.13			
	0.00	0.00	18.71	42.71	0.64	0.00	7.40	11.51	0.44	0.00	0.00	15.09			

Table 3.8.5 (contin.): Microprobe analyses of silicate phases in experimental slag

Metallic Sample No.	Fe	Cu	Ni	As	Mn	Cr	Ti	P	Si
XSm 3a	93.26				0.18		0.40	1.11	0.26
XSm 3c	77.12		11.36						
	74.76		10.75						
XSm 3b	79.15		3.79						
	91.01		1.53						
	66.24		33.04						
	82.63		14.04				0.36		0.38
XSm 3d.b1	92.53		6.19						
	87.36		13.07						
	87.54		12.37						
	86.90		12.65						
	94.10		5.51						
	85.29		13.66						
	82.95		16.45						
	82.22		18.42						
	79.88		20.28						
	95.76		3.18						
	96.51		1.93						
	96.89		1.15						
	97.12		0.87						
XSm 4	94.42		3.33						0.31
	95.63		3.37						0.18
	95.20		2.87						0.14
XSm 4c	96.31	0.28	2.22						
	95.96	0.22	2.94						
XSm 5	95.57		0.26						0.15
XSm 5Ib1	98.70								0.11
	97.83								0.16
XSm 5IC2	98.61								0.18
XSm5IIIa1	41.14		44.33						
	44.82		52.82						
	77.16		19.95						
	56.30		42.17						
	31.92		67.27						
	45.23		39.67						
	31.38		66.64						
	44.64		53.41						
XSm 7	91.84		7.98			0.41			
	83.41		17.46			0.94			
XSm 7e	93.69		1.56			0.48			
	95.83		1.23			0.25			
	94.28		1.63			0.62			
XSm 10a	45.49		54.18	1.48					
	89.29		7.57	0.48					
	83.43		15.11	0.38					
XSm 10d	62.80		43.04	9.42					
XSm 11a	97.81		1.04						
	96.22		1.83						

Table 3.8.6: Analyses of metallic phases in experimental slags and blooms

suggesting that it has a free-running temperature well within the range attained by our experimental furnace (estimated temperature 1250°C). It is clear from these analyses that nickel does not partition in the slag but only in the metal. This is due to the fact that the free energy of formation of the nickel oxides is quite low (c. 200 KJoule/mole O_2) at 1200°C compared with iron, suggesting that nickel oxide will reduce quite readily (see Ellingham diagram, appendix 3.8.1).

3.8.b.2 Experimental evidence: Smithed blooms and forge-welded objects

Before any comparison is drawn between the products of the experimental smelts and the Petres material, it is essential that the results of the experimental smithings are discussed first. A section of the bloom from Xsmelt5 (Plate 22d) was smithed at Kavala by the blacksmith Mr. Theocharis Piperides. The nickel content in the smithed bloom ranged between 0.5 and 2.8%. The structure is that of mild steel (ferrite with pearlite) with only a small number of inclusions, suggesting adequate consolidation of the bloom. This piece was only smithed but not forged.

A second piece of the same bloom was forge-welded by Mr. Piperides to a piece of Mn steel (Plate 22a). Fig 3.8.2 shows the distibution of Ni along the Ni-rich section, the interface (see insert in Fig. 3.8.2) and the mild steel section. The nickel distribution along the nickelrich phase is very homogeneous and drops to zero in the Mn steel zone phase which signifies there is no Ni diffusion along the boundary. At the interface the nickel

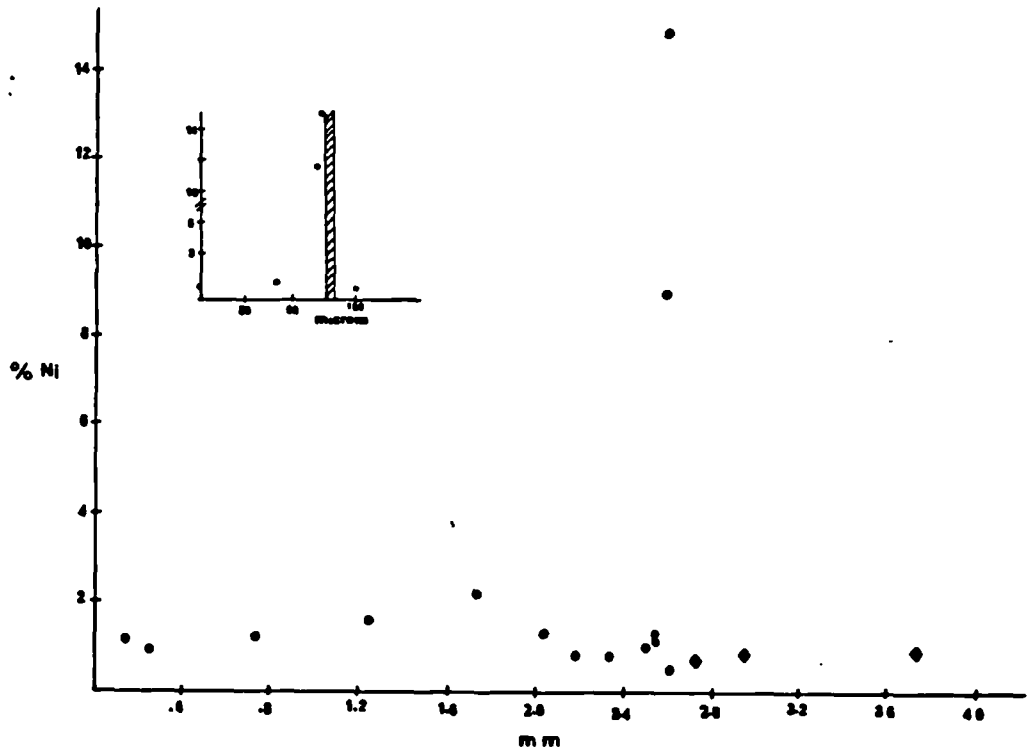

Fig. 3.8.2 Nickel distribution in bloom forge-welded to a piece of Mn steel (Plate 22a). Dots correspond to Ni content, diamonds to manganese. The insert is an enlargement of the interface (cross hatched area).

content rises to a high level (15%Ni). If slag inclusions are trapped in the interface, they are also characterised by a high nickel content. However, nickel does not concentrate in the silicate phases as such, but rather at the interface between slag inclusions and metal. Thus, if an iron object is suspected of having a nickel-rich iron source, the interface between metal and slag inclusion should be analysed to ascertain whether the metal is indeed made of nickel-rich iron.

Finally, a third Ni-rich section of a bloom (Plate 22b) was forge-welded to a piece of mild steel (Plate 22c), the interface shown by an extensive layer of slag. The metallography of all three smithed blooms indicates the presence of ferrite with various

amounts of pearlite.

The slags produced as a result of Mr. Piperides' smithing were characterised by the absence of chromite, whereas the slag produced from the smithing of the X-smelt7 bloom (Xsm7sa, Table 3.8.8), in our smithing hearth in Ashdown Forest, showed that chromite was still present, indicating an inefficiently smithed bloom. The mineralogy of the slag inclusions present in the forge-welded pieces (Xsmith4a and Xsmith5a) are similar to the smithing slags (Xsmith4f, Xsmith5s, Xsmith7sa in Table 3.8.7), consisting primarily of wustite and an iron-alumino-silicate matrix rich in calcium. Both of these phases have been observed in smelting and smithing slags and are also present in the slag inclusions of the forge-welded 'objects'. Sand was added by Mr. Piperides during forge-welding of Xsmith5a only.

Table 3.8.7a: Phase compositions of slag inclusions in forge-welded objects: Xsmith4a and Xsmith5a

	Xsmith4a		Xsmith5a	
%age	matrix	wustite	matrix	wustite
Na_2O	0.00	0.00	0.71	0.65
MgO	1.97	2.85	0.41	0.47
Al_2O_3	13.86	1.03	10.72	0.01
SiO_2	30.18	0.37	28.43	0.30
P_2O_5	0.99	0.00	0.52	0.00
K_2O	3.64	0.00	1.63	0.00
CaO	22.35	0.00	12.89	0.00
TiO_2	0.92	0.00	0.23	0.00
MnO	0.71	0.57	0.00	0.00
Cr_2O_3	0.00	0.85	0.00	0.25
NiO	0.00	0.00	0.26	0.00
FeO	24.14	93.59	44.46	94.10

Table 3.8.7: Silicate phases in experimental smithing slag

Sample No. Phase	Na_2O	Mg O	Al_2O_3	SiO_2	P_2O_5	SO_3	K_2O	CaO	TiO_2	Cr_2O_3	MnO	FeO	NiO
XSmith 4f	0.00	0.85	0.52	0.37	0.00	0.00	0.00	0.35	0.33	0.32	0.32	93.64	
	0.57	0.65	10.86	23.35	5.33	0.00	6.73	20.11	0.28	0.00	0.00	30.57	
	0.00	1.28	0.00	31.42	0.84	0.00	0.00	32.46	0.00	0.00	0.26	31.13	
XSmith 5a	0.69	0.50	8.93	21.57	0.66	0.84	1.15	8.71	0.21	0.21	0.00	59.28	
	0.56	0.56	12.67	33.44	0.71	0.52	2.20	17.57	0.29	0.00	0.00	31.57	
	0.65	0.47	1.01	0.30	0.00	0.00	0.00	0.00	0.00	0.25	0.00	94.10	
	0.71	0.55	0.97	0.29	0.00	0.00	0.00	0.00	0.00	0.55	0.00	95.08	
	0.71	0.41	10.72	28.43	0.52	0.70	1.63	12.89	0.23	0.00	0.00	44.46	0.26
	0.56	0.59	9.27	23.99	0.33	0.52	1.93	11.01	0.33	0.00	0.00	54.68	
XSmith 5s	0.00	1.07	0.75	0.28	0.00	0.00	0.00	0.13	0.23	0.47	0.26	94.72	
	0.00	0.74	1.82	26.74	0.67	0.00	3.79	14.29	0.21	0.00	0.32	47.92	
	0.46	0.81	11.08	27.91	0.55	0.00	3.01	19.79	0.25	0.35	0.28	38.41	
XSm 7sa	0.00	8.49	26.19	0.00	0.00	0.00	0.00	0.00	0.00	40.42	0.36	22.55	
	0.00	2.68	19.82	0.29	0.00	0.00	0.00	0.13	0.38	33.11	0.00	40.82	
	0.00	3.80	9.64	0.72	0.00	0.00	0.00	0.42	0.19	41.63	0.87	37.47	
	0.00	2.78	49.51	0.34	0.00	0.00	0.00	0.00	0.41	3.28	0.21	43.27	
	0.64	2.58	45.25	0.00	0.00	0.00	0.00	0.15	0.34	6.56	0.00	43.05	
	0.00	0.67	0.73	0.49	0.00	0.00	0.00	0.00	0.29	1.24	0.28	91.79	
	0.57	1.03	0.47	0.33	0.00	0.00	0.00	0.00	0.41	3.28	0.21	43.27	
	0.00	0.93	8.44	0.36	0.00	0.00	0.00	0.00	0.80	1.06	0.29	80.37	
	0.00	1.03	8.13	34.09	0.65	0.00	2.81	18.87	0.00	0.00	0.29	32.76	
	0.00	1.73	0.98	30.99	0.68	0.00	0.25	17.27	0.00	0.00	0.38	46.28	

Sample No.	Phase	Fe	Ni	Mn	Cr	As	Si
XSmith 4a	metal	97.78	1.72				
		99.06	1.12				
		98.00	0.92				
		99.02	1.15				
		96.53	1.61				
		96.26	2.16				
		99.13	1.32				
		97.92	0.87	0.21			
		96.87	0.82				
		97.75	1.32				
		97.34		0.77			
		96.15		0.87			
		96.44		0.97			
		98.29	1.08				
		97.69	0.99				
		87.67	9.11				
		82.53	15.04				
		86.68	11.49				
		97.85	0.56	0.21			
		82.09	16.46		0.56		
		69.63		0.69			
		96.03	2.19			0.12	0.16
		95.89	0.95				0.25
		97.79	1.79				0.13
XSmith 5a		97.98	1.39				
		95.59	3.73				
		95.77	3.49				
		96.32	2.87				
		96.95	2.15				
		97.80	1.13				
		98.58	1.60				
		96.89	1.26				
		97.98	1.83				
		98.44	1.88				
		98.60					
		97.09	1.97				
		88.77	10.27				
		87.25	8.93				
		84.27	15.19				
		97.40	2.03				
		95.65	3.47				
		94.60	4.16				
		92.64	5.85				
		80.63	19.59				
		97.75	1.55				
		97.01	1.61				
XSmith 5b		102.43					
		98.39	1.12				
		98.02	2.17				
		100.25	1.09				
		101.77	0.44				
		101.51					

Table 3.8.8: Microprobe analyses of experimental smithing slag

3.8.c Discussion

The analytical examination of the Petres material posed a set of questions which we attempted to solve by carrying out a set of experimental smeltings. The questions were the following:

a) Is it possible to smelt nickel-rich laterites in a shaft furnace and under what conditions? Is the resulting bloom workable and under what conditions?

b) Does the evidence of a few nickel-rich iron prills in the Petres slag and a nickel-rich lump of metal suggest that nickel-rich laterites were indeed smelted at Petres? Are the Petres slag smelting or smithing?

c) Finally, is it possible to clearly differentiate on the basis of chemical analysis and metallography nickel-rich iron produced from lateritic iron ores and meteoritic iron.

On the basis of the analytical data we believe that nickel-rich laterites were indeed smelted at Petres. This type of ore deposit is known to exist in the vicinity of the settlement (see Fig. 3.2.3) and it is very probable that smiths at Petres had noticed it at some stage. Evidence to that effect is the lump of iron found amidst the hoard of a blacksmith's tools and the few nickel-rich iron prills in some Petres slags. None of the analysed Petres objects was made of nickel-rich iron so the smith must have saved this piece either as a curiosity or to use it for some particular purpose. There is yet a third possibility that the slags are not contemporary with the objects (Photos et al, in press).

The Petres 'bloom' bears many similarities with our

experimental blooms. Its nickel content resembles that of Xsmelt 4, (c. 3% Ni), while its metallography resembles that of X-smelt 3 and 5 (ferrite and pearlite with some martensite). The experimental results focus on one particular point. What is the reason for the uneven distribution of nickel in the blooom?

The distribution of nickel in iron is governed by the rate of diffusion of nickel in alpha- and gamma-iron. Diffusion takes place in the solid phase and relies on the intimate contact an iron and a nickel prill. The rate of diffusion, or diffusivity, is dependent on the lattice structure, the temperature and the alloy composition (Carter 1979, 247). Diffusivity is different for nickel in face-centered cubic (FCC) iron (gamma-iron) and body-centered cubic iron (BCC) (alpha-iron). The rate of diffusion is slower in the former because nickel is an austenite stabiliser, that is, once it is in that phase it will not diffuse out; the rate of diffusion is lower at 1000°C than at 1400°C, and below 800°C diffusivity of nickel in FCC stops (Fig. 3.8.3). Rates of diffusion of nickel over a distace of 1.5 cm have been calculated for different nickel contents on the basis of data given by Carter (1979, Table 9.5).

Table 3.8.9: Effect on diffusion time of nickel impurities in iron at 1100 C, 1.5cm (calculated from data in Carter (1979, Table 9.5)

Composition	Time (hours)
Ni in pure Fe	19.6
99.8%Fe + .2% Ni	134
98%Fe + 2% Ni	1.9
96%Fe + 4% Ni	14

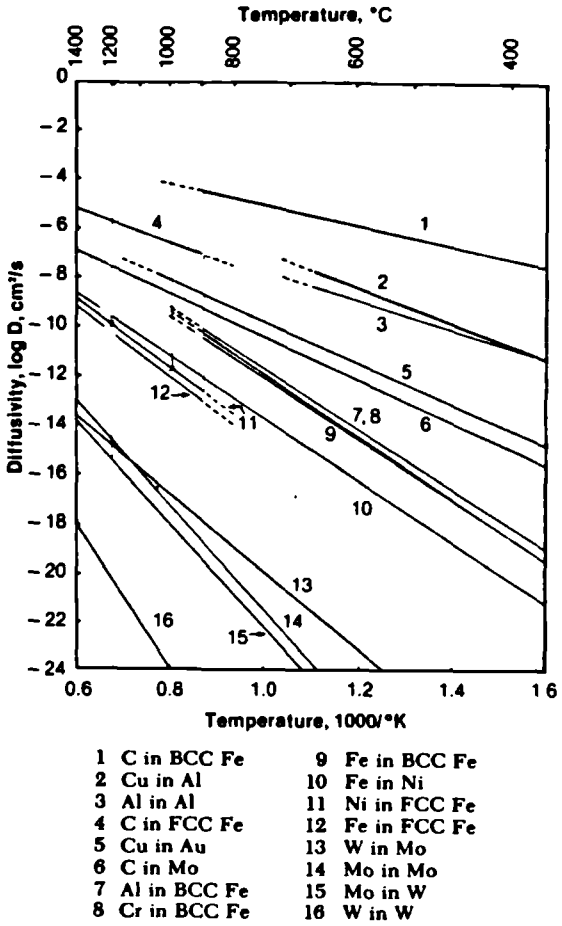

Fig. 3.8.3 Diffusivity as a function of temperature. Dashed lines indicate instability at these temperatures (after Carter 1979, 247)

This Table indicates that the rate of diffusion is fastest in iron with 2% Ni, but it decreases rapidly as the nickel increases to 4%, assuming the temperature remains constant at 1100°C. Such conditions did not prevail in our experimental furnace where the bloom would not have been exposed to that temperature for long. Once the bloom had reached the zone below the tuyere, where the temperature is substantially lower, diffusion probably stopped. Given the large variation in nickel distribution, in the mixed ore in particular, the short smelting cycles (no more than 4-5 hours), and the relatively short exposure to a uniform, high temperature

that the bloom experiences, it is not surprising that the experimental blooms had such a heterogeneous nickel distribution. Such inhomogeneities must, in all likelihood, have been inherent in the bloomery smelting of nickel-rich lateritic ores and were not the result of subsequent stages like piling and forge-welding. On only one occasion did we notice an even distribution of nickel in the iron and that was in the case of iron prills which had been molten.

Tylecote (forthcoming) has suggested that the high nickel areas found in Swedish and Polish artefacts are the result of oxidation enrichment or the forging together of a high- and a low-nickel iron. We are suggesting that there is an additional source of high nickel, namely the bloom itself. Chilton and Evans (1955) were correct in attributing the nickel segregation partly to the mechanism of solid state reduction and partly to enrichment during welding. Thalin (1973) was also correct in attributing the presence of Ni-rich areas in the Swedish metal to "the result of qualities proper to the ore or of irregularities in the reducing process". Hanssoon and Mod in (1973) found streaks of martensite in a ferrite matrix similar to those observed in our own blooms. These high and low areas seem to be due to the uneven diffusion of nickel in the bloom and are not high nickel areas produced during oxidation enrichment and flattening during forging (Tylecote forthcoming). Thus, although a number of previous investigators have suggested that the bloom itself may be the cause of the uneven distribution of nickel in the iron, this observation has only been verified by the present experimental smelts.

In view of this inhomogeneity of the bloom, it is suggested that the high nickel sections of the bloom would have been difficult to work due to their hardness originating from the presence of impurities like nickel carbon and phosphorus. It is possible that we, as well as the Kavala smith, were not experienced in the forging of the nickel-rich blooms, with resulting fracture and loss of large sections of the experimental bloom. Nevertheless, it is a fact that all the blooms that it was possible to work contained no more than 4% Ni and that the Petres bloom composition fell within that range.

The presence of only a few nickel-rich iron prills in the slag is in accordance with the experimental results, which showed that not all iron prills contained nickel. This was particularly true in the case of prills in smithing slags. The composition of the Petres slags is very similar to our experimental smithing slags. It is characterised by the absence of chromite, while the matrix of both is rich in alumina and magnesium. Chromium seems to be present in all analyses of nickel-rich iron laterites given by Albadakis (1981), and so it can be safely assumed that it was present in the source of the Petres laterites. Its absence therefore suggests that the majority of the Petres slags are smithing.

Thus to summarise, the results of the experimental smelts have shown that it is indeed possible to smelt lateritic iron ores, but the yields are not satisfactory given the low iron content in the ore (see appendix 3.8.1). The yields can be improved by

addition of hematites, but the blooms produced showed a large variation in nickel content. The high nickel areas of the bloom were not workable resulting in great losses. Consequently, the yield from the smelting of laterites was not much different from that obtained from the smelting of laterites on their own.

This discussion leads us to suggest that lateritic iron ores with 1% Ni could produce blooms with nickel contents ranging from 0-4%. These blooms could be forged in a smithing /forging hearth. The metal produced would, upon forge-welding, produce in turn enrichment zones up to 25% Ni accompanied by slag stringers and (possible) white lines. However, if laterites are mixed with high-grade hematite, high and low nickel areas would be produced in the bloom and would be reflected in the artefacts. These high nickel areas would be differentiated from enrichment zones by the absence of slag stringers and/or white lines. The limited amount of nickel-rich iron produced in our bloomery is likely to be the reason for its generally limited use. Its combination with nickel-poor iron led to laminations so beautifully exploited through etching in the making of the Malaysian daggers, the kris, discussed together with meteoritic iron in the following section.

3.8.d The question of smelted nickel-rich versus meteoritic iron

3.8.d.1 Review of the literature

Research into meteoritic iron and how to distinguish it from terrestial high-nickel iron has been conducted over many years by a number of investigators because of its relevance to many early iron

artefacts in many cultures.

Piaskowski's (1960) examination of a socketed axe from the Carpathian region revealed a 10% Ni content. This high amount was attributed not to meteoritic iron but to the smelting of a combination of ores, some rich in nickel, others not. Panseri and Leoni (1966)in their analyses of an Etruscan weapon found bands of high nickel and cobalt asociated with high carbon areas in the range of 0.2-0.5% C. There was also no attempt to interpret it as meteoritic. Recently, LiChung (1979) in China and Buchwald and Mosdal (1985) in Denmark examined chemically and metallographically meteorites and objects considered to have been produced from them. The latter showed that Eskimos never heat-treated meteorites and that sufficient hardness was imparted by mere cold working. The Chinese group proved that a Han dynasty axe was indeed made of meteoritic iron on the basis of metallography and line scans across the sample. Both these works are important since they concentrate on the criteria used for differentiating meteoritic from smelted iron.

As already mentioned in the previous section, Thalin (1973) analysed a number of Swedish artefacts with nickel contents not exceeding 1% and most below 0.5%. She explained that many Swedish ores contain nickel and cobalt in small amounts and that "irregularities in the course of smelting" can account for that nickel concentration in the artefacts. In their analyses with EPMA of two currency bars and a socketed axe also from Sweden, Hansson and Modin (1973) detected 1.4% Ni in the pearlite of the currency

bars and 10-25% Ni in the martensite streaks of the same objects. These martensite streaks have no particular shape in contrast to the lamelar martensite of the axe. Again there was no evidence for a meteoritic origin of iron. Tholander and Blomgren (see bibliography under either name) produced a series of papers on the examination of an axe from Eskilstuna, Sweden. They took blanks of high and low nickel content which they forge-welded and piled. The result was high nickel streaks ranging in width from 40 to 120 microns. Metallographic sections showed high nickel streaks of martensite embedded in a matrix of ferrite and some pearlite, signifying that with the piling of high and low nickel sheets of iron the nickel will segregate at the boundaries. Ni is an austenite stabilizer and so will concentrate at the areas with high carbon ontent, which explains its presence in the martensite in all of the objects discussed here. Tholander and Blomgren believed that the Eskilstuna axe had been produced in a similar fashion.

More recently, Clough (1986) measured clearly delineated enrichment zones in a Malaysian wave-bladded dagger, kris (or Keris), which comprised a steel core and layers of ferrite alternating with streaks of pearlite rich in nickel. The kerises display a wavy water pattern on the surface of the blade (damascening) due to the elaborate welding of nickel-rich and nickel-poor iron sheets. The pattern can only become visible when the blade is etched with arsenic sulfide and lime juices (B. Bronson, unpublished).

While in the Eastern Mediterranean and most of Europe, meteoritic iron has been assumed to represent man's first attempts

at working the metal, in Indonesia, meteoritc iron came into use relatively recently. In the 18th c. AD a meteorite fell on the island of Java . It is known that the manufacture of some kerises (probably those of high ranking officials) date to that period. However, previous to the use of meteoritic iron, evidence for smelting of lateritic iron ores has also been reported in Sulawesi (Indonesia) by Dutch officials who observed that this nickel-rich iron (0.4% Ni) was used in combination with ordinary iron in traditional small bloomery furnaces (B. Bronson, unpublished). It would be particularly interesting to find and analyse objects produced from this type of iron.

3.8.d.2 Canyon Diablo meteorite

The Canyon Diablo meteorite, a coarse octahedrite with a band width of 2.0+.5mm, fractured into thousands of fragments, 20,000 of which have been recovered and weigh between 50g to 639kg (Buchwald 1975, 381). Canyon Diablo meteorite consists of lamellae of kamacite (nickel in alpha-iron) and taenite (nickel in gamma-iron). EPMA analysis shown in Table 3.8.10 revealed that the nickel contents of taenite and kamacite were 35% and 7% respectively. It is important when analysing iron with alleged meteoritic origin to look for these lamellae, unevenly distributed though they may be. This was the case in our specimen of the Canyon Diablo meteorite. Plate 22f shows thin bands of taenite (high nickel) in a matrix of kamanite (low Ni)

(Fig. 3.8.4). The X-ray distribution map of Ni (Plate 22g) of the photographed area (Plate 22f) shows that high nickel (dark)

and low nickel areas. It is interesting to note that cobalt (another element characteristic of meteorites) increases in the opposite direction to nickel.

Table 3.8.10: Microprobe analysis of specimen from the Canyon Diablo Meteorite

Phase	Fe	Ni	Co
Kamacite	93.60	5.59	0.81
Kamacite	91.33	5.68	0.68
Kamacite	90.66	6.35	0.92
Kamacite	89.04	6.20	0.84
Kamacite	90.49	5.77	0.60
Taenite	58.69	37.74	0.00
Taenite	57.48	38.78	0.00

Analysis of CD meteorite after Buchwald (1975)

7.10 %Ni, 0.46 %Co, 0.26 %P, c.1 %C, c.1 %S,

80 ppm Ga, 320 ppm Ge, 1.9 ppm Ir.

The fine thin bands in Plate 22h are Neumann bands which are the result of rapid deformation of the meteorite upon impact with the earth's atmosphere (LiChung 1979). These Neumann bands have no connection with nickel variation in composition, and indeed on analysis with the microprobe showed 7% Ni as the surrounding matrix. On the other hand, the deformation on the left-hand side of the polished section of the Canyon Diablo meteorite (Plate 22f) is the product of shock annealing resulting from recrystallization. What this suggests is that upon impact with the earth and subsequent fragmentation some of the kinetic energy of the fragments was converted into thermal energy resulting in a brief reheating of kamacite to c. 600°C and subsequent recrystallization

(Buchwald 1975, 395).

Thus to summarise, high and low nickel areas in meteorites are associated with taenite and kamacite bands. The alteration is very characteristic and can be traced even within the corrosion area. Meteoritic iron could be cold worked and reach sufficient hardness without heat treatment. Upon cold working, taenite bands are elongated (Buchwald and Mosdal 1985, fig. 13).

A summary of the differences between meteoritic and terrestial iron are given here:

Meteorites

a) Regular high and low nickel areas corresponding to kamacite and taenite with Ni enrichment in the interface. No visible presence of white lines due to lack of local forge-welding and local depletion of C.

b) Absence of slag inclusions apart from those that may have been introduced during welding (wustite and/or fayalite). However, this assumes that the meteorites were hot worked and present evidence suggests that cold working was sufficient to impart necessary hardness.

c) Presence of elements like Ge, Ga or Co.

d) elongated kamacite/taenite grains when cold-worked.

Smelted iron

a) Irregular high and low nickel areas arising from the uneven distribution in the bloom and the enrichment zones along welding lines.

b) Presence of slag inclusions associated with ore.

c) Presence of slag stringers lining along the enrichment zones (white lines).

d) Almost always hot worked with resulting bands of high and low nickel content formed byforge-welding and/or piling.

The investigation of metallography and microprobe analysis of both the metal and the slag inclusions is absolutely essential in the differentiation of meteoritic from terrestrial iron. The careful examination of early nickel-rich iron artefacts in the Eastern Mediterranean has not always been possible. This is due to the fragile nature of the objects since they almost invariably date among the earliest iron artefacts made. As a result, archaeologists and museum curators are reluctant to commit them to full-scale investigation which has to be partly destructive.

In Greece there is evidence of smelting of laterites at least in the Hellenistic period. Whether the Mycenaean rings are indeed of meteoritic iron is a question pending future investigation. On the positive side, at least the criteria of distinguishing between the two types of metal are now quite clear.

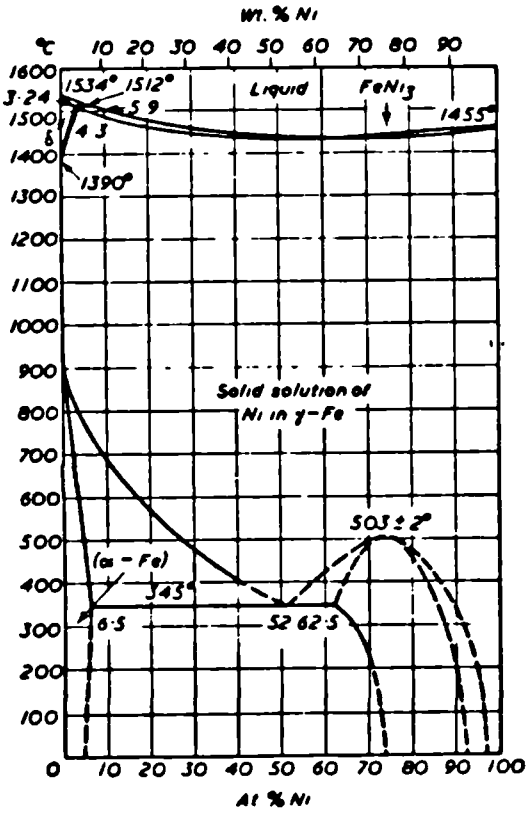

Fig. 3.8A Fe-Ni

Plate 21

(a) Petro 6 (400X) martensite

(b) Petro 6 (200X) pearlite in the previously austenite boundaries; ferrite at the grain boundaries.

(c) X-sm3a (200X) pearlite within the previously austenite boundaries; ferrite at the grain boundaries and globular.

(d) X-sm3 (200X) slag lathes of Ca-rich olivine; matrix: a eutectic of Ca-rich olivine and mellilite.

(e) X-sm5 (200X) bloom pearlite in the previously austenite boundaries; ferrite at the grain boundaries.

(f) X-sm10d (100X) slag with round (solidified from the molten state Ni-rich iron prills; tip of a large grain (bottom right corner) and angular shaped grains are chromite; lathes of Ca-rich olivine, dendrites (round globules) of wustite; pores (black); silicate matrix.

(h) X-smelt4e (200X) slag: angular grains of chromite (bottom left) and chromite exsolving out of a chromium rich spinel; broken up lathes of Ca-rich olivine (medium grey), silicate matrix (dark grey), very small metallic prills dispersed in the sample.

(g) X-smelt4c (200X) angular chromite grains, Ca-rich olivine lathes, very fine wustite dendrites, silicate matrix.

Plate 21

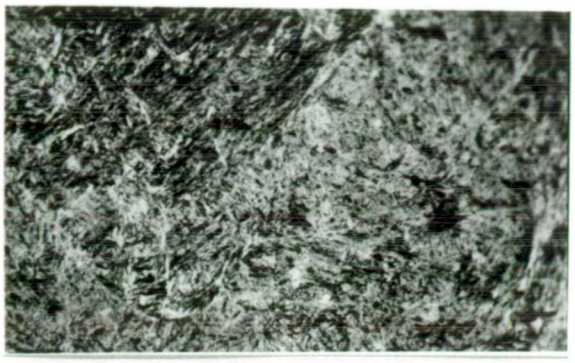

a

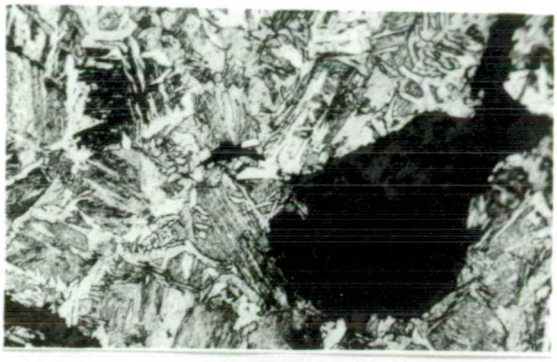

b

c

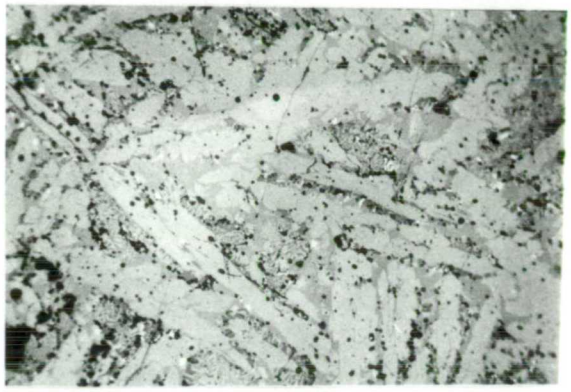

d

e

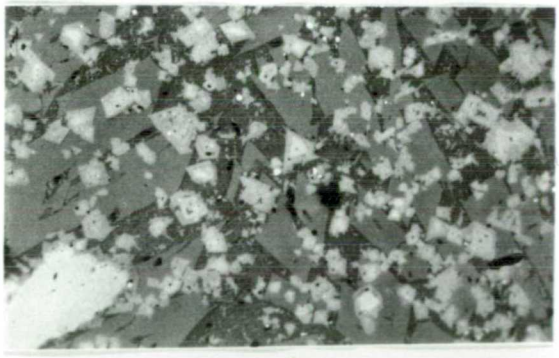

h

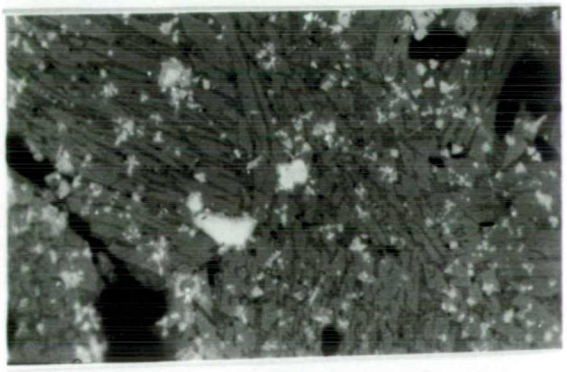

g

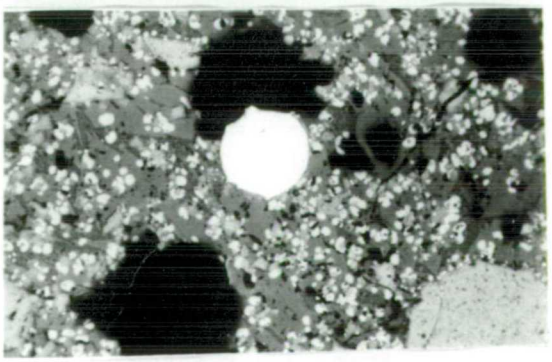

f

Plate 22

(a) X-smith4a (100X) Interface between ferritic bloom forge-welded to a piece of Mn-rich (pearlite and ferrite).Interface contains small slag inclusions.

(b) X-smith5a (200X) fraction of a bloom wrapped in an envelop of mild steel for easier handling. Bloom is ferritic.

(c) X-smith5a (200X9 interface between nickel-rich bloom (left, ferrite) and steel (right, ferrite and pearlite).

(d) X-sm5smithed (200X) ferrite with pearlite. A two phase slag inclusion (top right corner) is noted.

(e) X-sm5smithed (200X) slag associated with smithed bloom (d). Wustite (globular) in a mellilite matrix.

(f) Canyon Diablo meteorite (100X) Alternating areas of kamacite (low nickel matrix) and taenite (high nickel dark long needles) and triangular area in the middle of the section.

(g) Computer print out of the X-ray distribution map for nickel in area depicted in (f). High nickel areas (dark), low nickel areas (light).

(h) Neumann bands in Canyon Diablo meteorite (400X). Nickel composition in the bands is the same as in the mrest of the matrix.

Plate 22

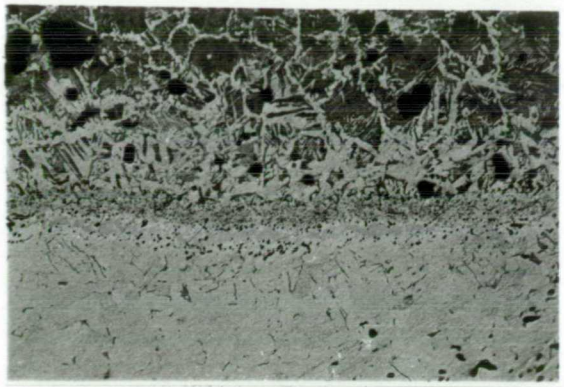

a

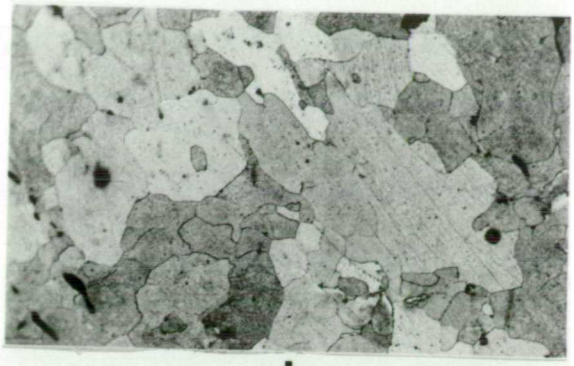

b

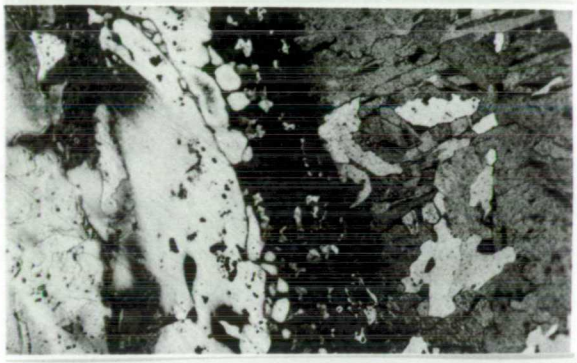

c

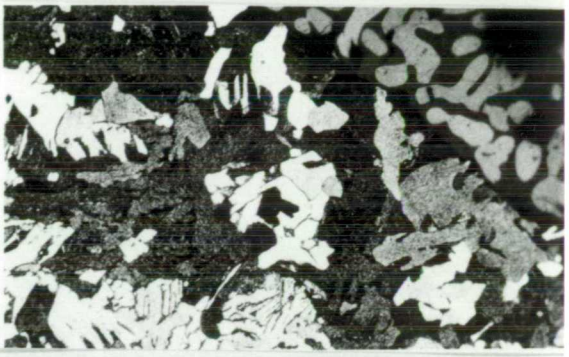

d

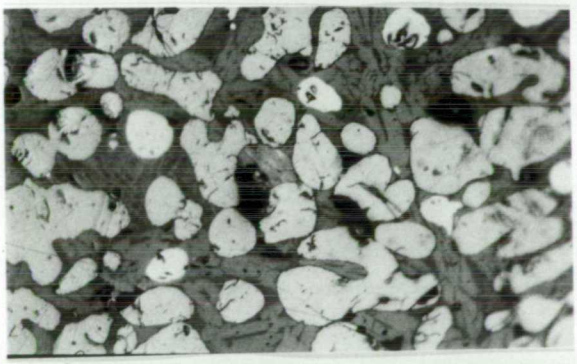

e

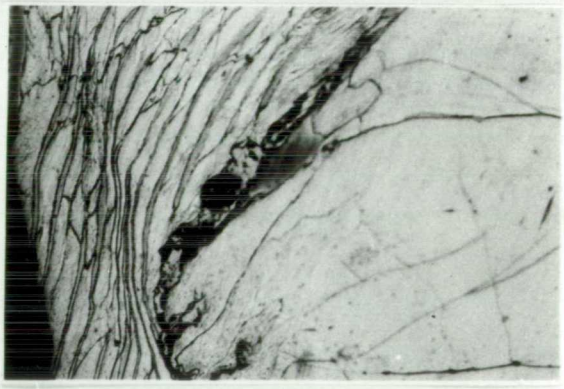

f

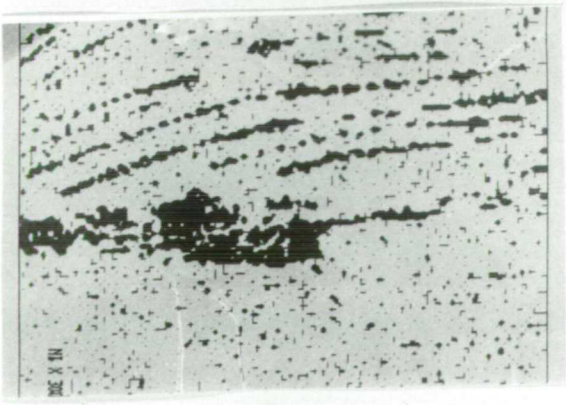

g

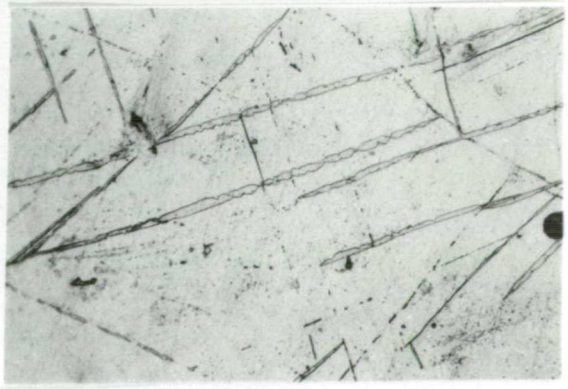

h

CHAPTER 4

METALLURGICAL FURNACES IN GREECE: ARCHAEOLOGICAL EVIDENCE, PICTORIAL REPRESENTATIONS AND DOCUMENTARY REFERENCES

It is a fact that every great center of population has worked out a set of elementary answers and has an unfortunate tendency to stick to them out of that force of inertia which is one of the great artisans of history.

F Braudel (1985)

4.1.a Introduction

Evidence of metallurgical furnace remains, whether smelting, melting or smithing, are not common in any period in Greece, while the remains of those extant have not always been thoroughly understood. The only available illustrations thereof are those depicted on Attic Black and Red Figure vases of the 6th and 5th centuries BC (Fig. 4.1.1). Although it has generally been accepted that most of the furnaces are associated with metal-making activities, there have been many attempts since the late 1800's to interpret their precise functions and the role of the ubiquitous cauldron on top of them, by drawing on information from the relevant but often controversial passages in the classical texts. However, although the interpretation of the function of the furnaces has been more or less straightforward, that of the

cauldron has remained a complete puzzle. One of the reasons is that since its foundations, the history of iron metallurgy in Greece has been based on the interpretations provided either by classicists or by metallurgists influenced by the suggestions of the former.

In this chapter a thorough reappraisal of the present position is given, and a novel approach to a previously suggested interpretation is offered. This approach has been based on two happy coincidences: a) the discovery in the literature of eye-witness accounts in the last century of Chinese wrought iron-conversion furnaces (finery hearths) with a cauldron on top, and b) the opportunity to carry out experimental simulations of the processes suggested here. Both are presented in support of the hypothesis that the furnaces on the vase illustrations are fining hearths for the production of wrought iron or steel. This suggestion implies that the ancient Greeks were intentionally producing cast iron (high carbon iron) which they proceeded to decarburize in a separate stage. However, presently, there exists no material evidence either in the form of artefacts or metallurgical waste for cast iron production in Greece.

4.1.b Archaeological Evidence

Understanding the nature and function of ancient furnaces and kilns in Greece (as elsewhere) presents many problems to the excavator. As a result there are a number of dubious, not to say wrong, identifications in the literature. For instance, the late Byzantine tile kilns of Steno near the modern town of Tripolis in

central Peloponnese (Photos et al, in preparation) were initially thought by the excavator, G Spyropoulos, to be Bronze Age furnaces for copper/lead smelting or melting operations (Kalogeropoulou 1981). Furthermore, a late Middle Bronze Age structure at the Minoan center at Kato Zakro in eastern Crete has also been interpreted as a metallurgical furnace (Platon 1981).

We can now mention those sites in Greece where metallurgical furnaces have been located. An Early Bronze Age furnace at Skouries on Kythnos in the Cyclades is currently being investigated by the Greek Department of Antiquities, Cyclades Division. A preliminary account of this important site is given by Gale et al (1985). Three smelting sites have been found in the Laurion, two by the coast (Thorikos and Puntazeza) and one in the hills (Megala Pefka) (Jones 1982; Jones 1984, 80). These sites, which probably date to the Classical period, consist of a row of small stone-built rooms open in the front and set against a long corridor. The back wall made of schist constitutes the back wall of the furnace proper and was vitrified by high temperature (Conofagos 1980, fig 11.9). In his pictorial reconstruction of one of these sites Conofagos (1980, 289) suggests that the back wall of the corridor was used as a loading platform for the charging of the furnace. The slag and metal ran into a hole in front of the furnace, as is apparent in the remains (Conofagos 1980, 275).

The only furnace (Plate 28c) to have been partly excavated in northern Greece is in the Pangaion range near the modern village of Nikisiani (Papastamataki 1986b, 61). The excavation report is not yet published, but the furnace is thought to belong to the Ottoman

period, as mentioned in section 3.7.

To summarize, although the present, cumulative evidence for metallurgical remains is minimal, the past few years have shown that there is a growing interest and demand for careful excavation of furnaces and metal-working areas, irrespective of period and that a considerable amount of relevant information is yet to come.

4.1.c Pictorial Representations

The present paucity of any substantial archaeological evidence for metallurgical furnaces in antiquity obliges the researcher to turn to the representations of metal-working activities which appeared on Attic Black and Red Figure vases of the late 6th and 5th centuries BC. These can be divided into two categories: those depicting furnaces and those with simple smithing scenes. It has been argued that the illustrations depicting furnaces are the result of the application of extensive artistic licence and thus lacking in technical detail. The clay plaques from Penteskoufi, near Corinth dating to the 6th c. BC, although votive and rather crude in design, nevertheless give very accurate illustrations of ceramic kilns (Furtwaengler 1886, pl. 8).

Accepting the approach that everything is subject to artistic licence leaves little room for a serious examination of the scenes from a metallurgical point of view. It is suggested here that the artists have depicted metallurgical scenes both accurately and to the best of their abilities, given the limitations of the medium. Our approach is corroborated by that of other researchers (D.

Williams, pers. comm.) who point out that the rarity of such craft-oriented scenes makes it almost certain that the painter had a first-hand experience of such operations either because of the proximity of his workshop to a metalsmith as in the Athenian Agora (Mattusch 1977a), or more appropriately because he was commissioned to paint exactly that scene.

The most up-to-date compilation of furnace scenes on both complete vases and sherds has been given by Oddy and Swaddling (1985). The authors provided a thorough survey of the extensive literature as well as interpretations surrounding these furnaces and their ubiquitous cauldron-with-lid arrangement. They interpreted the lid as a set of concentric rings fitting one within the other, and proposed that the cauldron was used as a water bath for the melting of wax for bronze casting. Only three of the scenes discussed by Oddy and Swaddling (1985) will be presented here. They are the least stylized and thus more representative of the operations themselves:

a. Oinochoe (Plate 23b) at the British Museum (GR 1846.6-29.45) of the first quarter of the 5th c. BC showing a smith with tongs and metallic mass on an anvil, an assistant with hammer in hand and a furnace with cauldron and lid.

b. Column crater (Plate 23c) from the Museum at Caltanisetta in Sicily (No 20371) also of the first quarter of the 5th c. BC. Furnace and lid of the same typology as the BM oinochoe. The smith holds an iron mass that he is hammering on an anvil. The satyr on the left is thought to raise a rather slim (deflated) pair of bellows (Oddy and Swaddling 1985, 47).

c. The Foundry Cup (Plate 23a) at the Staatliche Museum, Berlin (F 2294), dated to the first part of the 5th c. BC, depicts bronze working and wax shaping as well as a furnace in full operation. This is possibly the most famous metallurgical scene from Classical Greece relating to bronze-working activities and the subject of much discussion (Mattusch 1980).

The metallurgical illustrations on Attic vases depicting furnaces similar to those above have been compiled by Schwander et al (1983, 69) and are reproduced in Fig. 4.1.

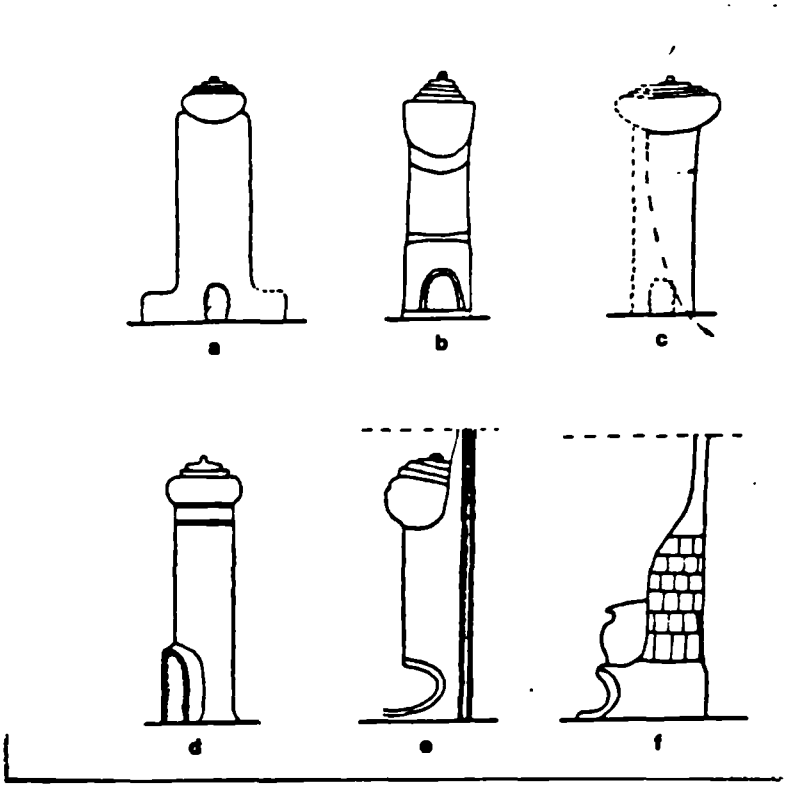

Fig. 4.1 Compilation of all furnace illustrations on 6th and 5th cents. BC vases (after Schwander et al 1983).
a, b and d appear on Plate 23

Previous investigators in their efforts to interpret the illustrations turned to relevant passages in the ancient texts. We shall be following the same approach, presenting first the documentary evidence in the classical texts, then the known literature on the interpretations of the texts and the vase illustrations, followed by our interpretations of both. Our conclusions are corroborated by an experimental melting of cast iron in the furnace used for our smelting experiments and by the presentation of ethnographic parallels drawn from China. The chapter concludes with a discussion of the furnace on the Foundry Cup and the arguments against this particular furnace being used for any bronze related activity.

4.1.d Documentary References

We present here five of the most well-known relevant passages relating to iron making and working. The aim of these texts was rarely to produce a detailed description of the process but rather to draw an analogy between iron smithing and events of everyday life, as for example Hippocrates' passage below. For the translations of the texts, the Loeb text series have been used.

a. Aristotle's Metereologica (IV, 6, 383) is full of technical details and is probably the most accurate account on steel-making we have today.

"Wrought (worked) iron indeed will melt and grow soft and then solidify again. And this is the way in which steel (stomomata) is made. For the dross sinks to the bottom and is removed from below,

and by repeated subjection to this treatment the metal is purified and steel is produced. They do not repeat the process often, however, because of the great wastage and loss of weight in the iron that is purified. But the better the quality of the iron the smaller the amount of impurity. Pyrimachus (fire resisting) stone will also melt and form drops; when it solidifies, after having been fluid, it regains its former hardness. Millstones too melt and become fluid: and when they solidify again afterwards they are black in colour but like lime in texture. (Mud and earth also melt)."

b. Hippocrates (Peri Dietis, Regiman I, XIII).

"Craftsmen melt the iron with fire, constraining the fire with breath; they take away the nourishment it has already; and when they have made it rare, they beat it and weld it and with the nourishment of other water it grows strong. Such is the treatment of the man by his trainer."

c. Plutarch's Moralia (Table Talk VIII, 9, 3)

"..which like iron, is made soft and fluid by heat then plunged into cold water to be tempered".

d. Plutarch's Moralia (De Primo Frigido, 19)

"Blacksmiths, when their iron becomes fiery and begins to melt, sprinkle on it marble chips and gypsum and cool it off before it melts too much."

e. In Plutarch's Moralia (De Defectu Oraculorum, V, 41 and 47) the first reference is about quenching and tempering of steel,

while the second attempts a scientific interpretation of the same process.

"When steel is dipped in cold water it is rendered tense and keen" and "he that goes into the details of the hardening and the softening of steel, how it is relaxed by the fire and becomes pliant and yielding for those who forge and fashion it then plunged anew into clear water, is contracted and compacted by the coldness because of the softness and looseness of texture previously engendered by the fire and acquires a tenseness and firmness which Homer called the "brawn of steel", does such an investigator any the less preserve intact the credit for the creation of the work?".

There is a plethora of other much shorter references involving quenching and tempering not to mention the occurrence of other synonyms for sideros and stomomata like, for example, adamas, all of which are included in the Liddell and Scott classical Greek dictionary.

4.1.e Previous investigators' interpretation of the texts and the vase illustrations

Kluge and Lehmann-Hartleben's (1927) interpretation of the bloom/metal in the BM oinochoe (Plate 23b) acting as a stopper closing the entrance to a channel, out of which the molten metal would run into an invisible casting pit, should be considered rather improbable since it does not take account of a large amount of circumstantial evidence.

In examining the scene on the BM oinochoe (Plate 23b),

Conofagos (1981a, 153) suggests that we are faced with the smithing of a bloom for the removal of residual slag. From ethnographic studies such operations are known to take place in a simple hearth without the necessary addition of a shaft. However, chimneys are known to exist in many smith workshops from medieval illustrations (Tylecote 1980, 44). Tylecote (1976, 45) is also of the opinion that the scene is depicting a smith forging a bloom in the vicinity of a shaft furnace, thus proposing that we have an iron-smelting furnace in a smithy. In a recent re-evaluation of the furnace, Prof. R.F. Tylecote (pers. comm.) thinks that there might be an opening (not visible) at the side, near the top of the furnace from which gases would escape once the rim was closed off by the cauldron. Oddy and Swaddling (1985, 47) believe that the subject of the BM oinochoe was smithing not of a bloom but rather of a metallic object. They also attempted to read the writing on the vase, but apart from the sentence "Mys is beatiful" little else makes any sense. 'Mys' means mouse and the word here may be used as a pun. There is a passage in Theophrastus about mice nibbling at iron (Bakhuizen 1976, 50). A bloom is a spongy mass, porous and not dissimilar to the texture of cheese. It is possible that the closest analogy Theophrastus could find to describe a bloom is that of mice nibbling at cheese.

One problem with all these interpretations is that they do not account for the function of the cauldron as an integral part of the furnace in iron making.

Livadefs (1956) was the first to analyze iron artefacts and attempt an interpretation of the texts and vase illustrations in

accordance with the results of his analytical investigations of the clamps and dowels of the Parthenon. The latter were heterogeneous in composition displaying bands of ferritic iron and steel ranging in composition from traces to 0.9% carbon. Slag stringers were found at the interface of the main body of each phase. Livadefs suggested that Aristotle's passage in Metereologica refers to co-fusion of smelted iron pieces. Co-fusion, he argues, takes place in a pot, the periodos, mentioned by the ancient lexicographer Polydeucis (VII, 99) as "the pot in which they mix iron". In the pot, Livadefs argues, the pieces of the bloom fuse without melting completely. Carbon-free iron, being the highest melting, sinks to the bottom of the pot and carbon-enriched iron (steel) forms the layer above. Slag, the lowest melting of the three, is the third layer. It was the middle layer, steel, that the ancient smith was seeking, Livadefs advocates, removing the slag carefully so as not to remove the layer below. Turning his attention to the BM oinochoe (Plate 23b), Livadefs comments that the smith has just removed a section of the bloom from the furnace hearth. He will subsequently hammer it to remove excess slag before placing it in the pot on the furnace mouth in order to co-fuse it in the method described above.

Livadefs' interpretation of the texts and the vase scenes is rather confusing. His use of the term co-fusion is loose since Biringuccio (in Pyrotechnia) used the term to imply the fusion of cast iron and wrought iron for the production of steel (Biringuccio, 68) rather than the fusion of wrought iron pieces. Such co-fusion at the top of the furnace and the resulting three-

layer formation of wrought iron, steel and slag is almost impossible in practice (Conofagos 1981a, 162). The temperatures in the top of the furnace would hardly exceed 700 C even if the shaft were completely stacked with fuel. Conofagos (1981c) himself argued that the lid on the cauldron served as a regulator of furnace conditions in the same way that a flue acts in a kiln.

In discussing co-fusion by the Chinese, practised as early as the 6th c. AD, Needham (1964, 27) correctly points out fallacies in Livadefs' translation of the Meteorologica. Although the classical text clearly notes that slag sinks to the bottom, Livadefs suggests the opposite (1956, 64). Putting aside these weaknesses in Livadefs' argument, we advocate that he is basically right in claiming that the furnace was used for steel-refining operations. In view of the lack of any material evidence one can only speculate. But textual, pictorial, experimental and ethnographic evidence strongly point in that direction.

4.2.a A proposed new interpretation

Before proceeding with the details of the furnace illustrations and Aristotle's text, it is important to give a few definitions relating to cast iron making and refining for the production of wrought iron.

The exact date of the introduction of the blast furnace to Europe, the furnace used for cast iron production, is a matter of ongoing research. Sweden claims the earliest blast furnace at Lapphyttan, with accompanying fining hearth (Magnusson 1986) and of

Vinarhyttan (Serning et al1982) dating to the 12th-14th c. AD and mid-14th c. AD respectively. This has prompted Tylecote (1985) to suggest that the introduction of cast iron technology from the East (China) to the West took place via Sweden by way of trade connections with peoples of present-day Russia.

In the bloomery furnace wrought iron (ferrite and low carbon steel) is produced in one step from the solid-state reduction of the iron ore (direct process). In the blast furnace iron rich in carbon is tapped out and cast into moulds (pigs). This product is the result of prolonged exposure of ore to fuel (initially charcoal but subsequently coke) in a high shaft furnace. The success of the blast furnace was primarily due to the high yields produced in one smelt compared to the bloomery which under the best conditions did not achieve more than 50% (excluding the Catalan hearth which gave c. 70% yields). To obtain wrought iron which was more in demand than cast iron, the latter had to be decarburised in a fining hearth and later, when coal substituted charcoal, in a puddling furnace. This means that the production of wrought iron from the ore was achieved indirectly.

Fining is the operation by which grey cast iron is decarburised by an oxidising blast in a fining hearth. The metal (pig iron) melts and falls, drop-like, into a slag bath (Fig 4.2). At the bottom of the hearth and away from the oxidising blast the metal becomes more pasty and can be lifted at the end of a rod. It is subsequently further exposed to an oxidising blast and further decarburised. Silicon in the metal is removed before it is

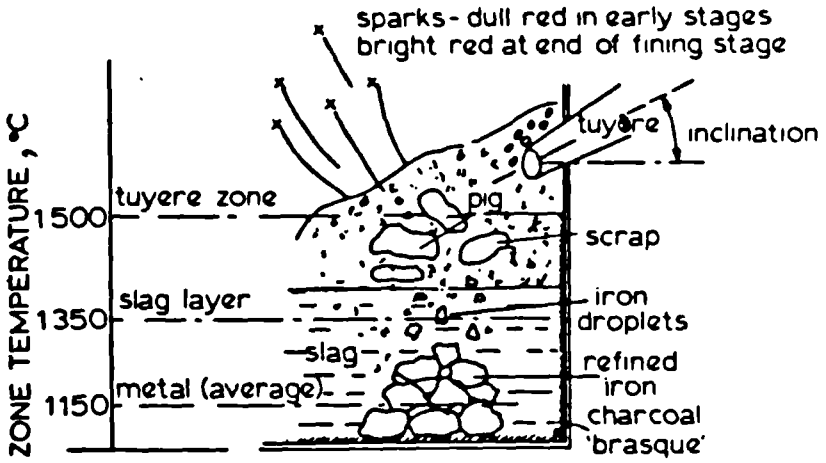

Fig. 4.2 Finery hearth (after Morton 1963)

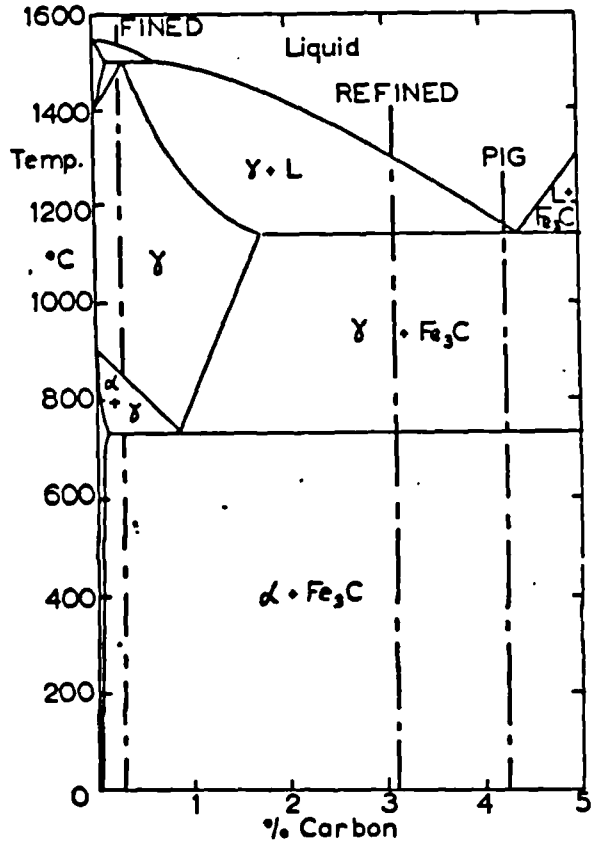

Fig. 4.3 Fe-Fe_3C phase diagram (after Morton and Wingrove 1970)

transfered to another hearth, the chaffery, of the Walloon process (den Ouden 1981), where it was forged into a bar. The Walloon process is the method of fining cast iron in the Low Countries and France. The fining is essentially divided into two steps, the removal of silicon stage (often called refining) in which the grey cast iron is converted to white cast iron and the second step, the fining proper, in which the cast iron is converted to malleable iron (Morton 1963). The effect of temperature variation with carbon composition of the cast iron and subsequently the pasty mass is plotted in the $Fe-Fe_3C$ diagram (Fig 4.3) (Morton and Wingrove 1970). The expertise of the finer lay in his correct estimation of when the iron mass was adequately fined because any subsequent rabbling would result in loss by oxidation. In puddling, fuel and metal had to be separated in a specially designed furnace (reverbatory), since the fuel was sulfur-rich coal. If sulfur entered into the iron, it would make it hot short (Schubert 1957).

One variation of fining which is of particular relevance to the present discussion, was recorded by E. Rocher, a French official stationed in the province of Yunnan in China at the end of last century (Rocher 1879, 203). Rocher provided a scale plan of both blast furnace and fining hearth and a detailed account of the process, as he himself witnessed it. The important feature of this Chinese furnace (Plate 23e) is the cauldron filled with water which rests on the top of the furnace. In brief, Rocher notes that cast iron was molten in the furnace. Once molten, a cold blast was applied from the bellows to decarburise it. For that purpose, it was essential that the furnace top was tightly closed. Rocher clearly points out that a tight fit was necessary, implying that

the positioning of a mere stone cover would not suffice. The cauldron was filled with water, but no lid was mentioned.

As Wagner states (1985, 95), traditional iron-working techniques varied greatly from region to region in China. Thus, a converting hearth in Henan province is very different from those described by Rocher in Yunnan. It is therefore of no surprise that this particular type of furnace was not known more widely.

We believe there is a direct analogy between Aristotle's passages in the Metereologica, the illustration of the furnace and cauldron on the BM oinochoe and the fining operation described by Rocher. In Metereologica Aristotle mentions that "worked iron will melt and grow soft and then solidify again". All three stages do indeed occur in the fining process. Iron has been previously worked but is not wrought iron in terms of its carbon content. The fact that iron melts does suggest that the carbon content must have been in excess of 2%. It cannot be certain whether by 'melt and grow soft' a liquid or semi-fused iron mass is implied, but we can confidently say that none of the two states would be achieved in the bloomery. The second line in Aristotle's passage involves, as he put it, "the way in which stomomata (steel) is made". Once the metal is molten, the top of the furnace is closed off with a cauldron filled with water and topped with a lid. The air blast is directed over the molten metal and out of the front arch since the top is sealed off. It slowly decarburises the iron mass, thus rendering it more viscous. The melting point of the metal rises inversely proportional to the carbon content, (Fig. 4.3), the

higher the carbon the lower the melting point of the iron-carbon alloy.

If the slag sank to the bottom, as Aristotle points out, then the metal must have been kept apart possibly at the end of a rod, by which it was manipulated. A similar rod is present in the Foundry Cup illustration held by the head smith (Plate 23a). The viscous mass needed to be exposed to the oxidizing blast if the decarburisation was to proceed. However, prolonged exposure would result in further oxidation and "in great wastage and loss of weight of the iron that is purified".

The "melting" of the refractory (pyrimachus) stone ensures that the temperature at the lower section in the furnace was in excess of 1250 C. Millstones probably refer to the furnace building material since a similar type was found at Laurion in the smelting furnaces at the Bay of Panormos (Conofagos 1980, fig.11.9).

As already mentioned, the cauldron served as a means of achieving a close fit. It must have been filled with water, as in Rocher's illustration. The multi-tiered lid must have acted as a distillation column, water vapour condensing on the upper tiers. This ensured a prolonged life for the cauldron and avoided the necessity of refilling it during furnace operation.

Recently, a vessel from Pompeii of Roman date (Chiurazzi and De Angelis 1910, 332) was brought to our attention (D. Williams, pers. comm.) which resembles the cauldron on the vase illustrations. The lid is clearly hammered rather than cast with a hoop, on the top, for the attachment of a chain (Plate 23d). It is

evident that such pots with lids were indeed being made possibly as kitchen ware. Their lids did not have a series of concentric circles inserted one within the other, as suggested by Oddy and Swaddling (1985), but neither is the depth of the concentric rings more than a few mm each.

4.2.b Experimental melting of iron in a shaft furnace

We attempted to simulate the above process in order to establish a) whether iron can indeed melt in such an arrangement and b) the function of the cauldron as an integral part of the decarburisation stage.

A cast iron grate (Plate 24a) was broken into small pieces which were stacked on a refractory brick base, reaching a height of 15cm below tuyere level (Fig. 4.4a). Wood and a small amount of preheating charcoal were lit around and above the refratory brick. A chimney was positioned on top to enhance natural draught. No bellows were used at this stage.

When the furnace was preheated the bellows were positioned in front of the front arch (Fig. 4.4a). Most of the arch was closed off, leaving just enough space for the tuyere (a long metal tube) to be inserted. The charcoal was charged up to the furnace rim twice, and pumping was kept at a steady pace of 32 strokes per minute (bellows volume: 60 litres). One and a half hours after the estimated beginning of the melting stage, the air supply was stopped. It was difficult to establish to what degree the cast iron pieces had melted.

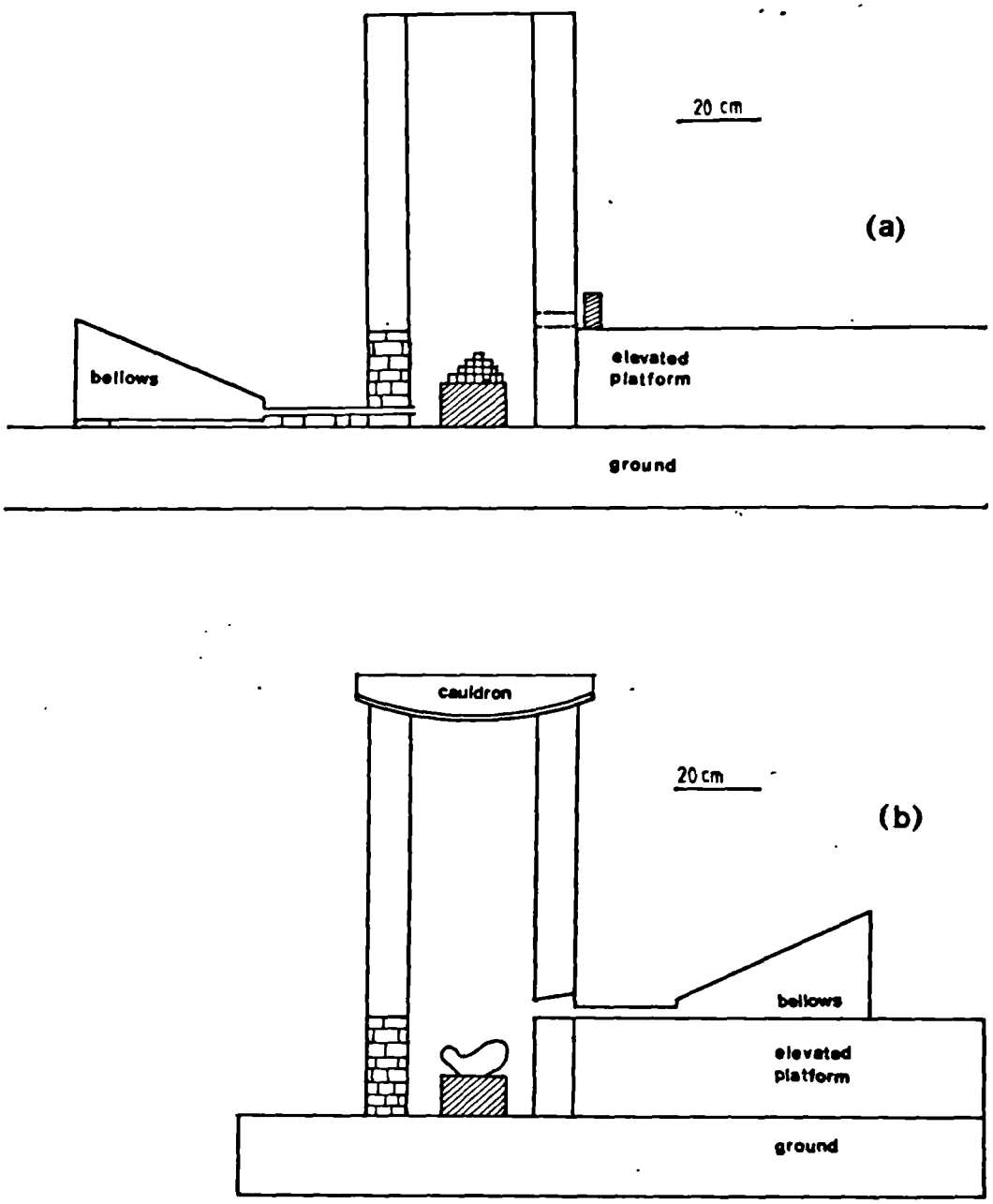

Fig. 4.4 Furnace and bellows arrangement during iron melting experiment to simulate those operations thought by the writer to be depicted on the vases

The bellows were moved back to their usual position (Fig. 4.4b) and a 'cauldron', or more precisely a rubbish bin lid, was fitted on the top of the shaft after it was checked for leaks. It was filled with water but did not have a cover. Plate 24d shows the 'cauldron' full of water being removed at the end of the operation. Harder blowing ensued (36 blows per minute) in an effort to decarburise the 'molten' iron. The temperature rose to 1165°C (thermocouple at 22cm above and to the right of the tuyere level) and then approximately 10 minutes later subsided to 950°C.

Sealing the furnace from the top forced furnace gases to escape from the front arch in a rather spectacular display of flames and gases. It took c. 15 mins. for the water in the cauldron to start boiling (Plate 24d). Approximately thirty mins. later the fused iron mass was removed with tongs from the front arch (Plate 24c), with minimal amount of slag (Plate 24b).

The experimental melting procedure is summarised in Table 4.1. The analyses of the products are shown in Table 4.2 . The cast iron grate (Xmelt2-raw material) is a high silicon, manganese, phoshorus cast iron, the metallographic section of which is shown in Plate 25c. The product, Xmelt2-product, the result of melting and decarburising, clearly suggests that the removal of silicon and manganese had indeed started, while the carbon content, as graphite, had decreased and substituted the depleted silicon by forming cementite (Plates 25d,f,e). This can be clearly seen in the form of mottled cast iron in Plate 25f. Analyses of the product (Xsmelt2-product) and the slag (Plate 25b) are given in Table 4.2.

The slag matrix contains magnetite crystals, kirschsteinite lathes and an aluminum-potassium-rich matrix of mellilite composition. Phosphorus from the metal has passed on to the slag. The amount of slag produced was rather small and was the result of reaction between the oxidised metal and fuel ash.

Table 4.1: Outline of iron melting in shaft furnace: summary of proceedings

11.30am	Position refractory brick with cast iron grate on top
11.45	Preheating with wood
11.45	Preheating with coarse charcoal (17 kg)
2.00	Finished stacking with charcoal
2.45	Added more charcoal
3.15	Added 1kg of iron and 1 kg of charcoal
3.20	Moved bellows to the back, put cauldron in place
3.50	Stopped pumping

The preliminary experimental melting results suggest that it is possible to melt cast iron in a furnace similar to those on the vase illustrations. The 'fined' cast iron analysed showed early stages of decarburisation, while the cauldron had a specific role to play in the decarburisation stage. Controlling the decarburisation and stopping it at the steel stage (c. 0.5% carbon), rather than continuing it to wrought iron, is a very tricky operation and requires considerable expertise.

Did Aristotle mean steel when he talked about stomomata or did he merely imply wrought iron produced via this decarburisation method? There is a need for further examination of more artefacts and metallurgical waste of that period but more importantly there

Analysis of products of experimental melt of cast iron

Sample		Fe	Si	Mn	P	Cr	Cu
Xmelt 2	raw mat.	90.79	3.86	0.34	0.42	0.00	0.00
		93.79	3.10	0.32	0.36	0.11	0.46
		92.62	3.13	0.42	0.37	0.00	0.36
		92.25	3.49	0.38	0.33	0.18	0.00
		93.11	3.63	0.42	0.44	0.00	0.39
		92.96	3.69	0.24	0.36	0.00	0.00
Xmelt 2	product	92.75	2.47	0.46	0.00	0.00	0.00
		92.40	0.57	0.00	0.61	0.28	0.00
		93.92	1.69	0.00	0.24	0.00	0.00
		94.08	1.08	0.00	0.55	0.00	0.00
		93.79	1.92	0.24	0.24	0.45	0.00

		Na_2O	MgO	Al_2O_3	SiO_2	P_2O_5	SO_3	K_2O	CaO	TiO_2	Cr_2O_3	MnO	FeO
Xmelt 2	slag	0.00	1.19	2.59	0.29	0.00	0.00	0.00	0.64	0.36	0.00	0.36	86.94
		0.00	0.00	19.54	34.12	2.04	1.26	22.24	7.16	0.00	0.00	0.00	11.19
		0.00	1.06	6.75	33.99	0.00	0.00	7.42	26.95	0.43	0.00	0.38	22.98

Table 4.2: Microprobe analysis of products of experimental melting of cast iron

is a need for further research into the identification of wrought iron produced from the direct and indirect processes.

What evidence is there for cast iron making in antiquity in the absence of any material finds? Pleiner (1969, 26) points out that Pausanias in his travels makes reference to iron statues which in all probability should have been cast. That aside, it seems that Plutarch's passage in Moralia (19), is the only clear documentary evidence presently available about cast iron making. Plutarch mentions that blacksmiths, after iron began to melt, 'sprinkled it with marble chips and gypsum to cool it off before it melts too much'. Addition of lime (a base) would remove silica (an acid) and other impurities from the iron at the same time ensuring that most of the iron stays in the metal rather than being lost in the slag. The addition of lime as flux is an integral step in blast furnace iron-making, and for that reason it is very unlikely that Plutarch would have been mistaken in his observation. In appendix 4.1 a description of a traditional iron foundry employing a cupola furnace in Kavala, EM is given. In addition to cast iron and scrap limestone is also added.

As an etymological footnote to this discussion, the word stomomata is most probably derived from the word stoma, meaning mouth or opening. It is possible to assume that stomomata could be considered as meaning "the products of the mouth of the furnace". In modern Greek and in reference to a cutting edge, the verb 'stomono' means developing a dull edge.

4.2.c Were the Greeks making cast iron?

It is unfortunately not posssible to know whether the Greeks of the 5th c. BC were indeed making cast iron. One of the major difficulties is the distinction between wrought iron produced from the bloomery (directly) and indirectly through the decarburisation of cast iron. Moreover, it is very difficult to distinguish slag from a finery and slag from a bloomery (Morton and Wingrove 1970). A sample of material thought to be iron from a finery at Saugus, Mass., USA kindly provided to us by Thelma Lowe displayed ferrite with long slag inclusions (Plate 25a), just as if it was wrought iron produced from the bloomery. Table 4.3 below presents the microprobe composition of the metallic phase of this sample. Gordon (1983) gives the metallographic analysis of an iron bar from Connecticut, and there again,it is not possible to tell whether this piece was produced in the bloomery or indirectly.

Table 4.3: Composition of iron from Saugus, USA

%age			
Fe	Si	P	Cu
96.96	0.89	0.16	0.00
95.79	0.87	0.21	0.00
92.38	0.99	0.49	0.36

In an attempt to distinguish bloomery iron from the two processes, the same author (Gordon 1983) suggested shape, size and distribution of slag inclusions as a means of distinction. Large inclusions are characteristic of iron produced from a bloomery, while small inclusions or no inclusions at all are indicative of cast iron, he argued. Wagner (1985, 73) suggested similar methodology for Chinese artefacts . However, the extent of slag

inclusion removal is related to the degree of carburisation of the metal as well as the smith's expertise in forging and so does not constitute an adequate criterion for differentiating bloomery iron produced from the two processes.

In producing cast iron, the ancient Greeks, unlike the Chinese, did not intend to use it for castings. Nor does it seem likely that they made it as an accidental byproduct, as was the case in the West, where cast iron bars have been found at Roman sites (Tylecote 1976, 57). On the contrary, it seems that Greek smiths would be producing wrought iron through the indirect process only for specific purposes, namely for weapons and armoury. Bloomery iron would have been quite adequate for utilitarian objects of everyday use, hence the contemporary clamps and dowels analysed by Livadefs (1956) and Conofagos (1981b). Perhaps, it should not surprise us that the cauldron-bearing furnaces appear in armourer's workshops. Decarburisation may have helped the blacksmiths of Classical Greece to achieve a better quality control of the iron billet in contrast to the more erratic results produced from the slow carburisation of an inhomogeneous iron bloom. It is also possible that classical Greeks were producing wrought iron indirectly as a result of using specific iron ores like iron sands. In view of their small particle size, iron sands would reduce readily and carburise extensively (see discussion in section 3.6). An ancient reference is brought to mind here by the 1st c. AD writer Eustathius (453, 25) about the four most famous steels in antiquity. These were the Chalybian, the Sinopic, the Lydian and the Laconian. The first two, on the Black Sea, and the

third in the western coast of Asia Minor are regions well known for their black iron sands.

Our experimental simulations were not aimed at proving that cast iron was indeed being produced in Classical Greece. Only material evidence can provide the necessary proof in the form of cast iron objects. Our purpose was to show that it is possible to melt cast iron in a furnace similar to those on the vase illustrations and subsequently decarburize it with the cauldron playing an integral role.

At this stage of the investigation, the writer is inclined to believe that the term 'stomomata' meant to Aristotle wrought iron/mild steel produced via the decarburisation of cast iron in a shaft furnace like those depicted in the vase illustration. The preliminary experimental melts suggested cast iron can indeed decarburise and produce wrought iron in a shaft furnace used for smelting.

4.3 Why the Foundry Cup depicts more than bronze casting

Before concluding this investigation, it is desirable to discuss the furnace on the Foundry Cup (Plate 23a) assumed by previous investigators to be related to bronze melting (Mattusch 1980). The furnace on the Foundry Cup is in full operation, since a boy is seen working at the bellows. We believe this is another example of a scene depicting iron fining activities for the following reasons:

a) no shaft is necessary in a bronze melting furnace.

Traditionally in Greece, bronze foundry furnaces are small (1m high) with just enough volume for the crucible and the fuel to fit in. They are usually closed off at the top with a lid resting just above the rim of the crucible (V. Pandelidis, pers. comm.). The purpose is to reflect the heat back into the crucible and thus keep the metal molten. With a shaft of that size the crucible would need to be removed from the arch, a rather difficult task which would imply pulling rather than lifting.

b) no arch is necessary at the side of the furnace; on the contrary, the furnace in which the crucible is placed should be well insulated and enclosed from all sides, thus raising the temperature by minimising heat losses.

c) Prof Tylecote (pers. comm.) has suggested that there may be a pit, not shown here, into which the molten metal would flow. Mattusch (1977a and b) found several casting pits for large statuary in the Agoras of Athens and Corinth, but none seemed to be in the vicinity of furnace remains. It is more probable that melting would have to be done in a crucible and poured in from there into a mould. Recently, Schneider (1986) has shown that at the workshop of Pheidias at Olympia bronze metal for large statuary was melted in large crucibles with the use of elbow tuyeres. This suggests that the furnace was more like a cupola furnace in which large quantities of bronze would be molten. In that case, firstly the front arch would only be wide open at the time of tapping of the molten metal and slag, and secondly there would be no need for the cauldron to close off the mouth of the furnace.

d) The role of the assistant, hammer in hand, ready to be

summoned by the head smith is rather dubious in a bronze foundry. Surely, he should be holding crucible tongs.

We believe the furnace, being similar to those in the other vase illustrations, is used in iron fining. The proximity of iron and bronze working in the same workshop are well established. Mattusch (1977a, 358) found iron slag in a smith together with clay impresssions of a cheek guard of a helmet. She concluded that this was an armourer's workshop where both metals could be worked. It is also interesting to note how the vase painter has separated the people involved in each activity spatially, those occupied with bronze working having their backs turned to the three figures involved in iron making and gathered around the furnace, that is the smith, the bellows boy and his assistant.

Plate 23

(a) Foundry Cup, Berlin Museum

(b) Oinochoe, British Museum

(c) Column Crater, Caltanisetta Museum, Sicily

(d) Vessel from Pompeii similar to that depicted on the top of the furnace in the vase illustrations (a), (b), (c). (Chiurazzi and De Angelis, 1910, no. 74766, p. 332). Maximum diameter approximately 37cm. A similar vessel exists at the British Museum. The ridges on the lid are shallow (depth: 1cm).

(e) Rocher's (1879) illustration of the fining hearth in the Yunan province as witnessed by the author himself. Note the cauldron (3) and the note ('casserole remplie d'eau, elle bouche le haut du fourneau quand le metal est fondue').

Plate 23

a

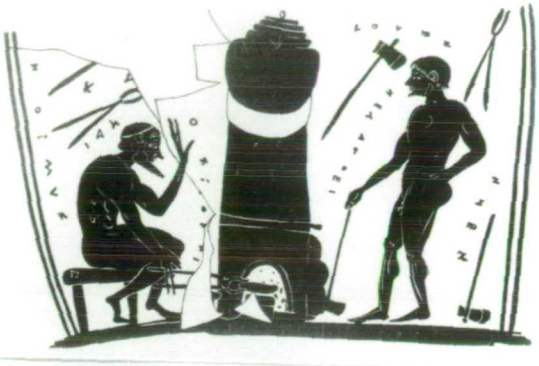

b

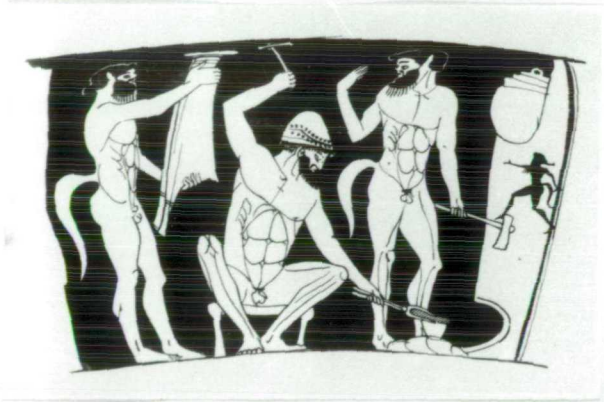

c

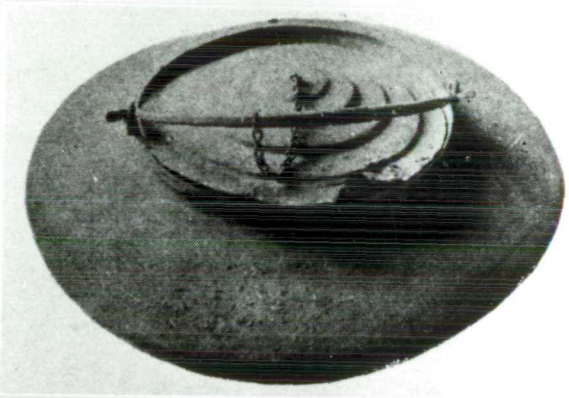

d

Fourneau employé pour le traitement de la fonte en fer ductile.

FIG. B.

1. Intérieur du fourneau.
2. Couche de sable réfractaire.
3. Couvercle rempli d'eau, elle touche le haut du fourneau quand le métal est fondu.
4. Massif du fourneau, il est lié au briquet autour du cône.
5. Tuyère.
6. Soufflet ou à bras.
7. Couche de brasque.
8. Ouverture par où on retire le métal.
9. Petite partie qui paroit de métal tuyère est obturée et de même la cuvette de l'opération.

Echelle

e

Plate 24

(a) Cast iron grate (together with other cast iron scrap) broken with a hammer to be melted into the furnace in the arrangement shown in Fig. 4.4.

(b) Slag resulting from the melting of cast iron scrap

(c) Mass of molten/fused cast iron retrieved from the furnace at the end of the melting cycle shown in Fig. 4.4.

(d) 'Cauldron' filled with boiling hot water removed cautiously from the furnace top at the end of operation. The cauldron sealed the furnace top very adequately with no detected leakage of gases. The cauldron was the most efficient and quick way of opening and closing the furnace top during the melting and decarburisation cycle.

Plate 24

a

b

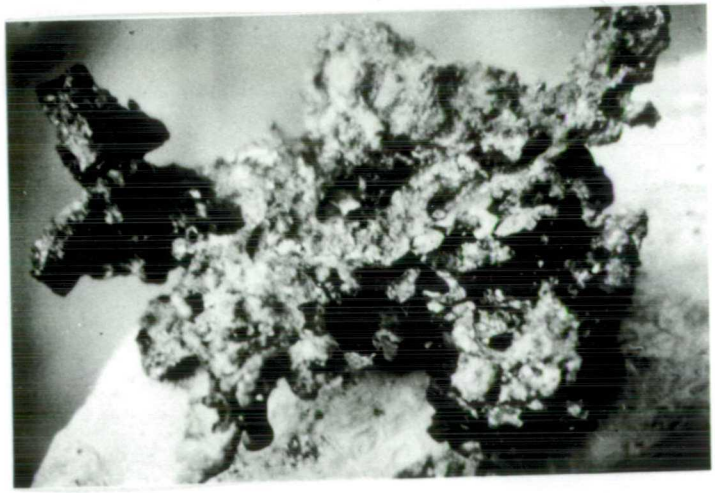

c

d

Plate 25

(a) Saugus, Mass. (USA). Bar iron and slag inclusion. Unetched; ferritic structure upon etching. 100x

(b) Experimental iron melting slag; magnetite (white plates), wustite (dendrities, globular), fayalite (lathes, light grey), silicate matrix (dark grey). 200x

(c) Raw metal (cast iron grate), graphite flakes (black); unetched. 100x

(d) Experimental product: fused/molten iron mass; graphite flakes, unetched. 400x

(e) Experimental product: fused/molten iron mass; graphite flakes, unetched. 100x

(f) Experimental product: fused/molten iron mass; graphite flakes, pearlite and inter-granular cementite. 100x

Plate 25

a

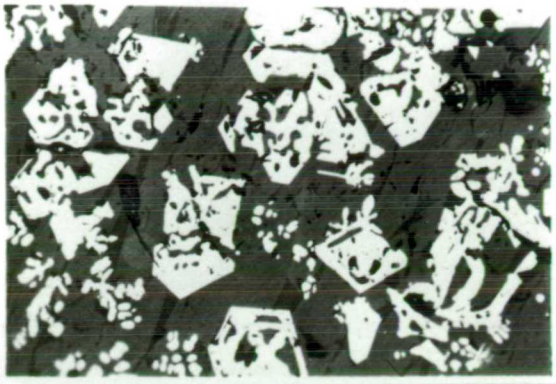

b

c

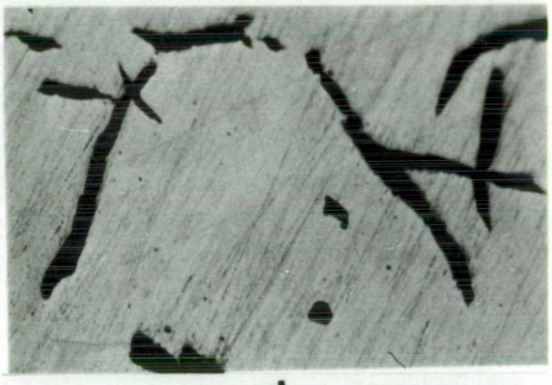

d

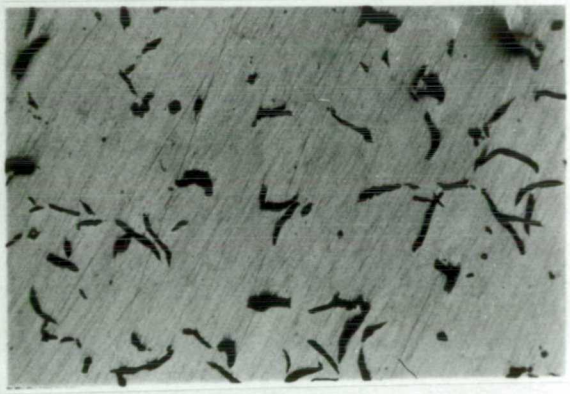

e

f

Plate 26

(a) Slag from iron foundry in Kavala. Cast iron prill (white) and black round holes, previously containing metallic prills which came off during sectioning and/or polishing. 400x

(b) Raw material. Grey cast iron with graphite flakes (black) in a matrix consisting of pearlite (greyish) and ferrite (white boundaries), etched. 400x

(c) Grey cast iron tapped at an intermediary stage in the process, etched. 100x

(d) Final product: grey cast iron with long graphite flakes, pearlite and ferrite. 100x

(e) Athenian Agora, AA 1508. Ca-rich fayalite lathes: dendrites of wustite. 200x

(f) LA (Lesvos). Ulvospinel plates : dendrites of wustite and metallic iron prill. 400x

(g) LA (Lesvos). Ulvospinel plates exsolving out of wustite (see Plate 14) in a background of Ca-rich olivine and silicate matrix. 400x

Plate 26

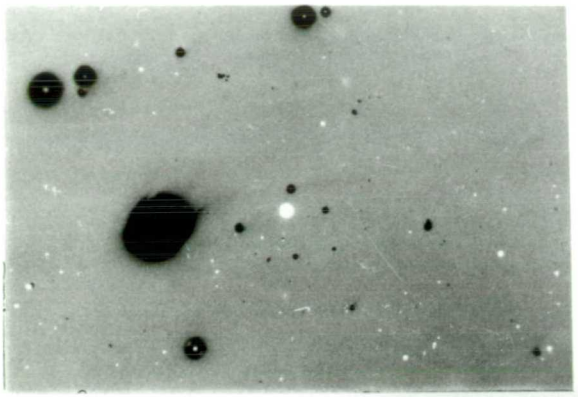

c

d

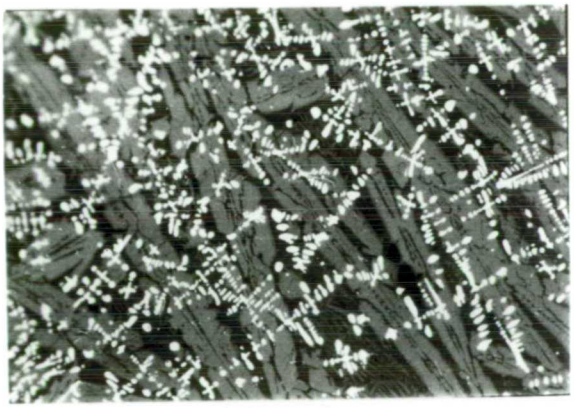

e

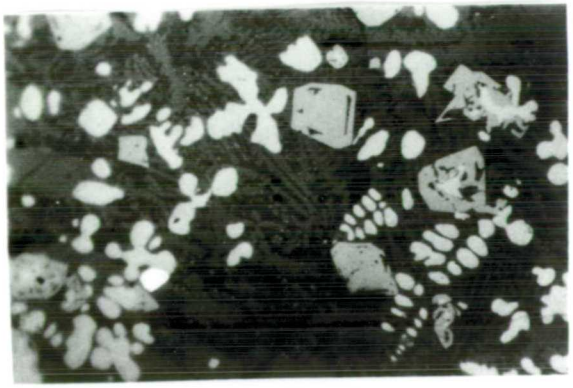

f

g

CHAPTER 5

CONCLUSIONS

Until recently, very little was known about early extractive iron metallurgy anywhere in Greece. Terms like bloomery iron, wrought iron produced by the direct versus the indirect method, fining and puddling were not familiar to most Greek archaeologists. Archaeometallurgical studies have generally concentrated first on non-ferrous metals and second on a handful of metallographic and analytical examinations of iron artefacts.

While in Western and Central Europe numerous bloomery furnaces have been excavated and an extensive typology has been worked out on the basis of regional variations in the material evidence, the present author knows of no identified or excavated iron-making furnace in Greece. In short, so limited was the existing information about iron making anywhere in the land at any period of its history that the subject needed urgently to be put on the map.

To this end, Macedonia, Greece's richest province in mineral resources, was chosen, and analyses were carried out on a considerable number of archaeological slags and artefacts as well as iron ores. In an attempt to elucidate the processes that gave rise to the archaeometallurgical finds, a set of experimental smeltings using the same types of ores were undertaken.

In the absence of any furnace remains, the archaeological slags

in Macedonia pointed to a continuous use of the bloomery process from the early periods of antiquity (EIA) on Thasos to the turn of the present century in Katafyto, EM. It is expected that the bloomery must have evolved during that period and indeed leat systems evident at Katafyto suggested the use of water-driven bellows. However, the development of the bloomery and the extent to which it was the product of local innovations and/or external influences will have to remain unknown for the present. The evidence for blast furnace slag at Avli, in the foothills of the Pangaion, suggests that bloomeries overlapped or even were superceded by blast furnaces at some periods. Thus, the evidence can, at best, be patchy given the lack of excavation of a metallurgical site or furnace. Industrial archaeology in Greece is still at its infant stages, while the documentary evidence for technological developments in N. Greece in recent centuries needs also to be researched in more depth.

It was the survey and analysis of slag from a considerable number of locations in EM Mainland and Thasos which pointed to a long tradition of smelting of iron sands, dating from the late Byzantine period and continuing to the beginning of the present century. In addition, artefact analyses suggested that iron sands may have been smelted earlier in antiquity, during the Hellenistic/Roman period, on Thasos or the Mainland. Given the major iron ore deposits on Thasos - there is evidence for galleries at Koupanada (probably of Byzantine date) - it seems at first hand curious that this additional source would be worked. It is however, very likely, that the local smelters would resort to iron sands at

times of hardship (war or occupation). This observation is corroborated by the location of these metallurgical sites, in inland rather inaccessible places, the inhabitants being driven there by fear of piracy (early Ottoman period).

Smelting of iron sands on Thasos and in EM Mainland may be seen as the continuation of a long tradition, extending to the northern Aegean (Lesvos) and the southern shores of the Black Sea where the mythological Chalybians are supposed to have smelted iron for the first time. There is documentary evidence for iron sand smelting in the Hellespont in the 10th c. AD and the Black Sea shores in the 14th c. AD. Thus, for the first time, material evidence corroborates the multitude of literary and documentary sources for an apparently widespread practice in the extended region of the northern Aegean and western and northern Asia Minor.

The relatively simple extraction of iron sands (see watercolour in frontispiece), and its dressing either by winnowing or washing, made them a particularly attractive source to smelters in many other parts of the world (Japan, Africa, India, North America). The main problem of containing the fine-particled sands in the furnace, vividly expressed in a letter by a colonial American to the Royal Society (Horne 1763), was eventually worked out in various ways. Buchanan (1910) gives an illustration of a funnel-shaped furnace in India, while the Chinese solved the problem by charging huge quantities at a time. Iron sands were smelted to produce cast iron in China, cast iron or bloomery in India and cast iron, steel and wrought iron in Japan.

Our attempts to smelt iron sands in a blomery shaft furnace proved rather unsuccesful in the sense that they did not simulate the archaeological material. The small quantity of ore charged proved difficult to contain and prevent from filtering down to the furnace floor. Reduction resulted in the production of small lumps of cast iron, as opposed to the wrought iron clearly produced at the Thasos and EM Mainland sites. Thus, in view of the importance of this source of iron ore, further research needs to be carried out on the experimental smelting of iron sands, preferably on a pilot plant scale, with control of the temperature and furnace conditions. Appropriate ore beneficiation would be essential before smelting with fine charcoal in an experimental furnace.

Another first indication for the smelting of a particular ore type in Greece is that of nickel-rich iron laterites. Although most researchers would agree that early nickel-rich iron in the East Mediterranean could not all have been meteoritic in origin, material evidence to that effect was lacking. It was the 'bloom' from the site of Petres and nickel-rich iron prills in the Petres slag which suggested for the first time that such ores were indeed smelted in Greece. The problem, however, is that none of the iron objects analysed contained nickel. There are two possible explanations: either slag and metal may not be contemporary or the production of the Petres 'bloom' may have been the result of an accidental smelt of the nickel-rich laterites. In view of the elusive nature of the nickel in the slag, one should be cautious before drawing conclusions at this early stage of the investigation.

Experimental smelts of Larymna nickel-rich iron laterites presently smelted for the production of a ferro-nickel alloy, gave rather low yields because of the low iron and high alumina contents. As a result, it was essential that these ores were mixed with a high grade hematite despite the fact that such a mixture resulted in a heterogeneous distribution of nickel in the bloom. The high nickel sections of the bloom were not forgeable. The bloom fractured and a large section of it was lost in the hearth. Thus, high nickel areas arise not only as a result of forge-welding of high- and low-nickel iron but possibly more often from local inhomogeneities within the bloom. The latter seems to be the origin of the martensitic streaks in iron artefacts away from welding seams.

The experimental bloom was smithed and forge-welded to a piece of Mn steel. The result was an enrichment zone at the interface between the two metals as well as between the slag inclusions and the metal. Thus when the nickel content in the iron is too low to allow any conclusions to be made about a nickel-rich iron source, the interface between slag inclusion and the metal should be analysed. The diffusion of nickel in iron in the bloom should be examined more closely in a laboratory reduction of iron oxide and nickel oxide. This work has presented only some preliminary results. Nickel diffusion in iron as a result of forge-welding of bars of nickel-iron alloys with various nickel contents has been undertaken by previous investigators, but it would be interesting to compare bloom and forge-welded bars produced experimentally.

The development of iron metallurgy has long been seen as emerging out of the practice of copper metallurgy. However, this assumption was primarily based on common sense and the analysis of copper artefacts in which iron was included. On Thasos there is evidence for the first time of copper ore extraction from a primary iron ore deposit, barium having been used as the tracer element. The indication is that, in the early stages, far from being an intentional addition as flux, iron ores were loaded in the furnace as charge together with the copper ores. During the course of the Bronze Age, the presence of iron ore in the furnace would have resulted in random metallic iron prill formation. The methodology for working the metallic iron would have developed slowly, but by the Early Iron Age it had already been mastered. This hypothesis carries the significant consequence that the origins of iron metallurgy should be sought during the Bronze Age. By the same argument, the origins and experimentation with copper metallurgy should be sought in the Late Neolithic because by the Early Bronze Age the concept of alloying seems to have been at least partially and empirically understood. If iron metallurgy indeed developed out of copper metallurgy, every copper smelting area had in principle the potential of experimenting with iron production. The independent development of iron metallurgy on Thasos and possibly the rest of Macedonia can be argued on the grounds of, first, abundant presence of metalliferous deposits and variety of iron ores, second, the evidence for exploitation of copper ores associated with iron deposits (on Thasos) and third the abundance of both bronze and iron artefacts in the large cemetery at Vergina suggesting no shortage of either the raw material or technological

know-how. Whether the knowledge to smelt iron ores arrived from outside, the writer believes is of little consequence. Theories about diffusion of technology should not be based on artefact typology and style since these two parameters relate only to the final stage in a long process and tend to ignore all steps relating to ore and metal extraction. It is the metallurgical waste, however scanty, which clearly heralds the introduction of a new technology by shedding light on the extraction stages.

It is proposed here that the smelting of copper ores should be attempted experimentally in the presence of various amounts or iron ores, in the field, since it is the random production of iron metal as a result of localised 'excessively' reducing conditions in a copper producing furnace that would be investigated.

Macedonia may have been known in the classical texts for its sources of iron, lead, cheese and bacon, but first and foremost it was known for its intensive precious metals exploitation in the Classical/Hellenistic and later on in the Ottoman periods. In the Chalkidiki, the large-scale precious metals processing has been well documented in contemporary Ottoman reports, and some metallurgical remains spanning both periods have recently been analysed. However, in EM, despite the known references about Ottoman exploitation in areas around Pravi or Sidirokastro and the abundance of slag heaps, very little was known about the type of activities and their date. One problem was the proximity of some of these sites to Mt. Pangaion, the classical source of Hellenistic gold. Our investigations of the metallurgical remains in EM have

concentrated on some of the (chronologically) later activities, but dates are still not available. It is quite clear that Mn-rich iron ores were smelted in furnaces similar to that found in Nikisiani, in conjunction with lead ore, the role of the latter being to act as a precious metals collector since both gold and silver were present in the iron ore. Speiss, obtained as a by-product together with lead-rich slag, was found to contain some precious metals, unbeknown to the smelters. Lead was subsequently cupelled and the gold, if sufficient, was separated from the silver. This is probably the first instance in Greece of an iron ore being used in non-ferrous metals extraction. It is in agreement with the modern approach to mining, that the economic value of an ore is based on more than one metal, since at least during the Ottoman period the speiss was remelted and cast into cannon shot. Such an approach towards mining in antiquity is already hinted at in Strabo's report that the mine above Chalkis in Euboea was worked for both its copper and iron.

The actual location of the Skapte Hyle, second only to the Pangaion as a source in antiquity of precious metals in EM, is a problem of major archaeological importance. A number of investigators presently believe that the ancient Skapte Hyle was probably located in the region of Palaia Kavala. Is the Skapte Hyle the source of silver and the Pangaion the source of gold? There is a great need for archaeological excavation and analyses of ores and slags from Palaia Kavala, mapping of the mines in the vicinity of the slag heaps, prospection for furnaces and last, and very important, the dating of the heaps. It is very likely that Ottoman

exploitation followed Byzantine and Hellenistic/Roman activities, and that the slag heaps represent the accumulated results.

The last issue tackled in this thesis relates to the furnace illustrations on the vases of the 6th and 5th c. BC. The writer believes that bloomery technology may have varied regionally in Greece, even coming close, in places, to blast furnace technology. Such a situation, however, had not become apparent simply because of the overwhelmingly accepted view that cast iron from a blast furnace was not introduced to the West until the 14th c. AD. Since high carbon iron was not produced for the purpose of being cast, as in China, but rather as an intermediary step, surviving evidence is inevitably elusive. Nevertheless, the few references in the classical texts and the depiction of the cauldron on all furnace vase illustrations deserve to be taken seriously. The reference to stomomata, steel, is clearly not suggestive of the product of quenching and tempering of wrought iron, a process which could have taken place in a forging hearth, but rather a distinct product as slag and iron are. So much is suggested by Aristotle's reference in the Metereologica. There is no way of knowing what the metallography of stomomata was. Was it wrought iron or was it actually steel? This question has considerable implications. It invokes the problem of distinguishing between wrought iron produced from the direct reduction of iron ores as opposed to decarburisation of cast iron. It should, in principle, be possible to distinguish wrought iron, fined, and puddled iron on the basis of both slag inclusions and metal. The importance of establishing the criteria for this differentiation is far-reaching, since it applies to iron

metallurgy in all those geographical regions that underwent the transition from the bloomery to the blast furnace. In addition, it is neceesary to determine when this transition first occurred in the West.

In the meantime, the references in the classical texts should be studied for possible variations in the meaning of stomomata, and the cauldron should be taken as representing the closing of the mouth of the furnace for the purpose of decarburising the molten or fused iron in a process similar to that taking place in the Chinese fining hearth, as witnessed by Rocher (1879). There are good indications that a figurine from Olympia (now in Olympia Museum) (A Moustaka, pers. comm.) may be of cast iron; its metallography should be investigated as a first step in elucidating the question of possible cast iron production in Classical Greece.

Appendix 2.1: Chronological Tables

Aegean

EN	6500-5500BC	(Early Neolithic)
MN	5500-4500	(Middle Neolithic)
LN	4500-3700	(Late Neolithic)
FN	3700-3000	(Final Neolithic)
EBA	3000-2000	(Early Bronze Age)
MBA	2000-1150	(Middle Bronze Age)
LBA	1550-1100	(Late Bronze Age)
DA	1100- 850	(Dark Ages)
GEO	850- 700	(Geometric)
ARCH	700- 480	(Archaic)
CLASS	480- 323	(Classical)
HELL	323BC-23AD	(Hellenistic)

Macedonia

Sitagroi I	5400 - 5300 BC
II	5200 - 4800
III	4600 - 4200
IV (=Early Bronze I)	3300 - 3100
Va (=EB II)	2600 - 2450
Vb (=EB III)	2250 - 2150
Middle & Late Bronze Ages	2000 - 1050
Early Iron Age	1000 - 700
Archaic	700 - 480
Classical	480 - 323
Hellenistic	323 - 23AD
Roman	23 - 333AD
Early Byzantine	6th - 9th c. AD
Middle Byzantine	9th - 12th c. AD
Late Byzantine	12th - 15th c. AD
Ottoman	1453 - 1912
Macedonia annexed to Greece	1912

The Aegean dates are as given in Jones (1986, 888); Sitagroi: Renfrew (1979, 201); Macedonia (Archaic to Roman): Hammond (1972)

Appendix 3.1.1: Pangaion

On the Pangaion a number of slag heaps have been surveyed and sampled by Papastamataki (1975; 1986a; 1986b) and her co-workers. She has published a number of analyses of ores and slags but made litle attempt at offering any suggestions as to the metallurgical processes involved.

A sample of speiss collected during a visit to Nikisiani (site Livadia), showed the same composition as speiss from Palaia Kavala region suggesting similar methods for precious metals extraction. Slag from Valtouda, also on the Pangaion, showed the same phases as the Palaia Kavala slags (see analyses below).

At the site of Avli, there is the first evidence for cast iron making suggesting the operation of a blast furnace. This is the only place in EM, the author came across, with other than bloomery iron making activities. The analysed sample (see Table below) suggests that Mn-rich iron deposits were smelted in a blast furnace producing glassy slag rich in alumina, silica, calcium and manganese. The metallic prills in the slag were grey cast iron with graphite flakes with silica, phosphorus and manganese.

ıple	Na_2O	Mg O	Al_2O_3	SiO_2	P_2O_5	SO_3	K_2O	CaO	TiO_2	MnO	FeO	ZnO	AS_2O_3
ıg													
ltouda	0.00	6.41	0.00	32.08	0.00	0.00	0.58	4.96	0.00	2.28	50.46	1.61	0.00
	0.00	0.00	7.89	1.94	0.00	0.00	0.00	0.65	1.62	0.78	80.40	2.57	1.13
"	0.00	0.00	22.09	54.44	0.00	0.00	18.65	1.75	0.26	0.00	3.29	0.00	0.00
li	1.36	1.75	15.12	44.18	0.71	0.00	2.17	18.84	4.01	9.61	0.28	0.00	0.00

:al mple	Fe	As	Cu	S	Sb	Pb	Mn	P	Si
ltouda	54.43	31.97	6.85	4.05	0.42	0.75	0.00	0.00	0.00
:issiani	57.89	36.78	1.22	0.14	1.57	0.00	0.00	0.00	0.00
li	95.28						1.99	1.01	1.05

Appendix 3.1.1 Analysis of slag and metal from ferrous and non-ferrous production sites in EM

Appendix 3.1.2

DIRECTORY OF SITES AND THEIR ABBREVIATIONS

AA	Athenian Agora
Ag. Dimi	Aghios Demetrios, S Euboea
Ag. Elis	Aghios Elissaios, Neapolis, S. Laconia
AIA	Aiani, near Kozani
Archam, Sev. Arch	Archampolis, S. Euboea
ART	Artemission, Limenas, Thasos
Ast	Astris, Thasos
Avli	Avli, Pangaion
Dyp	Dypotama, Palaia Kavala region
D	Kavala and Thasos Museums
Doma	Domatia, Pangaion
EL	Eleftheroupolis, EM
Fl-Pet	Petres (slope), WM
KALF	Kallirachi-Fournoi, Thasos
KALO	Kalovria, Thasos
Kara-3	Tria Karagatsia, Palaia Kavala region
Karys	Karystos, S. Euboea
Kasta	Kastanas, Palaia Kavala region
KATA	Katafyto, EM
Kaza	Kazani, Thasos
Kehro	Kehrokampos, Palaia Kavala region
KIMX	Kimmeria, Xanthi, Thrace
K.Lar	Kato Larnaki, Thasos
Kn	Knossos (Unexlored Mansion), Crete
Kupyelo, Kupblor	Koupanada mine, Thasos
LA, B, C	Thermi, Lesvos
Lep Mag	Lepoura Magoula, Euboea
Makro	Makrychori, Palaia Kavala region
Man, MANTM	Mantaloudi, Thasos
M.Th	Thessaloniki Museum
M.Th7	Vardaroftsa (Axiochori), CM
M.Th8	Vardaroftsa (Axiochori)
Myl	Myloudi, Chalkidiki
N AGH	Nea Aghialos, nr. Thessaloniki
Nero, Ner.	Nerotrivia, Euboea
N Styra	Nea Styra, S. Euboea
Oly	Olympias, Chalkidiki, CM
OXI, OXIM	Oxia, Thasos
PAI	Paidouli, Thasos
Pano	Panorama, EM
Pet	Petres (slope)
Pet Acro	Petres (acropolis)

Phil	Philippoi
Piga	Piges Angiti, EM
Pilion	Pilion, Thessaly
Pyr	Pyrgiskos, Palaia Kavala region
Pyrg. Apo.	Pyrgos Apollonias, W. of Kavala
SEVR	25th km on the SerresVrontou road
Sidi	Siderochori, EM
SKR	Skries, Thasos
THE	Theologos, Thasos
Trag, Tragm	Tragi, Thasos
TSI, TSICE, TSIAR, TSIM	Tsigganadika, Thasos
Valt	Valtouda, Pangaion
Vath, Vatt	Vathytopos, EM

Appendix 3.1.3

INVENTORY OF METALLURGICAL WASTE COLLECTED DURING SURVEYS ON THASOS AND THE MAINLAND

Site/Location	Date	Slag macrostructure	N	Dimensions (cm)
Thasos Ti-rich iron slags				
Mandaloudi	7/83	spongy	10	4,4,6,9,7,7, 8,8,7,4,3,3
		compact (ropey)	7	4,5,4,3,4,8,5
		furnace lining	2	3,3
		sherd	1	
Paidouli	3/83	spongy (blocky)	7	9,8,6,4,4,6,8
		sherd	1	
Kalovria	3/83	compact (ropey)	2	6,4
		drop like	1	7
		spongy	8	8,9,7,6,4,5,4,
Astris	3/83	semi spongy/semi compact	7	6,5,4,6,4,6,6
		compact	1	4
		spongy	1	6
		drop like	1	5
		ore pieces	2	5,6
Theologos, cemetery	3/83	spongy	8	9,8,4,4,4,6,4,
		compact	4	3,2 2,3
		semi spongy/semi compact	13	4,2,4,4,3,4,5, 6,3,4,3,4,4
		furnace lining	1	3
		sherd	1	3
Oxia	3/83	semi spongy	2	4,4
		spongy	5	6,5,7,4,3
		tuyere frag (9cm long, inner diam 4cm, outer diam 7.5, one end vitrified, depth of vitrification 2cm)	1	
Kazani	3/84	bloom	1	6
		ore piece	1	4
		tuyere frag (4 cm long, inner diam 2 cm)	1	
Tragi	3/84	spongy	2	6,5
MAINLAND: Ti-rich iron slags				
Piges Agiti	1/85	spongy	4	6,4,5,5
		compact/glassy, various pore sizes	10	4,5,6,4,4,5, 3,4,4,4
		semi spongy, heavy	5	3,5,3,3,3
		ceramic frag	2	6,3
		iron handle	1	
		soil		

Siderochori, Rema	2/85	compact	12	5,5,4,4,3,5,4, 4,4,6,5
		semi spongy/semi compact	18	7,6,7,7,7,6,6, 7,4,4,3,3,3,5
		soil		
Vathytopos, Miloi	1/85	spongy/semi compact	2	9,8
		compact/semi compact	17	9,6,7,8,6,6,5, 6,5,6,6,7,6
Vathytopos, entrance	1/85	compact (v. small gas holes)	6	6,4,5,8,4,4
		porous (light)	2	4,4
Kimeria	1/85	very compact	6	3(5sl),5(3sl),6(5(2sl),3(4sl),4((
		porous (glassy)	2	4,3(1sl)
		furnace wall	1	17 x 9 x 3
		ore (Cu/Fe)	1	
MAINLAND: Mn-rich 'iron' slags				
Domatia	2/85	spongy	2	7,3
		drop like	1	4
		compact	9	4,6,6,6,5,7,!
		semi compact, porous	3	9,6,6
		cinder	3	8,7,7
		furnace lining	3	3,5,3
		furnace lining, slagged	1	12 x 8
		furnace lining, cindered	2	7,6
		furnace lining, low fired	3	4,3,8
		tuyere (7cm long, outer diam 7cm, inner diam 4cm)	1	
		soil		
Panorama, Aghios Demetrios	1/85	semi spongy, heavy	1	5
		semi spongy	3	4,4,3
		compact (ropey), heavy	1	7
		compact	12	7,4,6,8,6,5,5 4,6,3,3,4
		drop like	1	6
		sherds	10	2 to 8
		furnace lining	2	6,6
		ore pieces	1	5
		trachyte stone	1	9 x 6
Panorama, Kampania	1/85	very spongy	3	9,9,6
		iron pieces	2	
		sherd	1	
Eleftheroupolis (church)	1/85	compact	2	5(5sl),6(6sl)
		speiss	1	8 x 4 (4sp)
Eleftheroupolis (Pano Rema)	1/85	compact	4	4(1sl),3(3sp), 4,2(4sl)

Dipotamos, 'furnace'	1/85	speiss	3	3(4sp),3(3s) 4(5sp)
		compact	1	3(2sl)
Kastanies	1/85	compact (small pores)	5	6(3sl),5(1sl),3 3(4sl),3(2sl)
Makrychori Slag heap	1/85	compact, heavy	4	4(13sl),5(11sl) 2(12sl),4(10sl)
		speiss	1	
		furnace lining	2	
Makrychori 'melting furnace'	1/85	compact/ropey	3	4(1sl),3(2sl),4
Makrychori 'modern furnace'	1/85	compact, small pores	2	4,5
MAINLAND: other slags				
Pyrgos Apollonias	2/85	compact/ropey	3	9,6,8
		semi compact	14	5,4,3,4,4,2, 3,3,2,2,3,2
		ore	1	10

Samples not included in this inventory are:
a) Tsigganadika and Kato Larnaki (Thasos)
b) 25th km of Serres-Vrontou road (Mainland:Ti-rich iron slags)
c) Pyrgiskos (Mainland:Mn-rich 'iron' slags)

*sl and sp refer to slag and speiss respectively. The number associated with them is the sample number in the classification system.

Appendix 3.2.1: Analysis of Thasos gneiss

The composition of Thasos gneiss determined by G. Gialoglou using AA (Photos et al, in press) is given below:

%age Fe_2O_3	CaO	SiO_2	MgO	Na_2O	K_2O	Al_2O_3	TiO_2	MnO
13.15	12.75	49.1	5.3	3.2	0.45	1.5	1.8	0.8

Cu	Pb	Zn	V_2O_5	Cr_2O_3
0.02	0.02	0.02	0.06	0.04

Analysis of the Vrontou graniodiorite, a coarse-grained plutonic rock containing quartz, ferromagnesian minerals (biotite) is given below, adapted from Karamatzani and Kaklamani (1983, Table 2):

%age SiO_2	Al_2O_3	Fe_2O_3	K_2O	Na_2O	CaO	MgO
67.84	15.95	3.33	4.00	3.2	2.84	0.79

Mineralogical composition revealed quartz, feldspars, biotite, amphibole and epidote.

Appendix 3.6.1: Analyses of Titanium-rich iron slags from Lesvos

The samples and their analysis by XRF were kindly provided by Dr E. Pernicka of the Max Planck Institute, Heildeberg. The six samples were collected at the following locations:

a) LA,LD,LF : 3 km SW of Thermi, the EBA site, on a ridge about 320m above sea level. Location: Louloudia. Fragments of tuyeres and furnace lining were also observed. A total of 100kg of slag was estimated on the site. The local ore source was thought to be ankerite and limonite.

b) LC: scattered slag fragments on the slope of the valley. Location: To Lagadi tis Toksani.

c) LB: scattered slag fragments in a stream valley. Location: Lagaria tou fournou. Fragments are quite large (up to 10cm) and coarse pottery fragments are also present.

The chemical analyses provided by Dr Pernicka are included below. No titanium was measured, possibly because it was not expected to be present.

	%age FeO	SiO_2	CaO	Al_2O_3	MgO	K_2O
LA(TG119A)	67.0	11.9	6.1	3.0	1.5	0.0
LC(TG119C)	11.6	34.0	27.2	7.3	2.8	1.5
LF(TG119F)	13.5	51.0	7.5	14.9	3.4	1.5
LB1	55.0	21.0	10.6	5.2	1.6	1.2
LB2	75.0	10.0	3.6	2.7	1.4	0.0
LD(TG119D)	31.0	28.0	17.9	7.1	2.5	1.0

The microprobe analyses are provided in a separate table. The Lesvos slags are titanium-rich with ulvospinel, wustite and a matrix of mellilite composition (Plate 26f,g).It is not likely that the slag samples found near Thermi were indeed of BA date but

rather of smelting of titanium-rich sands at later periods, possibly Ottoman. The scattered nature of the finds and the relatively small quantity of slag (100kg) in three different locations are reminiscent of the situation on Thasos, where similar slag was found in the vicinity of Tsigganadika at the prehistoric settlement of Kastri. It is likely that Ti-rich iron sands may have been exploited in other islands in the northern Aegean, like for example Samothrace. Further field surveying is necessary in the future.

Titanium-rich Iron slags from Lesvos

Sample no.	Phase	Na_2O	MgO	Al_2O_3	SiO_2	P_2O_5	K_2O	CaO	TiO_2	Cr_2O_3	V_2O_5	MnO	FeO
LC	wustite	0.00	0.61	1.77	2.79	0.00	0.00	0.98	6.38	0.00	0.00	0.00	88.13
	matrix	0.00	0.79	5.11	34.98	1.40	2.56	18.00	0.85	0.00	0.00	0.29	34.74
LA	ulvo	0.00	0.98	5.78	0.47	0.35	0.00	0.00	21.25	0.00	6.29	0.46	65.17
	matrix	0.00	1.18	6.08	35.51	2.49	1.62	15.69	1.22	0.00	0.00	0.28	34.36
LD	wustite	0.00	0.37	1.26	0.53	0.00	0.00	0.38	1.97	0.00	0.00	0.27	95.35
	ulvo	0.00	0.89	14.21	0.34	0.00	0.00	0.00	1.72	0.00	3.93	0.37	63.62
	matrix	0.00	0.71	6.04	33.37	1.58	1.38	20.61	0.48	0.00	0.00	0.34	35.66

Appendix 3.6.2 Table of silicate phases in experimental slag

Sample No.	Na_2O	MgO	Al_2O_3	SiO_2	P_2O_5	SO_3	K_2O	CaO	TiO_2	Cr_2O_3	MnO	FeO	NiO	CuO
XSm2a	0.00	0.82	0.00	31.52	0.44	0.00	0.17	23.16	0.26	0.00	0.21	41.85		
	0.00	0.00	16.02	35.04	2.29	0.22	4.77	6.51	5.95	0.00	0.00	13.62		
	0.00	0.00	15.42	29.93	1.76	4.15	3.30	3.46	8.49	0.00	0.00	21.05		
XSm2b	0.00	0.87	8.06	32.64	0.42	0.00	1.71	12.27	1.04	0.00	3.28	37.32		
XSm 6Ia	0.00	2.00	18.66	40.29	0.00	0.00	3.52	17.07	8.65	0.00	5.44	0.36		
	0.00	1.92	17.43	37.85	0.00	0.00	2.73	15.85	8.94	0.00	4.40	0.29		
	0.00	1.08	18.92	42.54	0.00	0.00	3.69	15.11	5.83	0.00	5.45	0.28		
XSm 6Ic.dr	0.00	0.38	1.79	3.14	0.00	0.00	0.23	0.83	0.18	0.00	0.19	85.90		
	0.00	0.46	2.43	1.10	0.00	0.00	0.11	0.23	0.16	0.00	0.20	85.51		
	0.00	0.66	4.50	41.08	0.67	0.00	4.75	11.47	0.00	0.00	0.30	33.90		
XSm 6Ie	0.00	2.04	11.84	44.39	0.00	0.00	0.15	14.03	2.30	0.00	24.29	3.81		
	0.00	0.00	31.68	42.72	0.00	0.00	0.27	17.99	0.47	0.00	3.28	4.41		
XSm 6	0.00	0.80	12.37	8.30	0.00	0.00	0.31	3.16	8.23	0.00	1.91	68.94		
	0.00	1.12	13.65	10.97	0.00	0.00	0.54	4.26	11.43	0.00	2.50	54.45		
	0.00	0.67	9.36	26.76	0.38	0.00	1.55	10.10	4.44	0.00	2.89	43.86		
XSm6IIIb.p	0.00	0.33	8.67	0.92	0.00	0.00	0.00	0.32	14.80	0.00	3.28	68.33		0.35
	0.00	0.26	1.53	0.44	0.00	0.00	0.00	0.00	8.92	0.00	1.66	83.23		0.31
	0.00	0.00	10.69	1.02	0.00	0.00	0.00	0.32	9.42	0.00	1.88	71.94		
	0.00	0.00	0.00	0.34	0.00	0.00	0.00	0.00	4.56	0.00	0.98	87.13		
	0.00	0.00	16.68	40.97	0.54	0.12	0.69	18.11	0.95	0.00	1.33	21.10		0.29
XSm6V.cd	0.00	0.89	12.38	0.53	0.00	0.00	0.00	0.14	17.35	0.00	1.94	56.09		0.43
	0.00	1.35	12.47	0.55	0.00	0.00	0.00	0.25	11.61	0.00	1.45	61.15	0.45	
	0.00	0.80	12.09	1.20	0.00	0.00	0.10	0.49	16.89	0.51	2.02	54.18		
	0.00	1.16	8.57	0.54	0.00	0.00	0.00	0.32	15.73	0.26	1.31	46.23	0.29	
	0.00	0.76	10.58	0.44	0.00	0.00	0.00	0.24	15.08	0.00	1.71	66.25		
	0.00	0.96	0.98	0.46	0.00	0.00	0.00	0.00	9.88	0.00	1.00	79.18	0.74	
	0.00	0.56	6.80	0.46	0.00	0.00	0.00	0.25	7.03	0.00	1.44	76.47		
	0.00	1.77	2.23	29.98	0.42	0.00	0.67	15.13	0.36	0.00	1.78	29.20		
	0.00	1.49	4.63	32.62	0.43	0.00	1.62	13.49	0.48	0.00	2.07	29.26		
	0.00	1.70	1.80	28.65	0.00	0.00	0.54	14.67	1.05	0.00	2.03	32.61		
	0.00	1.19	8.01	37.93	0.39	0.00	3.10	13.64	1.34	0.00	2.17	33.26		
XSm12.ABci	0.00	0.44	5.33	12.85	0.00	0.00	0.24	2.38	41.12	0.00	2.49	36.03		
	0.00	0.60	10.66	35.09	0.00	0.00	1.31	20.51	2.51	0.34	2.22	21.53		
	0.00	0.45	11.86	42.69	0.28	0.00	0.83	6.96	9.76	0.23	2.04	22.65		
	0.00	0.68	13.27	47.57	0.00	0.00	1.49	7.87	7.81	0.00	2.11	18.51		
	0.00	0.50	13.18	49.14	0.43	0.00	11.89	8.94	6.71	0.00	2.03	16.40		
	0.00	1.55	9.44	52.17	0.00	0.00	2.08	10.99	3.99	0.00	2.83	14.95		
	0.00	0.76	13.54	50.49	0.00	0.00	1.45	10.47	3.62	0.00	1.91	13.67		
	0.00	0.78	13.62	50.71	0.34	0.00	1.94	10.20	2.89	0.00	2.09	14.83		
	0.00	0.00	25.48	50.03	0.00	0.00	0.56	13.55	1.19	0.00	0.54	5.36		
XSm15a	0.00	0.00	2.59	11.87	0.00	0.00	0.51	1.37	20.79	0.53	0.21	58.64		
	0.00	0.00	5.50	37.95	0.36	0.00	1.48	7.31	6.98	0.00	0.37	37.39		
	0.00	0.41	4.24	35.99	0.26	0.00	1.42	4.09	4.34	0.00	0.59	47.56		
	0.00	0.68	3.13	34.24	0.25	0.00	1.23	2.79	4.30	0.00	0.64	50.72		

Sample No.	Fe	Ni	Cu	Mn	Cr	Mg	Al	Si	P	Ca	Ti
Xsm 2	2.31		97.80			1.49	0.26	0.17			
	90.34		7.94					0.12			
	93.67		1.74					0.10			
XSm 6	96.38			0.55				0.19	0.26		
	95.47			0.53				0.18	0.29		
	88.06				0.21				7.29		
	95.42							0.15			
XSM 6Ia	96.87		0.26								
	1.91		97.07								
	58.39		38.56								
	78.37		16.67								
	95.54		3.36								
XSM 6Ie	96.85			0.40						0.12	0.83
	96.46			0.26							0.86
XSm 12AB c	94.33							0.16		0.21	0.24
	94.32							0.12	0.21		
								0.17	0.19	0.14	

Appendix 3.6.2 Table of metallic phases in experimental 'blooms' and slag

X-Ti sands

X-Smelt 13
Clay-bound Ti-rich magnetite sands in shaft furnace

Total amount of magnetite sands	8.6kgr
clay slurry	1.8kgr
Ore/clay slurry	4.77/1 or 5/1
Total ore charged	17kgr
total fine charcoal	24kgr
preheating charcoal	10.5kgr
ore size	ball shape, 5cm diam
charcoal size	1.25-.63cm
coarse charcoal size	5cm

Smelting Cycle

12:00	preheat with wood	
1:30	preheat with charcoal	7kgr
1:45	preheat with charcoal	3.5kgr
1:50	fine charcoal	2kgr
1:55	1st charge	2kgr ore/2kgr char
2:05	2nd charge	2kgr ore/2kgr char
2:15	3rd charge	2kgr ore/2kgr char
2:25	4rth charge	2kgr ore/2kgr char
2:45	5th charge	2kgr ore/2kgr char
3:05	6th charge	2kgr ore/2kgr char
3:20	7th charge	2kgr ore/2kgr char
3:45	8th charge	2kgr ore/2kgr char
3:50	9th charge	2kgr ore/2kgr char
3:55	fine charcoal	1kgr
4:15	x-tra fine charcoal	1 kgr
4:30	x-tra fine charcoal	3kgr
5:15	shutdown	
5:30	furnace sealed	

Appendix 3.7.1: Speiss

Speiss can be iron, copper, or nickel, arsenides or antimonides produced in the smelting of complex ores (fahlerz) or a copper ore containing substantial amounts of iron and arsenic. Speiss is grey, hard, brittle and magnetic due to the presence of iron. The fractured surface is bright and crystalline and resembles cast iron. Speiss can be argentiferous or auriferous or even contain members of the platinum family. Platinum and gold have high affinities for speiss as opposed to matte (a copper sulfide or copper iron sulfide) while silver has the same affinity for both. The thermodynamics of speiss and their stability with matte and slag have not been worked out given their limited modern industrial usage (Rosenquist 1983, 343).

The method of speiss formation as a result of smelting of a copper ore is the following. When a copper carbonate ore is smelted, a cake of metal is formed at the bottom of the furnace with slag floating on top, because of the difference in specific gravity (slag 3.5-4.0 gm/cm^3, copper 8.9 gm/cm^3). If a sulfide ore with small amounts of antimony and arsenic is smelted, the last two elements will be taken up by the matte which will form underneath the slag layer. Thus, copper will collect at the bottom of the furnace covered by a layer of matte and slag. If, however, arsenic and antimony occur in substantial amounts, a layer of speiss will form under the matte and above the molten copper. The specific gravity of speiss is 5-8 gm/cm^3. Thus, the sequence would be copper(8.9), speiss(5-8), matte(5), slag(4) (Tylecote 1985).

Speiss was first reported in Greek lands in a Mycenaean context in 14th c. BC at Tiryns in the N.E. Peloponnese (Kilian 1983). It was suggested that it come from the Pangaion and that it may have been used for soldering. We analysed a section from this sample, kindly provided to us by Prof. Dr. K Kilian, and found it contained iron, arsenic and some sulfur. It presumably originated from the smelting of mixed sulfide ores, probably the result of copper reduction. Rather than coming from the Pangaion in Macedonia, it is more likely to have been the result of local experimental smelting attempts. However, more work is needed to establish the presence of sulfidic ores in the vicinity of Tiryns.

Analysis of Mycenean speiss from Tiryns

%age Fe	As	S	Cu
57.37	33.95	3.45	1.26
64.90	31.05	2.29	1.03
86.14	12.39	0.18	0.34

Speiss contemporary with the Mycenaean sample from the Hittite city of Hattusas was analysed by Maddin (1986) and reported by him and Muhly et al (1985, 77). The authors argue that speiss is the result of smelting of arsenopyrite with metallic iron forming at the bottom of the furnace. But, it is unlikely that metallic iron and speiss would form in the same furnace since metallic iron and speiss require different furnace conditions: rather reducing rather oxidising conditions respectively. Concentrations of precious metals in speiss has been reported at levels in excess of 1000gr/ton (Lupu 1961, 196).

To retrieve the precious metals, speiss is roasted and smelted with lead products (Percy 1879, 313). This is possible since speiss is immiscible in lead. Lead is an overall better collector of precious metals and has been used in that capacity since the Roman times. Rickard (1888) reported a method developed in the United States to desilverise speiss. During that procedure, speiss (800lb) was tapped in a converter lined with fire brick. About 160-200 lb of liquid lead was added and a blast of air (17oz pressure) was introduced through the bottom of the converter. The blast stirred the speiss and lead, burning some arsenic in the process. Precious metals were taken up by the lead. The converter was then turned down, and the contents were allowed to pour into a cast iron receiver (a slag pot) with a hole in the bottom. The speiss solidified quickly in the slag pot, but the still liquid lead ran through the hole in the pan underneath. The desilverised speiss was discarded. It was claimed that 86% and 90% of the original Ag and Au contents in the speiss were recovered.

Such yields suggest that it may be posssible to process the substantial amounts of speiss (an estimate not available presently) scattered amidst the slag heaps of Palaia Kavala and Chalkidki for the purpose of recovering the precious metals. However, the cost of collecting and roasting the speiss, the main difficulty being in the expulsion of arsenic as arsenic oxide, will have to be balanced against the demand for these metals at the time.

Appendix 3.7.2: Experimental Smelts with Petropigi Ore

Ore and slag was collected during a field survey at Petropigi in the region of Palaia Kavala in May 1986. Some shafts were evident in the vicinity of a disused lime kiln. Another mine was known to exist N.W. of Petropigi but was not visited during that fieldtrip. It was assumed that the surface slag which did not exceed a few kg must have been the product of the smelting of local ore. The ore was hematite/limonite. No analysis was available at the time of this writing.

Smelting of Petropigi ore

Two experimental smelts were undertaken in a shaft and a bowl furnace, using this ore either on its own or in combination with high-grade Australian hematite kindly provided by British Steel Co., Llanwern, South Wales. Only X-smelt 8 is outlined here.

Date	Smelt	Fuel/Ore	Furnace type	Ore
27.7.86	X-smelt8	3/1	shaft	Petropigi ore
31.7.86	X-smelt9	2/1	bowl	Petropigi ore and Australian hematite

Roasting

Pre-roasted ore	16.8kg
Roasted ore	14.1kg
Lost on Ignition	2.7kg

Smelting cycle

12:30	preheat with wood	
2:30	preheat with coarse charcoal (10kg)	
2:45	charge the rest of preheated charcoal (3kg). Total 13kg	
2:50	charge fine charcoal (3kg)	
3:00	1st charge	1kg ore/3kg charcoal
3:15	2nd charge	1kg ore/3kg char
3:30	3rd charge	1kg ore/3kg char
4:00	4rth charge	1kg ore/3kg char
4:30	5th charge	1kg ore/2kg char
4:50	6th charge	1kg ore/2kg char
5:15	7th charge	1kg ore/3kg char
5:45	8th charge	1kg ore/3kg char

6:25 9th charge 1kg ore/3kg char
6:45 charge 1kg fine char
7:15 shutdown
7:30 cover furnace

Results

Primary bloom weight: 3.18kg
Associated slag 1.4kg
Dimensions: 10 x 15 x 7cm
Fettled bloom weight: 2.5kg

Smelting furnace contents
Above bloom: 6.8kg (larger than 2.5cm)
3.6kg (less than 2.5cm)
0.9kg sintered and partially reduced ore

Below bloom: 4.1kg (larger than 2.5cm slag and charcoal)
1.8kg (less than 2.5cm slag and charcoal)
1.4kg slag

Furnace efficiency: 72% of the fuel was consumed (12.6kg retrieved out of the 46kg charcoal charged in the furnace).

Typology of macrostructure of primary bloom:

a. drop-like: weight: 0.51 kg
size distribution: 4.3cm
magnetism: non-mildly magnetic

b. compact to spongy fine:
weight: 0.7kg
size distribution: 3.7 cm average
magnetism: mildly magnetic

c. spongy fine: weight: 0.3kg
size distribution: 3.4cm average
magnetism: mildly magnetic

d. fines: weight: 1.1kg
size: less than 0.5cm (consists of dust and scale)
magnetism : very magnetic

Typology of macrostructure of furnace (smelting)slag

Below bloom (B/B)
a: drop-like: size: 2.8cm
b. spongy fine: 2.9cm average
c. shiny drop or plate-like: size: 2.4cm average
d. dust: 0.15kg
total weight: 1.2kg
magnetism: non-mildly magnetic

Sample No.	SiO_2	TiO_2	Al_2O_3	Fe_2O_3	MnO	MgO	CaO	K_2O	P_2O_5	PbO	BaO	Zn	As	Cu	Ag
KALF 1	30.78	0.25	*	19.01	0.10	1.38	4.28	1.29	0.28	7.33	13.25	6877	447	29	21
KALF 2a	30.33	0.24	*	18.67	0.19	1.86	4.09	1.31	0.22	n.d.	n.d.	4213	238	15	2
KALF 2b	30.55	0.24	*	18.75	0.18	1.87	4.13	1.31	0.22	n.d.	n.d.	*	*	*	*
KALF 4	4.14	0.11	*	78.33	0.04	0.16	0.25	*	0.15	0.67	0.14	1279	168	10	6
KALF 3	20.93	0.27	*	33.70	0.14	0.78	3.30	1.17	0.32	4.40	11.65	3547	427	6	1
SKR 1	19.26	0.27	0.34	22.72	0.72	1.28	6.60	1.34	0.30	2.62	14.92	8668	250	29	1
SKR 3a	15.10	0.31	2.39	15.45	0.99	1.39	6.35	1.41	0.23	1.40	20.93	4472	160	63	1
SKR 4a	14.00	0.29	1.38	17.24	0.68	1.29	8.28	0.95	0.29	1.57	18.80	3613	165	66	1
MYL 1.4	71.36	0.36	13.13	7.14	2.15	0.61	1.78	4.55	0.16	4.80	0.99	6882	447	29	21
MYL 1.2	36.35	0.36	3.91	26.59	9.13	1.42	3.43	1.73	0.26	1.30	0.07	5694	255	23	7
MYL 1.3a	37.60	0.44	4.95	26.29	9.10	0.62	1.11	2.07	0.25	2.93	0.07	2723	294	25	9
MYL 1.1	30.04	0.30	2.17	22.43	9.28	0.59	1.79	1.66	0.13	1.58	0.05	6732	194	18	7
MYL 2.3	23.55	0.26	1.09	23.06	9.11	0.80	2.31	1.23	0.18	4.86	n.d.	16523	412	14	9
MYL 2.4b	16.25	0.22	*	21.95	8.63	0.97	1.82	0.32	0.16	5.17	n.d.	29488	496	24	19
MYL 2.1wv	13.95	0.28	1.30	17.48	0.69	1.23	8.25	0.92	0.29	3.57	0.11	14200	327	14	8
MYL 2.2	31.60	0.24	0.01	38.69	7.63	0.67	2.09	1.15	0.19	1.38	0.68	7630	139	4	16
MYL 3.1a	13.40	0.23	*	26.49	7.07	0.69	2.58	0.59	0.15	3.94	0.01	24931	381	103	13
MYL 3.2	36.17	0.38	5.04	41.63	8.75	0.55	2.70	1.88	0.45	0.38	3.02	4242	38	7	1
MYL 3.4	14.44	0.21	*	35.34	7.02	0.59	2.16	0.67	0.14	5.20	0.06	26439	493	106	14
MYL 3.3	16.30	0.22	*	21.68	7.70	0.66	1.95	0.70	0.12	3.76	n.d.	26827	391	82	14

* not measure d n.d. not detecte Zn,As, Cu,Ag are in ppm

Appendix 3.7.3 XRF analyses of non-ferrous slag from the Chalkidiki, CM (MYL) and Thasos (KALF and SKR)

e No.	Phase	Na_2O	MgO	Al_2O_3	SiO_2	P_2O_5	SO_3	K_2O	CaO	TiO_2	Cr_2O_3	V_2O_5	MnO	FeO	BaO	PbO	ZnO	CuO
	matrix	0.00	0.00	2.75	47.14	0.00	0.00	1.53	9.06	0.00	0.00	0.00	14.01	15.77	3.20	1.28	2.91	
	'grain'	0.00	0.00	2.87	47.72	0.00	0.00	1.49	9.22	0.00	0.00	0.00	14.02	16.33	3.25	1.51	3.34	
	matrix	0.00	0.00	6.86	47.77	0.39	0.49	3.13	5.22	0.00	0.00	0.00	18.91	8.87	6.59	0.68	0.99	
	matrix	0.00	0.00	10.35	48.74	0.34	0.16	4.72	3.43	0.00	0.00	0.00	14.27	10.18	7.12	0.00	1.01	
	matrix	0.00	0.00	0.00	46.78	0.00	0.00	0.16	9.04	0.00	0.00	0.00	27.84	13.78	0.52	0.00	0.82	
	'grain'	0.00	0.00	1.21	48.39	0.00	0.00	0.49	10.78	0.00	0.00	0.00	29.69	9.15	1.11	0.00	0.68	0.30
	matrix	0.00	0.00	0.00	30.20	0.00	0.00	0.00	1.39	0.00	0.00	0.00	38.38	27.45	0.35	0.00	2.69	
	matrix	0.00	0.00	6.17	43.43	0.00	1.18	3.35	5.12	0.00	0.00	0.00	19.86	17.52	0.27	2.75	2.24	
	matrix	0.00	0.00	0.96	30.82	0.00	0.50	0.48	1.81	0.00	0.00	0.00	24.18	35.01	0.51	1.11	4.97	0.29
	matrix	0.00	0.00	0.00	0.00	0.00	33.45	0.00	0.00	0.00	0.00	0.00	5.54	13.74	0.27	1.03	48.33	0.54
	matrix	0.00	0.00	0.12	0.30	0.00	33.19	0.12	0.00	0.00	0.00	0.00	3.98	12.76	0.00	0.00	50.76	0.66
.2	matrix	0.00	0.00	0.00	30.24	0.00	0.00	0.00	4.44	0.00	0.00	0.00	26.67	33.47	0.38	0.00	3.78	
	matrix	0.00	0.00	0.00	0.00	0.00	0.00	0.00	0.00	0.00	0.00	0.00	3.35	13.47	0.00	0.00	50.81	0.32
	matrix	0.00	0.00	0.13	0.00	0.00	0.00	0.05	0.00	0.00	0.00	0.00	3.42	14.23	0.00	0.00	50.98	0.27
n	matrix	0.00	0.00	6.60	40.00	0.73	1.20	2.89	13.69	0.00	0.00	0.00	0.00	19.07	0.54	7.71	9.16	
	matrix	0.00	0.00	2.66	43.01	0.41	0.57	0.97	19.73	0.00	0.00	0.00	0.00	16.19	0.33	2.89	6.87	
	matrix	0.00	0.00	2.23	45.91	0.00	0.34	1.30	21.04	0.00	0.00	0.00	0.00	16.55	0.52	3.70	6.23	
	matrix	0.00	0.00	2.85	47.65	0.32	0.72	1.63	19.69	0.00	0.00	0.00	0.00	17.58	0.44	4.30	5.90	
	matrix	0.00	0.00	2.22	47.57	0.41	0.13	0.28	22.70	0.00	0.00	0.00	0.00	19.49	0.31	0.51	4.77	
	matrix	2.07	2.77	1.46	28.08	0.10	2.26	0.00	3.92	0.00	0.00	0.00	0.86	13.58	37.02	1.40	2.51	
	matrix	1.70	1.13	4.50	22.87	0.30	1.88	0.00	10.80	0.00	0.00	0.00	1.21	26.16	27.51	0.94	1.82	
	matrix	1.32	0.37	5.74	22.30	0.63	7.03	0.00	0.65	0.00	0.00	0.00	0.16	14.88	33.91	1.31	1.36	
	matrix	1.05	0.46	6.00	8.32	0.00	1.02	0.00	1.00	0.07	0.00	0.00	1.24	61.68	14.67	0.24	0.53	
	matrix	3.48	1.80	3.34	30.32	0.43	1.44	0.00	8.74	0.00	0.00	0.00	0.94	20.90	20.26	0.77	4.11	
	matrix	3.92	2.71	2.81	32.11	0.25	0.41	0.00	4.37	0.00	0.00	0.00	1.30	20.93	30.60	0.31	5.65	
	matrix	3.05	1.16	3.96	13.08	0.24	0.70	0.00	4.34	0.47	0.00	0.00	0.68	62.93	6.02	0.50	3.12	
	matrix	1.80	1.19	4.08	0.73	0.04	0.13	0.00	0.21	0.97	0.00	0.00	0.69	79.65	1.58	0.23	3.22	
	matrix	3.11	1.57	4.43	30.90	0.00	2.48	0.00	11.16	0.07	0.00	0.00	1.10	23.24	17.74	2.53	4.73	

Appendix 3.7.3 (contin.) Analysis of non-ferrous slag from Chalkidiki, CM (OLY, MYL), Pelion (Thessaly) and Thasos (SKR)

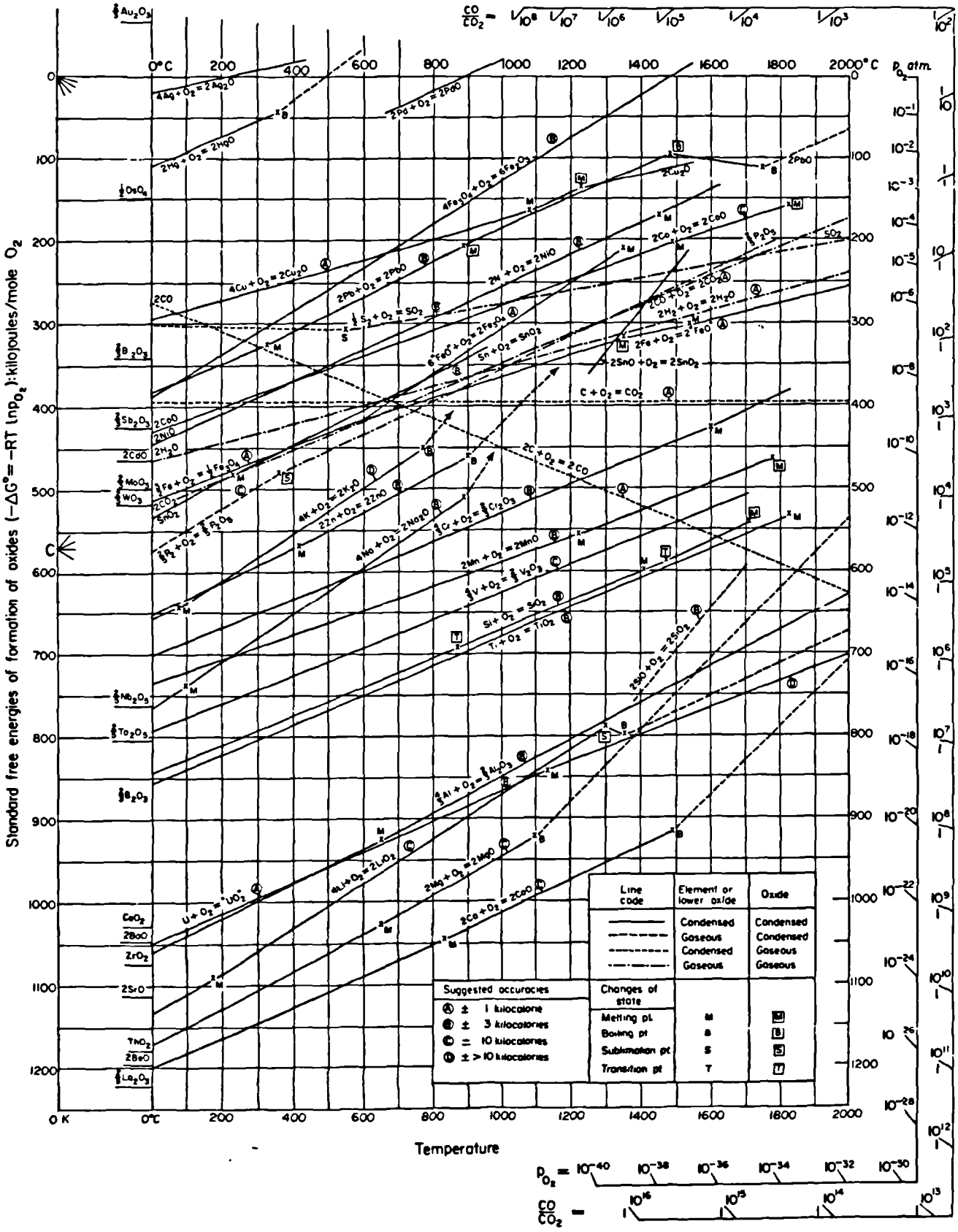

FIG. 45. The standard free energies of formation of oxides, the standard states being the pure condensed phases and gases at 1 atm pressure. Grids for P_{O_2} and CO/CO_2 values are indicated by scales round the right margin and radiate from foci marked on the temperature axis. Where values are not known accurately or where inclusion would lead to confusion the oxide is indicated by its formula at the approximate value of ΔG° at 0°C. (Based on diagrams by Ellingham[39] and Richardson and Jeffes.[33])

Appendix 3.8.2: Experimental smelts with Ni-rich iron laterites

The ore was nickel-rich iron laterite from Boeotia in Central Greece from the Larco plant at Aghios Ioannis, Larymna. It was rather friable and often pulverised extensively. Associated with it were fragments of calcite which were stained red and could not be distinguished from the ore unless hit with a hammer. Thus, the ore was broken on a cast iron plate into 1-1.5cm pieces and in the process calcite fragments were also removed.

The composition of the sample was determined by EPMA and is shown below. Although it cannot be totally representative of the ore as a whole, it corresponds well with the compositions of ores given by Albadakis (section 3.2) and particularly that from Kastoria.

EPMA analyses of Larymna ore used in smelting experiments (sample size 2 cm^2). Area analysed: 800 square microns:

	%age		
	A	B	C
SiO_2	1.94	3.12	2.56
NiO	0.46	1.10	1.22
Cr_2O_3	0.71	1.86	2.13
Fe_2O_3	79.52	65.52	70.30
Al_2O_3	9.05	11.64	9.49
CaO	0.25	0.33	0.36
TiO_2	0.26	0.65	0.65

The stratigraphy as well as metallogenesis of the Larymna ore body have been extensively studied. The deposit is economically viable, the ore beng currently mined and smelted after preroasting in electric furnaces to produce a ferro-nickel alloy (Albadakis 1981). Nickel is found in minerals like garnierite, pimelite which accompany hematite, the main mineral. Chromite is also present, as

well as bauxite which explains the high aluminium contents in the compositions above. Smaller minerals found are gibbsite and pyrite. Apart from the hematite, chert, a quartz constituent is also present.

A number of ore combinations were charged in the shaft furnace with a variety of fuel to ore ratios. The smelts, fuel/ore ratios and type of ore discussed here are summarised below.

Smelt No.	Fuel/Ore	Ore
X-smelt 3	3/1	Hematite and NiO powder
X-smelt 4	3/1	Laterites
X-smelt 10	3/1	Laterites
X-smelt 5	2/1	Hematite and Laterites(4/1)
X-smelt 7	3/1	Hematite and Laterites(1/1)
X-smelt 11		Clay-bound laterites

No roasting was carried out for any of the laterites. The ore and fuel specifications for each smelt are set out below.

	X-smelt 4	X-smelt 10
Ore charged	5.5kg	6kg
Fine charcoal	17kg	20kg
Fuel/Ore	c.3/1	c.3/1
Preheating charc.	15kg	15kg
Fine charc. size	1/2-1/4in	1/2-1/4in
Ore size	0.3-1cm	0.3-1cm

X-smelt 5		X-smelt 7
Total ore charged	12kg	9.4kg
Laterites	2.4kg	4.7kg
Hematites	9.6kg	4.7kg
Hematite/Laterite	4/1	1/1
Fine charcoal	26.5kg	25.5kg
Fuel/ore	2/1	3/1
Preheating char.	15kg	17kg
Fine char. size	1/2-1/4 in	1/2-1/4 in
Laterite ore size	0.5-1cm	0.5-1cm
hematite ore size	1-1.5cm	1-1.5cm

Outline of four smelting cycles using Ni-rich iron ore:

X-smelt 4

11:45	preheat with wood
12:45	preheat with charcoal (5kg)
12:30	preheat with charcoal (10kg)
12:45	charge fine charcoal 0.5kg
1:00	1st charge 0.5kg ore/1.5kg charcoal
1:10	2nd charge 0.5kg ore/1.5kg char
1:20	3rd charge 0.5kg ore/1.5kg char
1:40	4th charge 0.5kg ore/1.5kg char
1:45	5th charge 0.5kg ore/1.5kg char
1:55	6th charge 0.5kg ore/1.5kg char
2:05	7th charge 0.5kg ore/1.5kg char
2:20	8th charge 0.5kg ore/1.5kg char
2:45	9th charge 0.5kg ore/1.5kg char
3:00	10th charge 0.5kg ore/1.5kg char
3:20	11th charge 0.5kg ore/1.5kg char
4:00	shutdown
4:15	furnace sealed

X-smelt 5

11:00	preheat with wood
1:00	preheat with charcoal
1:30	preheat with remaining charcoal (total 15kg)
1:35	1st charge 0.5kg hema/1.5kg charcoal
1:40	2nd charge 1kg hema/2kg char
1:50	3rd charge 1kg hema/2kg char
2:00	4th charge 1kg hema+1kg lat/4kg char
2:20	5th charge 1kg mixed+1kg hema/4kg char
2:45	6th charge 1kg mixed+1kg hema/4kg char
3:15	7th charge 1kg mixed+1kg hema/4kg char
3:30	8th charge 0.5kg hema/1.5kg char
3:45	9th charge 1kg hema/2kg char
5:15	shutdown
5:40	furnace sealed

X-smelt 7

11:45	preheat with wood
1:00	preheat with charcoal (5kg)
1:30	preheat with remaining charcoal (12kg)
1:45	1st charge 1kg mixed(0.5kg lat+0.5kg hema)/2.5kg char
2:10	2nd charge 1kg mixed/2.5kg char
2:15	3rd charge 1kg hema/2.5kg char
2:40	4th charge 2kg mixed/5kg char
3:00	5th charge 2kg mixed/4kg char
3:10	6th charge 1kg lat/1.5kg char
3:45	7th charge 0.7kg hema/2.5kg char
4:00	8th charge 0.7kg lat/2.5kg char
4:20	2.5kg char
5:15	shutdown
5:30	furnace sealed

X-smelt 10

12:30	preheating with wood	
1:30	preheating with charcoal (20kg)	
2:00	charge fine charcoal 2kg	
2:05	1st charge	1kg ore/3kg char(2 fine+1 extra fine)
3:45	2nd charge	1kg ore/3kg char(same as above)
3:10	3rd charge	1kg ore/3kg char(same as above)
3:25	4th charge	1kg ore/3kg char(same as above)
4:20	5th charge	1kg ore/3kg char(same as above)
4:40	6th charge	1kg ore/3kg char(same as above)
5:20		1kg fine char
6:15		1kg fine char
7:00	shutdown	
7:15	furnace sealed	

X-smelt 11

Laterites (sand particle size, bound with a clay slurry) and hematite.

Clay/ laterite sand ratio	2.7kgr/11.8kgr or 1/4.3
hematite	8kgr
Total charcoal	22kgr
Fuel/ore ratio	20kgr/13kgr or 1.5
Peheating charcoal	20kgr
preheating wood	12.5kgr
Clay-bound laterite size	1.5x5x2.5
charcoal size	1.25-.63cm

Smelting Cycle

1:30	preheating with wood (12.5kgr)	
2:30	preheating with coarse charcoal (12.3kgr)	
3:00	charge 2kgr fine charcoal	
3:15	1st charge	2kgr ore (1kg clay-bound later+1kg hem 2kgr char
3:30	2nd charge	2kgr ore (as above)/3kgr char
4:10	3rd charge	2kgr ore (as above)/3kgr char
4:30	4th charge	2kgr ore (as above)/3kgr char
4:55	5th charge	2kgr ore (as above)/3kgr char
5:15	6th charge	2kgr hema/3kgr char
5:45	7th charge	1kgr hema/3kgr char
7:00	shutdown	
7:15	furnace sealed	

Results

Bloom 6.4kgr
Bloom remains after the bloom crushed to the furnace floor:8.2
Furnace charge above bloom 9.5kgr
Furnace charge below bloom 3.2kgr

Appendix 4.1: A Traditonal Iron Foundry in Kavala

The cast iron foundry in Kavala, 20 Amyntaion Street, run by Mr S. Demertzoglou, is probably one of the few of its kind remaining in Greece today. It specialises in the making of man-holes, cast iron covers for sewer shafts and occasionally aluminium castings for propellers. In the past, Mr Demertzoglou did bronze castings as well, but he no longer carries out this type of work.

The focal point of the workshop is a cupola furnace firmly built onto the floor on a cement base. The shaft is about 2-2.5m height and about 40cm inner diameter. The wall thickness is equivalent to that of a single refractory brick. The furnace is charged from the top, from a platform accessed by a ladder.

Cupola furnaces were first patented in England in 1794 (Schubert 1956). Their purpose is to remelt cold pig iron which is tapped at intervals and cast into moulds. The furnace is fired with coke, and as a result the iron picks up some excess carbon.

In a normal run, Mr Demertzoglou uses the following material: a) 15-20 kg of imported grey cast iron (grade 18, from Russia). This constitutes 15-20% of the total charge b) car spare parts c) broken-up pieces of wood stoves. The metal/fuel ratio is 3 parts of iron to 1 part of coke. The charges are estimated by weight rather than by volume. Limestone is added continuously after the first twenty minutes of operation, the ratio being 1 kg of limestone to 10 kg of coke. During the first fifteen minutes only a small amount of slag runs out, but later on both slag and iron are tapped from different tapping holes in the furnace, slag

from the side, iron from the front.

Samples of the material used and produced by Mr Demertzoglou were provided by the founder himself. Their metallographic structures are presented here (Plate 26); the raw material (Madhyt d) (Plate 26b), the tapped slag (Madhyt c) (Plate 26a), tapped iron during melt (Madhyt b) (Plate 26c) and the final product (Madhyt a) (Plate 26d).

Madhyt c (Plate 26a) is tapped slag with iron prills caught in the glassy matrix. Madhyt d (Plate 26b) is the raw material, grey cast iron containing slag inclusions, probably silicates. The matrix is pearlite and ferrite. Madhyt a (Plate 26d), the final product, resembles the raw material except for the added amount of graphite flakes present in the iron. The extra graphite was probably picked up from the coke.

Glossary of technical terms
(after Tylecote (1976), Tylecote (forthcoming), Neeley (1984) and the writer)

Annealing The process of softening a metal hardened by cold working, ie hammering. The lowest temperature at which a metal will soften varies with the degree of cold working, greater amounts of work tending to reduce the temperature.

Austenite A non-magnetic form of iron normally existing only at high temperatures (above about 720° C). Carbon can disolve in it up to about 1.8% at 1150° C and diffuse readily.

Bloom or bloomery iron Iron that has been produced in a solid condition as the result of the reduction (smelting) of iron ore. Pure iron melts at 1535°C, but bloomery was not normally heated above 1250°C. The carbon content varies but is usually low.

Brittleness The property of materials that will not deform under load but tend to break suddenly, like cast iron or glass. It is the opposite property to plasticity.

Cast iron An impure iron containing more than 1.9% C and other elements like silicon, phosphorus, formed in the liquid. Not malleable, hot or cold, and very brittle. It exists in two forms, white and grey, which describes the appearance of the surface exposed when it is fractured.

Catalan hearth Hearth blown by a 'trompe' for making wrought iron by the direct process. Used in some Mediterranean regions. Often used loosely for a bellows-blown low hearth from which the bloom is extracted through the top.

Cementite Iron carbide, Fe_3C, very hard and brittle, forming one of the constituents of pearlite (qv).

Cold-working When hammered at low temperatures, metals increase in hardness and strength.

Cupellation A process for extracting silver and gold from lead, involving the oxidation at c. 1000° C of lead to litharge in a crucible, leaving the precious metals behind as a molten globule.

Decarburization The loss of carbon from the surface of a ferrous alloy as a result of heating it in the presence of a medium, such as oxygen, that reacts with the carbon.

Direct process The iron-making process by which wrought iron is reduced directly from ore.

Etching Developing the structure of a metal by attacking it with aid or other solutions.

Fayalite Iron silicate.

Ferrite A magnetic form of iron, almost devoid of carbon but capable of containing various amounts of other elements such as phosphorus.

Fettled bloom Cold-hammered bloom in preparation for smithing.

Finery hearth The hearth in which decarburization (oxidataion of carbon in the cast iron by air) takes place.

Flux Lime or other material added to the smelting charge to render a slag easy-flowing.

Free-running temperature The temperature at which the viscosity of a metal is low enough for it to be poured.

Eutectic The alloy composition that freezes at the lowest constant temperature, causing a discrete mixture to form in definite proportions.

Forge-welding Welding by heating two pieces of iron or steel and forging them together with a hand or mechanical hammer.

Gangue The commercially undesirable portion of an ore that must be removed before the ore is processed into a metal. Normally removed in smelting by fluxing.

Graphite The form of carbon occurring in cast iron containing more than c. 1% silicon and slowly cooled.

Hammer scale The scale removed from iron during forging. This consists of metal which has reacted with air and wich has thereby been converted mainly to iron oxides.

Hardness The hardness of metals is usually measured by indentation tests. Two popular scales of hardness are the diamond pyramid (HV) and the Brinell (HB).

Hematite Iron oxide, Fe_2O_3, usually red.

Hot-short Brittleness in hot metal. The presence of excess amounts of sulfur in steel causes hot-shortness.

Inclusions Particles of impurities that are usually formed during solidification and are usually in the form of silicates, sulfides and oxides.

Indirect process The iron-making process by which wrought iron is produced indirectly through cast iron. The sequence is: reduction of ore in the blast furnace, cast iron production, decarburization of cast iron in fining hearth, and then wrought iron.

Leaching The removal of elements from the soil or a metal deposit by aqueous solutions.

Limonite Mixture of hydrated and other oxides of iron.

Litharge Lead oxide, PbO.

Martensite A hard product produced by quenching iron containing carbon from temperatures above 720°C.

Matte A liquid or solid mixture of sulfides, usually FeS and Cu_2S.

Mild steel Modern equivalent of wrought iron but without the slag which gives the latter its fibrous structure.

Neumann lines or bands Markings on ferrite which occur as a result of great shock at low temperatures (below 500°C). They disappear when the metal is heated above c. 600°C.

Pearlite One of the constituents of iron containing carbon in excess of about 0.02%; a mixture of ferrite and cementite, usually laminated in form.

Phase A portion of an alloy, physically homogeneous throughout, that is separated from the rest of the alloy by distinct bounding surfaces.

Pig A term now used to denote large lumps of metal which, like the ingot, are destined for breaking up and remelting.

Puddling furnace A reverbatory furnace used for converting cast iron into wrought iron, using a stirring or 'puddling' action in the later stages.

Quenching The process of rapid cooling of metal alloys for the purpose of hardening.

Recrystallization A process in which the distorted grain structure of metals that are subjected to mechanical deformation is replaced by a new strain-free grain structure during annealing.

Reverberatory furnace A type of furnace in which the heating flame is reflected onto the charge from the roof.

Scale The surface oxidation on metals caused by heating in air or in other oxidising atmospheres. It is produced at all stages in iron making including smelting and smithing (see Hammer Scale), and constitutes one of the most common wastes at a metallurgical site.

Slag A fused product occurring in the melting of metals and composed of oxidised impurities of a metal and a fluxing substance, such as limestone.

Smelting Involves a chemical reaction between the ore and the fuel, or between a heated sulfide ore and the atmosphere.

Speiss A residue of lead or copper smelting containing a high proportion of metallic arsenic compounds.

Sorbitic pearlite Unresolvable pearlite formed during rapid cooling in the range 500-600° C.

Spheroidized pearlite Globular cementite particles formed when iron/steel with lamellar pearlite is heated for a prolonged period near or below 700°C.

Stringer (slag) Aligned silicate (slag) inclusions following the direction of working.

Stueckofen A bloomery furnace with a high shaft (up to 5m), originating in Austria in the 18th c.

Tap slag Slag run off from a furnace in liquid condition.

Tempering The operation of softening the hard and brittle constituent, martensite, by heating it for a short time at temperatures between 100 and 650° C.

Walloon finery Finery developed in Flanders in the 16th c. in which the hearth was used: a finery in which decarburization took place and a chafery in which the wrought iron of the finery was reheated for forging.

Widmanstä tten structure The structure occurring in steels which have been fairly rapidly cooled from high temperatures, c. 1000° C.

Wrought iron Iron made either by the direct (bloomery) process or resulting from a conversion process such as puddling or fining.

BIBLIOGRAPHY

Abbreviations

AJA	American Journal of Archaeology
BSA	Annual of the British School at Athens
AD	Archaeologikon Deltion
BCH	Bulletin Coorespondence Hellenique
BMOP	British Museum Occasional Papers
JAS	Journal of Archaeological Science
JFA	Journal of Field Archaeology
JHMS	Journal of the Historical Metallurg Society
JISI	Journal of the Iron and Steel Institute
PPS	Proceedings of the Prehistoric Society

Adam-Veleni, P.
1983 First report on a new Hellenistic town in West Macedonia. Proc. XII Internat. Congress in Classical Archaeology, Athens 1983, 39. In Greek.

Albadakis, N.
1981 The nickel-bearing ores in Greece. In Internat.Symp. on the Metallogeny of Mafic and Ultramafic Complexes in the Eastern Mediterranean, Western Asia and its Comparison with Similar Environments. Athens, Vol 1, 194-213.

Alexander, J.
1962 Greeks, Italians and the ancient Balkan Iron Age, Antiquity 36, 123-30.

Ammen, C.W.
1984 Recovery and refining of precious metals. Van Nostrand-Reinhold.

Anastopoulos J, C Koukoulas, and G Hatziyannis
1976 The iron deposits of Greece. In Iron Ore Deposits of Europe I, 187-91.

Andronikos, M.
1969 Vergina I. Athens.

Anhegger, R.
1943 Beitrage zur Geschichte des Bergbaus in Osmanichen Reich: Europeanische Turkei. Istanbul.

Assimenos C.
1983 Technological and analytical research of precious metals from the chamber tomb of Philip II. 2nd Int. Symp. Hist. Technologie der Adel Metal, Meersburg. 2-4.

Assimenos, C.
1984 Metallographic analysis of the Vergina armour. In Science in Archaeology, R.E. Jones and H.W. Catling, eds., Anthropologika 6, 64. In Greek.

Avery, D.H. and P. Schmidt
1979 A metallurgical study of the iron bloomery, particularly as practiced in Buhaya. J. Metals, October, 14-20.

Bachmann, H-G.
1982 The Identification of slags from archaeological sites, Institute of Archaeology Occ. Paper 6.

Backe-Forsberg, Y. and Ch. Risberg
1986 Metal working at Asine; 'New' finds from the 1926 season. Opuscula Atheniensia 16(10), 123-5.

Backhuizen, S.C. (and R. Kreulin)
1976 Chalkis-in-Euboea: Iron and the Chalcidians abroad, Chalcidian Studies III, Leiden. Part II.2.

Bakirtzis, Ch.
1980 AD 31, Chronika.

Balmuth M. and R.F. Tylecote
1976 Ancient copper and bronze in Sardinia:excavation and analysis.JFA 3, 195-201.

Beaujour, P.
1829 Voyage militaire dans l'empire Ottoman. Paris.

Belon, P.
1553 Les Observation de Plusieurs Singularites et Choses Memorables trouvees en Grece. Paris.

Bielenin, K.
1974 Starozytne Gortnictwo i Hutnictwo Zelaza w Gorach Swietokryskich, Warsaw-Krakow.

Biringuccio, V.
Pyrotechnia. Translated from the Italian by S.C. Smith and M.T. Gnudi, MIT Press, 1943, 68.

Bjorkman, J.K.
1973 Meteors and meteorites in the ancient Near East. Center for Meteorite Studies, Arizona State University, Publication 12.

Blomgren, S.
1980 The possibilities of producing iron nickel alloys in prehistoric times. JHMS 14/2, 103-4.

Blomgren, S.
1982 Changes in carbon distribution during the production of laminated nickel steel tools in prehistoric times. Scandinavian J. Metallurgy 11, 197-202.

Blomgren, S. and E. Tholander
1983 A prehistoric engraving tool of nickel-alloyed steel found in Sweden.Polhem: Tidskrift for Teknikhistoria 1, 1-11.

Bon, A.
1930 Les ruines antiques dans l'isle de Thasos. BCH 54, 147-94.

Branigan, K.
1974 Aegean metalwork of the Early and Middle Bronze Age. Oxford.

Braudel, F.
1985 Civilisation and Capitalism, 15th-18th century. Vol. 1. The Structures of Everyday Life. Fontana Paperbacks, London.

Bronson, B.
1985 Patterns in the early Southeast Asian metals trade. Paper presented at the Research Conferece on Early Southeast Asia, Bangkok and Nakhon Pathom, April 1985.

Bronson, B. and P. Charoenwongsa
1986 Eyewitness acoounts of the early mining and smelting of metals in mainland South East Asia. Thailand Academic Publising Co.

Bronson, B.
unpub. Terrestrial and Meteoritic Nickel in the Indonesian Keris.

Bryer, A.A.M.
1983 The question of Byzantine mines in the Pontos: Chalybian iron, Chaldian silver, koloneian alum and the mummy of Cheriana. Anatolian Studies 32,133-50.

Buchanan, F.
1930 Report on survey of the district of Bhagalpur in 1810-11. CEA Oldham, ed. Government Printing, Patna.

Buchwald, V.F.
1975 Handbook of Iron Meteorities II. University of California Press, 381-404.

Buchwald, V.F. and G. Mosdal
1985 Meteoritic iron, telluric iron and wrought iron in Greenland. Meddelelser om Gronland, Man & Society 9, 1-49.

Casson, S.
1926 Macedonia, Thrace and Illyria. Oxford.

Carter G.
1979 Principles of Physical and Chemical Metallurgy. American Society for Metals, Ohio.

Charles, J.A.
1973 Heterogeneity in metals. Archaeometry 5(1), 105-14.

Charles, J.A.
1979 Metallurgical Examination of S.E. European copper axes. In Problems in European Prehistory, C Renfrew. Edinburgh, 171-4.

Charles, J.A.
1979 From copper to iron; the origin of metallic materials. Journal of Metals 31, 7-14.

Charles, J.A.
1980 The coming of copper and copper base alloys and iron. In The Coming of the Age of Iron, T A Wertime and J D Muhly, eds., Yale University Press, 151-81.

Chernych, E.N.
1978 Aibunar: A Balkan copper mine of the fourth millennium BC. PPS 44, 203-18.

Chilton, J.P. and U.R. Evans
1955 The corrosion resistance of wrought iron. JISI 183, 113-22.

Chiurazzi, J. and R. de Angelis
1910 Catalogue de bronze, marbre, argenterie, Fonderie Artistiche Riunite, Naples.

Cleere, H.
1972 Iron making in a Roman furnace. Britannia 2, 203-17.

Cline, W.
1937 Mining and metallurgy in Negro Africa. General series in Anthropology 5. Wisconsin.

Clough, R.E.
1986 Iron: Aspects of the Industry during the Iron Age and Romano-British periods. Unpublished PhD thesis, University of London.

Collart, P.
1937 Philippe. Paris.

Conofagos, C.
1980 The Ancient Laurion. Athens. In Greek.

Conofagos, C. and G. Papadimitriou
1981a La technique de production de fer et acier par les Grecs Anciens en Attique pendant la période classique. Proc. Academy of Athens 56, 148-72. In Greek with French summary.

Conofagos, C. and G. Papadimitriou
1981b Les crampons en acier de l'Erechtheion ont été fabriques selon la technique qu'on retrouve au Moyen Âge pour les 'Épées Damassées'. Proc. Academy of Athens 56, 173-90. In French with Greek summary.

Conofagos, C. and G. Papadimitriou
1981c Interprétation du pot placé par les Grecs anciens sur le gueulard des fours pendant la période classique. Proc. Academy of Athens 56, 191-211. In Greek with French summary.

Conofagos, C. and G. Papadimitriou
1982 La metallurgie du fer et de l'acier en Grece, pendant la periode classique. In Early Metallurgy in Cyprus, J.D. Muhly, R. Maddin and V. Karageorghis, eds., Nicosia, 363-72.

Cooke, S.R.B. and S. Aschenbrenner
1975 The occurrence of metallic iron in ancient copper. JFA 2, 251-66.

Cooke S.R.B. and B.V. Nielsen
1978 Slags and other metallurgical products. In Excavations at Nichoria in SW Greece, Vol 1. Site, Environs and Techniques, G Rapp and S E Aschenbrenner, eds, Minneapolis. 182-325

Cousinery, E.M.
1831 Voyage dans la Macedoine. Paris.

Craddock, P.T.
1976 The composition of the copper alloysused by the Greek, Etruscan and Roman Civilisations. I: The Greeks before the Archaic period. JAS 3, 93-113.

Craddock, P.T.
1977 The composition of the copper alloys used by the Greek, Etruscan and Roman civisilations. II: The Archaic, Classical and Hellenistic Greeks. JAS 4, 103-23.

Crossley, D. W.
1981 Medieval Iron Smelting. In Medieval Industry, CBA Research Report 40, 29-41.

Davies, O.
1926 Report on the excavations at the toumba and tables of Vardaroftsa, Macedonia, 1925, 1926. BSA 28, 195-9.

Davies, O.
1935 Roman mines in Europe. Oxford.

Den Ouden, A.
1981 The Production of Wrought iron in Hearths. De Archaeologische Pers. Nederland.

Fells, S.
1983 The Structure and Constitution of Archaeological Ferrous Process Slags. Unpublished PhD thesis, University of Aston, Birmingham.

Forsdyke, E.J.
1926-27 The Mavrospelio Cemetery at Knossos.BSA 28, 243-96.

Filippakis S., E. Photos, C. Rolley and G. Varoufakis
1983 Bronzes Grecs et Orientaux: Influences et Apprentissages. BCH 107, 111-32.

François, J.
1843 Recherche sur le gisement el le traitement direct des mineraux de fer dans les Pyrenées particulièrement dans l'Aviège. Paris.

Furtwaengler, A.
1886 Beschreibung der Vasensammlung zu Berlin , I. In Antike Denkmaeler I. Berlin.

Gale, N.H., W. Gentner and G.A. Wagner
1980 Mineralogical and geographical silver sources of Archaic Greek coinage. In Metallurgy in Numismatics I,D.M. Metcalf, ed., Royal Numismatic Society Special Publication, Oxford, 3-54.

Gale, N.H. and Z.A. Stos-Gale
1982 Bronze Age copper sources in the Aegean: a new approach. Science 216, 11-19.

Gale, N.H. and Z.A. Stos-Gale
1984 Cycladic Metallurgy in The Prehistoric Cyclades. Contributions to a Workshop on CycladicChronology, J.A. MacGillivray and R. Barber, eds. Edinburgh, 255-74.

Gale, N. H., A. Papastamataki, Z. Stos-Gale and K. Leonis
1985 Copper sources and copper metallurgy in the Aegean Bronze Age. In Furnaces and Smelting Technology in Antiquity, P.T.Craddock and M.J.Hughes, eds. BMOP 48, 81-101.

Garagounis, K. N.
1971 Peri Lateritikon Sidironikeliouchon kitasmaton periochis Edessis. Deltion Hellinikis Geologikis Etaireias VIII, 181-93.

Gaskell, D. R.
1973 Introduction to Metallurgical Thermodynamics McGraw-Hill.

Georgiev, G.K.
1971 Die alte eisengewinnugsindustrie in Bulgarien. Geologie 4/5, 597-608. Berlin.

Gettens, R. J., R. S. Clarke and W. T. Chase
1971 Two early Chinese Bronzes with Meteoritic Iron Blades.Freer GalleryofArt Occasional Paper, 4(1). Washington DC.

Gialoglou, G. and D. Drymonitis
1983 Northeastern Greece: mining activities, mineral exploration and future developments. Trans. Institute of Mining and Metallurgy (Section A: Mining industry), Athens, 92, 180-85.

Gilchrist, J.D.
1980 Extraction Metallurgy. Pergamon Press.

Gimbutas, M.
1977a Gold Treasure at Varna. Archaeology 30, 44-51.

Gimbutas, M.
1977b Varna: a sensational rich cemetery of theKaranova civilisation, about 4500 BC. Expedition 19-20, 39-47.

Gordon, R.B.
1983 Materials for manufacturing: the response of the Connecticut iron industry to technolgical change and limited resources. Technology and Culture 24(4), 602-34.

Gordon, R.B. and N.J. van der Merwe
1984 Metallographic study of iron artefats from the Eastern Transvaal, South Africa. Archaeometry 26(1), 108-27.

Grammenos, D.
1984 Neolithic studies in Central and Western Macedonia. Published PhD dissertation, University of Thessaloniki.

Hammond, N.
1972 History of Macedonia. I. Cambridge.

Hammond, N. and G.T. Griffith
1979 History of Macedonia. II. Cambridge.

Haaland, R. and P. Shinnie (eds)
1985 African Iron Working. Norwegian University Press.

Hansson, T. and S. Modin
1973 A metallographic examination of some iron findings with a high nickel and cobalt content. Early Medieval Studies 5, 5-23 (Antikvariskt archiv 50).

Healy, J.F.
1979 Mining and processing gold ores in the Ancient World. J. Metals 8, 11-16.

Hedges, R.E.M. and C.J. Salter
1979 Source determination of iron currency bars through analysis of the slag inclusions. Archaeometry 21(2), 161-75.

Hereward, D.
1965 Where was Skaptesule?. Palaeologiae 12, 50-4.

Hermelin, G., E. Tholander and S. Blomgren
1979 A prehistoric nickel-alloyed iron axe. JHMS 13/2, 69-94.

Heurtley, W. A.
1925-6 Report on excavation at the Toumba and Tables of Vardaroftsa, Macedonia 1925,1926. Part I: The Toumba. BSA 27,1-68.

Heurtley, W.A.
1939 Prehistoric Macedonia. Cambridge.

Hoddinot,
1981 The Thracians. Thames and Hudson, London.

Horne, H.
1763 Observations on Sand Iron, Philos. Trans. Royal Soc. 53, 48-61.

Iakovides, S.
1970 The appearance of iron in Greece. Athens Annals of Archaeology 3, 293-6.

Jirecek, C.
1886 Archaeologische fragmente aus Bulgarien. Archaeologische Epigraphische Mitteilungen X, 75.

Jirecek, C.
1912 Staat und Geselschaft,II,44.

Jones, J.E.
1982 The Laurion silver mines: a review of recent researches and results. Greece and Rome 29(2), 169-83.

Jones, J.E.
1984 Ancient Athenian silver mines, dressing floors and smelting sites. JHMS 18(2), 65-81.

Jones, R.E.
1980 Analysis of bronze and other base metal objects from the Lefkandi cemeteries, Appendix in Lefkandi: The Iron Age: The cemeteries, MR Popham, LH Sackett and P Themelis, eds, London, 447-64.

Jones, R.E.
1986 Greek and Cypriot Pottery: A Review of Scientific Studies. Athens.

Jovanovic, B. and B.S. Ottoway
1976 Copper mining and metallurgy in the Vinca group. Antiquity 50, 104-13.

Jovanovic, B.
1980 Primary copper mining and the production of copper. In Scientific Studies in Early Mining and Extractive Metallurgy. P T Craddock ed., BMOP, 20, 31-40.

Junghans, S., E. Sangmeister and M. Schroeder
1960 Studien zu den Anfängen der Metallurgie I. Berlin.

Junghans, S., E. Sangmeister and M. Schroeder
1968 Studien zu den Anfängen der Metallurgie II. Berlin.

Ivanov, I.
1978 Treasures of the Varna Chalcolithic Metropolis. Sukrovishtata na Varnenskiya Khalkoliten Nekropol. English text 49-65. Sofia. Durzahavno Izdatelstvo 'Septemrbrii'.

Institute for Geology and Mineral Exploration (IGME)
1975 Explanatory Issue of the Metallogenic Map of Greece. Epexegematikon Teuchos tou Metallogenetikou Chartou tis Hellados. Athens, 1965 edition.

Kalogeropoulou, A.
1981 The ancient metallurgical furnaces at Steno, Arkadias. Kathimerini 16.2.81. In Greek.

Karamatzani, K. and N. D. Kaklamani
1983 Feasibility Study for the Exploration of the Vrontou-Drama granodiorite. IGME. Athens. (In Greek).

Katsikatsos, G., N. Fytrolakis and V. Perdikatsis
1981 Contribution to the genesis of lateritic deposits of the upper Cretaceous transgression in Attica and central Boeotia (Greece). Proc. Int. Symp. on Metallogeny of Mafic and Ultramafic Complexes Athens, Vol I, 279-313.

Keene Congdon, L.O.
1971 Steel in antiquity: a problem of terminology. In Studies presented to G.M.A. Hanfmann. Fogg Art Museum, Harvard University monograph in Art and Archaeology II, 17-27.

Kense, F.J.
1983 Traditional African Iron Working. African Occasional Papers No. 1, University of Calgary.

Kilian, K.
1983 Ausgrabungen in Tiryns. Arch. Anzeiger 98, 277-328.

Kluge, K. and K. Lehmann-Hartleben
1927 Die antike Grossbronzen. Berlin and Leipzig.

Koukouli-Chrysanthaki, H.
1975 AD 30B, 278.

Koukouli-Chrysanthaki, H.
1977 AD 32, Chronika, 244.

Koukouli-Chrysanthaki, H.
1978 AD 33B, Chronika, 285-6.

Koukouli-Chrysanthaki, H.
1979a AD 34B, Chronika,

Koukouli-Chrysanthaki, H.
1979b Eastern Macedonia. In Treasures of Eastern Macedonia. Arch. ReceiptsFund.Thessalonike, 86-98.

Koukouli-Chrysanthaki, H.
1980 AD 35, Chronika.

Koukouli-Chrysanthaki, H.
1983a AD 38, Chronika, in press.

Koukouli-Chrysanthaki, H.
1983b Excavations in ancient Tragilos. Archaia Makedonia 111, 139. In Greek.

Koukouli-Chrysanthaki, H.
1980 The colonies of Thasos in the N. Aegean. In Kavala and its Surroundings. Idryma Meleton tou Haimou, 189, 309-25.

Koukouli-Chrysanthaki, H.
1985 Protohistoric Thasos. Unpublished PhD thesis. University of Salonika. In Greek.

Koukouli-Chrysanthaki, H. and G. Weisgerber
1982 AD 37, in press.

Kubota, K.
1970 Japan's original steel making and its development under the influence of foreign techniques. Report of the International Cooperation in History and Technology. Pont-à-Mousson, France, March 1970.

Kubler, K.
1939 Kerameikos I. Berlin.

Lazarides, D.
1976 Thasos and its Peraia. Athens.

Lemerle, P., A. Guillou, P. Papachrysanthou and N. Svoronos
1979 Chrysovounion Stefan Dusan, no. 128, Actes de Lavra III. Paris.

Levin, E.M., C.R. Robbins and H.F. McMurdie
1964 Phase diagrams for Ceramicists. Ohio, The American Ceramics Society.

Li Chung
1979 Studies on the iron blade of a Shang dynasty bronze yueh-axe unearthed at Kao-Ch'eng, Hapei, China, Ars Orientalis,11, 259-89.

Light, J.D. and H. Unglik
1984 A frontier fur trade blacksmiths shop. Parks Canada, Ottawa.

Livadefs, S.
1956 The structural iron of the Parthenon. JISI, 49-66.

Lucas, P.
1712 Voyage de sieur Paul Lucas faite par ordre du Roi dans la Grece, l'Asie Mineur, la Macedoine et Afrique. Paris.

Lupu, A. and L. Dragan
1961 Contributii Cu privere la natira si possibilitatile de valorificare a speisului de la uzinele de plumb diu reqiunea Maramures In Studii di cercetari de Metalurgie Extras 2, Annul VI.

MacDonald Encyclopedia of Rocks and Minerals. MacDonald.
1983

McDonnell, J.
1987 The classification of early iron-working slag. Unpublished PhD thesis, University of Aston, Birmingham.

McGeehan-Liritzis, V.
1983 The relationship between metalwork, copper sources and the evidence for settlement in the Greek Late Neolithic and Earaly Bronze Age. Oxford J. of Archaeology 2 (2), 147-80.

McGeehan-Liritzis, V. and N. H. Gale
forthcoming Chemical and lead isotope analyses of Greek Late Neolithic and Early Bronze Age Metals. Archaeometry.

McNeil, M.
1974 Lateritic Soils. In Planet Earth. Readings from Scientific American. Freeman, 221-6.

Mack, E.
1983 Auriferous Mineralization in N Greece: History, Exploration, Evaluation. In Mineral Deposits of the Alps and of the Alpine Epoch in Europe. H J Schneider. Springer Verlag, 375-84.

Maddin, R.
1975 Early Iron Metallurgy in the Near East. Trans. Iron and Steel Institute of Japan 15, 59-68.

Maddin, R.
1985 The technology of ironmaking. In Medieval Iron in Society. Jernkontoret and Rikantikvareambetet.

Stockholm, 127-57.

Maddin R., T. Stech Wheeler and J.D. Muhly
1980 Distinguishing artifacts made of native copper. JAS 7, 211-25.

Magnusson, G.
1986 Lagteknisk Jarnhantering I Jamptlands Lan Stockholm.

Maratos, G. and B. Andronopoulos
1966 The Minerals Wealth of Greece. Institute for Geology and Subsurface Research. Athens.

Marinos, G.
1982 Greece in Mineral Deposits of Europe 2, F.W. Dunning, W. Mykura and D. Slater, eds., London, 233-53.

Mastoris, K., P. Licos, K. Katsiavalos and S. Koutsinos
1979 The placer gold deposit of Aghios Mandilios. IGME Report 12.

Mattusch, C.C.
1977a Bronze and iron working in the area of the Athenian Agora. Hesperia 46, 340-79.

Mattusch, C.C.
1977b Corinthian metalworking: the Forum area.Hesperia 46, 380-89.

Mattusch, C.C.
1980 The Berlin Foundry Cup: the castings of Greek bronze statuary in the early fifth century BC. AJA 84, 435-444.

Merkel, J.
1983 Ore beneficiation during the Late Bronze Age-Early Iron Age at Timna, Israel. MASCA 3, 164-68.

Morton, G.R.
1963 The Products of Nibthwaite Iron-works. The Metallurgist (Sept.) 2, 259-68.

Morton, G.R. and J. Wingrove
1969 Constitution of bloomery slags: Roman. JISI 207, 1556-64.

Morton, G.R. and J. Wingrove
1972 Constitution of bloomery slags: Medieval. JISI 210, 478-88.

Morton, G.R. and J. Wingrove
1970 The charcoal finery and chafery forge.JHMS, 24-8.

Muhly, J.D., R. Maddin, T. Stech and E. Özgen
1985 Iron in Anatolia and the nature of the Hittite Iron industry. Anatolian Studies 67-84. 34.

Müller, A.
1979 La mine de l'Acropole de Thasos. BCH, Suppl. V. Thasiaca, 315-44.

Murphey, R.
1980 Silver production in Rumelia according to an official Ottoman report, circa 1600. Ost Forschung, 75-102.

Needham, J.
1964 The development of iron and steel technology in China. Second Biennial Dickinson Memorial Lecture to the Newcomen Society, 1956. London.

Nishida, E. (ed.)
1973 History of Steel in Japan. Nippon Steel Corporation.

Nosek, E.
1977 The investigation of the iron-sponge fragments from Burgenland. Wiss. Arbeiter Bgld. 59, 71-82.

Notton, J.H.F.
1974 Ancient Egyptian gold refining: a reproduction of early techniques. Gold Bulletin 2, 50-6.

Oddy, W.A. and J. Swaddling
1985 Illustrations of metalworking furnaces on Greek vases. In Furnaces and Smelting technology in Antiquity, P.T. Craddock and M.J. Hughes, eds., BMOP 48, 43-58.

Osborne, R.
1985 Demos. The Discoveryof Classical Attika. Cambridge.

Panseri, C. and M. Leoni
1966 On the Etruscan technique for making iron arms: Examination of a sword from Montefiascone, Metallurgia Italiana 58, 381-9.

Papastamataki, A.
1975 The exploitation of mineral wealth of ancient Greece: Study on the gold and silver content of ancient Greek metallurgy. IGME publication, Athens.

Papastamataki, A.
1986a A study of ancient slags and their contribution to the revealing of ancient metallurgical technology - geological and geophysical research, Special Issue (IGME publication) 329-39. In Greek.

Papastamataki, A.
1986b Ancient Greek metallurgical slags. Proc. of Conference on Ancient Greek Metalurgical Slags, IGME publication. Athens, 40-67. In Greek with english summary.

Parlama, L.
1973-74 AD 29, Chronika, 788.

Pedrizet, Z.
1910 Scaptesyle. Klio 10, 1-25.

Percy, J.
1861 Metallurgy: Fuel; Fire clays; Copper; Zinc; Brass. London. A fascimile reprint of the original source of Metallurgical reference books. 1860-1880. De Archaeologische Press, Nederland.

Percy, J.
1864 Metallurgy: Iron and Steel. London.

Percy, J.
1870 Metallurgy: Lead. London.

Pernicka, E., W. Gentner, G.A. Wagner, M. Vavelidis and N.H. Gale
1980 Ancient Lead and silver production on Thasos, Greece. Revue d'Archeometrie 3.

Petsas, P.
1964 The multiple brush on a local Early Iron Age pithos from Pieria. Essays in Memory of Karl Lehmann, Marsyas, (1). Institute of Fine Arts. New York University, 255-8.

Photos, E., S.E. Filippakis and C.J. Salter
1985 Preliminary investigations of some metallurgical remains at Knossos, Hellenistic to 3rd c. AD. In Furnaces and Smelting Technology in Antiquity, P.T. Craddock and M.J. Hughes, eds., BMOP 48, 189-98.

Photos, E. and C. J. Salter
1986 A reapraisal of phase characterisation in slags. In Proc. 24th Internat. Archaeometry Symposium, J Olin and M J Blackman, eds., Smithsonian Institution, Washington, 259-266.

Photos, E., H. Koukouli-Chrysanthaki and G. Gialoglou
in press Iron metallurgy in Eastern Macedonia; a preliminary report. Paper presented at the UISPP Symposium of the Comite pour la siderurgie anciennne, Belfast, September 1984.

Photos, E., R F. Tylecote and P. Adam-Veleni
in press The possibility of smelting nickel-rich lateritic iron ores in the Hellenistic settlement of Petres, NW Greece. Proc. Meeting on Ancient Mining and Metallurgy - a British School at Athens Centenary Conference. University College of N. Wales, Bangor, April 1985.

Photos, E., S. Papamarinopoulos and G. Spyropoulos
forthcoming An analytical investigation of the furnaces at Steno, Tripolis.

Piaskowski, J.
1960 An interesting example of early technology: a socketed axe from Uretrznobobrka in the Carpathians. JISI 194(3), 336-8.

Piaskowski, J.
1982 A study of the origin of the ancient high-Ni iron generally regarded as meteoritic. In Early Pyrotechnology, T.A. Werthime and S.F. Werthime, eds., Smithsonian Institution, Washington DC, 237-43.

Pigott, V. C., P. E. McGovern and M.R. Notis
1982 The earliest steel from Transjordan. MASCA 2(2), 35-9.

Pigott, V.C.
1982 The Innovation of iron: cultural dynamics in technological change. Expedition 25, no. 1, 20-5.

Platon, N.
1981 Metallurgical furnace in Zakro, Crete. Proc. 4th Cretological Conference, Herakleion 1976, A' (2), 436-46. In Greek.

Pleiner, R.
1968 Problems of direct steel production in early ferrous metallurgy. Steel Times 196, 312-18.

Pleiner, R.
1969 Iron working in Ancient Greece. National Museum, Prague.

Pleiner, R.
1973 Metallography of early artefacts: the problem of welding together iron and steel. Early Medieval Studies Antikvariskt Arkhiv 53, 17-28.

Pleiner, R.
1980 Early Iron Metallurgy in Europe. In The Coming of the Age of Iron, T.A. Werthime and J.D. Muhly, eds. New Haven, 375-416.

Popham, M. R., L. H. Sackett and P. G. Themelis
1980 Lefkandi I: The Iron Age Settlement. BSA Supplementary Volume 11. London.

Poulios, B.
1983 AD 38, Chronika, in press.

Price, G. D.
1982 Exsolution in titanomagnetites as an indicator of cooling rates . Mineralogical Magazine, 46(3), 19-25.

Ramdohr, P.
1980 Ore Minerals and their Intergrowth. London.

Renfrew, C.
1969 The autonomy of the S.E. European Copper Age, PPS 35, 13-47.

Renfrew, C.
1979 Problems in European Prehistory. Edinburgh University Press.

Renfrew, C., M. Gimbutas and E. Elster
1986 Excavations at Sitagroi I. Los Angeles, California.

Richardson, H.G.
1934 Iron, prehistoric and ancient. AJA 38, 555-83.

Richard, T.
1838 Etudes sur l'art d'extraire immediatement le fer de ses mineraux sans convertir le metal en fronte. Paris.

Rickard, J.
1888 Engineering and Mining J. XLV, 474.

Ridley, C. and K.A. Wardle
1979 Rescue excavations at Servia, 1971-73: a preliminary report. BSA 64, 185-230.

Rocher, E.
1879 La Province Chinoise du Yunnan. Vols I and II. Leroux, Paris.

Rosenqvist, T.
1983 Principles of Extractive Metallurgy. McGraw-Hill. London.

Rostoker, W. and E.R. Gebhard
1981 Iron smelting at Isthmia. JHMS 15(1), 41-3.

Rouge, J. (ed)
1966 Expositio Totius Mundi et Gentium. Sources Chretiennes. Paris.

Salkied, L.U.
1987 A Technical History of Rio Tinto Mines: Some Notes on Exploitation from Pre-Phoenician Times to the 1950's. Institution of Mining and Metallurgy.

Salviat, F. and J.J. Mattre
1980 Artemission: secteur proche de l'autel monumental et peribole carre. BCH 104, 726-30.

Schmidt, P. and D.H. Avery
1978 Complex iron smelting and prehistoric culture in Tanzania. Science 201, 1085-89.

Schmidt, P.R. and Avery, D.H.
1983 More evidence for an advanced prehistoric iron technology in Africa. JFA 10, 421-34.

Schneider, G.
1986 Investigation of crucibles and moulds from bronze foundries in Olympia and Athens. Paper presented at the 25th Internat. Archaeometry Symposium, Athens. To be published.

Schwander, E-L., G. Zimmer and U. Zwicker
1983 Zum problem der ofen griechischer Bronzegiesser. Archaeologische Anzeiger 98, 57-70.

Schubert, H.R.
1957 History of the British Iron and Steel Industry from 450 BC to 1775. London.

Serning, I., H. Hagfeldt and P. Kresten
1982 Vinarhyttan. Jernkontorets Bergshistonska Utskott (Nov.), 21.

Snodgrass, A.M.
1980 Iron and early metallurgy in the Mediterranean. In The Coming of the Age of Iron, W.A. Werthime and J.D. Muhly, eds., Yale University Press, 335-74.

Snodgrass, A. M.
forthcoming The coming of the Iron Age in Greece: Europe's earliest bronze to iron transition. In The Transition from Bronze to Iron in Europe, Cambridge University Press.

Spathi, K., C. Kouvelos and V. Perdikatsis
1982 The Manganese-iron Mineralisation in the area of Palaia Kavala, Mineralogical and Petrological Research, 3. IGME. Athens. (English summary).

Stavropodis, I.
1983 Radienerges metallourgikes skouries Makedonias ke Thrakis. Oryktos Ploutos 24, 41-6. (English summary).

Stavropodis, I. and S. A. Pourni
1971 Radiometric Survey of Northern Greece. Greek Atomic Energy Commis sion. Athens.

Tebbutt, C. F. and H. Cleere
1973 A Roman-British bloomery at Pippingford, Hartfield, Sussex Archaeological Collections 3, 28-40.

Theocharis, D. (ed.)
1973 Neolithic Greece. National Bank of Greece, Athens.

Theocharis, D. and K. Romiopoulou
1961 Excavations at Dikili-Tash. Praktika tis Archaeologikis Etaireias, 81-9.

Theophilopoulos, D.
1982 Meleti siderometallevmaton Thasou. Institute of Geological and Mining Exploration. Athens. (English summary).

Tholander, E.
1971 Evidence of the use of carburised steel and quench hardening in LBA Cyprus. Opuscula Atheniensia, 10(3), 15-22.

Tholander, E. and S. Blomgren
1980 Reconstruction of techniques used to produce prehistoric nickel-rich iron artefacts. JHMS 14/2, 94-102.

Tholander, E. and S. Blomgren
1985 On the classification of ancient slags by microstructure examination. Proc.Third Nordic Conference on the application of scientific methods in Archaeology, Mariehamn, Aland, Finland 415-25.

Tholander, E.
1986 Temperature determination in furnaces used in early iron-making. Proc. 24th Internat. Archaeometry Symp. J Olin and J Blackman, eds, Smithsonian Institution, Washington.

Todd, J.A.
1979 Studies of the African Iron Age. J. Metals. November, 39-45.

Todd, J.A. and J.A. Charles
1977 The analysis of non-metallic inclusions in ancient iron. PACT 1, 204-20.

Todd, A. and J.A. Charles
1978 Ethiopian bloomery iron and the significance of inclusi on analysis in iron studies. JHMS 12/2, 63-87.

Tsountas, Ch.
1908 The Prehistoric Acropoleis of Dimini and Sesklo. Athens. In Greek.

Tylecote, R. F.
1974 Can copper be smelted in a crucible? JHMS, 8(1),

Tylecote, R.F.
1976 History of Metallurgy. London.

Tylecote, R.F.
1981a Iron sands from the Black Sea. Anatolian Studies 31, 137-39.

Tylecote, R.F.
1981b The medieval smith and his methods. In Medieval Industry, CBA Research Report 40, 42-50.

Tylecote, R.F.
1982 Smelting of copper ore from Rudna Glava, Yugoslavia, PPS 48, 459-65.

Tylecote, R.F.
1985 The examination of archaeometallurgical remains; some recent examples and conclusions. Proc. Third Nordic Conference on the Application of Scientific Methods in Archaeology, ISKOs 5, 543-60.

Tylecote, R.F.
forthcoming European Metallurgy. Institute of Metals, London.

Tylecote, R.F.
forthcoming Oxidation enrichment in nickel-rich iron. Paper presented at Conference 'Primo Ferro'. San Vincenzo, Italy, October 1983.

Tylecote, R.F., J.N. Austin and A.E. Wraith
1971 Mechanism of the bloomery process in shaft furnaces. JISI 209, 342-62.

Tylecote, R.F. and R. Thomsen
1973 The segregation and surface enrichment of arsenic and phosphorus in early iron artifacts, Archaeometry 15(2), 193-98.

Tylecote R.F. and B.J.J. Gilmour
1986 The Metallography of Early Ferrous Edge Tools and Edged Weapons. BAR. British Series 155.

Vakalopoulos, A.
1973 History of Macedonia 1354-1833. Salonika. Institute of Balkan Studies.

Valmin, M. N.
1938 The Swedish Messenia Expedition. Lund.

Varoufakis, G.
1973 Investigation into three iron spearheads of the 7th and 6th centuries BC. Metalleiologica ke Metallourgika Chronika 10, 23-34. In Greek.

Varoufakis, G.
1979 Chemical and metallurgical study of nineteen iron tripod legs dating to the Geometric period. PhD thesis, University of Athens. Privately published; in Greek.

Varoufakis, G.
1980 Metallurgical investigation of the bronze crater from Derveni. In Aspects of Early Metallurgy, W A Oddy (ed), BMOP 17, 71-86.

Varoufakis, G.
1981 Investigation of some Minoan and Mycenaean iron objects, Frühes Eisen in Europa, Feschrift for W Guyan, Schaffhausen, 25-35.

Varoufakis, G.
1982 The Origin of the Mycenaean and Geometric iron on the Greek mainland and in the Aegean Islands. In Early Metallurgy in Cyprus, J.D. Muhly, R. Maddin and V. Karageorghis, eds., Nicosia, 315-24.

Voreadis, G.
1953 Geologikai ke koitasmatologikai erevnai en Thaso. IGEY. Geologikai ke Geophysikai Meletai 11, 227-82. (English summary).

Vryonis, S.
1962 The question of the Byzantine mines, Speculum, 37(1), 1-17.

Wagner, D.B.
1985 Dabieshan. Traditional Chinese iron production techniques practised in southern Hennan in the twentieth century. Scandinavian Institute of Asian Studies Monograph Series 52. Curzon Press.

Wagner, G.A., E. Pernicka, G. Gialoglou and M. Vavelidis
1981 Ancient gold mines on Thasos. Naturwissenschaften 68, 263-4.

Waldbaum, J.
1978 From Bronze to Iron: the Transition from the Bronze Age to the Iron Age in the Eastern Mediterranean. Studies in Mediterranean Archaeology 54. Göteborg.

Waldbaum, J.
1980 The first archaeological appearance of iron and the Transition to the Iron Age.In The Coming of the Age of Iron, T A Wertime and J D Muhly, (eds.), Yale University Press, 69-98.

Wardle, K. A.
1980 Excavations at Assiros, 1975-9. BSA 75, 229-67.

Wardle, K.A.
1982 The Early Period. In Macedonia: 4000 years of Greek History and Civilisation, M Sakelariou, ed., Athens.

Wertime, T.
1973 The beginning of metallurgy: a new look, Science 182, 875-7.

Westerink, L.G. (ed.)
1973 Nicetas Magistros. Lettres d'un Exile (928-946). Paris.

Wynne, E.J. and R.F. Tylecote
1958 An experimental investigation into primitive iron-smelting tehnique. JISI 190, 339-48.

Yenner, K. A. and H. Özbal
1986 Bolkardag mining district: survey of silver and lead in ancient Anatolia. In Proceedings of the 24th International Archaeometry Symposium. J Olin and M J Blackman eds, Smithsonian Institution Press, Washington, 309-20.